Earth-Science Reviews 244 (2023) 104519

Contents lists available at ScienceDirect

Earth-Science Reviews

journal homepage: www.elsevier.com/locate/earscirev

Tectonostratigraphic evolution and significance of the Afar Depression

Valentin Rime [a,*], Anneleen Foubert [a], Joël Ruch [b], Tesfaye Kidane [c,d]

[a] Department of Geosciences, University of Fribourg, Ch. Du Musée 6, 1700 Fribourg, Switzerland
[b] Department of Earth Sciences, University of Geneva, Rue des Maraîchers 13, 1205 Geneva, Switzerland
[c] School of Agricultural, Earth and Environmental Sciences, University of Kwazulu-Natal, Westville Campus, H1 Building, Geology Department 4001, Durban, South Africa
[d] Department of Environmental Science and Geology, Wayne State University, Detroit MI-48202, USA

ARTICLE INFO

Keywords:
Rift
Red Sea
Gulf of Aden
Passive margin
Hotspot
Continental breakup

ABSTRACT

The Afar Depression is a unique place on Earth where active rift processes can be directly observed. It is believed to be close to continental breakup. The Afar hotspot has a strong influence on the geology of the Depression. Despite the strong geological interest in the region, difficult field access slowed scientific discoveries. During the last two decades, new projects and studies resulted in a better characterization of the region. New field data and global advances in understanding rift processes call for an integrative and holistic review of the tectonostratigraphic evolution of the Afar Depression. This study compiles new geological maps and reviews the stratigraphy and the geological history of the Afar Depression and the Afro-Arabian Rift System. A new kinematic evolution model and integrative paleogeological maps are proposed. Results show that geological events are diachronous throughout the region. We consider the Afar Rift to be distinct from the Red Sea Rift, both being separated by the Arrata Microplate. The Afar Rift is propagating northwards and forms a relay structure with the Red Sea Rift, linked to the counter-clockwise rotation of the Danakil Block since the Mid- to Late Miocene. The Afar Depression can be segmented into two distinct domains, Central Afar and the Danakil Depression. Central Afar experienced significant extension, protracted and extensive magmatism and magma-compensated thinning. It is believed to be strongly influenced by the Afar hotspot. In comparison, the Danakil Depression is younger and went through less extension and less magmatic activity until Recent (~0.6 Ma) times. The absence of magma-compensated thinning allowed the development of an evolved stage of continental breakup. The tectonostratigraphic evolution of the Afar Depression with distinct rifting styles shows the complexity of continental break-up.

1. Introduction

The Afar Depression is the only emerged region on Earth that is close to continental breakup. It furthermore experiences the unique influence of a hotspot. As such, the Afar Depression is a unique place to study ongoing rift mechanisms that shaped planet Earth.

The Afar Depression has triggered geological interest since the 19th century (Blanford, 1869; Munzinger, 1869). The geological significance of the region was heavily debated during the rise of the continental drift theory and the understanding of plate tectonics (e.g. McKenzie et al., 1970; Mohr, 1967; Tazieff et al., 1972; Teilhard de Chardin, 1930; Wegener, 1929). The kinematic reconstruction of the Afar region has been at the core of this discussion for nearly a century. Wegener (1929) argued for continental drift based on the fitting between the African and Arabian continents when removing Afar. Conversely, Mohr (1967) denied this theory based on the presence of pre-rift blocks in the Afar Depression. It remains a spectacular natural laboratory for the study of tectonic processes, such as the transition from rifting to drifting, crustal structure, strain accommodation, the evolution of tectonic styles, mechanical extension vs magma assisted rifting, seismic activity, fault nucleation, propagation and interactions, and rift linkage, among others (e.g. Ahmed et al., 2022; Bastow et al., 2018; Bastow and Keir, 2011; Doubre et al., 2017; Illsley-Kemp et al., 2018a, 2018b; Keir et al., 2013; La Rosa et al., 2022; Moore et al., 2021; Pagli et al., 2014, 2019; Rowland et al., 2007; Ruch et al., 2021; Sangha, 2021; Stab et al., 2016; Zwaan et al., 2020b). It is also an essential site for studies related to the understanding of mantle dynamics (e.g. Armitage et al., 2015; Chambers et al., 2019; Chang and Van der Lee, 2011; Civiero et al., 2015; Faccenna et al., 2013; Hammond et al., 2013; Hansen et al., 2012). The region constitutes the second most recent Large Igneous Province (after

* Corresponding author.
E-mail address: valentin.rime@unifr.ch (V. Rime).

https://doi.org/10.1016/j.earscirev.2023.104519
Received 7 December 2022; Received in revised form 19 May 2023; Accepted 24 July 2023
Available online 2 August 2023

Yellowstone) with ~30 Ma old Ethiopian flood basalts (Courtillot et al., 2003), but is also characterized by a Recent volcanic cover, leading to numerous studies on petrology, volcanology and volcano-tectonics (e.g. Acocella, 2010; Ayele et al., 2007; Barberi et al., 1972b; Barberi and Varet, 1975; Barnie et al., 2016; Ebinger et al., 2010; Ferguson et al., 2013b; Hagos et al., 2016a; Kieffer et al., 2004; Medynski et al., 2016; Mohr and Zanettin, 1988; Pagli et al., 2012; Rooney et al., 2013; Rooney, 2017, 2020a; Tortelli et al., 2022; Wright et al., 2006; Xu et al., 2017). While dominated by magmatic products, the sedimentary architecture and infill of the Afar Depression are particular. The Danakil Depression witnessed episodic marine flooding that led to the formation of marine sediments as well as thick evaporite deposits, possibly forming a modern analogue for salt giants (Atnafu et al., 2015; Holwerda and Hutchinson, 1968; Jaramillo-Vogel et al., 2019, 2023). The interaction of sediments and magmatism formed the unique Dallol salt volcano that is believed to be a Mars-analogue for the study of extremophiles (Belilla et al., 2021; Cavalazzi et al., 2019; López-García et al., 2020; Otálora et al., 2022; Sanz et al., 2021). The Pliocene to Pleistocene sediments in the Afar Depression yielded crucial Hominine discoveries (Abbate et al., 1998; Alemseged et al., 2006; Johanson et al., 1982; Pan et al., 2002; Villmoare et al., 2015). During Late Pleistocene times, the region provided a critical corridor for the early waves of *Homo sapiens* out-of-Africa migration (Abbate and Sagri, 2012; Beyin, 2006, 2021; López et al., 2015; Tierney et al., 2017).

Due to challenging environmental conditions, complex logistics and geopolitical instability, few field studies have been performed considering the significant scientific interest. The emergence of new projects and field data and advances in understanding rifts and passive margin development during the last two decades call for an integrative and holistic review and reassessment of the current knowledge on the tectonostratigraphic evolution of the Afar Depression. This holistic approach implies the consideration of the entire Afar Depression and its margins, as well as the Afro-Arabian Rift System. It requires not only the study of the dominant volcanic rocks, but also sediments (including pre-rift and syn-rift sediments) and the basement. Likewise, the structural analysis includes pre-rift and Precambrian structures that might have influenced the rifting processes.

The core of this work is the compilation of more than 750 datings and more than 120 geological maps, along with other published geological data, new field mapping and remote sensing analysis. All data are integrated, resulting in a new geological map of the Afar Depression (Rime et al., 2022a). It is the first detailed (1:1′000’000) map comprising the complete Afar Depression and its margins. The map combines basement, sedimentary, intrusive and volcanic units, including pre-rift units. Lithological formations are homogenized and age constraints are improved. This map, combined with revised maps of the surrounding regions (section 3) and a review of the geological history of the Afar region (section 4), allows for (1) reevaluation of the tectonic structure of the Depression (section 5), (2) reassessment of the tectonostratigraphic evolution of area with a new kinematic model (section 6), and (3) discussion of concepts and mechanisms of rift evolution in the Afar Depression (section 7).

This revised tectonostratigraphic review will form the base for further detailed studies in the fields of volcanology, structural geology, tectonics, petrology, sedimentology, geo(micro)biology, hominid evolution and human dispersal, and the exploration of the limits of life in extreme settings. The map of the Afar Depression will help local communities in risk assessment of natural hazards and the exploitation of natural resources such as water, salt, and geothermal energy, among others (Battistelli et al., 2002; Gardo and Varet, 2018; Hearn, 2022; Pasquet et al., 2022; Rizzello et al., 2021; Schaegis et al., 2021; Varet, 2018; Varet and Gardo, 2020).

The full review of the magmatic petrology and geochemistry of the Afar Depression is out of the scope of this study. For more information on this topic, the reader is referred to the book of Varet (2018), the reviews of Rooney (2017, 2020b, 2020c, 2020a) and references therein.

2. Geological setting

The *Afar Depression* (also called *Afar Triangle*) is a low-lying triangular region of approximately 600 km by 300 km covering about 105′000 km^2 and extending in Ethiopia, Djibouti and Eritrea (Fig. 1). It is bordered in the west by the Ethiopian plateau, in the south by the Somalian plateau and in the east by the Danakil Block. In the south-west, it opens up towards the Northern Main Ethiopian Rift (NMER). While the elevation of the Depression is situated between – 154 m (lake Asal) and approximately 1000 m, the plateaus reach more than 3000 m. The broader *Afar region*[1] term used in this paper encompasses the Afar Depression, the Danakil Block, the southern Red Sea, the western Gulf of Aden and the surrounding margins of the Ethiopian, Somalian and Yemenite plateaus.

The Afar Depression is situated at the border between the Nubian, Arabian and Somalian plates, forming a triple junction (McClusky et al., 2003; McKenzie et al., 1970; Reilinger et al., 2006; Reilinger and McClusky, 2011; Viltres et al., 2022, Fig. 2). The present-day plate velocities show that the movement of the Arabian plate relative to the Nubian and Somalian plates is significantly larger (~20 mm/yr in the southern Red Sea) than the movement between the Nubian and the Somalian plates (~5 mm/yr in northern MER) (e.g. McClusky et al., 2010; Stamps et al., 2021). The Arabian plate has constantly been moving northward relative to the Eurasian plate since 56 Ma due to the closure of the Neotethys (McQuarrie et al., 2003). The Bitlis and Zagros sutures (Fig. 2) mark the closure of this former ocean at least 10 Ma ago (Darin and Umhoefer, 2022; McQuarrie et al., 2003). At ~25 Ma, the collision in the Mediterranean was probably locked while the Makran was still actively subducting. This caused a significant slowing of the northward relative movement of the Nubian plate and led to the opening of the Red Sea and Gulf of Aden (ArRajehi et al., 2010; Bellahsen et al., 2003; Jolivet and Faccenna, 2000; McQuarrie et al., 2003; Reilinger et al., 2015; Reilinger and McClusky, 2011). This collision also caused the westward escape of the Anatolian plate (e.g. Reilinger et al., 2006, Fig. 2). The East African Rift System (EARS) experienced localized extension since late Eocene, but widespread rifting started to propagate since the Mid to Late Miocene and separated the Somalian plate from the Nubian plate (Michon et al., 2022).

The opening of the Afro-Arabian rift system was preceded by the emplacement of the Ethiopian flood basalts. The first basalts emplacement took place in the Eocene (since 45 Ma) in Southern Ethiopia and Northern Kenya (Fig. 3, see also Rooney, 2017). The main eruptive phase occurred during a short time period around 30 Ma in Ethiopia and Yemen, forming the classical Traps or flood basalts (Coulié et al., 2003; Eid et al., 2021; Hofmann et al., 1997; Ukstins et al., 2002).

This Large Igneous Province (LIP) is related to the African Superplume or African Large Low Shear Velocity Provinces (LLSVP) rooted at the core-mantle boundary (Bastow et al., 2005; Cottaar and Lekic, 2016; Hansen et al., 2012; Ritsema et al., 2011; Rooney, 2017). While some authors argued for a minimal plume influence in Recent times in the Afar Depression (Hammond et al., 2013; Rychert et al., 2012), others associated it with an elevated mantle temperature (Armitage et al., 2015; Bastow and Keir, 2011; Ferguson et al., 2013b; Rooney et al., 2012) and resulting in dynamic topography, explaining the high elevations around the Afar region (Lithgow-Bertelloni and Silver, 1998; Moucha and Forte, 2011).

There is a long-standing and unsolved controversy about the number and configuration of plumes in the upper mantle. While some authors argue that the Ethiopian flood basalts were formed by one single plume/superplume (Ebinger and Sleep, 1998; Hansen et al., 2012; Hassan et al., 2020), others argue for distinct Kenyan and Afar plumes or several different heads rooted in the African Superplume (Chang and Van der

[1] Which should not be confused with the Afar Region (with capital R) representing a political division of Ethiopia.

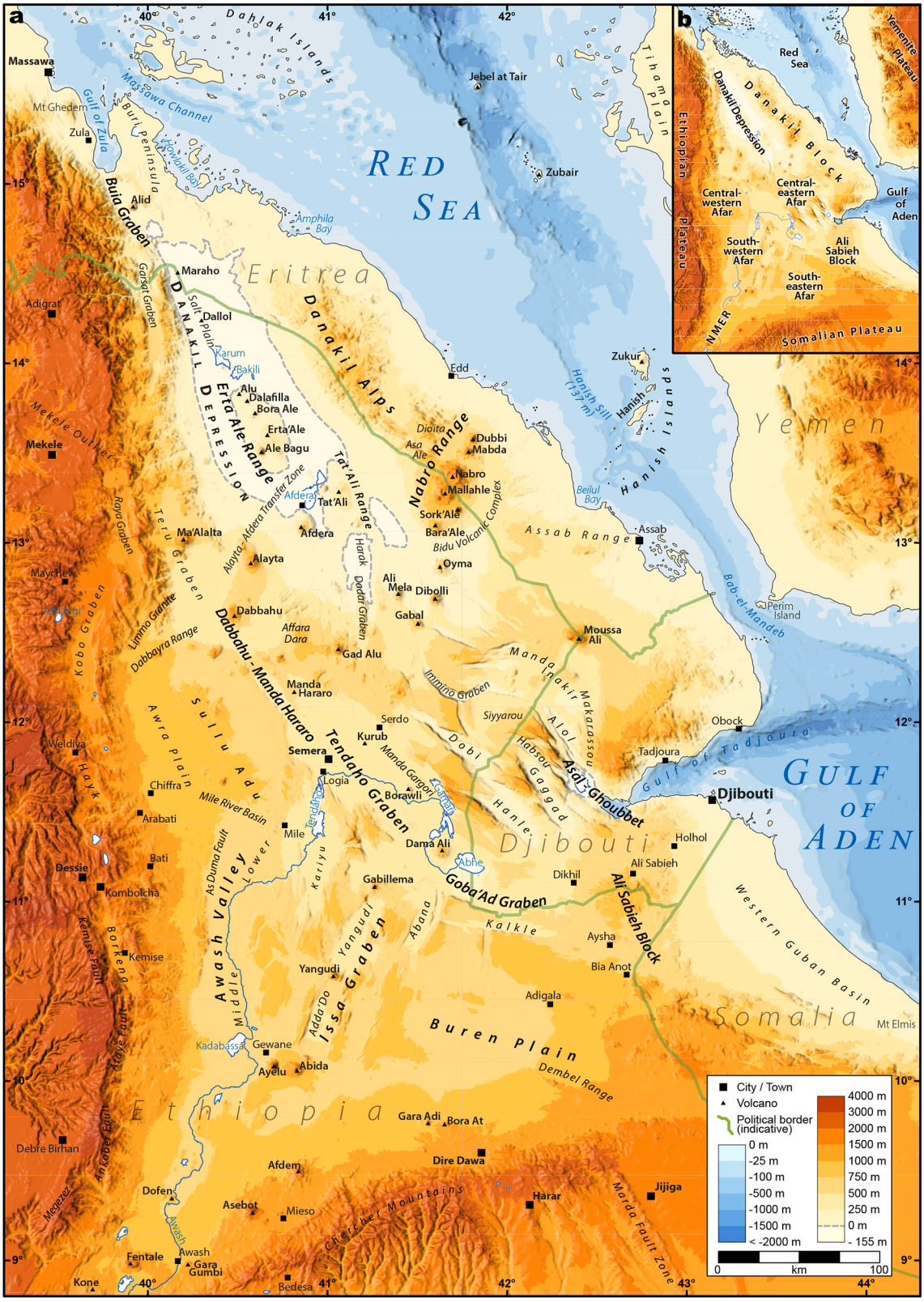

Fig. 1. Topographic map of the Afar Depression.
Topography data are from SRTMGL1 and GEBCO. a) The different regions, basins, structures, volcanoes (block triangles), cities (black squares), lakes and river discussed in the text are shown. Green lines represent political boundaries (Openstreetmap, retrieved on 06.01.2020). Multiple names and spelling are common in the region. The most commonly used names in the scientific literature were favoured. The list of sources for the nomenclature is presented in section Table 1. More local names are presented in Rime et al. (2022a). b) Names of the main regions used in the text and in Fig. 7.

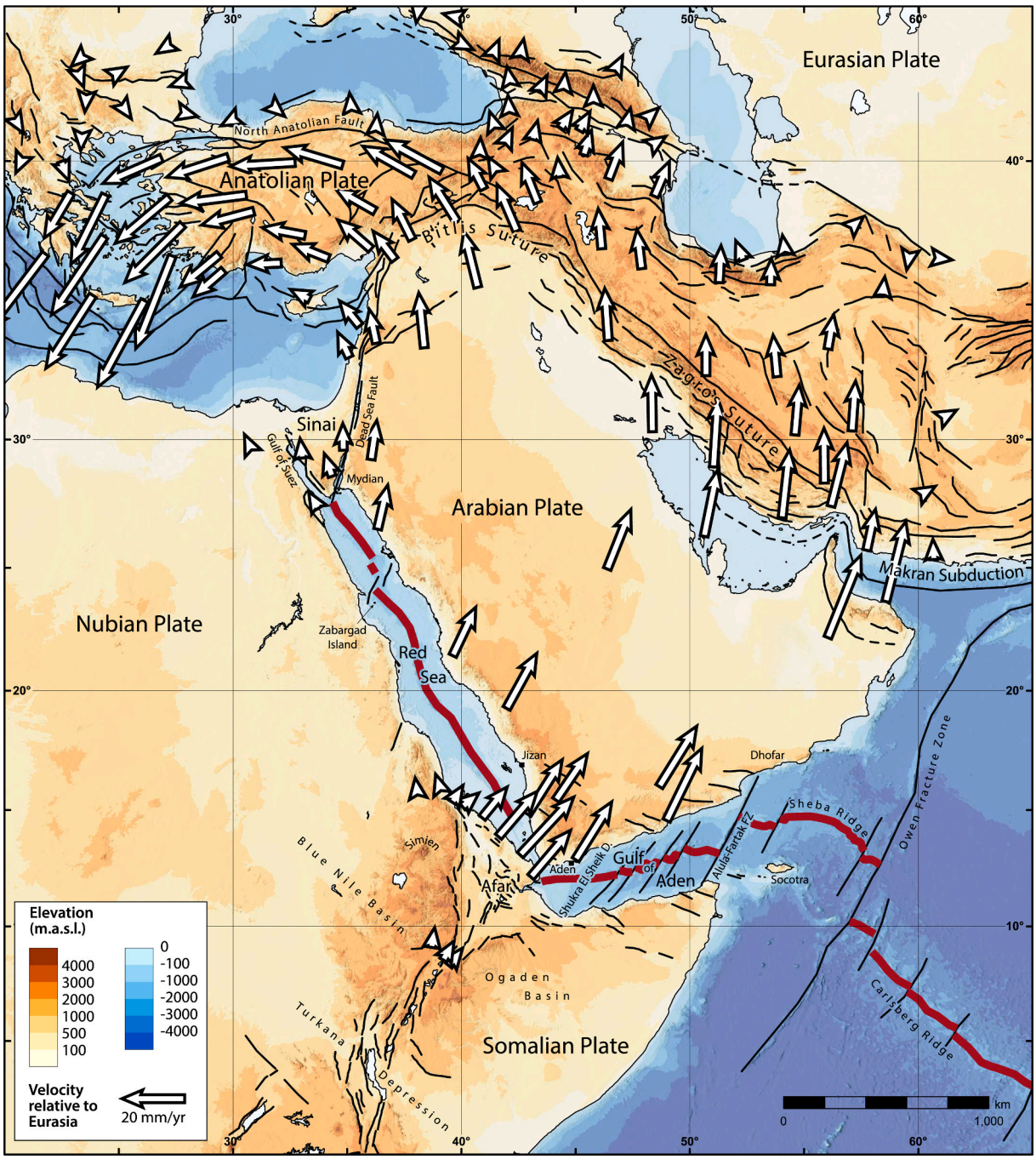

Fig. 2. Geodynamic and topographic map of the Middle East. The white arrows represent GPS velocities relative to stable Eurasia. Data from Reilinger et al. (2006) and Reilinger and McClusky (2011). Black lines indicate major faults and thrust, thick red lines indicate oceanic ridge (after Aghanabati, 1993; Aksu et al., 2021; Ali and Watts, 2016; Augustin et al., 2021; Barrier et al., 2004; Fournier et al., 2010; Pubelier, 2008; Rime et al., 2022a, 2022b; Thiélemont, 2016).

Lee, 2011; Chang et al., 2020; Civiero et al., 2015, 2022; Furman et al., 2006; George et al., 1998; Halldórsson et al., 2014; Lin et al., 2005; Montelli et al., 2006; Rogers et al., 2000).

The origin of the driving force causing the extension of the Afro-Arabian Rift System is often debated (Aldaajani et al., 2021; Michon et al., 2022). For the East African Rift System, plume and mantle effects seem to provide the most significant contribution, mainly as gravitational potential energy (Kendall and Lithgow-Bertelloni, 2016; Michon et al., 2022; Stamps et al., 2014, 2015). For the Red Sea and the Gulf of Aden, the individual contributions of mantle effects and slab-pull linked to the subduction of the Neotethys remain unclear (Bellahsen et al., 2003; Bosworth et al., 2005; Faccenna et al., 2013; Mouthereau et al., 2012; Petrunin et al., 2020). While slab-pull forces were probably important during the first phase of rifting, they significantly reduced after the Arabian slab breakoff in Zagros around 11 Ma (Mouthereau et al., 2012). Most authors agree that the weakening of the Arabian-Nubian lithosphere by plume activity played an significant role in the localization of the Afro-Arabian Rift System (Bellahsen et al., 2003; Bosworth et al., 2005; Brune et al., 2023; Guan et al., 2021; Khalil et al., 2020; Koptev et al., 2018a, 2018b; Reilinger et al., 2015).

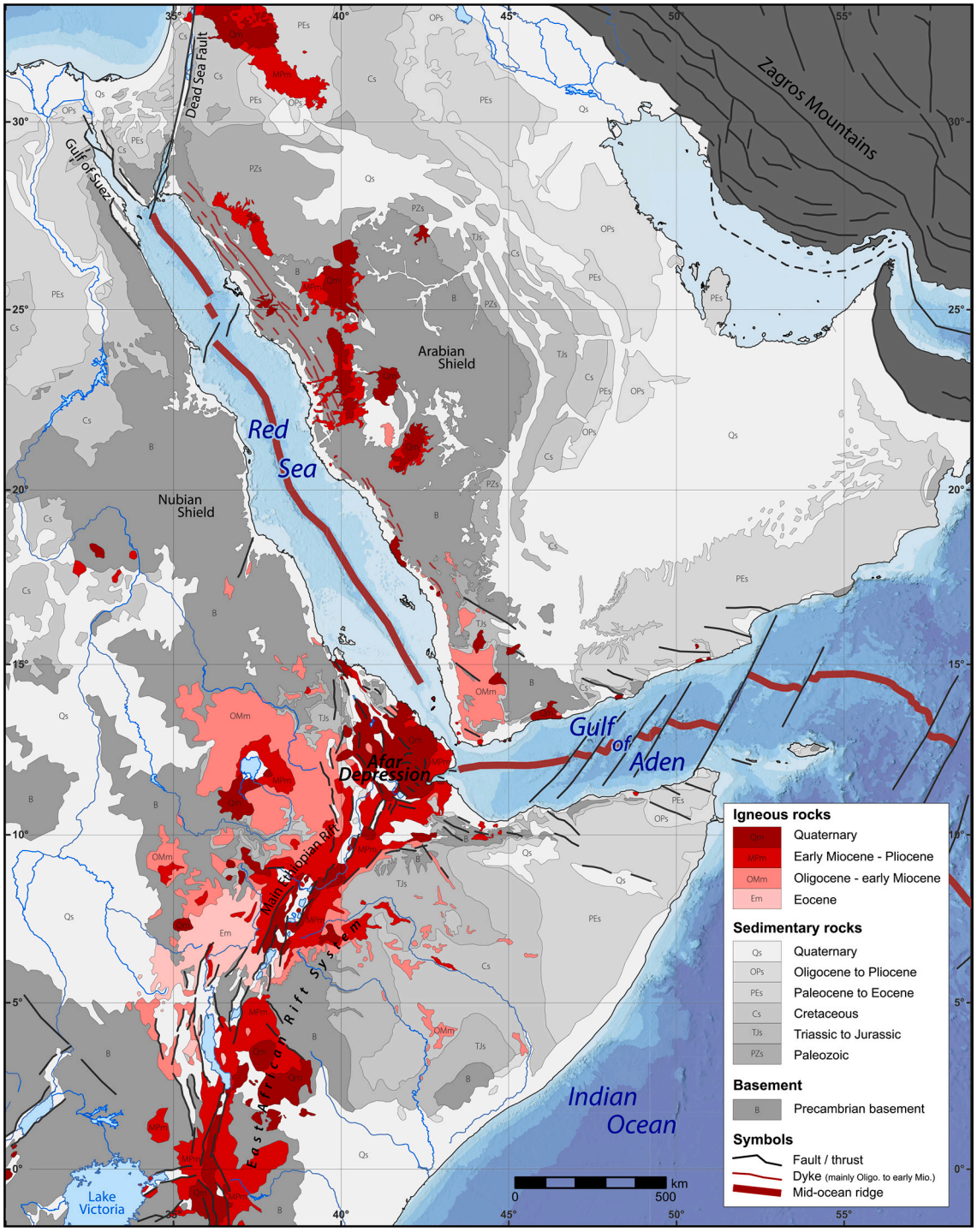

Fig. 3. Geological map of the Afro-Arabian Rift System. This map particularly shows the extent and chronology of Cenozoic volcanic rocks. References listed in Table 3.

3. Geological mapping

3.1. Geological map of the Afar Depression

One of the first geological maps of the Afar region was the *Sketch of the Geological Formations of Abyssinia* of Rüppel (1834). However, until the 70s', no detailed geological map existed. During the 70s', high-quality maps were published after field exploration and access to new satellite imagery. Brinckmann and Kürsten (1970) published detailed 1:250′000 maps of the Danakil Depression. Barberi et al. (1971) and Varet et al. (1975) published 1:500′000 maps covering almost entirely the Afar Depression but excluding the margins and pre-rift rocks. The Geological Survey of Ethiopia (1973) published the first 1:2′000'000 geological map of Ethiopia (including present-day Eritrea). Until today, the only geological map covering the complete Afar Depression and its margins are the 1:2′000'000 maps of Kronberg et al. (1974a, 1974b) (accompanying paper: Kronberg et al., 1975). Small-scale maps were since then published in single articles (e.g. Ayalew et al., 2019; Beyene and Abdelsalam, 2005; Stab et al., 2016) and as part of regional maps (e.g. Thiélemont, 2016).

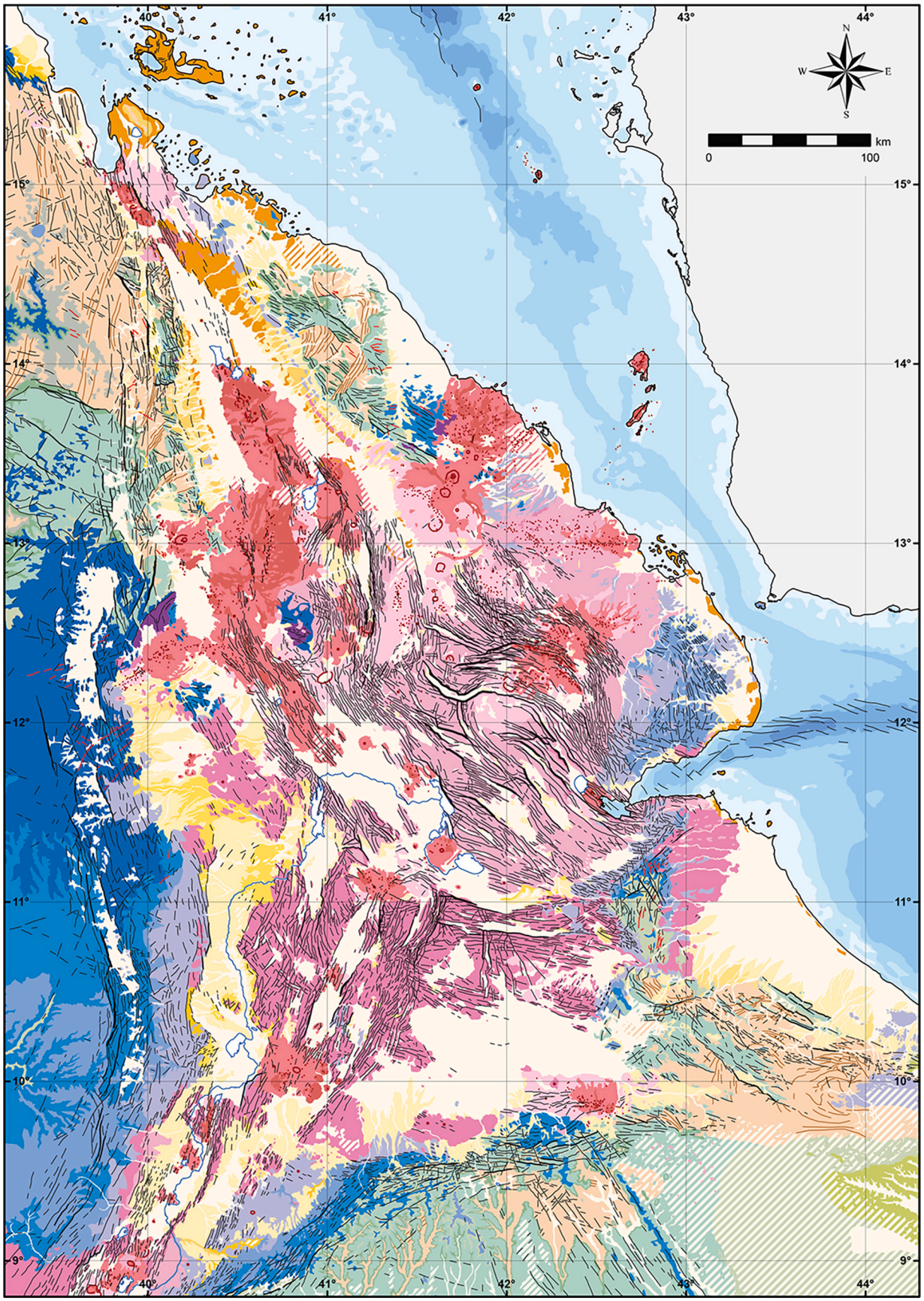

Fig. 4. Geological map of the Afar Depression. The full-scale version of this map is available in Rime et al. (2022a). References listed in Table 1.

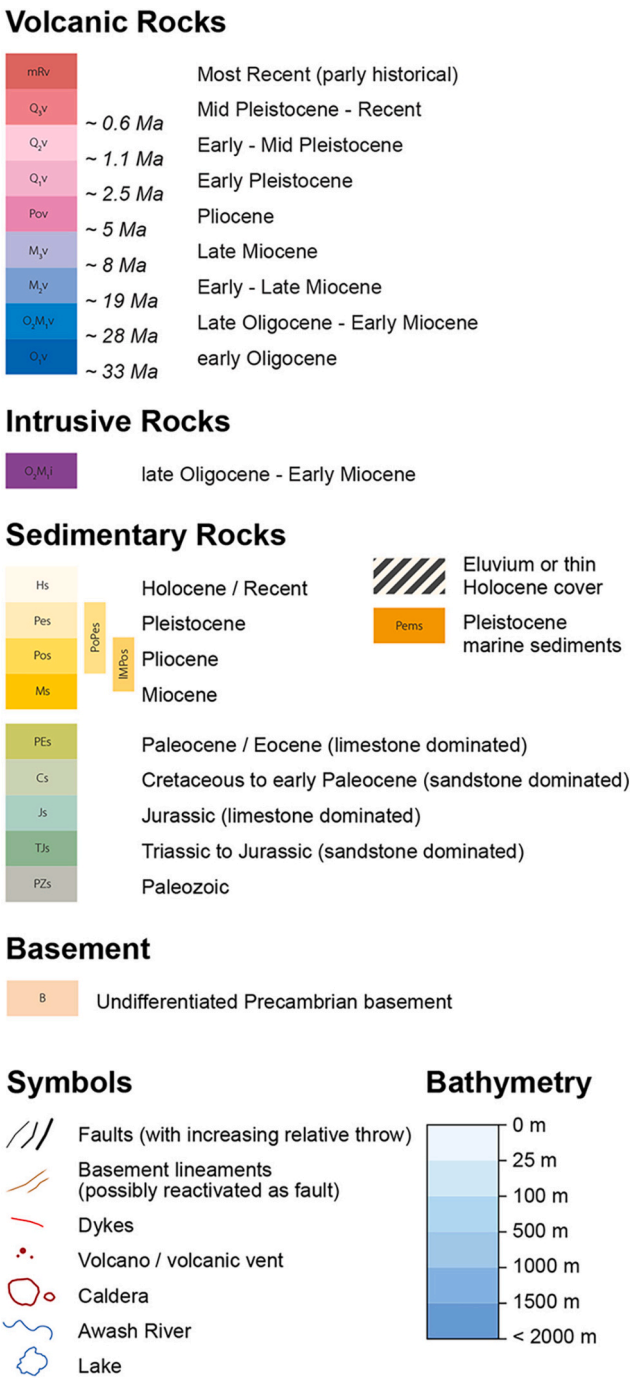

Fig. 4. (*continued*).

The new geological map of the Afar Depression (Rime et al., 2022a, simplified version in Fig. 4) covers the Danakil Depression and adjacent regions from 8.8°N to 16°N and from 39.2°E to 44.3°E at a scale of 1:1′000’000. It includes the northernmost part of the Main Ethiopian Rift, the less-studied Southern Afar Depression and Somalian margins, as well as the rift margins. To keep the scale of 1:1′000’000, certain structures were simplified, and some rare outcrops of important geological significance were upscaled to remain visible.

The map was compiled in Esri’s ArcGIS Pro. All GIS data and files, as well as the dating database are available through the Zenodo open-access database (Rime et al., 2022a). An uncertainty map and the descriptive uncertainty of each mapped region are also available. The attributes of the single mapped polygons further contain source information and comments on the reliability. Finally, on the full-sized geological map, unit codes followed by “*?*” indicate higher uncertainty levels (e.g. contradictory interpretation in the literature, poor age constraint, extrapolation over long distances, unclear remote sensing data, missing coordinates or vague descriptions).

3.1.1. *Material*

More than 120 published geological maps of different sizes, scales, precision and reliability were considered for the mapping (see Table 1 and Rime et al., 2022a). The mapped units across the different maps are mostly lithostratigraphic. Some maps also follow a chronostratigraphic approach and/or provide information on geochronology.

We complied an extensive database of published datings (Rime et al.,

Table 1
Reference for the geological map of the Afar Depression.

	Geological maps	Datings	Other
Gulf of Zula, Danakil Depression and Danakil Alps	Abbate et al. (2004), Antonielli et al. (2009), Barberi et al. (1971), Barberi and Varet (1972), Brinckmann and Kürsten (1970), Buffler et al. (2010), Civetta et al. (1975a), De Fino et al. (1978), Drury et al. (1994), Duffield et al. (1997), Frazier (1970), Gasse, 1974, Geological Survey of Ethiopia (1971, 1978a), Ghebreab (1998, 1999), Ghebreab and Talbot (2000), Hagos et al. (2016b), Le Gall et al. (2018), López-García et al. (2020), Lowenstern et al. (2006), Mège et al. (2021), Sagri et al. (1998), Sani et al. (2017), Teklay et al. (2005), Tortelli et al. (2021), Watts et al. (2020)	Barberi et al. (1972a, 1975), Brinckmann and Kürsten (1971), Buffler et al. (2010), Civetta et al. (1975a), Drury et al. (1994), Duffield et al. (1997), Frazier (1970), Le Gall et al. (2018), Lowenstern et al. (2006), Shoshani et al. (2006)	Bannert et al. (1970), Barberi et al. (1970), Barberi and Varet (1970), Brinckmann and Kürsten (1971), Bruggemann et al. (2004), Buffler et al. (2010), Bunter et al. (1998), Duffield et al. (1997), Frazier (1970), Holwerda and Hutchinson (1968), Munzinger (1869), Park (2010), Varet (2018), Walter et al. (2000)
Ethiopian plateau	Ayalew et al. (2021), Geological Survey of Ethiopia (1971, 1978a, 2009a, 2009b, 2010b, 2011), Hagos et al. (2020), Sembroni et al. (2017), Tesfamichael et al. (2010)	Chernet et al. (1998), Coulié et al. (2003), Drury et al. (1994), Eid et al. (2021), Feyissa et al. (2017), Hofmann et al. (1997), Kieffer et al. (2004), Mohr and Zanettin (1988), Morton et al. (1979), Rooney et al. (2013), Stab et al. (2016), Ukstins et al. (2002), Wolfenden et al. (2005)	Mohr and Zanettin (1988)
Ethiopian central-eastern Afar (including here Dabbahu – Manda Hararo and Tendaho)	Ayalew et al. (2019), Field et al. (2013), Gasse et al. (1974, 1980, 1987), Geological Survey of Ethiopia (2013a, 2014), Kidane et al. (2003), Lahitte et al. (2003a, 2003b), Medynski et al. (2015, 2016), Stab et al. (2016), Varet et al. (1975)	Barberi et al. (1972a, 1975), Brinckmann and Kürsten (1971), Civetta et al. (1975a, 1975b), Ferguson et al. (2013a), Field et al. (2013), Kidane et al. (1999, 2003), Lahitte et al. (2003b), Medynski et al. (2015)	Global Volcanism Program (2013), Varet (2018)
Western Afar	Adamson and Williams (1987), Alene et al. (2017), Asfaw et al. (2002), Black et al. (1972), Chorowicz et al. (1999), Christiansen et al. (1975), Clark et al. (2003), De Heinzelin et al. (1999), DiMaggio et al. (2009, 2015a, 2015b), Garello (2019), Geological Survey of Ethiopia (2009a, 2010b, 2011, 2014), Geraads et al. (2021), Kalb (1995), Kalb et al. (1982), Levin et al. (2004), Mège and Korme, 2004, Mohr (1983), Mohr and Zanettin (1988), Niespolo et al. (2021), Quade et al. (2004, 2008), Semaw et al. (2005), Stab et al. (2016), Taieb et al. (1976), Tiercelin (1986), Varet et al. (1975), Wolfenden et al. (2005), Wynn et al. (2008), Zwaan et al. (2020a, 2020b)	Alemseged et al. (2020), Aronson et al. (1977), Ayalew et al. (2019), Barberi et al. (1972a, 1975), Black et al. (1972), Braun et al. (2019), Clark et al. (1994), Coulié (2001), Coulié et al. (2003), Deino et al. (2010), DiMaggio et al. (2015a, 2015b), Haile-Selassie et al. (2015), Kidane et al. (2003), Kleinsasser et al. (2008), Kunz et al. (1975), Lahitte et al. (2003b), Niespolo et al. (2021), Renne et al. (1999), Rooney et al. (2013), Saylor et al. (2019), Stab et al. (2016), Ukstins et al. (2002), White et al. (1993), WoldeGabriel et al. (2001, 2013), Wolfenden et al. (2005)	Black et al. (1972), Campisano (2012), Clark et al. (1984), Hall et al. (1984), Justin-Visentin and Zanettin (1974), Kleinsasser et al. (2008), Rowan et al. (2022), Varet (2018), WoldeGabriel et al. (2013)
NMER	Abebe et al. (2005), Benito-Calvo et al. (2014), Chernet et al. (1998), Feyissa et al. (2017), Geological Survey of Ethiopia (1978b, 1985, 2007, 2009b), Hujer et al. (2015), Juch (1975), Morbidelli et al. (1975), Popp and Scholger (2017), Sickenberg and Schönfeld (1975), Siegburg et al. (2018), Williams et al. (2004), WoldeGabriel et al. (1992b), Wolfenden et al. (2004)	Benito-Calvo et al. (2014), Chernet et al. (1998), Feyissa et al. (2017), Hujer et al. (2015), Kazmin et al. (1980), Kidane et al. (2006, 2010), Kunz et al. (1975), Lahitte et al. (2003b), Morbidelli et al. (1975), Morton et al. (1979), Siegburg et al. (2018), Tiercelin et al. (1979), Ukstins et al. (2002), Vogel et al. (2006), Williams et al. (2004), WoldeGabriel et al. (1992a, 1992b), Wolfenden et al. (2004, 2005)	Rooney (2020b), Tiercelin et al. (1979)
South-eastern Afar and Somalian plateau	Black et al. (1975), Geological Survey of Ethiopia (1985, 2007, 2010a, 2014, 2015), Juch (1975), Mège et al. (2016), Varet et al. (1975)	Audin et al. (2004), Barberi et al. (1975), Berhe (1986), Black et al. (1975), Chernet et al. (1998), Kunz et al. (1975), Mège et al.	Varet (2018)

(*continued on next page*)

Table 1 (*continued*)

	Geological maps	Datings	Other
		(2016), WoldeGabriel et al. (1992a)	
Somalia	Ali (2015, 2009), Ali et al. (2018), Ali and Watts (2013), Geological Survey Somali Democratic Republic (1957, 1970a, 1971a, 1971b)		
Djibouti	Arthaud et al. (1980), Audin et al. (2004), Black et al. (1975), Boucarut et al. (1985), Chessex et al. (1975), Daoud et al. (2011), Le Gall et al. (2010, 2015), Manighetti et al. (1997, 1998), Muller and Boucarut (1975)	Audin et al. (2004), Barberi et al. (1972a, 1975), Chessex et al. (1975), Civetta et al. (1975a, 1975b), Courtillot et al. (1984), Daoud et al. (2011), Lahitte et al. (2003b), Le Gall et al. (2010), Manighetti et al. (1998), Piguet and Vellutini (1991), Zumbo et al. (1995b)	Gasse et al. (1980, 1986), Varet (2018)
Southern Danakil Block (excl. Djibouti)	Barberi et al. (1971), Civetta et al. (1975a, 1975b), De Fino et al. (1973), Ganci et al. (2020), Wiart and Oppenheimer (2005)	Barberi et al. (1975), Brinckmann and Kürsten (1971), Civetta et al. (1974, 1975a, 1975b), Piguet and Vellutini (1991)	Civetta et al. (1974), De Fino et al. (1973), Varet (2018), Wiart and Oppenheimer (2000), Wiart et al. (2000)
Red Sea and Gulf of Aden (incl. islands)	Carbone et al. (1998), Dauteuil et al. (2001), Frazier (1970), Gass et al. (1973), GEBCO Compilation Group (2020), Lambeck et al. (2011), Le Gall et al. (2015), Mallick et al. (1990), Purkis et al. (2012), Xu et al. (2015)	Mallick et al. (1990)	Al-Mikhlafi et al. (2018), Angelucci et al. (1975), Conforto et al. (1976), Frazier (1970)
Seasonally flooded areas	2019/2020/2021 Landsat 8 images (Earth Resources Observation and Science (EROS) Center, 2018a)		
Geographic features	Rivers, lakes, roads, coastlines and political boundaries from Openstreetmap (https://www.openstreetmap.org, 06.01.2020). River, lakes, roads and coastlines are manually modified. Data for insert globe from Natural Earth (naturalearthdata.com).		
Names	Ali (2015), Angelucci et al. (1975), Ayalew et al. (2019), Ayele et al. (2009), Black et al. (1972), Campisano (2012), Chernet et al. (1998), Christiansen et al. (1975), Clark et al. (2003), Frazier (1970), Geological Survey of Ethiopia (1978b, 1985, 2007, 2010a, 2011, 2013b, 2014, 2015), Global Volcanism Program (2013), Kidane et al. (2003), Lahitte et al. (2003a, 2003b), Le Gall et al. (2015), Manighetti et al. (2001), Munzinger (1869), Nanis and Aly (2020), Stab et al. (2016), Varet (2018), Varet et al. (1975), Wiart and Oppenheimer (2005), Williams (2016), Wolfenden et al. (2005), Wynn et al. (2008), Zwaan et al. (2020b) and the EthioGIS MapServer Ethiopia (www.ethiogis-mapserver.org). Multiple names and spelling are common in the region. We favoured the most commonly used names in the scientific literature. Names with comments are also featured as a shapefile of Rime et al. (2022a).		

2022a, see also Suppl. Mat. 1). This database contains 773 datapoints extracted from 75 publications. Most datings have been performed on volcanic material. 63% of the samples were dated using the K/Ar technique, 23% using Ar/Ar, 8% by unknown dating techniques, and the last 6% include a variety of techniques like (U-Th-Sm)/He, 36Cl, 14C, Fission track and 3He. Some techniques are known to be less reliable, particularly, K/Ar datings compared to Ar/Ar datings (Kidane et al., 2003; Lahitte et al., 2003b). The higher uncertainty related to the technique used and the published uncertainty range for each datapoint were weighted during the mapping process (see discussion on reliability in Rime et al., 2022a). The precision and reliability of the localisation were also evaluated and rated for each datapoint. When possible, the position of the datapoints was reviewed based on the sampling description or maps presented in the publication. Several (>40) errors in coordinates and/or inconsistencies were identified, corrected and indicated in the database.

Outcrop descriptions, cross-sections and sedimentological descriptions were also used for the mapping (Table 1).

The map is complemented by lithological and structural field observations conducted during six field trips (2013, 2015, 2016, 2017, 2019, 2020) led by teams of the universities of Addis Ababa (Ethiopia) and Fribourg (Switzerland) within the framework of the SNF-funded project SERENA 'Sedimentary Record of the Northern Afar' (200021_163114). Observations focussed on the Danakil Depression and its western margin, including western Harak graben, the basins N, NE and E of the Tat'Ali Range, the Erta Ale Range, the basin W of the Erta Ale Range, the Salt plain and its western margin, several transects between the salt plain and the Garsat Graben and the road outcrops between Afdera-Mekele and Dallol-Mekele.

Remote sensing data were used to complement, improve and interpolate published data and field observations. Multispectral satellite images from Landsat 8 OLI and TIRS Level-1 data (Earth Resources Observation and Science (EROS) Center, 2018a) were used for the complete study area. The bands 7–6-5 were used to enhance geological contrasts. Other commercial orthophoto providers (Google Earth, Bing Maps, Esri) were used for higher-resolution images. The digital elevation models (DEM) used were the SRTMGL1 (Earth Resources Observation and Science (EROS) Center, 2018b) for the complete study area and the ALOS PALSAR RTC (doi:https://doi.org/10.5067/Z97HFCNKR6VA) for the Danakil Depression.

3.1.2. Lithological units

Different stratigraphic classifications have been proposed in the literature for the Afar Depression and its margins since the first lithostratigraphy was presented by Blanford (1869) for the Ethiopian Plateau. Suppl. Mat. 2 compiles the most commonly used formal and informal lithostratigraphic classifications in the area for the Paleogene, Neogene and Quaternary based on magmatic and sedimentary units. Fig. 5 compiles the lithostratigraphy from the Ordovician to the Paleogene. As noted by Mohr and Zanettin (1988) and Rooney (2017, 2020a), lithological units and Formation names used in Afar are based on petrological, morphological or genetic relationships, and distinct Formations sometimes have overlapping ages. Conversely, identical terms are used for rocks of significantly different ages (e.g. Stratoid, Termaber Fm. on Suppl. Mat. 2). Also, most studies focus either on magmatic stratigraphy or sedimentary stratigraphy but an integrated stratigraphic approach is rarely proposed.

Considering the principal aim of this study is the overall understanding of the tectonostratigraphic evolution of the study area, the authors took an unconventional chronostratigraphic-approach while – where possible – respecting the historically defined lithostratigraphic units. As such, the map is the first of its kind for the Afar Depression and integrates volcanic, magmatic and sedimentary rock units. The authors are aware of the limits of this combined chrono-lithostatigraphic approach. Still, they are convinced that this is the only way to understand better rift evolution at a regional scale.

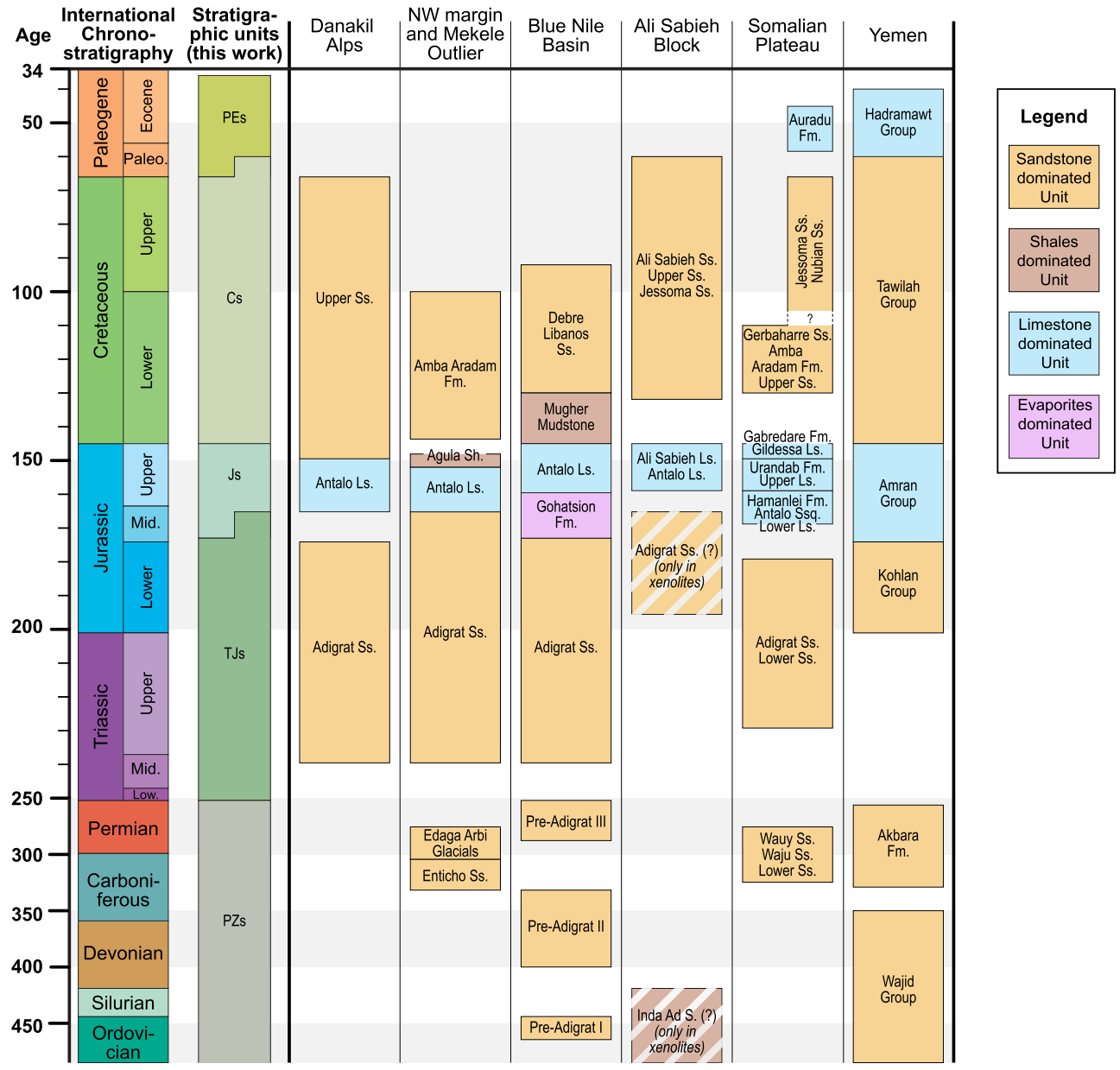

Fig. 5. Pre-rift lithological units of the margins of the Afar Depression. Compilation of the most common lithological units. Note that the chronostratigraphy is often poorly constrained. The reader is referred to the original publications for detailed information. Abbreviations: Fm. = Formation; Gr. = Group; Ls. = Limestone; S. = Series; Sh. = Shales; Ss. = Sandstone; Ssq. = Supersequence. Sources: Danakil Alps: Brinckmann and Kürsten (1971), Sagri et al. (1998); NW margin and Mekele Outlier: Beyth (1972), Hagos et al. (2020), Kidane et al. (2013), Sembroni et al. (2017); Blue Nile basin: Chernet et al. (2020); Ali Sabieh Block: Chessex et al. (1975), Gasse et al. (1986), Kidane (2016), Le Gall et al. (2015); Somalian plateau: Ali and Watts (2016), Bosellini et al. (2001), Geological Survey of Ethiopia (1985, 1996, 2007, 2010a), Geological Survey Somaliland Protectorate (1956); Yemen: As-Saruri et al. (2010), Grolier and Overstreet (1978), van der Gun and Ahmed (1995).

3.1.2.1. Volcanic stratigraphy. The volcanic units are defined mainly based on their age and not necessarily on historical defined Formation names. The units represent lavas erupted synchronously but often have very different petrology, chemistry or origin. Conversely, one former defined single, homogeneous lithostratigraphic unit might exceptionally be mapped in this study by two separate units due to significant age differences at the bottom and top of the succession. Nevertheless, most of the volcanic stratigraphic units defined in this study follow the lithostratigraphic consensus presented in recent literature. The encountered lithologies of volcanic rocks cover various compositions from basalts to rhyolites (e.g. Barberi et al., 1970; Rooney, 2020a; Varet et al., 1975). On the full-scale map (Rime et al., 2022a), rhyolite outcrops are indicated with a pattern. Because of significant contradictions among different sources, ignimbrites were not included in this category.

The following volcanic stratigraphic units are defined:

- *mRv*: most Recent volcanics. This unit is not defined solely by age but corresponds to the last eruptions identified and mapped easily due to their very dark color. It considers historical eruptions, including the very Recent Erta Ale or Nabro eruptions (Global Volcanism Program, 2018, 2019; Goitom et al., 2015).
- Q_3v: Mid-Pleistocene to Recent volcanics younger than ~0.6 Ma. This unit is comparable to the Recent formations of Kidane et al. (2003), Stab et al. (2016) and Varet (2018), or the *Axial Series* of Rooney (2020a) and Zumbo et al. (1995b).

- Q_2v: Early – Mid-Pleistocene volcanics, with ages between ~0.6 and ~ 1.1 Ma. This unit is comparable to the *Gulf Basalts* of Kidane et al. (2003) and Stab et al. (2016) or the upper part of the *Stratoid series* of Varet et al. (1975).
- Q_1v: Early Pleistocene volcanics between ~1.1 and ~ 2.5 Ma old. This unit is comparable to the upper *Stratoid Series* of Kidane et al. (2003).
- *Pov*: Pliocene volcanics between ~2.5 and ~ 5 Ma old. This unit includes the lower *Stratoid Series* of Kidane et al. (2003) and Rooney (2020a), most of the *Sullu Adu Series* of Stab et al. (2016), the *Bachi Fm.* of Wolfenden et al. (2004), and the upper part of the *Somali* and *Dalha Basalts* of Le Gall et al. (2015).
- M_3v: Late Miocene volcanics between ~5 and ~ 8 Ma old. This unit is shorter but comparable to most of the *Dahla Series* defined in the literature (Kidane et al., 2003; Le Gall et al., 2015; Varet et al., 1975; Wolfenden et al., 2005).
- M_2v: Early to Late Miocene volcanics between ~19 and ~ 8 Ma old. This unit covers an extended period but a relatively small extent (Suppl. Mat. 1c) and includes the *Mabla Series*.
- O_2M_1v: late Oligocene to Early Miocene volcanics between ~28 and ~ 19 Ma old. It corresponds to the upper part of the *Traps series* (holding a wide variety of names across the region) and includes the *Ali Sabieh basalts* (Le Gall et al., 2015) and the Ogaden dyke swarm (Mège et al., 2016).
- O_1v: early Oligocene volcanics between ~28 and ~ 34 Ma old corresponding to the lower part of the *Traps series*.

3.1.2.2. Intrusive rocks. Mapped Cenozoic intrusive rocks in the study area are relatively rare. They are mainly formed by granites and some dolerite (Bannert et al., 1970; Barberi et al., 1975; Black et al., 1972; Civetta et al., 1975a; De Fino et al., 1978; Geological Survey of Ethiopia, 1978a). The major intrusions are the Limmo, Affara Dara, Dioita and Asa Ale intrusives (Barberi et al., 1975; Black et al., 1972; Civetta et al., 1975a; De Fino et al., 1978). Because they all have similar age, a single unit was defined:

- O_2M_1i: late Oligocene to Early Miocene intrusive magmatic bodies between ~28 and ~ 19 Ma old. They include the Limmo, Affara Dara, Dioita and Asa Ale intrusives (Barberi et al., 1975; Black et al., 1972; Civetta et al., 1975a; De Fino et al., 1978).

3.1.2.3. Sedimentary stratigraphy. Stratigraphic units for the syn-rift sedimentary rock are defined following the International Chronostratigraphic Chart. Except for the *Pems* unit, these units are chiefly composed of siliciclastic sediments ranging from very coarse conglomerates to mudstones, but lacustrine carbonates and evaporites are also present.

The following syn-rift stratigraphic units are defined:

- *Hs*: Holocene sediments covering mainly the basin floor and the Red Sea and Gulf of Aden coasts.
- *Pes*: Pleistocene sediments mainly present at the margin of the Danakil Depression, "Terraces gravel" of Brinckmann and Kürsten (1971), in the lower and middle Awash valley, forming the *Busudima Fm.* (e.g. Quade et al., 2008), in some graben structures of central-eastern Afar (e.g. Gasse and Street, 1978) and in the NMER (WoldeGabriel et al., 1992b).
- *Pems*: Pleistocene marine sediments. This unit is distinguished from the other Pleistocene deposits due to its marine nature and lithology being significant to understand the basin dynamics of the Danakil Depression.
- *Pos*: Pliocene sediments. They are mainly present in the Awash valley as clastic sediments forming the *Sagantole* and *Hadar Formations* (e.g. Quade et al., 2008; Renne et al., 1999) and in the eastern Goba'Ad basin (Gasse et al., 1987).
- *PoPes*: Pliocene to Pleistocene sediments. This unit is mainly present in the Awra plain and Guban basin.
- *Ms*: Miocene sediments. They are present as the *Chorora* and *Adu-Asa Fm.* in the NMER (Sickenberg and Schönfeld, 1975; WoldeGabriel et al., 2001) and as the *Dogali Fm.* near Massawa (Drury et al., 1994; Sagri et al., 1998).
- *lMPos*: Late Miocene to Pliocene sediments. This unit is almost exclusively used for the Red Bed Series around and at the margins of the Danakil Depression.

Pre-rift lithostratigraphic units are well defined in former studies with a homogenized nomenclature (Fig. 5). However, timing is poorly constrained. Based on the recurrent, almost synchronous pattern of facies associations, the stratigraphic units defined in this study mostly conform to the former lithostratigraphic units.

The following pre-rift stratigraphic units are defined (see legend of Fig. 5 for sources):

- *PEs*: Paleocene to Eocene sediments dominated by marine limestone. They are only present in the SE part of the map forming the *Auradu Fm.*
- *Cs*: Cretaceous sediments dominated by sandstones. The upper part of this unit (*Jessoma sandstones*) might, however, be early Paleocene in age (Grolier and Overstreet, 1978; Kidane, 2016; van der Gun and Ahmed, 1995). Note that the *Mugher Mudstones* of the Blue Nile basin are incorporated in this *Cs* unit.
- *Js*: Jurassic sediments dominated by marine limestones (often named *Antalo limestones*). This unit includes the *Agula Shales* of the Mekele outlier and the evaporitic *Gohatsion Fm.* of the Blue Nile basin.
- *TJs*: Triassic to Jurassic sediments dominated by sandstones (often named *Adigrat sandstones*)
- *PZs*: Paleozoic sediments dominated by continental tillites, sandstones and shales.

Finally, the *B* unit represents the undifferentiated Precambrian basement, formed by various plutonic rocks, metasediments and metavolcanic rocks.

Often, thin (a few meters or less) Holocene sedimentary cover (aeolian or lacustrine) or, in the case of the Somalian plateau, eluvium cover is present on top of older units. As it only concerns a very thin layer, they are not mapped as distinct 'Holocene' units (*Hs*) but indicated with hatched symbols.

3.1.3. Structural mapping

In addition to the newly defined stratigraphic units, faults, basement lineaments, dykes, volcanoes/volcanic vents and calderas are mapped. Faults are classified into three categories reflecting the relative throw of the fault. The authors are aware that fault mapping mainly based on remote sensing has inherent limitations related to erosion, vegetation cover, lithology contrast, topography and fault orientation. The density of mapped faults is thus not necessarily reflecting the actual fault density, and the classification by throw is only relative at a local scale. Also, differentiation between faults and dykes based on DEM data is not always evident when vegetation covers the area. The basement lineaments represent any visual lineation identified in the basement that cannot be attributed to a fault. They were identified based on color/lithology contrasts and/or lineaments visible on the DEM.

3.2. Other maps

3.2.1. Geological map of the Southern Red Sea & Western Gulf of Aden Region

The *Geological map of the Southern Red Sea & Western Gulf of Aden region* (Fig. 6 and Rime et al., 2022b) was compiled to serve as a base for the kinematic reconstruction. The mapping was performed at an approximate scale of 1:3'000'000 and using a similar

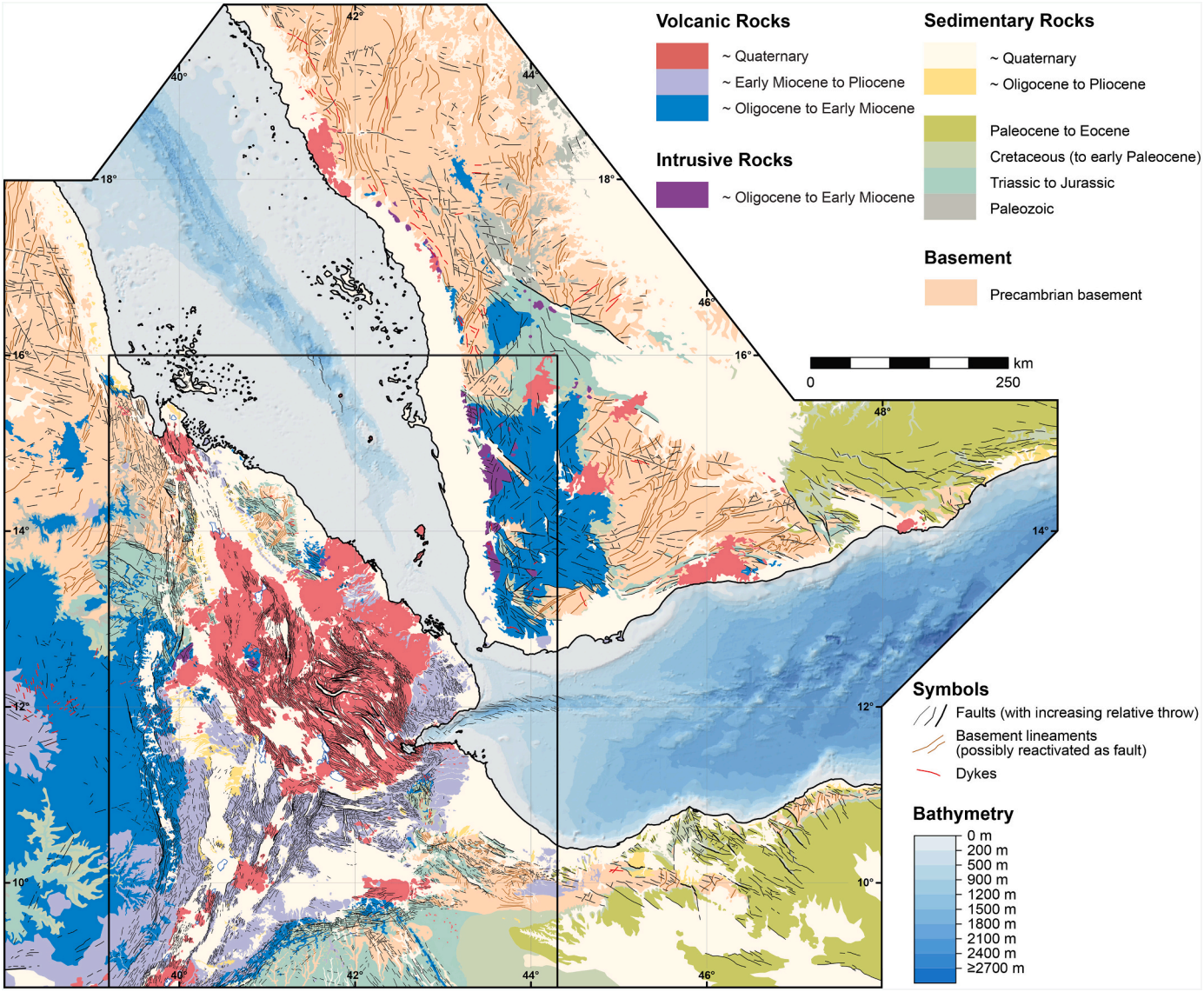

Fig. 6. Geological map of the Southern Red Sea & Western Gulf of Aden Region. The full-scale version of this map is available in Rime et al. (2022b). References are listed in Table 2.

chronostratigraphic-lithostratigraphic approach as described for the map of the Afar Depression. Due to the lower resolution of mapping, only the following stratigraphic units are mapped:

- *Qv*: Quaternary volcanic rocks. Includes *mRv, Q_3v, Q_2v* and *Q_1v* units of the geological map of the Afar Depression.
- *MPv*: Early Miocene to Pliocene volcanic rocks. Includes *M_2v* and *M_3v* units of the geological map of the Afar Depression.
- *OMv*: Oligocene to Early Miocene volcanic rocks. Includes *O_1v* and *O_2M_1v* units of the geological map of the Afar Depression.
- *OMi*: Oligocene to Early Miocene intrusive rocks. Similar to the *O_2M_1i* units of the geological map of the Afar Depression.
- *Qs*: Quaternary sediments. Includes *Hs* and *Pes* units of the geological map of the Afar Depression.
- *OPs*: Oligocene to Pliocene sediments. Includes *Pos, PoPes, lMPos* and *Ms* units of the geological map of the Afar Depression and some older sediments (up to Oligocene) on the coasts of the Gulf of Aden (e.g. Ali, 2015; Leroy et al., 2012; USGS and Arabian American Oil Company, 1963).
- *PEs*: Paleocene to Eocene sediments dominated by marine limestones and including the Auradu Fm. on the Somalian plateau and the Hadramawt Group on the Yemenite plateau (see Fig. 5).
- *TJs*: Triassic to Jurassic sediments, including the sandstone-dominated *TJs* and the limestone-dominated *Js* units of the geological map of the Afar Depression.
- *PZs*: Paleozoic sediments similar to the geological map of the Afar Depression.
- *B*: Undifferentiated Precambrian basement.

Sources and reference maps used are summarized in Table 2. Remote sensing data (Landsat imaging and SRTMGL1 DEM) were used to discriminate between the interpretations of different authors, to compensate lack of data and to improve the mapping of faults, dykes and basement lineaments. All data are available in Rime et al. (2022b).

3.2.2. *Geological map of the Afro-Arabian rift system and basement map of the Red Sea*

The geological map of the Afro-Arabian Rift System (Fig. 3) was mapped at an approximate scale of 1:17′000’000 and mainly summarizes the Cenozoic magmatic units. Sedimentary units are the same as

Table 2
References for the geological map of the southern Red Sea & western Gulf of Aden region.

Afar Depression	Geological map of the Afar Depression (Rime et al., 2022a, see Table 1 for references)
Ethiopia	Abebe et al. (2005), Chernet et al. (1998, 2020), Chorowicz et al. (1998), Coulié et al. (2003), Drury et al. (1994), Geological Survey of Ethiopia (1971, 1978a, b, 1996, 2009a, 2009b, 2010b, 2011), Hagos et al. (2017), Hofmann et al. (1997), Kieffer et al. (2004), Mège and Korme, 2004, Mohr and Zanettin (1988), Morton et al. (1979), Rooney (2017, 2020b), Sembroni et al. (2017), Teklay et al. (2005)
Somalia	Ali (2009, 2015), Ali et al. (2018), Billi (2022), Geological Survey Somali Democratic Republic (1970b, 1970c, 1970d, 1970e, 1971c), Geological Survey Somaliland Protectorate (1954, 1956, 1959a, 1959b, 1959c)
Yemen and southern Saudi Arabia	Baker et al. (1996), Brown et al. (1989), Capaldi et al. (1987a, 1987b), Davison et al. (1994, 1998), Fairer (1985), Garzanti et al. (2001), Grolier and Overstreet (1978), Kruck (1980, 1984), Kruck et al. (1984), Mallick et al. (1990), Prinz (1984), Stern and Johnson (2019), USGS (1963), van der Gun (1995), Windley et al. (1996)
Geographic features	Lakes, coastlines and borders from Openstreetmap (https://www.openstreetmap.org, 06.01.2020) and Natural Earth (naturalearthdata.com). Lakes and coastlines are manually modified. Data for insert globe from Natural Earth.

the *Geological map of the Southern Red Sea & Western Gulf of Aden region.* Volcanic and intrusive rocks are merged as "igneous rocks". Age divisions are identical except for adding a new unit showing the Eocene lavas in the southern part of the Main Ethiopian Rift. Sources and reference maps used are summarized in Table 3. Another version of this map focused on basement structures was produced (Suppl. Mat. 3).

Table 3
References for other maps.

Geological map of the Afro-Arabian Rift System (Fig. 3)	Abbate et al. (2015), Abebe et al. (2005), Aghanabati (1993), Ali and Lee (2019), Ali and Watts (2016), Altherr et al. (2019), Augustin et al. (2021), Barrier et al. (2004), Berhe et al. (1987), Bosworth and Stockli (2016), Brown et al. (1989), Camp et al. (1991, 1992), Camp and Roobol (1989), Chernet et al. (2020), Dawit (2016), Duncan and Al-Amri (2013), Egyptian Geological Survey (1981), Fantozzi and Ali Kassim (2002), Fournier et al. (2010), GEBCO Compilation Group (2020), Geological Survey of Ethiopia (1996), Kenea et al. (2001), Lucassen et al. (2008), Mège et al. (2016), Ministry of mines and energy (1985), Ministry of Petroleum and Mining (2004), Moufti et al. (2012), Mutebi et al. (2019), Pollastro et al. (1999), Pubelier (2008), Rime et al. (2022a, 2022b), Rooney (2017, 2020b), Scoon (2020), Sebai et al. (1991), Sneh et al. (1997a, 1997b, 1997c, 1997d), Stern and Johnson (2019), Survey of Kenya (1962), Thiélemont (2016), Trifonov et al. (2011), USGS (1963), van der Gun (1995), Vrbka et al. (2008), Zawacki et al. (2022) and Natural Earth.
Simplified basement map of the Red Sea and surrounding regions (Suppl. Mat. 3)	Geological map of the Afro-Arabian Rift System (references above), Brown et al. (1989), Flowerdew et al. (2013), Fritz et al. (2013), Johnson (2021), Johnson et al. (2011), Osman and Fowler (2021), Quick (1991), Rime et al. (2022b), Stern and Johnson (2019), Windley et al. (1996) and Esri orthophoto.

4. Geological history of the Afar Depression and Afro-Arabian Rift System

In order to achieve a comprehensive understanding of the Afar Depression, the tectonic, magmatic and sedimentological history of different regions are first reviewed and discussed individually in this section. A chronological chart (Fig. 7) summarizes these events. As the Afar Depression is part of and genetically linked with the whole Afro-Arabian Rift System, the latter is also included in this section. The division of the regions discussed in this section is indicated in Fig. 1b while local names are presented in Figs. 1a and 2. First, the pre-rift history is shortly discussed, followed by the detailed Cenozoic evolution of the Gulf of Aden, Red Sea, Ethiopian Plateau, Yemenite Plateau, Danakil Block, Ali Sabieh Block, NMER, south-western Afar, central-western Afar, central-eastern Afar and the Danakil Depression. A shorter, summarized, interpretative and chronological description of the tectonostratigraphic evolution of the Afar region is presented in section 6.2.

4.1. Pre-Rift history

The basement of the Afar region is part of the Arabian-Nubian Shield and formed during the Neoproterozoic as part of a supercontinent cycle including the breakup of Rodinia and the East African Orogen. The East African Orogen comprises the accretion of several island-arc terranes, the formation of sedimentary and volcano-sedimentary basins, as well as a complex history of intrusion, volcanism, metamorphism and faulting. By the end of the Ediacaran, the eroded and weathered Arabian-Nubian Shield formed a vast low-relief peneplain (Johnson, 2021; Johnson et al., 2011).

During Paleozoic and Mesozoic times, eastern Africa was influenced by two main tectonic phases (Frizon de Lamotte et al., 2015; Macgregor, 2018). The first phase (Karoo phase) lasted from Permian to Triassic times and mainly affected the southern part of eastern Africa, as well as the southern Ogaden basin (Hunegnaw et al., 1998; Shawel et al., 2022; Worku and Astin, 1992), characterized by mainly NE-SW oriented structures. The "late Karoo" phase of rifting during the Lower Jurassic led to the separation of Madagascar and India. The second phase of rifting happened in the Upper Jurassic and Lower Cretaceous, forming multiple NW-SE oriented basins, including the Mekele Basin (Beyth, 1972; Sembroni et al., 2017), the Blue Nile Basin (Chernet et al., 2020; Gani et al., 2009), the Somaliland basins (Ali and Lee, 2019; Ali and Watts, 2016) and the southern Yemenites basins (As-Saruri et al., 2010; Redfern and Jones, 1995). As these structures were also active during the Cenozoic, it is sometimes unclear when faulting occurred (Hagos et al., 2020; Macgregor, 2018).

In the Afar region, the first sediments were deposited during Paleozoic times. They consist of terrestrial sediments, often with glacial and peri-glacial affinities (e.g. Enticho Sandstone, Edaga Arbi Glacials, Fig. 5). The Triassic to Lower/Middle Jurassic is dominated by widespread terrigenous conditions with the deposition of the Adigrat sandstones. During the Middle and Upper Jurassic, a major marine transgression synchronous with the initiation of the second rifting phase led to the deposition of marine sediments in the Afar region (e.g. Antalo Limestone, Fig. 5, Abbate et al., 2015; Beyth, 1972, 1991; Bosellini et al., 2001; Chernet et al., 2020; Gasse et al., 1986; Guiraud et al., 2005; Sagri et al., 1998; Sembroni et al., 2017). During the Cretaceous, an large regression resulted again in terrestrial conditions around the Afar Depression while marine deposition continued in the southern Ogaden basin (Abbate et al., 2015; Ali, 2015; Beyth, 1991; Guiraud et al., 2005). One last marine flooding in the Ogaden and Yemen basin occurred from the Paleocene till the Eocene (Auradu Fm. and Hadramawt Group on Fig. 5, Abbate et al., 2015; Ali, 2015; As-Saruri et al., 2010; Guiraud et al., 2005).

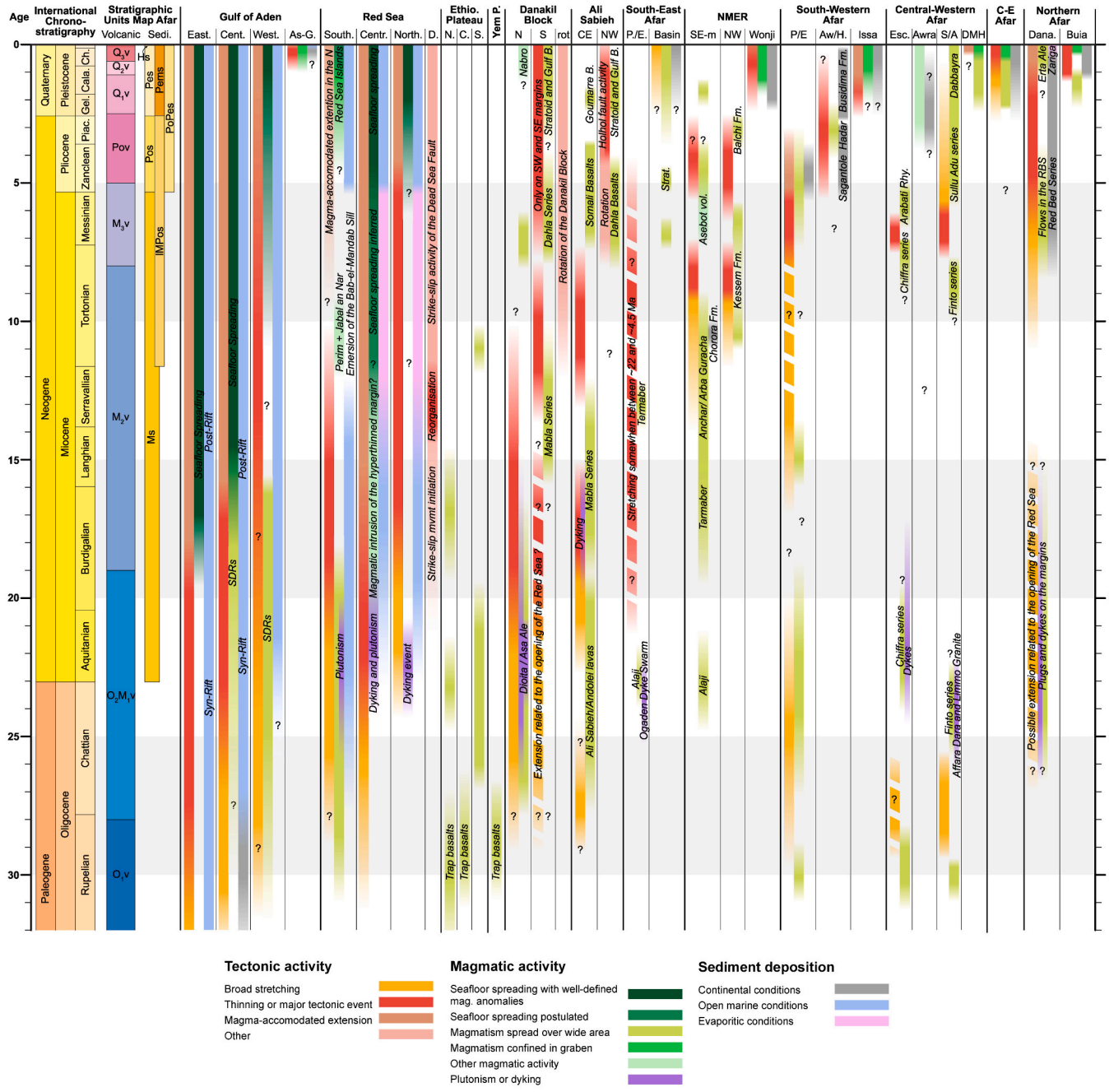

Fig. 7. Chronological event chart of the Afar and surrounding regions. This figure summarizes the geological evolution of different regions discussed in section 4. The abbreviated regions are, as defined in Figs. 1, 2 and section 4: the eastern (East.), central (Cent.), western (West.) Gulf of Aden and the Asal-Ghoubbet (As-G.) graben; the southern (South.), central (Centr.) and northern (North.) Red Sea, along with the Dead Sea fault (D); the northern (N.), central (C.) and southern (S.) Ethiopian Plateau; the Yemenite Plateau (Yem P.); the northern (N) and southern (S) Danakil Block, as well as its rotation (rot); the Ali Sabieh Block segmented in its central and eastern part (CE) and its north-western part (NW); the south-eastern Afar with its plateau/escarpment (P./E.) and its basin; the Northern Main Ethiopian Rift (NMER) with its south-eastern margin (SE-m), its north-western margin (NW) and the Wonji segments; the South-Western Afar with its plateau/escarpment (P/E), the Awash valley and the horst east of it (Aw/H.), and the Issa Graben; the central-western Afar with its escarpment (Esc.), the Awra plain, Sullu Adu + Affara Dara + Dabbayra + Limno (S/A) and the Dabbahu/ Manda Hararo rift segment (DMH); the central-eastern Afar (C-E Afar); the northern Afar with the Danakil Basin (Dana.) and the Buia Graben.

4.2. Gulf of Aden

The Gulf of Aden, situated east of the Afar Depression, is segmented into four zones (Figs. 1, 2). The Alula-Fartak Fault Zone separates the eastern and central Gulf of Aden, while the central and western Gulf of Aden are separated by the Shukra El Sheik Discontinuity. We included the Asal-Ghoubbet graben in the Gulf of Aden region as it constitutes its eastern tectonic prolongation. Note that more in-depth reviews of the geological history of the Gulf of Aden and the Red Sea are available (Bosworth et al., 2005; Leroy et al., 2012; Stockli and Bosworth, 2019).

Leroy et al. (2012) and references therein show that the first syn-rift sediments of the eastern Gulf of Aden in the region of Dhofar (Oman) and Socotra Island (Arabian Sea) are dated to late Priabonian/early Rupelian, and dominated by shallow marine facies. The first tectonic

activity is already recorded at the end of the mid-Eocene. Major faults are registered at the end of the Oligocene and a significant unconformity during the Burdigalian, interpreted to represent the onset of the break-up of the continental crust. Post-rift sedimentation has been recorded since Langhian times. These timings are consistent with the initiation of seafloor spreading before 17.5 Ma in the same area (Fournier et al., 2010; Ogg, 2020).

The age for the initiation of clastic syn-rift sedimentation at the Yemenite margin in the central Gulf of Aden is believed to have initiated during the lower Oligocene (Ali and Watts, 2016; Leroy et al., 2012; Nonn et al., 2019; Watchorn et al., 1998), coherent with ages of ~32 Ma for rift initiation on the Somalian margin (Ali and Watts, 2013; Fantozzi and Ali Kassim, 2002). The first marine sediments of the central Gulf of Aden are dated to ~29.5–27 Ma (Hughes et al., 1991; Speijer et al., 2020). On the Yemenite coasts, the facies changes from continental to marine in the Aquitanian/Burdigalian (Leroy et al., 2012). Syn- to post-rift transition probably happened between 21 and 17 Ma (Watchorn et al., 1998). The formation of SDR (Seaward Dipping Reflectors) is described between 21 Ma and 18 Ma, coinciding with significant thinning of the crust (Nonn et al., 2019). In the westernmost part of this zone, near the Shukra El Sheik Discontinuity, these SDRs are better developed over longer time periods (~30 to 16 Ma), probably due to the more significant influence of the Afar plume (Leroy et al., 2012; Tard et al., 1991). Seafloor spreading starts before 16.3 Ma (Fournier et al., 2010; Ogg, 2020).

West of the Shukra El Sheik Discontinuity, the nature of the crust changes (e.g. Hébert et al., 2001; Manighetti et al., 1997, see also Bouguer anomaly, Suppl. Mat. 4). The crust ranges from oceanic to the east to continental with an axial valley in the west (Hébert et al., 2001). Few data exist on the rift history before seafloor spreading. SDRs are mentioned between ~30 and 16 Ma offshore Aden (Leroy et al., 2012; Tard et al., 1991). In the Somalian Guban basins, Ali (2015) mentions extensive basaltic lavas of potential Miocene age. The marine connection between the Gulf of Aden and the Red Sea was established during the late Oligocene (Hughes et al., 1991). Seafloor spreading in the eastern part began between 9 and 6 Ma (Leroy et al., 2012) or 9 and 11.6 Ma (Fournier et al., 2010; Ogg, 2020). Further west, oceanic spreading is believed to have started around 3 Ma ago (Fournier et al., 2010; Leroy et al., 2012; Manighetti et al., 1997; Ogg, 2020). However, all authors do not accept the oceanic nature of the spreading in this westernmost part of the Gulf (Hébert et al., 2001). In the Gulf of Tadjoura, Daoud et al. (2011) report the initiation of faulting to be around 1.7 Ma, coherent with the interpretation of Manighetti et al. (1997).

Manighetti et al. (2001, 1998) mention the onset of diffuse rifting of the Asal-Ghoubbet rift at ~0.9 Ma with the establishment of a fully developed graben by ~0.3 Ma. This rift segment possibly propagated towards Manda Inakir around 0.2 Ma ago. Extension in Asal-Ghoubbet is now partially accommodated by magmatic intrusions (Cattin et al., 2005).

Marine flooding of the Ghoubbet basin occurred around 9 ka ago, but it is plausible that it was also connected to the Gulf of Aden during previous interglacial(s) (Audin et al., 2001). Lake Assal is now evaporitic but was lacustrine until 5–6 kyr ago (Gasse and Fontes, 1989).

4.3. Red Sea

4.3.1. Tectonic and magmatic history

There is a long-standing debate about the nature of the crust in the Red Sea and the position of the Ocean-Continent Transition (Almalki et al., 2014, 2015; Augustin et al., 2014, 2016, 2021; Bohannon, 1986; Bonatti, 1985; Bonatti et al., 2015; Bonatti and Seyler, 1987; Cochran, 1983; Egloff et al., 1991; Girdler, 1985; Girdler and Southren, 1987; Girdler and Styles, 1974; Girdler and Underwood, 1985; Hall, 1989; Issachar et al., 2022; Izzeldin, 1987; Le Magoarou et al., 2021; Ligi et al., 2018; Makris et al., 1991; Mitchell and Park, 2014; Okwokwo et al., 2022; Rihm and Henke, 1998; Schettino et al., 2016; Shi et al., 2018; Stockli and Bosworth, 2019; Sultan, 1992; Sultan et al., 1993). While all studies agree on the oceanic nature of the central trough in the central and southern Red Sea, the nature of the crust in the northern Red Sea and the one underlaying the platforms in central and southern Red Sea is under debate. Most models acknowledge the presence of a thin crust (~20–8 km, Almalki et al., 2014; Egloff et al., 1991; Mooney et al., 1985) in these areas, thicker however than normal oceanic crust. The presence of significant magmatic material is testified by magnetic, gravimetry, as well as seismic refraction and reflection surveys in the central and southern Red Sea (Almalki et al., 2014; Bohannon and Eittreim, 1991; Hall, 1989; Izzeldin, 1987; Mitchell and Park, 2014; Mooney et al., 1985). It is, however, debated whether these geophysical data indicate heavily intruded continental crust or oceanic crust (e.g. Hall, 1989; Izzeldin, 1987). Overall, the distinction between heavily intruded continental crust and thickened oceanic crust is subtle and has only small implications for tectonic reconstructions. Both imply that significant crustal material was accreted during the rifting process.

On the southern margin of the Red Sea (south of approx. 15.5°N), significant volcanism was recorded between 31 and 18 Ma (Davison et al., 1994; Huchon et al., 1991), together with the emplacement of plutons between 20 and 26 Ma (Capaldi et al., 1987b). Renewed phases of post-tectonic volcanic activity occurred at ~10 Ma at the foot of the escarpment (Jabal an Nar) and on Perim Island (Capaldi et al., 1987a; Huchon et al., 1991; Mallick et al., 1990). Huchon et al. (1991) indicate extension starting at least 25 Ma ago and ending before 10 Ma, with a major pulse of tectonism between 18 and 10 Ma. In the same area, Menzies et al. (1992) show cooling ages of 16 Ma, and Davison et al. (1994) indicate exhumation since 20 ± 5 Ma.

On the Bab-el-Mandeb platform, Mitchell et al. (1992) mention flat beds with only minor subsidence and tectonic influence in the Plio-Pleistocene sequence. These observations, along with the Late Pleistocene tectonic quiescence (Al-Mikhlafi et al., 2018; Faure et al., 1980) and the absence of volcanic material younger than the Mid-Miocene (Capaldi et al., 1987a; Mallick et al., 1990) indicate that tectonic activity in the area ceased after the Mid- to Late-Miocene. North of Bab-el-Mandeb, seismic and recent volcanic activity is recorded, forming the Hanish, Zubair and Jebel at Tair islands (Ruch et al., 2021; Xu et al., 2015).

Further north, on the SW Saudi Arabian margin (central Red Sea on Fig. 7), Bohannon (1986), Bohannon et al. (1989) and Bohannon and Eittreim (1991) show faulting activity between 29 and 23 Ma and an intense period of extension around 25 Ma, just before significant diking between 24 and 21 Ma and the emplacement of plutons between 21 and 22 Ma (Sebai et al., 1991). Magmatic extension probably dominated afterwards, while the uplift of the margins began at ~20 Ma and accelerated since 13.8 Ma (Bohannon et al., 1989). On the Eritrean coast, Abbate et al. (2002), Balestrieri et al. (2005) and Ghebreab et al. (2002) similarly report denudation between 23 and 15 Ma. Omar and Steckler (1995) interpret a further uplift phase around 34 Ma in SW Saudi Arabia.

In the northern Red Sea, rifting style and chronology differ. While Augustin et al. (2021), Makris and Rihm (1991) and Rihm and Henke (1998) consider seafloor spreading along the whole Red Sea, many authors consider that the northern Red Sea has not yet attained this state or only partially, as testified by geophysical studies and the presence of Precambrian basement and granitic rocks on Zabargad Island and in offshore wells (Ali et al., 2022; Almalki et al., 2014, 2016; Bonatti et al., 1981; Bonatti and Seyler, 1987; Bosworth et al., 1993, 2005; Cochran, 2005; El Khrepy et al., 2021; Le Magoarou et al., 2021; Mitchell and Park, 2014; Saada et al., 2021; Stockli and Bosworth, 2019). This part of the Red Sea probably represents intruded and hyperextended continental crust with a thickness reduced to <14 km (Ali et al., 2022; Le Magoarou et al., 2021).

At the NW Saudi Arabian margin, no significant extension or tilting occurred before 23 Ma. 23 Ma also corresponds to a significant dyking event (Bosworth and Stockli, 2016; Stockli and Bosworth, 2019) and the

first syn-rift sediments in Egypt (Bosworth et al., 2005). In Saudi Arabia, thermochronometry showed the initiation of extension at ~23 Ma with a second rift pulse at ~15 Ma (Stockli and Bosworth, 2019; Szymanski et al., 2016). Stockli and Bosworth (2019) provide a comprehensive review of timing.

The oldest measurable anomalies, identified in the central Red Sea (between roughly 16° N and 19° N), are C3n.2n (4.6–4.8 Ma) according to Schettino et al. (2016) and 3A (6.3–7.2 Ma) according to Izzeldin (1987) (age updated after Ogg, 2020). Other authors estimate the initiation of seafloor spreading around 10 Ma (Okwokwo et al., 2022), between 10 and 12 Ma (Izzeldin, 1987; Rihm and Henke, 1998), at ~13 Ma (Augustin et al., 2021; Le Pichon and Gaulier, 1988) and ~ 14 Ma (Makris and Rihm, 1991). Augustin et al. (2016) suggest younging of the initiation of seafloor spreading northward, from 12 Ma at 20°N to 8–9 Ma at 23°N.

Mid-Miocene ages are also coherent with the ~14–12 Ma major structural event recorded in the southern Gulf of Suez and Midyan (Bosworth et al., 2005), interpreted to represent the abandonment of the Gulf of Suez rift with the strain being accommodated by the Dead Sea Fault system (or Aqaba-Levant fault). This reorganisation is thought to be caused by the very thick and strong lithosphere of the Eastern Mediterranean hindering the northward propagation of the Gulf of Suez, while the Levant area provided a weaker lithosphere (El-Sharkawy et al., 2021; Steckler and ten Brink, 1986). Based on data from the Gulf of Suez, Bosworth et al. (1998, 2005) estimate that this ~14 Ma reorganisation caused a change in extension direction from rift normal to rift oblique (parallel to the Dead Sea Fault). It also corresponds to a significant increase in the Arabia – Nubia relative motion around 11–13 Ma ago (ArRajehi et al., 2010; McQuarrie et al., 2003; Reilinger et al., 2015) and to the closure of the Neotethys ocean (McQuarrie et al., 2003). Motion along the Dead Sea fault is thought to have initiated before this ~14 Ma reorganisation, around 20 Ma ago (Craddock et al., 2021; Garfunkel, 2014; Morag et al., 2019; Nuriel et al., 2017). The sinistral transform movement of the fault accommodates 100–110 km of displacement (Quennell, 1958; see also Garfunkel, 2014 and references therein).

4.3.2. Sedimentary environments

According to Crossley et al. (1992), Hughes et al. (1991) and Hughes and Beydoun (1992), the marine connection between the Gulf of Aden and the Red Sea was established during the late Oligocene (NP25, i.e. ~27 to 23 Ma, Speijer et al., 2020), when adverse marine conditions are observed offshore Eritrea (Thio-1 well), but no indication of syn-rift sediments are reported further north or offshore Yemen. The configuration of this potential connection between the Gulf of Aden and the Red Sea is puzzling as it is not recorded in the sediments of the Tihama Plain (Hakimi et al., 2021, 2022) and some authors (Smith and Santamarina, 2022) suggest that this initial flooding occurred from the north. In the Gulf of Suez and the northern Red Sea, the first syn-rift sediments are reported during the late Oligocene - Early Miocene (Bosworth et al., 2005; Evans, 1988; Hughes et al., 1999; Montenat et al., 1998; Plaziat et al., 1998), with Early Miocene marine waters probably coming from the Mediterranean Sea (Hughes et al., 1991; Mandur, 2009; Mitchell et al., 1992; Orszag-Sperber et al., 1998). During the Early Miocene, open-marine conditions were reached offshore Eritrea and marine, but adverse conditions, possibly due to high clastic inputs, are reported offshore Sudan and Egypt (Hughes and Beydoun, 1992). During the Early or Mid-Miocene, the appearance of marine conditions is also reported below the Tihama Plain in Yemen (As-Saruri et al., 2010; Hakimi et al., 2016, 2021). Near Massawa (Eritrea), the Early Miocene lower Dogali Fm. show continental deposits (Drury et al., 1994; Sagri et al., 1998). The overlying Mid to Late Miocene upper Dogali Fm. is characterized by coastal conditions (Sagri et al., 1998).

During Langhian to Serravallian, the basin became underfilled and evaporitic conditions prevailed throughout the Red Sea, while deep marine conditions were maintained in the Gulf of Aden, clearly indicating a decoupling of both basins (Hughes and Beydoun, 1992; Mitchell et al., 1992, 2021; Orszag-Sperber et al., 1998; Plaziat et al., 1998; Savoyat et al., 1989; Smith and Santamarina, 2022). On the Bab-el-Mandeb platform, Mitchell et al. (1992) mention the absence of salt, possibly indicating emersion of the sill.

Following this evaporitic crisis, the re-establishment of open-marine conditions occurred in the Pliocene, establishing shallow to moderately-deep (except for the central trough) marine conditions in the Red Sea (As-Saruri et al., 2010; Crossley et al., 1992; Hakimi et al., 2016, 2021; Hughes and Beydoun, 1992; Mitchell et al., 1992; Savoyat et al., 1989; Stoffers and Ross, 1974).

4.4. The Ethiopian Plateau

The Ethiopian plateau represents the western margin of the Afar Depression (Fig. 1b). In the north, it merges with the Red Sea's western margin. The northern part of the Ethiopian plateau (N of approx. 13°N) is characterized by the sparse Cenozoic volcanic cover. In Eritrea, the main volcanic event is coeval with the emplacement of the Trap Series reported for the whole region and having early Oligocene ages (32.9–28.0; Drury et al., 1994; Zanettin et al., 2006). The second phase of volcanism is reported in the late Oligocene/Early Miocene (datings between 24.6 and 22.1 Ma; Zanettin et al., 2006). In Ethiopia, datings in the Adigrat region (Hofmann et al., 1997) and in the Mekele area similarly indicate the main phase of volcanic activity during the early Oligocene, possibly extending from 33 to 26 Ma (Justin-Visentin, 1974; Sembroni et al., 2017). A Miocene phase of volcanism (19–15 Ma) formed the Adwa Phonolite and trachyte, as well as volcanic rocks found along the coast (Drury et al., 1994; Hagos et al., 2017; Natali et al., 2013), being synchronous with a late pulse of activity of the Simien Shield volcano (Kieffer et al., 2004). Hagos et al. (2020) report some fault reactivation in the Mekele basin after the emplacement of the flood basalts.

In the central part of the Ethiopian plateau (approx. between 11 and 13°N), datings are scarce but Ayalew et al. (2021), Eid et al. (2021), Hofmann et al. (1997), Kieffer et al. (2004) and Ukstins et al. (2002) indicate ages ranging from 31.2 to 26.7 Ma. In contrast to the northern highlands, these Oligocene lavas almost entirely cover pre-Cenozoic rocks.

The southern part of the Ethiopian plateau (approximately between 11 and 9°N) similarly shows a wide magmatic cover of the pre-Cenozoic rocks, but their ages are younger than in the north. South of approx. 11° N, no early Oligocene lava is present (Chernet et al., 1998; Coulié et al., 2003; Feyissa et al., 2017; Kieffer et al., 2004; Morton et al., 1979; Ukstins et al., 2002; Wolfenden et al., 2004, 2005), the oldest being 26.7 ± 1 Ma (Feyissa et al., 2017). Coulié et al. (2003) even measured a 20.7 ± 0.3 Ma flow directly overlying the Mesozoic sandstones. The bulk of the datings indicate ages between 26.7 and 19.7 Ma, and the uppermost plateau lavas are as young as 12–10 Ma (Chernet et al., 1998; Ukstins et al., 2002; Wolfenden et al., 2004).

4.5. The Yemenite plateau

The Yemenite plateau forms the eastern margin of the southern Red Sea and the northern margin of the Gulf of Aden (Fig. 1b). Dating of lavas on this plateau indicate that the eruption of the traps was a very brief event lasting from ~30.9 to ~26.5 Ma, (Baker et al., 1996; Riisager et al., 2005; Thines et al., 2021; Ukstins Peate et al., 2005; Zumbo et al., 1995a). Recent publications indicate that the volcanic phase was even shorter, ending around 27.7 Ma. This contrasts with the Ethiopian plateau, where volcanism continued during the late Oligocene and the Miocene.

4.6. Danakil Block

The Danakil Block refers to the broad area of relatively more elevated topography and Bouguer gravity anomaly situated between the Gulf of

Zula and the Gulf of Tadjoura (Fig. 1, Suppl. Mat. 4). The geological history of the Danakil Block is poorly constrained due to the lack of detailed field studies since the 70s. We segment the Danakil Block into two parts: the northern part (approx. North of 13.2°N) exposes mainly Precambrian basement, Mesozoic sediments and the massive Nabro volcanic range. The southern part is almost entirely covered by Neogene and Quaternary volcanics. This limit also marks a possible tectonic block boundary (Viltres et al., 2020; section 5.1.1).

On the northern Danakil Block, Frazier (1970) reports two datings on volcanic rocks in the Howlakil Bay and N of the Amphila Bay at 15 and 23 Ma, respectively. Similarly, Brinckmann and Kürsten (1971) report the presence of isolated igneous rocks of ages ranging from ~25 to ~16 Ma in the Danakil Alps. In the southern Danakil Alps, the Dioita Massif is covered by 27 to 23 Ma lavas (Brinckmann and Kürsten, 1971; Civetta et al., 1975a). Two ~21–23 Ma old granitic plutons are described: the Dioita granite and the Asa Ale granite (Barberi et al., 1975; Brinckmann and Kürsten, 1971; Civetta et al., 1975a). They are overlain by ~19 Ma old rhyolites and a few Recent lava flows (Civetta et al., 1975a; De Fino et al., 1978).

The relative chronology of the Nabro volcanic range is well-defined (Wiart and Oppenheimer, 2005; Wiart et al., 2000) with the latest eruption in 2011 (e.g. Goitom et al., 2015), but the oldest lavas have not been dated. A maximal Pleistocene age is generally agreed upon (Varet et al., 1975; Wiart and Oppenheimer, 2005). The lavas situated SE of the Nabro range have ages between 8 and 6 Ma (Brinckmann and Kürsten, 1971; Civetta et al., 1975b).

On the southern Danakil Block, the age of the lavas covering most of the Danakil Block between 12.4°N and 13.2°N is poorly constrained. Datings from Barberi et al. (1975), Civetta et al. (1975b) and Zumbo et al. (1995b) indicate Mid-Late Miocene to Recent ages. The youngest lavas are found in the Assab and Gufa volcanic ranges (Civetta et al., 1975b; De Fino et al., 1973). The oldest rocks exposed on the Djiboutian part of the Danakil Block are the Mabla Rhyolites (and associated basalts, sometimes called Andolei basalts). Zumbo et al. (1995b) dated this formation between 15.4 and 11.8 Ma. Older K/Ar datings of Barberi et al. (1975) indicated a minimum age of 9.5 Ma. Extrapolation of the same units found on the Ali Sabieh Block suggests that volcanic activity began significantly earlier (Oligocene), but the absence of older outcrops on the Danakil Block does not allow to confirm this hypothesis. The overlying Dalha basalts in this part of Djibouti yield ages of 6.5 and 6.7 Ma (Barberi et al., 1975; Zumbo et al., 1995b). Comparison with the same unit in Ali Sabieh indicates that this unit might expand from 8.6 to 3.8 Ma (Audin et al., 2001; Barberi et al., 1975; Chessex et al., 1975; Daoud et al., 2011; Zumbo et al., 1995b). These units are overlain in the NW by the Quaternary stratoid basalts (Zumbo et al., 1995b) and near the shore in the SSE by Gulf Basalts with ages ranging from 3.5 to 1 Ma (Barberi et al., 1975; Daoud et al., 2011).

No complete interpretation of the tectonic history of the Danakil Block is available in the literature, but a chronology can nevertheless be proposed. The similarities of the volcanic and plutonic events of the northern Danakil Block and the Yemen coast (Fig. 7) suggest a similar tectonic history related to the opening of this part of the Red Sea, i.e. starting before 25 Ma and ending before 10 Ma (see section 4.3.1). The observation that the ~19 Ma rocks of the Dioita Massif are heavily faulted, while the ~7 Ma rocks situated south of the Nabro range are not affected by tectonism (Barberi et al., 1975) strengthens the hypothesis of a cessation of tectonic activity in the Mid-Miocene. Also, C.N.R - C.N.R.S. Afar Team (1973) mention that Jurassic sediments are tilted in another direction compared to the Red Bed Series, implying deformation before deposition of the latter (~8.5 Ma, see section 4.13.2). The northern Danakil Block experienced a second phase of deformation on its westernmost margin linked to the opening of the Danakil Depression. This phase is discussed in section 4.13.2.

The detailed tectonic history of the southern Danakil Block is unknown before the Mid-Miocene, but Makris et al. (1975), Makris and Ginzburg (1987) and Redfield et al. (2003) showed that the crust of the Danakil Block is thinner than the plateaus and thus experienced significant extension. It is reasonable to assume that the early tectonic history of the southern Danakil Block is similar to the one of the northern part of the Danakil Block, Yemen and Ali Sabieh Block, i.e. extension related to the opening of the Red Sea from late Oligocene to Mid Miocene. Surface geology shows that along the Red Sea coast, the Mabla Series is heavily faulted and tilted with an orientation parallel to the Red Sea trend (NNW-SSE) (Barberi et al., 1975). The Dahla/Dalha basalts lie unconformably on them and are only slightly tilted and faulted (Barberi et al., 1975; Chauvet et al., 2023), a further indication of the cessation of tectonism in the Bab-el-Mandeb area during the Late Miocene (see also section 4.3.1). In contrast, on the SW margin of the block (Makarassou region), thickness changes indicate continuous tectonic activity during the eruption of the Dahla basalts (Chauvet et al., 2023; Geoffroy et al., 2014; Le Gall et al., 2011). The overlying Plio-Quaternary lavas similarly show very little faulting except in Moussa Ali, Makarassou fault system and on the coasts of the Gulf of Tadjoura. The faults in the latter zone are parallel to the ones found on the floor of the Gulf of Tadjoura (Dauteuil et al., 2001), and we interpret it as being caused by the Quaternary opening of the Gulf (Daoud et al., 2011; Manighetti et al., 1997; see also section 4.2).

Paleomagnetic data of Manighetti et al. (2001) show that the Danakil Block rotated 10.7° since ~8 Ma. Assuming a constant rotation rate and a total rotation of 30°, they estimated the initiation of rotation around 20 Ma ago, but several other authors agree on a significantly younger age, i.e. at least at ~11 Ma (Eagles et al., 2002), 9.3 ± 4 Ma (McClusky et al., 2010) and 11 ± 2 Ma (Reilinger and McClusky, 2011).

4.7. Ali Sabieh Block

The Ali Sabieh Block (or Aisha Block) is an elevated area situated at the border between Ethiopia, Djibouti and Somalia (Fig. 1), covered by Mesozoic sediments attesting the continental nature of the block (e.g. Chessex et al., 1975; Geological Survey of Ethiopia, 2015; Le Gall et al., 2015). It was intruded and covered by trap basalts (19–28 Ma, alternatively named Ali Sabieh basalts, Adolei/Andolei basalt or Galile Fm., Audin et al., 2004; Barberi et al., 1975; Black et al., 1975; Chessex et al., 1975; Le Gall et al., 2010, 2015; Zumbo et al., 1995b). The overlying Mabla series have ages ranging between 19 and 13 Ma (Barberi et al., 1975; Black et al., 1975; Chessex et al., 1975; Zumbo et al., 1995b) of which many dykes intrude the Ali Sabieh basalts (Chessex et al., 1975; Zumbo et al., 1995b). The Dahla series lies unconformably on the Mabla Series and mainly yields ages between 8 and 4.5 Ma (Audin et al., 2004; Barberi et al., 1975; Black et al., 1975; Chessex et al., 1975) while some authors consider rocks as recent as 3.5 Ma being part of this unit (Le Gall et al., 2015; Zumbo et al., 1995b). The rocks dated between 3.5 and 4.5 Ma were all sampled on the eastern side of the Block and classified by other authors as part of the Somali Basalts. This latter unit was dated between 7.2 and 3.6 Ma (Daoud et al., 2011) and is sometimes topped by the Pleistocene Goumarre Basalts (~2.5–1.7 Ma; Daoud et al., 2011). Near the Gulf of Tadjoura, Stratoid and Gulf basalts with ages ranging from ~2.8 to 0.8 Ma (Audin et al., 2004; Courtillot et al., 1984; Daoud et al., 2011) represent the last volcanic events of the Ali Sabieh Block. On the SW side of the Block, the Dahla Series is covered by Stratoid lava of unknown age but probably being Pliocene based on the extrapolation of this unit in south-eastern Afar (see section 4.8).

South of the Ali Sabieh Block sensu stricto, the geological history of the region South of Aisha and E of Adigala is similar to the one of the Block itself (Audin et al., 2004; Black et al., 1975; Geological Survey of Ethiopia, 2015).

Towards the coast of the Gulf of Tadjoura, the Ali Sabieh Block is covered by the previously described Dahla unit and by Quaternary Stratoid and Gulf basalts with ages ranging from 2.5 to 0.8 Ma (Audin et al., 2004; Barberi et al., 1975; Courtillot et al., 1984; Daoud et al., 2011).

From a tectonic point of view, Chessex et al. (1975) mention a first

faulting event before the deposition of the Ali Sabieh lavas. The second stage of deformation occurs after the emplacement of the Ali Sabieh lavas, between 16 and 22 Ma, according to Chessex et al. (1975), or between 15 and 20 Ma, according to Black et al. (1975). The next faulting event is reported between the emplacement of the Mabla and Dahla Series. After the emplacement of the Dahla Series, renewed faulting activity is described (Arthaud et al., 1980; Chessex et al., 1975; Daoud et al., 2011; Muller and Boucarut, 1975), followed by the faulting of the Stratoid and Gulf basalts in the Quaternary. This faulting is related to the opening of the Gulf of Tadjoura and the Asal – Ghoubbet graben, where most of the present-day tectonic activity is concentrated (Audin et al., 2004; Daoud et al., 2011; Manighetti et al., 1997).

Paleomagnetic studies (Kidane, 2016) showed a 30° clockwise rotation of the Ali Sabieh Block somewhen between 60 and 8 Ma. Audin et al. (2004) show a clockwise rotation of the NW margin of the Ali Sabieh Block between 8 and 4 Ma and propose that the movement between the Ali Sabieh and Danakil Block was accommodated by the strike-slip activity of the NE-SW Holhol fault between ~4 and 1 Ma before the strain was transferred in the present-day Gulf of Tadjoura.

On the eastern side of the Block, the absence of faulting indicates tectonic stability, at least since Late Miocene times (Audin et al., 2004; Barberi et al., 1975).

4.8. South-eastern Afar

The south-eastern Afar is situated between the Goba'Ad graben, the Issa graben and the Somalian Plateau (Fig. 1). The Somalian Plateau differs from the Ethiopian Plateau with a smaller volcanic coverage, almost exclusively confined to the escarpment. The first activity recorded in south-eastern Afar is the formation of the Ogaden Dyke Swarm at 22–25 Ma in the Marda Fault Zone, postulated to be a Precambrian reactivated structure (Black et al., 1974; Mège et al., 2016; Purcell, 1976). More than 200 km further south in Ogaden, the continuation of the same dyke swarm indicates older ages, reaching 30 Ma (Mège et al., 2016). Between 24 and 22 Ma, the Alaji basalts erupted at the present-day escarpment and on the nearby plateau (Chernet et al., 1998; Kunz et al., 1975). Mid-Miocene lavas (~13 Ma, Berhe, 1986) are also present on the plateau.

At the foot of the escarpment, lava flows of Late Miocene ages (6.8–7.4 Ma) have been reported (Berhe, 1986). They are topped by slightly younger Stratoid basalts with ages ranging from 4.5 to 5.1 Ma (Berhe, 1986; Chernet et al., 1998; WoldeGabriel et al., 1992a).

It is unclear when stretching of the escarpment took place (e.g. Black et al., 1975), mainly because it does not expose much syn-rift volcanism. The late Oligocene/Early Miocene traps lie conformably above the Mesozoic sediments (Geological Survey of Ethiopia, 2010a; Juch, 1975). Late Miocene lavas are not outcropping enough to be conclusive, but Pliocene lavas have only undergone limited faulting, mainly towards the N and the Buren plain or towards the W and the NMER, which we interpret as evidence for post-tectonic magmatism, consistently with the results of Tortelli et al. (2022) who show that these lavas were probably emplaced on an already thinned lithosphere. The main stretching phase could thus have happened anytime between ~22 and ~ 4.5 Ma.

The Dembel Volcanic Range in the easternmost part of the region has experienced volcanic activity since 3.35 Ma ago, which continued until Recent times, along with some faulting activity (Audin et al., 2004; Black et al., 1975). However, data from Doubre et al. (2017), Moore et al. (2021) and Sangha et al. (2022) show that this region currently hardly accommodates any extension. The Buren Plain is mainly covered by Holocene/Recent sediments, suggesting active subsidence.

The history of the horst between the Buren Plain and the Goba'Ad graben has never been investigated in detail. The oldest rocks are dated at 6.3 Ma (Black et al., 1975,) or 4.3 Ma (Barberi et al., 1975). The youngest is 2.4 Ma (Barberi et al., 1975), but Geological Survey of Ethiopia (2015), Varet et al. (1975) and our mapping results indicate the presence of younger, undated lavas, hypothetically assigned to Early/Middle Pleistocene. The orientation of feeder dykes (coinciding with magnetic lineations (Purcell, 2018) in the area indicates a SSW-NNE extension during the Pliocene (Christiansen et al., 1975). This would fit the hypothesis of Audin et al. (2004), Hammond et al. (2011) and Wolfenden et al. (2004) that this area was an active rift segment during the Mio-Pliocene.

4.9. NMER

The Northern Main Ethiopian Rift (NMER) forms a rift valley between the Somalian and Ethiopian Plateaus, south of approximately 10°N (Fig. 1). On the eastern side of the NMER, the geological history of the plateau corresponds to the geological evolution of South-Eastern Afar with Trap basalts between 24 and 22 Ma (Alaji Group). Few datings are reported between 20 and 16 Ma on the present-day escarpment, but datings cluster mainly around 13 Ma (on the plateau and the escarpment) and between 9 and 11 Ma (at the base of the escarpment), indicating renewed magmatic activity in the Mid to Late Miocene (Berhe, 1986; Chernet et al., 1998; Kunz et al., 1975; Morbidelli et al., 1975) (Tarmaber Fm, Anchar Basalts and Arba Guracha Silicics acc. to Chernet et al., 1998; Geological Survey of Ethiopia, 1985). Intercalated between this volcanic material, the diatomite-dominated Chorora Fm indicates the presence of a lacustrine basin at ca. 10 Ma. This basin was localized between the future Afdem, Asebot and Gara Gumbi volcanoes and the foot of the escarpment (Geraads et al., 2002; Sickenberg and Schönfeld, 1975; Tiercelin et al., 1979). This timing corresponds to the initiation of subsidence according to Chernet et al. (1998). NE of Mieso, Juch (1975) reports the first angular unconformity in the Arba Guracha Silicics, which are slightly older (~10–14 Ma; Chernet et al., 1998). Berhe (1986) also reports the first rifting at 14 Ma with the formation of this unit. SE of Mieso, this unit is conformable (Juch, 1975).

The large volcanic edifices of Asebot and Gara Gumbi have been dated between 5 and 6.85 Ma, and the Afdem volcano is assumed to have a similar age (Chernet et al., 1998; Feyissa et al., 2017; Geological Survey of Ethiopia, 1985; Kunz et al., 1975; WoldeGabriel et al., 1992a). They show little faulting except on their W side towards the NMER and were thus probably emplaced after the first stretching phase. Juch (1975) reports unconformities in the lowermost part of this Late Miocene unit which we interpret as a second phase of stretching restricted to the rift floor. At the NW foot of the volcanoes, the rift is floored by Mio-Pliocene volcanic products and sediments (~5.6 Ma to ~3.8 Ma) covered near Awash by mostly undeformed Early Pleistocene lavas (Chernet et al., 1998; Hujer et al., 2015; Kidane et al., 2010; WoldeGabriel, 1987). This second tectonic event therefore probably lasted from the Late Miocene to the Pliocene.

On the NW margin of the NMER, Wolfenden et al. (2004) similarly note the first unconformity at ~10.6 Ma, linked with significant magmatic production until ~6.6 Ma (Kessem Fm.) (Chernet et al., 1998; Ukstins et al., 2002; Wolfenden et al., 2004) and a regional southeastward basinal tilt (Wolfenden et al., 2004). Deformation before 11 Ma cannot be excluded but must have been minor. Slightly further N along the Ankober fault, Wolfenden et al. (2005) note the first tectonic activity in the ~11 Ma Aliyu Amba Fm. A significant hiatus with a major unconformity is recorded between ~6.6 and ~ 3.5 Ma and is interpreted to be diachronous with strain migrating towards the centre of the rift. Pliocene (~3.6–2.5 Ma, Ukstins et al., 2002; Wolfenden et al., 2004) magmatic products are found in the lower part of the escarpment (Balchi Fm.).

The *Wonji segments* or the *Wonji fault belt* are narrow belts of intense recent faulting in the MER (Mohr, 1967). In the study area, they include the Kone, Fentale, Dofen and Hertali volcanoes. Their age range from ~1.8 Ma to very Recent (Chernet et al., 1998; Feyissa et al., 2017; Kazmin et al., 1980; Morton et al., 1979; Siegburg et al., 2018; Vogel et al., 2006; Williams et al., 2004), Deformation was focused in the Wonji belt since ~2 Ma (Corti, 2009; Wolfenden et al., 2004). Deformation is accommodated by both brittle and magmatic processes (Kurz

et al., 2007). One Lower Pleistocene fluvial and lacustrine clastic unit is reported near the Dofen volcanic centre by WoldeGabriel et al. (1992b). Sedimentation was probably nearly continuous since then.

4.10. South-western Afar

The south-western Afar comprise the area between the Issa Graben and the Ethiopian Plateau (Fig. 1). The geological history of the south-western Afar margin has been well studied, particularly by Wolfenden et al. (2005). Early Oligocene flood basalts are reported in the northern part of the region (Coulié et al., 2003; Rooney et al., 2013; Ukstins et al., 2002), but, as discussed in section 4.4, the traps outcropping in the southern part are younger.

The first stage of deformation initiated between 29 and 26 Ma along border faults and lasted until ~20 Ma (Wolfenden et al., 2005). Deformation was accompanied by significant acidic volcanism (Feyissa et al., 2017; Rooney et al., 2013; Ukstins et al., 2002; Wolfenden et al., 2005). In the southern part of the region (9.95°N, transect E-E' of Wolfenden et al., 2005), the first tectonic event is recorded along the Ataye border fault before the deposition of the ~25 Ma old Brikitu Fm. This strongly contrasts with the initiation of tectonic activity ~12 Ma ago in the NMER, only 40 km south (see Wolfenden et al., 2005 and section 4.9).

At ca. 16 Ma, the locus of extension shifted towards the east (Wolfenden et al., 2005), associated with basaltic and intermediate volcanism (~16–14 Ma; Ukstins et al., 2002; Wolfenden et al., 2005).

Around 7 Ma, the strain again migrated eastward towards the foot of the escarpment, corresponding to the 3rd stage of deformation (Wolfenden et al., 2005) and accompanied by volcanic products restricted to the foot of the escarpment (~7–3 Ma; Barberi et al., 1975; Coulié, 2001; Feyissa et al., 2017; Kleinsasser et al., 2008; Kunz et al., 1975; Wolfenden et al., 2005). The absence of large offset faults in this unit is interpreted by Wolfenden et al. (2005) as an indication that strain was mainly accommodated by dyke injection. At the SE base of the escarpment, WoldeGabriel et al. (2013,2001) report fluvio-lacustrine clastic sedimentary units with ages from 5.77 to 3.8 Ma.

The oldest deposits of the Awash valley are found in the middle Awash (ca. 10.4°N) with ages ranging from 5.5 to 4 Ma (Renne et al., 1999), and in the ~5.2–3.9 Ma fluvio-lacustrine Sagantole Formation formed in an eastward-dipping half-graben localized in the present-day Lower Awash valley (ca. 11.1°N, Quade et al., 2008).

The fluvio-lacustrine Pliocene (3.9–2.9 Ma, Quade et al., 2008) Hadar Formation in the lower Awash probably formed in response to extension parallel to the Red Sea Rift System, as testified by the north-northeast depositional direction observed in this unit (Campisano, 2012; DiMaggio et al., 2015a; Wynn et al., 2008), indicating that the region was not yet dominated by MER tectonics. Few studies, however, propose another interpretation with a N-S-oriented basin (see Campisano, 2012 and references therein). Deposits of comparable age (3.39–4.26 Ma, White et al., 1993) in the middle Awash valley are believed to belong to a distinct basin (Wynn et al., 2008). The deposition of the fluviatile Busidima Formation (2.7–0.15 Ma, Quade et al., 2008) marks a significant change in the dynamic of the basin, the activation of the N-S As Duma fault and the formation of a marginal graben (Quade et al., 2008; Wynn et al., 2008). Simultaneously, sedimentation began in the axial Adda'Do and Yangudi Basin (Issa Graben), according to Wynn et al. (2008). Sedimentation in the lower Awash valley ended approx. 0.15 Ma ago, probably related to base-level drop (Quade et al., 2008) and the formation of the Kariyu Basin (Kalb, 1995).

Magmatic rocks situated on the horst east of the Awash basin were dated between 4 and 2.3 Ma (Barberi et al., 1975; Kunz et al., 1975; Lahitte et al., 2003b) and were emplaced in a thinned lithosphere (Tortelli et al., 2022). One dating of 7.1 Ma is presented by Barberi et al. (1975) at the base of the eastern fault scarp of the Issa graben, suggesting that Late Miocene rocks are buried below the outcropping Pliocene lavas.

The age of the Issa graben is probably Quaternary, as proposed by Varet et al. (1975) and Wynn et al. (2008), and possibly related to the reorganisation of the Awash valley at ~2.8 Ma. This is comparable in age with the tectonic activity of the Wonji segment of the NMER (see section 4.9). No volcanic material in this graben has been dated. Only a few flows on the Abida and Ayelu volcanoes yield ages younger than 0.8 Ma (Kunz et al., 1975; Lahitte et al., 2003b; Rees et al., 2023).

4.11. Central-western Afar

The central-western Afar comprises the area between the Affara Dara and the Ethiopian Plateau (Fig. 1). At the margin, the trap series were dated between 31.2 Ma and 28.5 Ma (Ayalew et al., 2019; Eid et al., 2021; Hofmann et al., 1997; Kieffer et al., 2004; Ukstins et al., 2002). Datings between ~23 and ~ 20 Ma are reported by Ayalew et al. (2019) and Stab et al. (2016) in the lavas of the Chifra series. The top of this formation was dated at 7 Ma (Stab et al., 2016). It is unclear whether low-volume but continuous volcanism existed between these two Miocene age clusters. No thickness variations, unconformities or growth strata were observed in the Trap and Chifra series, but it is postulated that limited extension without block tilting formed marginal grabens (Stab et al., 2016). The Chifra series is unconformably overlain by the flat-lying Arabati Rhyolite, probably ~6.8–5.5 Ma old (Ayalew et al., 2019; Coulié, 2001). This indicates that significant tectonic activity only occurred during the Late Miocene. Ayalew et al. (2019) measured WSW - ENE dykes of 24.3–17.4 Ma old in the same region.

At the foot of the escarpment, the Awra plain is covered by poorly studied sediments. Erosion features indicate that most of those sediments are not Recent. Studies lack in this basin except along the Mille River Basin, where sediments were dated as Pliocene (3.4 to 3.8 Ma, Deino et al., 2010; Haile-Selassie et al., 2015; Saylor et al., 2019). Extrapolation to the whole basin is difficult but remains plausible. Volcanoes in the northern part of the basin were dated at 3.5 and 1.6 Ma (Coulié, 2001; Stab et al., 2016). Very recent volcanic cones are visible in the centre of the basin. Faults are rarely identified, and the relative scarcity of Recent sediments could indicate that the basin is not actively subsiding.

Whereas the escarpment seems to lack deformation during the early rifting phase, the Sullu Adu area shows a different evolution. In the northern part, Coulié (2001) and Stab et al. (2016) describe an angular unconformity between the Early Oligocene (30.6 to 29.7 Ma) lavas and the Miocene (25.4 to 8.6 Ma) Finto rhyolites. Stab et al. (2016) mentions the base of this unit to be 23.5 Ma old but Coulié (2001) shows an age of 25.4 Ma, probably in the same unit. It is unclear whether this long-lasting unit represents continuous deposition or whether it corresponds to two eruptive phases. In each case, the unit lacks any internal deformation or unconformity, evidencing tectonic quiescence during most of the Miocene. Renewed tectonic activity between this series and the Sullu Adu Series (i.e. between 8.6 and 5.4 Ma) formed a second major angular unconformity (Stab et al., 2016). The Sullu Adu series (5.4–3.9 Ma) are horizontal but cut by faults. In the southern part of the Sullu Adu horst (region of Mille), these lavas yield slightly younger ages (3.5–2.7 Ma, Coulié, 2001; Kidane et al., 2003; Kunz et al., 1975; Stab et al., 2016). Barberi et al. (1975) report an age of 7.4 Ma for a tilted block covered by the Sullu Adu series.

NNW of the Sullu Adu horst is the Recent Dabbayra volcanic range. The timing of the initiation of volcanic activity (in the eastern part of the area) is unknown, but extrapolation from datings of Coulié (2001) and Stab et al. (2016) in the Awra plain points towards a possible Plio-Pleistocene age. Further to the NNW, the 23 Ma Limmo Granite forms one of the few outcropping plutons of the Afar Depression, intruding in 23–26 Ma porphyritic and extrusive rocks (Black et al., 1972).

East of the Dabbahu – Manda Hararo volcanic range, the Affara Dara is formed by another granitic body with intruding trap basalts at ~25 Ma (Barberi et al., 1972a; C.N.R - C.N.R.S. Afar Team, 1973; Varet, 2018). This body is covered by Early-Middle Pleistocene lavas (Barberi et al., 1975). This massif was most probably linked to the Sullu Adu horst

before being separated by the proto-Dabbahu- Manda Hararo range.

The Dabbahu-Manda Hararo volcanic range is formed by lavas younger than 0.3 Ma (Barberi et al., 1972a; Ferguson et al., 2013a; Field et al., 2013; Lahitte et al., 2003b; Medynski et al., 2015). During this timeframe, the range formed the locus of extension, with most of the strain being accommodated by dyke intrusion rather than faulting (Ebinger et al., 2010; Ferguson et al., 2013a), as exemplified by the 2005–2010 event (e.g. Ayele et al., 2009; Barnie et al., 2016; Grandin et al., 2009, 2010; Wright et al., 2006). This area shows low crustal contamination, high partial melting, shallow Moho, linear magnetic anomalies, an extensive and long-lasting magma reservoir and is believed to be heavily intruded, representing an almost oceanic crust, close to continental breakup (Ahmed et al., 2022; Ayalew et al., 2019; Ayele et al., 2009; Bridges et al., 2012; Desissa et al., 2013; Didana et al., 2014; Hammond et al., 2011; Johnson et al., 2016; Lewi et al., 2016; Reed et al., 2014). The margins of the Dabbahu-Manda Hararo volcanic range are formed by Pleistocene lavas (2.3–0.6 Ma, Barberi et al., 1975; Kidane et al., 2003; Kunz et al., 1975; Lahitte et al., 2003b).

4.12. Central-eastern Afar

The central-eastern Afar is situated between the Tendaho and Goba'Ad grabens and the Danakil Block (Fig. 1). The central-eastern Afar is almost exclusively covered by rocks of Quaternary age, hiding part of its geological history. A few late Pliocene K/Ar datings were obtained near the Assal Rift and two on the Gamarri fault scarp (Barberi et al., 1975). Dating of the same scarp by Ar/Ar techniques indicates that previous datings were probably imprecise (Ar/Ar ages ~2 Ma, Ahn et al., 2016; Kidane et al., 1999, 2003; Lahitte et al., 2003b). Other datings (> 130 datapoints) indicate ages of 2.3 Ma or younger, assigned to the upper Stratoid series (Barberi et al., 1975; Brinckmann and Kürsten, 1971; Civetta et al., 1975a, 1975b; Courtillot et al., 1984; Kidane et al., 1999, 2003; Lahitte et al., 2003b; Manighetti et al., 1998; Zumbo et al., 1995b). Besides the few pre-Quaternary datings discussed above, most of the oldest datings are found between the Tendaho / Goba'Ad graben and the Asal – Ghoubbet graben. The age of the lavas tends to be young towards both of these active rift segments and Manda Inakir. The Recent (< ~0.6 Ma) lavas are restricted to four areas: the Tendaho/Goba'Ad graben, the Dadar graben, Manda Inakir and Asal-Ghoubbet (the latter discussed in section 4.2 above). Except for Manda Inakir, Recent lavas are confined to active rift segments. Stab et al. (2016) named this phase the "localizing phase".

The central-eastern Afar is dissected by numerous grabens. They are mainly filled by Pleistocene-Recent sediments (e.g. Gasse and Street, 1978; Gasse et al., 1980). The early tectonic history of the area is mainly unknown due to the ubiquitous Quaternary cover. However, data from Tortelli et al. (2022) suggest that the lithosphere was still relatively thick during the emplacement of the Early Pleistocene *Upper Stratoid Fm.*, indicating a late thinning. The Tendaho graben is filled in some parts by more than 1000–1300 m of sediments intercalated with basaltic lava flows (Battistelli et al., 2002). Formation of this graben has been postulated to have started 1.8 Ma ago (Acocella et al., 2008; Acton et al., 1991). However, this value is only constrained by the average age of the Stratoid basalts. We instead consider the graben to be initiated around 1.1 to 0.6 Ma ago, as argued by Lahitte et al. (2003b), coherently with petrological indications of rift focusing since 1.1 Ma (Tortelli et al., 2022). According to Acocella et al. (2008), the rifting activity decreased in the Tendaho Graben since ~0.2 Ma, in favour of Manda Hararo. However, lakeshore markers indicate still active subsidence during the Holocene (Mologni et al., 2021). The eastern part of the Goba'Ad graben comprises older sediments, up to Pliocene, indicating an earlier formation (Fig. 4, Gasse et al., 1987). Doubre et al. (2017), Moore et al. (2021), Pagli et al. (2014), Sangha et al. (2022) show that the Goba'Ad graben hardly accommodates any shortening nowadays.

4.13. Danakil Depression

The Danakil Depression sensu *lato* forms an area of lower elevation between the Gulf of Zula, the Ethiopian Plateau, the Affara Dara and the Danakil Block (Fig. 1). We segment it here in the Afar-Danakil transition zone, the Danakil Depression sensu stricto and the Buia graben.

4.13.1. Afar-Danakil transition zone

The *Afar-Danakil transition zone* refers in this study to the area situated between 12.8°N and 13.4°N (Fig. 1). This zone marks important changes in morphology, magmatism, tectonics and sedimentology between central Afar south of it and the Danakil Depression sensu stricto situated north of it (see also section 7.1). This area is characterized by vast zones covered by Recent (< ~0.6 Ma) lavas of the Ma'Alalta, Alayta and Tat'Ali massifs. Older lavas of unknown age are present on Afdera volcano. Barberi et al. (1975) published an age of 3.1 Ma at the foot of the volcano, but this age is questionable. Varet et al. (1975) map this volcano as belonging to the upper stratoid series, corresponding to our Q_2v unit. Tectonically, the area is dominated by the Alayta – Afdera Transfer Zone, which links the Dabbahu – Manda Hararo rift segment to the Tat'Ali and Erta Ale rift segments (Schaegis et al., 2021 and references therein). This transfer zone similarly affects Early Pleistocene to Recent lavas.

The Teru Graben and the Ma'Alalta volcano form the northern prolongation of the Dabbahu-Manda Hararo range. The Recent (<0.6 Ma, Barberi et al., 1972a; Tortelli et al., 2021) lavas of the Ma'Alalta volcano directly cover Mesozoic sediments towards the E, indicating a possibly relatively recent age for the formation of this rift segment. Local seismicity and the very recent filling of the Teru graben, which is possibly cut by active faults (12.827 N, 40.317E), indicate that this area is still active.

4.13.2. Danakil Depression sensu stricto

The Danakil Depression sensu stricto comprises the topographic depression between ~13.3°N and 14.65°N (Fig. 1). Its geological history remains debated. Magmatic material at the eastern margins is dated by Brinckmann and Kürsten (1971). However, dating results have large uncertainties (sometimes 200% error ranges). Subvolcanic samples from plugs and dykes at the western edge of the Danakil Alps showed results ranging from ~26 to ~16 Ma, probably corresponding to the same magmatic events studied in the southern Danakil Alps by Civetta et al. (1975a) (section 4.6). The rare Syenite and Dolerite sills mapped by the Geological Survey of Ethiopia (1978a) on the western margin probably have similar ages.

The basin itself is filled by the syn-rift Red Bed Series (also called Danakil Fm. by Brinckmann and Kürsten, 1971) or Polychromatic Fm. by C.N.R - C.N.R.S. Afar Team, 1973 and Varet, 2018) and unconformably overlay the basement and the Mesozoic cover (Beyth, 1973, 1978; Brinckmann and Kürsten, 1971; Le Gall et al., 2018). This unit is formed by alluvial and lacustrine sediments dominated by conglomerates, sandstones and siltstones with some basaltic intercalations (Beyth, 1973, 1978; Brinckmann and Kürsten, 1971; Le Gall et al., 2018). On the eastern margin of the Depression, Brinckmann and Kürsten (1971) dated lava flows embedded within the Red Bed Series. The datings with reasonable uncertainty range from 8.5 to 6 Ma, with an exception being 3.4 Ma. These values are comparable to the datings on the western margin ranging from 5.7 to 6.2 Ma (Brinckmann and Kürsten, 1971; Le Gall et al., 2018) and to Early Pliocene datings reported by Park (2010) on the eastern margin.

Continental sedimentation continued until present-day times. Continental conditions were interrupted by Middle to Late Pleistocene marine incursions identified as the Zariga Fm by Brinckmann and Kürsten (1971) and composed of fringing coralgal reefs covered by gypsum. At least four marine incursions were observed based on field observations, of which the two most recent ones were dated as MIS 5e and MIS 7 (i.e. ~0.125 and ~ 0.2 Ma, respectively, Jaramillo-Vogel et al., 2019,

Foubert et al., in prep.). Desiccation after the marine incursions resulted in the deposition of thick evaporite units (Bastow et al., 2018; Holwerda and Hutchinson, 1968) recycled by continental water forming a large salt pan that is still active today. The sediment thickness below the salt plain is probably more than 2 km (Behle et al., 1975; Makris and Ginzburg, 1987).

The Erta Ale volcanic range is situated on the rift axis in the southern Danakil Depression. It is formed by Recent lava and is still active nowadays (Burgi et al., 2002; Global Volcanism Program, 2021; Pagli et al., 2012; Xu et al., 2017, 2020). Barberi et al. (1972a) propose two datings of the lava deposits, resp. 0.35 ± 0.14 and 1.2 ± 0.5 Ma. However, as mentioned by Watts et al. (2020), it is challenging to date very young material, and most authors consider the Erta Ale lavas as Recent, i.e. probably younger than 0.6 Ma.

Rifting in the Danakil Depression has traditionally been postulated to initiate in the Early Miocene (~23–25 Ma), such as proposed by Barberi et al. (1972a), C.N.R - C.N.R.S. Afar Team (1973) and Le Gall et al., 2018) based on datings of magmatic material published by Brinckmann and Kürsten (1971). However, we challenge this hypothesis. As discussed above, all Early to Mid-Miocene datings were sampled in plugs and dykes of the Danakil Alps and not in the syn-rift Red Bed Series as described by Brinckmann and Kürsten (1971) and shown on their maps Brinckmann and Kürsten (1970). Only one single dating (sample 438, 22 ± 2 Ma, presumably taken at 13.802 N, 40.984E according to their geological map) cannot unambiguously be attributed to either the Red Bed Series or pre-rift rocks. The presence of igneous products in pre-rift rocks is not diagnostic for the formation of the Danakil basin. As shown in other parts of the Afar Depression, volcanic activity is not always linked with tectonic activity. If the plugs and dykes are linked to a tectonic event, we suggest relating them to the opening of the Red Sea basin occurring around the same time (see sections 4.3.1 and 4.6 above). The deposition of the Red Bed Series, however, is diagnostic for the formation of an incipient Danakil basin (Brinckmann and Kürsten, 1971; Le Gall et al., 2018; Varet, 2018). As discussed above, all datings unambiguously attributed to the Red Bed Series are 8.5 Ma or younger. This younger age is also much more consistent with the kinematic models of Eagles et al. (2002), McClusky et al. (2010) and Reilinger and McClusky (2011) that determined the initiation of the Danakil Block rotation at ~11 Ma (see section 4.6 above) and with the 9 to 3 Ma heating event recorded in fission tracks on Mt. Ghedem (Ghebreab et al., 2002). We thus conclude that the rifting of the Danakil did not start before the Mid to Late Miocene, although we cannot exclude prior faulting activity linked with the opening of the southern Red Sea. The late onset of tectonic activity in the Danakil Depression could also explain the unusual N-S fault orientation observed in the Garsat Graben and east of the Mekele Outlier (Fig. 4). As shown by Zwaan et al. (2020b), the rotation of the Danakil Block changed the stress field from N*E*-SW to E-W on the western Afar margin. In the southern part of this margin, the NNW-SSE faults were formed by initial stress fields, while near the Danakil Depression, the major faults formed later under the E-W stress field, forming N-S faults.

The occurrence of the Red Bed Series decreases towards the northern part of the Danakil Depression. On the western margin, no Red Bed sediments are found north of 14.24°N. They are visible further on the eastern margin but not north of 14.50°N. This, along with the change in topography and the larger tectonic uplift in the north, has been used as an argument for the younger age of the rift in the north (Rime et al., in prep., see also section 5.2.1), but the absence of dated material prevents any quantification.

4.13.3. Buia Graben

The Buia graben is situated between the Danakil Depression and the Gulf of Zula (Fig. 1a). We only discuss the opening of the graben itself, representing the northern extension of the Danakil rift. This area experienced denudation since ~15 Ma, which is not linked to the opening of the Danakil Depression but to the opening of the Red Sea discussed in section 4.3.1 (Balestrieri et al., 2005).

The Buia graben is not filled by a large amount of syn-rift sediments or lavas, as testified by the basement outcropping inside the crater of the Alid volcano, on the eastern fault scarp (Duffield et al., 1997) and on the hills separating the Buia graben and the Danakil Depression (see Fig. 4). The faulted stratoid lavas found on the shoulders of the graben were dated between 2.1 and 1.1 Ma (Buffler et al., 2010; Duffield et al., 1997). Recent (< 0.5 Ma) lavas were also reported by Buffler et al. (2010) in the north of the graben. The central Alid volcano erupted between ~0.212 and 0.015 Ma, and the basaltic flows at the foot of the volcano are believed to be younger (Duffield et al., 1997; Lowenstern et al., 2006).

The SW part of the graben forms the Dandiero basin and features approximately 500 m of Pleistocene sediments studied in detail after the discovery of Hominid fossils (Abbate et al., 2004; Ghinassi et al., 2009, 2014; Papini et al., 2014; Sani et al., 2017). These continental sediments are Pleistocene in age.

The Buia graben started forming at ~1.2 Ma (Sani et al., 2017) with the first phase of N-S faulting followed by NNW-SSE faulting. The graben is nowadays tectonically active as recorded by coral terrace elevations (Buffler et al., 2010, Rime et al., in prep), geodetic velocities (Viltres et al., 2020), earthquake swarms and a likely dike intrusion in Bada in 1993 (Ruch et al., 2021).

5. Tectonic structure of the Afar region

In light of the complex geological history of the Afar region (section 4) and studies on present-day tectonic activity, the tectonic structures and kinematic of that area are discussed in this section.

5.1. Plates, microplates, blocks and fragments

Three main tectonic plates play a major role in the region: the Nubian plate, the Arabian plate and the Somalian plate (Fig. 2, 8). Several smaller tectonic elements of varying extent and importance are also present. The most important are the Danakil Block and the Ali Sabieh Block, besides some smaller, minor crustal elements.

5.1.1. The Danakil Block

Most authors classify the Danakil Block as a microplate (e.g. Acton et al., 1991; Eagles et al., 2002; Keir et al., 2013; McClusky et al., 2010; Schettino et al., 2016; Sichler, 1980). The counter-clockwise rotation of this Block has been postulated since the early 70s based on geological evidences such as fault orientation, paleo stress analysis, comparison between Ethiopian plateau and Danakil Block geology, the distribution of young magmatic materiel and early plate tectonic reconstructions (Mohr, 1970, 1972; Sichler, 1980; Souriot and Brun, 1992; Tazieff et al., 1972; Zwaan et al., 2020b). Paleomagnetic (Manighetti et al., 2001; Schult, 1974) and InSAR studies (Moore et al., 2021), as well as GNSS data (ArRajehi et al., 2010; McClusky et al., 2010; Viltres et al., 2020, see Fig. 9) confirmed this hypothesis. However, the assumption of one single rigid Danakil Block is an oversimplification. Barberi et al. (1975), Barberi and Varet (1977, 1975) and Varet, 2018 already mentioned that the southern Danakil Block "has to be considered as an accretion of the Arabian plate" that behaves independently from the northern Danakil Block, which has been named as the *Arrata Microplate.* This configuration also explains the low seismicity (Fig. 10) and tectonic quiescence in the Bab-el-Mandeb Strait (section 4.3.1 and references therein). Recent GNSS data confirm this hypothesis (Viltres et al., 2020). They show the absence of relative movement between the southern Danakil Block and Arabia – both being thus part of the same plate -, and confirm that the Arrata Microplate is rotating rigidly and independently from both the Nubian and Arabian plates (see Fig. 9). It should, however, be noted that even if the southern Danakil Block nowadays represents an accretion to the Arabian plate, paleomagnetic (Manighetti et al., 2001) and geological data (see above) indicates that this was not the case in the past when the whole Danakil Block rotated and rifted away from Arabia.

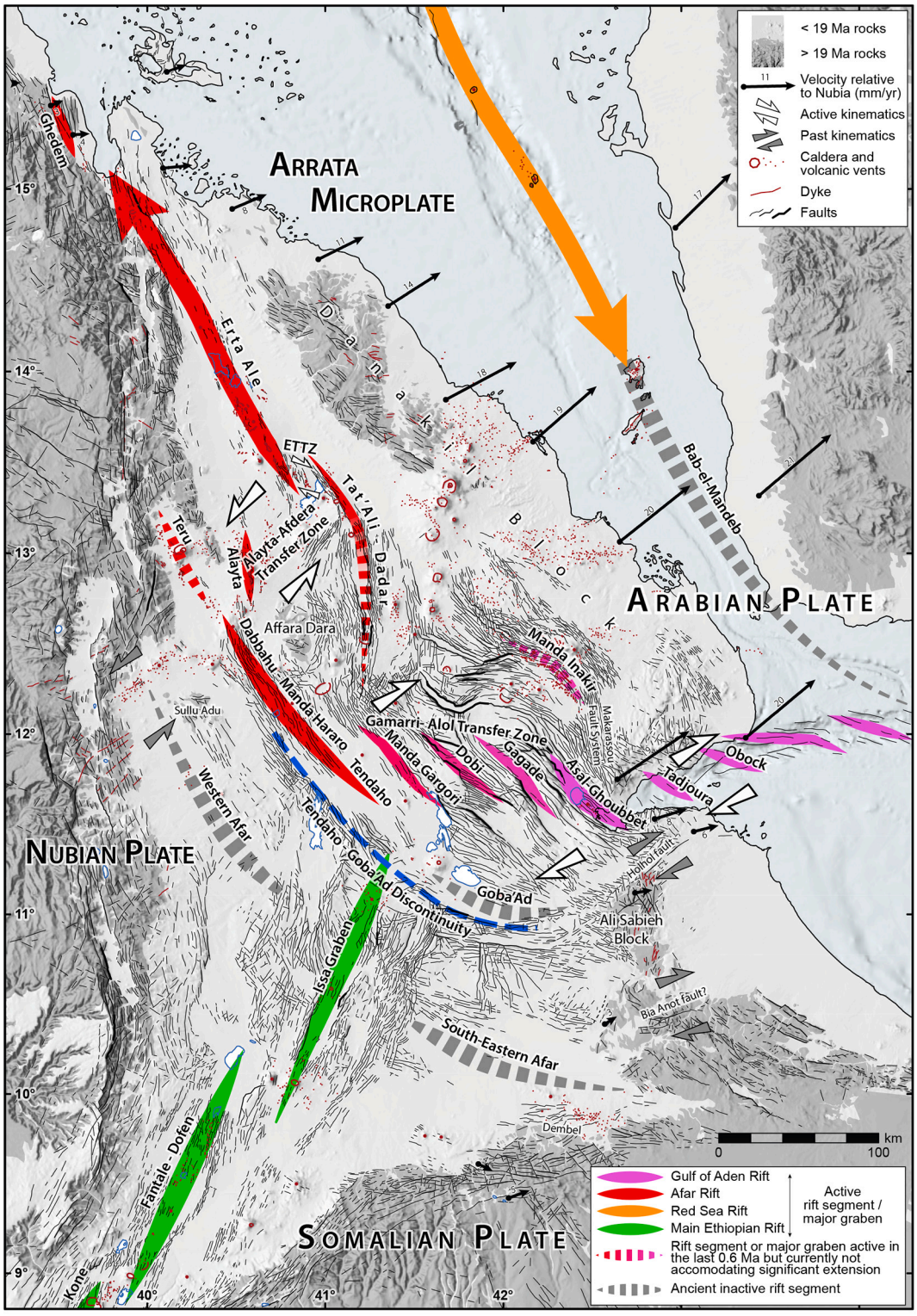

Fig. 8. Rift dynamics of the Afar Depression. Rift segments are discussed in section 5.2. After Corti (2009), Doubre et al. (2017), Moore et al. (2021), Pagli et al. (2014), Ruch et al. (2021), Sangha et al. (2022), Viltres et al. (2020) and discussion in section 5.2. ETTZ = Erta Ale – Tat'Ali Transfer Zone.

The south-eastern and north-western limits of the Arrata Microplate are poorly defined. As shown by Viltres et al. (2020), they are probably situated on the Euler poles of the Arabia-Arrata and Nubia-Arrata rotations, respectively (Fig. 9). As such, they should only accommodate little strain to no strain at the Euler pole. The limit between the Arrata Microplate and the southern Danakil Block (part of the Arabian plate) is unclear and is probably situated between the Nabro range, the Hanish island and the Beilul Bay (Barberi and Varet, 1977; Varet, 2018; Viltres et al., 2020, see Fig. 9). Earthquake data show seismic activity with sinistral strike-slip focal mechanisms in the Nabro Range (Fig. 10). The Hanish Islands show NE-SW fissures and vent alignment (Gass et al., 1973; Viltres et al., 2020, Fig. 8). Free air anomaly and vertical gravity gradient data (Suppl. Mat. 5 and 6) also indicate that the Beilul Bay might represent the southernmost continuation of the Red Sea Rift.

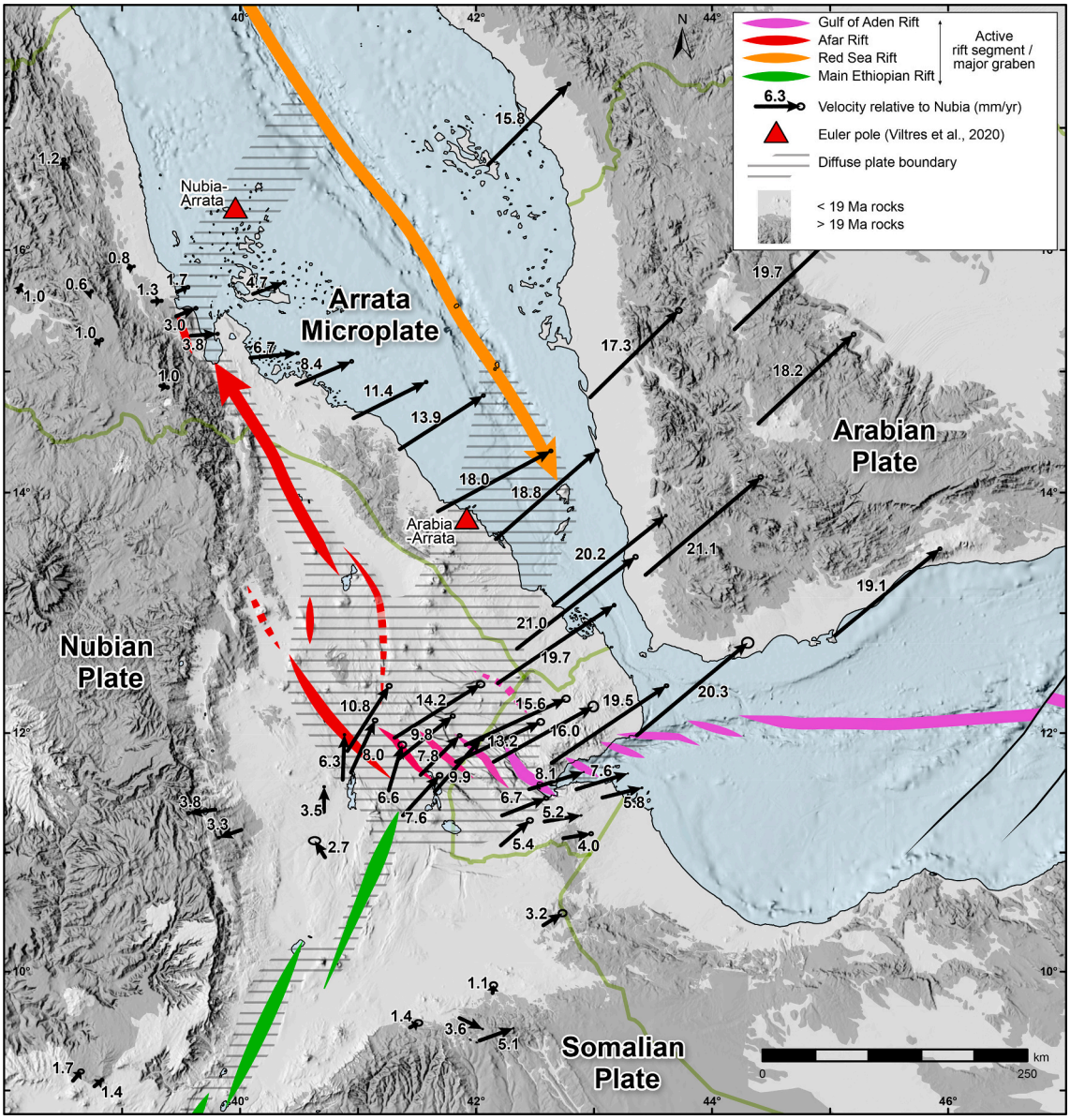

Fig. 9. Plate kinematics of the Afar region. GNSS velocities are from Doubre et al. (2017), McClusky et al. (2010) and Viltres et al. (2020). Only datapoints reflecting inter-dyking periods where used in the data of Doubre et al. (2017). Rift segments and diffuse plate boundary are discussed in section 5.

However, the onshore area of Beilul Bay is devoid of major fault sets.

The northern limit of the Arrata Microplate is similarly ill-defined and probably runs NE of Massawa (Viltres et al., 2020). Ruch et al. (2021) show the occurrence of a WSW-ENE-oriented earthquake swarm in Massawa in 2002. The earthquake cluster can be followed until the Red Sea trough at 17°N where several possibly sinistral strike-slip focal mechanisms have been recorded (see Fig. 10). Compressive focal mechanisms recorded in the vicinity of Massawa (Fig. 10) are coherent with an Euler pole situated on the plate boundary. Lineaments in free air anomaly and vertical gravity gradient data can also be observed in the same zone, albeit in a slightly different orientation (SSW-NNE, Suppl. Mat. 5 and 6). Further lineaments and earthquakes could even indicate that some of the strain is accommodated SE of the Dahlak Islands and the Howlakil Bay.

These elements point towards diffuse strain accommodation patterns for the NW and SE limits of the Arrata Microplate. As such, Fig. 9 only presents diffuse plate boundary.

5.1.2. *The Ali Sabieh Block*

The continental Ali Sabieh Block significantly complicates regional plate tectonic reconstructions (Beydoun, 1970; Collet et al., 2000; Purcell, 2018) and was ignored by some authors (Le Pichon and Francheteau, 1978; Redfield et al., 2003).

While some authors consider the Ali Sabieh Block as autochthonous (Christiansen et al., 1975; Kronberg et al., 1975; Purcell, 2018), others inferred that it was part of the southern Danakil Block also rotating counterclockwise (Garfunkel and Beyth, 2006; Mohr, 1970; Sichler, 1980). Other studies proposed a “saloon door mechanism” where both the Danakil and Ali Sabieh Blocks were rotating in opposite directions (Audin et al., 2004; Manighetti et al., 2001). The latter hypothesis was confirmed by paleomagnetic data showing a 29° clockwise rotation for the Ali Sabieh Block between 55 Ma and 8 Ma (Kidane, 2016). While it was since then accreted to the Somalian plate, it should be considered a distinct block during its geological history.

The southern extent of the Ali Sabieh Block and the mechanisms of movement are poorly defined. Most authors mention the *Bia Anot fault* as its southern limit (Audin et al., 2004; Black et al., 1975). According to

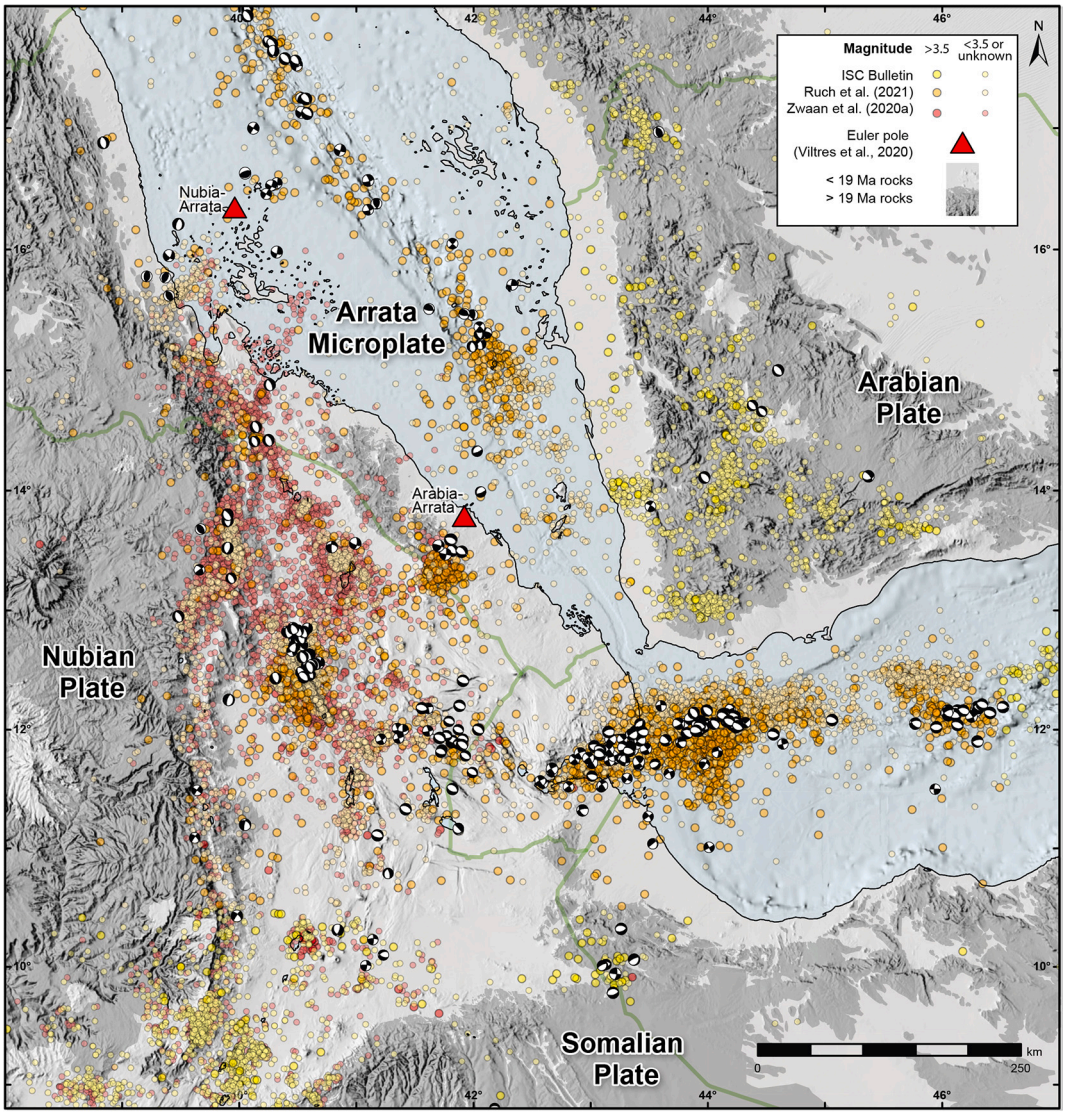

Fig. 10. Earthquake map of the Afar region. Earthquakes from Ruch et al. (2021), Zwaan et al. (2020a) and ISC Bulletin (Bondár and Storchak, 2011; International Seismological Centre, 2021; Storchak et al., 2017, 2020; Willemann and Storchak, 2001, retrieved on 22.09.2021). Focal mechanisms are from Hofstetter and Beyth (2003) and Global CMT Catalogue (Dziewonski et al., 1981; Ekström et al., 2012, retrieved on 27.11.2021).

the model of Audin et al. (2004), a significant amount (several tens of km) of dextral strike-slip movement would have been accommodated by this fault. The absence of major visible faults and the continuity of the basement and Mesozoic structure (Fig. 4 and Suppl. Mat. 7) argues against the presence of both faults indicated by Audin et al. (2004) or Black et al. (1975) (see Suppl. Mat. 7). We identified a major fault SE of Bia Anot (eastern Bia Anot fault on Suppl. Mat. 7) that might have accommodated strike-slip movement but that has an orientation (ENE-WSW) that is not strictly parallel to the strike-slip faults of the Gulf of Aden. Another major fault (probably buried beneath younger volcanic rocks) is indicated by the Ayisha geological map (Geological Survey of Ethiopia, 2015), SW of Bia Anot (western Bia Anot fault on Suppl. Mat. 7). This lineament also marks a major boundary between rocks of different ages and structure orientation (WNW-ESE faulted Pliocene and younger in the West, NNE-SSW faulted and tilted Mid-Miocene to pre-rift in the East, Fig. 4). North of Bia Anot, this fault might connect with a WNW-ESE oriented zone at ~10.6°N where no pre-rift rock crops out (northern Bia Anot discontinuity on Suppl. Mat. 7). This northern Bia Anot discontinuity also coincides with a significant change in the orientation of the structures in the pre-rift rocks from WNW-ESE south of it and NNE-SSW on the Ali Sabieh Block. It might represent the southern limit of the Ali Sabieh Block. Even though we used the eastern Bia Anot fault in our kinematic model (section 6.1), our work cannot bring a clear conclusion, and further field and paleomagnetic studies would be needed to understand the complex tectonic history of the area.

5.1.3. *Crustal fragments*

Several other continental crustal fragments have been proposed in the Afar Depression, and probably more are present but not reported. The Affara Dara, exposing Trap basalts intruded by a ~ 25 Ma granitic body (Barberi et al., 1972a; C.N.R - C.N.R.S. Afar Team, 1973; Varet, 2018, Fig. 4) represents a clear continental fragment. Hammond et al. (2011) also shows lower crustal Vp/Vs seismic velocities in the area, confirming the presence of a crustal body. The northern Sullu Adu region also exposes early Oligocene flood basalts and similarly represents a continental fragment. Based on geophysics, Hammond et al. (2011) proposed another continental fragment extending further south, near Mile. The presence of this block is however debated (see Wang et al., 2021). Hammond et al. (2011) further hypothesize a possible block in central-eastern Afar (roughly centred on Siyyarou).

5.2. Rifts, rift segments and rift propagation

We discuss here the *rifts* and *rift segments* of the Afar region. We define *rifts* as strain-accommodating areas separating rigid and extensive blocks, i.e. tectonic plates or microplates.

At a smaller scale, rifts are segmented into *rift segments* (e.g. Nelson et al., 1992). They represent continuous, mainly linear strain accommodating areas testified by faulting and, in some cases, magmatic activity and/or formation of sedimentary basin. They are the equivalent of the distinct Wonji Fault Belts in the MER.

5.2.1. Re-evaluation of rift propagation in the Afar

The literature usually mentions the presence of three rifts in the Afar Depression: the Gulf of Aden Rift, the (Northern) Main Ethiopian Rift ((N)MER), which is part of the East African Rift System, and the Red Sea Rift. They separate the Arabian, Nubian and Somalian plates. These rifts are often described as "propagators" considering the direction of propagation. We call for a re-evaluation of rift propagation in the Afar Depression at a regional scale. For this discussion, we define rift propagation as the along-strike migration of the part of a rift that experienced a certain amount of lateral extension.

The Northern Main Ethiopian Rift (NMER) accommodates extension between the Nubian and Somalian plates. At the scale of the East African Rift System, rifting is propagating southwards (Chorowicz, 2005; Macgregor, 2015), consistent with an Euler pole situated far south (DeMets and Merkouriev, 2016; Stamps et al., 2021) but a northward propagation from the Turkana Depression has also been proposed (Michon et al., 2022). At the scale of the study area, while Tesfaye et al. (2003) and Wolfenden et al. (2004) propose a northward propagation from the Central MER, most authors suggest a southward propagation from the Afar Depression towards Central MER (Abebe et al., 2010; Bonini et al., 2005; Keranen and Klemperer, 2008; Rooney et al., 2007). The long distance to the Euler pole implies that, at the scale of our study area, the Nubia-Somalia extension can be considered almost parallel, and rift propagation mechanisms are thus less significant.

It is well-defined that the Gulf of Aden propagated westwards into the Afar Depression. This was shown by the magnetic anomalies in the Gulf of Aden sensu stricto (Fournier et al., 2010; Leroy et al., 2012) and by the presence of a young rift segment in the Gulf of Tadjoura towards Asal-Ghoubbet (Courtillot, 1980; Daoud et al., 2011; Manighetti et al., 1997, 1998, 2001, see section 4.2). This westward propagation is coherent with the anticlockwise rotation of the Arabian plate.

What traditionally is called the "Red Sea rift" is characterized by two distinct rift arms (see Figs. 8, 9). One is situated "offshore", in the Red Sea trough, possibly reaching the Hanish islands as far south as 14°N. The other one comprises the Danakil Depression and central Afar.

The "offshore" Red Sea rift is thought to propagate northward in the central and northern part of the Red Sea (Augustin et al., 2016; Courtillot, 1982; Courtillot et al., 1987; Ghebreab, 1998; Izzeldin, 1987; Khalil et al., 2020; Schettino et al., 2016, see also section 4.3). Conversely, it propagates southward in its southern part (south of approx. 17°N, Courtillot, 1982; Courtillot et al., 1987; Ghebreab, 1998; Khalil et al., 2020; Schettino et al., 2016). The northward propagation from ~17°N is linked to the counter-clockwise rotation of the Arabian plate relative to the Nubian one, and the southward propagation linked to the counter-clockwise rotation of the Danakil Block and Arrata Microplate with respect to the Arabian plate.

The propagation of the second arm of the Red Sea rift, comprising the Danakil Depression and central Afar, is more controversial. (Barberi and Varet, 1975, 1977; Tazieff et al., 1972) proposed decreased spreading rates, crustal separation and opening, as well as a younger ages towards the northern part of the Afar, therefore implying a northward propagation. Since the late 90s', however, rifting in the Afar has mostly been described as a southward propagation of the Red Sea Rift (the "Red Sea propagator"). This concept was first mentioned and published by Manighetti et al. (1998). However, the study focused on the Gulf of Aden rift and the authors probably assumed the same concept of inland (centipede) propagation to be true for the other side of the Afar Depression or they extrapolated the southward propagation of the Red Sea Rift (sensu stricto) to the Afar. Since its first publication, this hypothesis has been mentioned by many authors (Acocella et al., 2008; Audin et al., 2004; Beyene and Abdelsalam, 2005; Bridges et al., 2012; Chauvet et al., 2023; Dumont et al., 2017, 2019; Hofstetter and Beyth, 2003; Kidane et al., 2003; Lahitte et al., 2003a, 2003b; Manighetti et al., 2001; Mologni et al., 2021; Muluneh et al., 2013, 2017; Purcell, 2018; Reed et al., 2014; Rowland et al., 2007; Wang et al., 2021; Wolfenden et al., 2004). Only few publications consider a northward rift propagation (Collet et al., 2000; Eagles et al., 2002; Gaulier and Huchon, 1991; Ghebreab et al., 2002; Molnar et al., 2018; Sani et al., 2017). The controversy on the northward versus southward rift propagation in the Danakil Depression and central Afar has however never been discussed in detail.

The following facts argue for northward rift propagation in the Danakil Depression and central Afar:

1) The counter-clockwise rotation of the Danakil Block postulated for a long time (Mohr, 1970; Sichler, 1980; Souriot and Brun, 1992; Tazieff et al., 1972), is now proven by GNSS velocity measurements, InSAR and paleomagnetic studies, as well as geological evidences (see section 5.1.1 and references therein). Rotation implies rift propagation towards the Euler Pole, i.e. towards the north (see Suppl. Mat. 16). This geometrical observation is confirmed by numerous analogue and numerical modelling studies of rotational rifting and field analogues (Benes and Scott, 1996; Khalil et al., 2020; Maestrelli et al., 2020; Molnar et al., 2017, 2018, 2020; Mondy et al., 2018; Le Pourhiet et al., 2018; Schmid et al., 2022; Zwaan et al., 2019; Zwaan and Schreurs, 2020).
2) Overall northward younging of the main outcroping magmatic products is observed in the Afar Depression (Fig. 4). While the southern Afar is dominated by Pliocene magmatic products, they are mainly Early- to Mid-Pleistocene in central-eastern Afar and mainly Recent (<0.6 Ma) in the Danakil Depression, with the exception of the thin Early Pleistocene basalts east of the Buia Graben.
3) The northward younging of the rifting age is noticeable (see section 4, Fig. 7). While rifting is reported since 27 Ma in central-western and south-western Afar (Stab et al., 2016; Wolfenden et al., 2005), rifting started probably ~11 Ma ago in the Danakil basin (section 4.13.2) and at 1.2 Ma ago in the Buia graben (Sani et al., 2017).
4) At a smaller scale, this trend of rifting with ages becoming younger towards the N is also observed from Goba'Ad (Pliocene) to Tendaho (~1.1 to 0.6 Ma, Lahitte et al., 2003b) to Manda Hararo (~0.2 Ma Acocella et al., 2008). Dumont et al. (2019) furthermore shows a northward propagation of faulting from Manda Hararo to Dabbahu at ~0.1 Ma.
5) The topography corroborates this northward younging trend (Suppl. Mat. 8). The topography in the south is wider, smoother and less steep, while in the north, it is steeper, indicating a less mature topography. This trend is also noticeable at the scale of the Danakil depression (Rime et al., in prep.).
6) The presence of pre-rift rocks shows a N-S gradient in the Danakil Depression. Basement crops out on the Buri peninsula, the eastern coast of the Gulf of Zula, the Howlakil Bay, and even the rift axis, on the Alid volcano (Fig. 4, Duffield et al., 1997). Volcanic material from the axial Maraho volcano in the northern part of the Depression contains xenoliths of the basement and Mesozoic cover (Kürsten, 1975), indicating the deep presence of pre-rift rocks. Further south, the magma of the Erta Ale range does not show any crustal contamination, probably indicating the absence of basement (Barberi et al., 1970; Barberi and Varet, 1970; Barrat et al., 1998; Hagos et al., 2016a; Watts et al., 2020). This evidences an overall crustal separation gradient, increasing from north to south.

Overall, we consider that rifting in central Afar and Danakil

Depression is not propagating southward but northward. The northward propagation implies that the northern Afar has experienced less stretching and lower extension rates than the central Afar (see also sections 6.1 and 7.1). It also implies that the same stage of extension happens later towards the Euler pole, i.e. northwards. Rifting in the Afar Depression would thus represent a large-scale en-echelon relay structure of the Red Sea, with the Danakil Block (nowadays only the Arrata Microplate) rotating between two rifts propagating in opposite directions.

This northward rift propagation calls for reconsidering the "Red Sea Rift" nomenclature referring to rifting in central Afar and the Danakil Depression. Northward propagation implies that the Red Sea Rift did not propagate southward from the Red Sea central trough through the Gulf of Zula into the Danakil Depression, as often described. The southern Red Sea Rift (the offshore arm of the Red Sea Rift) and the described Rift in central Afar/Danakil Depression (interpreted previously as the onshore segment of the Red Sea Rift) mark the SW and NE limit of the rigid (Viltres et al., 2020) Arrata Microplate. Both rifts overlap for >300 km and are >100 km apart. Of course, both arms have the same overall orientation and separate the Nubian and Arabian tectonic plates at a global scale. However, at a regional scale, if the Arrata/Danakil Block is considered a microplate, then both rifts (as defined above) should be considered distinct. We suggest calling it the *Afar Rift*. Barberi et al. (1972a) already named this segment the "*Afar Rift*" and "*Danakil Rift*". Viltres et al. (2020) also mention the "*Danakil-Afar rift*" and Le Pichon and Francheteau (1978) the "*Danakil Rift*". We prefer the "*Afar Rift*" because it encompasses both the Danakil Depression (northern Afar) and central Afar. The authors acknowledge that this distinction is not necessarily useful for global plate tectonic models but valuable at a regional scale to avoid confusion among scientists.

As shown in Fig. 8, the Gulf of Aden Rift and the Afar Rift are linked in central-eastern Afar, gradually accommodating extension in a series of en-echelon grabens. The formal distinction between the Gulf of Aden Rift and the Afar Rift at a regional scale is that the former accommodates extension between the Somalian and the Arabian plates while the latter accommodates extension between the Nubian and the Arrata plates. As no precise localization of the MER can be identified north of the Tendaho – Goba'Ad Discontinuity (TGD) and the limit between the Arrata and southern Danakil Block is gradual and ill-defined (see section 5.1.1), the boundary between what belongs to the Afar Rift and the Gulf of Aden Rift is also vague. It highlights the fact that the Gulf of Aden and Afar Rifts are forming a single, near-continuous structure (Fig. 8), propagating in the same overall direction. This continuity led Eagles et al. (2002) to consider the whole structure (the Afar Depression, including the Danakil Depression) as part of the Gulf of Aden rift.

We conclude that the Afar region is structured by the westward propagation of the Gulf of Aden Rift, the northward propagation of the Afar Rift, the southward propagation of the Red Sea Rift and close to parallel extension of the Main Ethiopian Rift (Fig. 8). This conforms to the counter-clockwise rotation of both the Arabian and Danakil plates. This rift propagation pattern and its associated timing (section 4) confirm the conclusion proposed by Girdler (1991), Hébert et al. (2001), Khalil et al. (2020), Maestrelli et al. (2022), Manighetti et al. (1997), Mohr (1972, 1970), Purcell (2018) and Wolfenden et al. (2004) that the triple junction models showing three rifts propagating synchronously away from one hotspot does not apply to the Afar region, just as it does not apply to the south Atlantic and the Etendeka and Paraná flood basalts or to the north Atlantic and the Iceland hotspot (Foulger et al., 2020; Franke, 2013; Peace et al., 2020).

5.2.2. Active rift segments

The position and configuration of rifts and rift segments in the Afar region varied significantly throughout its history. The most critical change corresponds to the abandonment of the Bab-el-Mandeb rift segment after Mid to Late Miocene times (see section 4.3.1). An extinct rift segment was also active between the Late Miocene and Pliocene in present-day Western and South-Eastern Afar (see sections 4.10, 4.11 and Fig. 7). As discussed in section 4.12, the Goba'Ad graben was probably active in the Pliocene and Pleistocene and represents another extinct rift segment.

At a shorter temporal scale, transient rifting processes, where individual rift segments accumulate strain for protracted periods before release during short volcanotectonic events, are known in the Afar Depression, such as in Iceland and in other rifts (Bourgeois et al., 2005; Ebinger et al., 2013; Foulger et al., 1992, 2020; Grandin et al., 2010; LaFemina et al., 2005; Ruch et al., 2016; Sigmundsson, 2006; Smittarello et al., 2016; Vigny et al., 2007; Wright et al., 2006, 2012). For example, Sangha et al. (2022) show that the distribution of extension changed before and after the 2005–2010 volcano-tectonic event in Dabbahu-Manda Hararo, and suggest that "surface deformation patterns in Afar changed drastically over periods of less than a million years". Another example is Manda Inakir which experienced significant Recent volcanic and tectonic activity as shown by the dense fault network in Recent lavas (Fig. 4) and by the 1928–1929 tectono-magmatic crisis (Audin et al., 1990). However, GNSS, InSAR and seismicity data show that the Manda Inakir currently hardly accommodates any strain (Doubre et al., 2017; Moore et al., 2021; Pagli et al., 2014, 2019; Ruch et al., 2021; Sangha et al., 2022, see also Figs. 9 and 10). This shows that the strain accommodation pattern in the Afar Depression can change over very short time scales.

The following sections discuss the present-day active rift segments. It is mainly based on very short observations of movement by GNSS, InSAR or seismicity methods and are not necessarily representative of the long-term evolution of the area.

5.2.2.1. The Northern Main Ethiopian Rift. In the studied area, the Northern Main Ethiopian Rift comprises 3 Wonji Fault Belt (WFB) segments: the northernmost part of the Kone segment, the Fantale segment and the Issa Graben. The latter is technically not situated in the NMER but in southern Afar. Nevertheless, as it accommodates strain between the Nubian and Somalian plates, it is considered part of the MER here. The MER rift ends northward abruptly on the Tendaho – Goba'Ad Discontinuity (TDG). Structures north of this discontinuity are related to the Gulf of Aden and Afar rifts (Hayward and Ebinger, 1996; Tesfaye et al., 2003), Figs. 4, 10).

5.2.2.2. The Gulf of Aden Rift. In the Afar Depression, the Gulf of Aden rift is commonly described as comprising the Gulf of Tadjoura, the Asal-Ghoubbet graben and the Manda-Inakir segments, linked by the Makarassou fault system (e.g. Le Gall et al., 2011; Manighetti et al., 1998, 2001; Tapponnier and Varet, 1974, see Fig. 8). Two rift segments are identified in the southwestern Gulf of Tadjoura,: the Obock and Tadjoura Troughs, linked by the Maskali fault zone (Dauteuil et al., 2001). The Asal-Ghoubeet rift segment witnessed a major rifting episode in 1978 (Abdallah et al., 1979; Kasser et al., 1981; Ruch et al., 2021; Smittarello et al., 2016; Vigny et al., 2007). GNSS and InSAR data indicate that this segment accommodates a significant part of the strain between the Arabian and Somalian/Nubian plates on a narrow zone with approx. 12–14 mm/yr of extension (Doubre et al., 2017; Pagli et al., 2014; Sangha, 2021; Sangha et al., 2022; see also Fig. 9), while Moore et al. (2021) indicate a more distributed extension.

The Manda Inakir rift segment is traditionally mentioned as an active rift segment linked to the Gulf of Aden rift (Barberi and Varet, 1975, 1977; Lahitte et al., 2003b; Manighetti et al., 1998; Tapponnier and Varet, 1974; Varet, 2018). As discussed above, it does not currently accommodate measurable extension although it probably did in the last century.

5.2.2.3. The link between the Gulf of Aden Rift and the Afar Rift. As discussed in section 5.2.1, the limit between the Gulf of Aden Rift and the Afar Rift is vague. Traditionally, only the Asal-Ghoubbet and Manda

Inakir segments are considered part of the Gulf of Aden Rift. However, considering the position of the MER, one could argue that the Gagade and Dobi grabens also belong to the Gulf of Aden Rift. As a formal limit is not useful, the transition area is considered here separately.

Strain in central-eastern Afar is distributed over more than 100 km (Doubre et al., 2017; Kogan et al., 2012; Moore et al., 2021; Pagli et al., 2014; Sangha et al., 2022). Data from Doubre et al., 2017, Pagli et al. (2014), Sangha (2021) and Sangha et al. (2022) show that most of the strain is currently accommodated in a zone going from Assal to Gagade, Dobi, Manda Gargor, Manda Hararo and Dabbahu, forming an en échelon graben pattern, similar to what is observed in the Gulf of Tadjoura (see Figs. 8 and 9). It furthermore represents an area with intense faulting (Fig. 4); the highest extensional strain (Polun et al., 2018; Sangha, 2021); high fault slip rates (2–3 mm/yr) during the Holocene and Quaternary (Manighetti et al., 2001); the most significant seismic activity (Fig. 10); the highest cumulative seismic moment release during the 1950–2017 period (La Rosa, 2020) and earthquake swarms recorded between 1960 and 2017, indicating magmatic processes at depth (Ruch et al., 2021). This broad area linking the Gulf of Aden Rift and the Afar Rift is named the Gamarri-Alol Transfer Zone. This complex transfer zone has been interpreted as bookshelf faulting, explaining the clockwise rotation of the Stratoid lavas of central-eastern Afar (Acton et al., 1991, 2000; Courtillot et al., 1984; Kidane et al., 2003; Manighetti et al., 2001; Tapponnier et al., 1990). Conversely, Pagli et al. (2019) argue for a distributed extension and rift-perpendicular shearing model.

5.2.2.4. The Afar Rift. The Dabbahu – Manda Hararo rift segment constitutes the southernmost rift segment that is indisputably part of the Afar Rift. It currently accommodates a significant amount of strain. This area shows low crustal contamination, high partial melting, shallow Moho, linear magnetic anomalies, an extensive and long-lasting magma reservoir and is believed to be heavily intruded, representing an almost oceanic crust, close to continental breakup (Ahmed et al., 2022; Ayalew et al., 2019; Ayele et al., 2009; Bridges et al., 2012; Desissa et al., 2013; Didana et al., 2014; Hammond et al., 2011; Johnson et al., 2016; Lewi et al., 2016; Reed et al., 2014). Towards the southeast, the Dabbahu-Manda Hararo rift segment is prolonged by the Tendaho graben. The Tendaho Graben accommodates approximately 6 mm/yr of extension, mainly along its northern fault (Gamari Fault) and in the Manda Gargori graben (Doubre et al., 2017, see also Fig. 9). This area witnesses strong seismic activity (e.g. Ruch et al., 2021 and Fig. 10), as shown by the deadly 1969 Serdo earthquake (Gouin, 1979).

The Teru Graben and the Ma'Alalta volcano represents the northernmost prolongation of the Dabbahu – Manda Hararo rift segment and is considered to be an active rift segment (Tortelli et al., 2021). The data of Moore et al. (2021) show that this segment is probably not accommodating significant extension and that most of the strain is transferred from the Dabbahu – Manda Hararo rift segment to the Tat'Ali – Dadar and Erta Ale rift segment by the Alayta – Afdera Transfer Zone (Barberi et al., 1974; Barberi and Varet, 1977; Schaegis et al., 2021).

The Tat'Ali – Dadar forms a rift segment with active faulting (Sangha et al., 2022), Recent acidic and basaltic volcanism but most of the strain seems to be currently accommodated by the Dabbahu – Manda Hararo rift segment except for the northern part of the segment (Lahitte et al., 2003a; Moore et al., 2021; Sangha et al., 2022). Further north, the Erta Ale – Tat'Ali Transfer Zone links the Tat'Ali and Erta Ale rift segments (Illsley-Kemp et al., 2018a, 2018b; La Rosa et al., 2019, 2021, 2022).

The Erta Ale Rift Rift Segment runs from Lake Afdera in the south to the Gulf of Zula in the north. It shows an alignment of very active Recent (see section 4.13.2) shield volcanoes (Barberi and Varet, 1970, 1972; Barrat et al., 1998; Global Volcanism Program, 2013; Hagos et al., 2016a; Magee et al., 2017; Pagli et al., 2012; Watts et al., 2020; Xu et al., 2017, 2020). Based on the structure of this part of the basin as well as the petrology of the Erta Ale Range, several authors postulated that it represents the point of continental breakup or even proto-oceanic spreading (Barberi et al., 1970; Barberi and Varet, 1970, 1977; Barrat et al., 1998; Hurman et al., 2023; Watts et al., 2020). In the north, the basin is covered by a rapidly subsiding salt plain punctured by the Dallol and Maraho volcanoes (Bastow et al., 2018; Hurman et al., 2023). In the north, finally, the Erta Ale Rift Segment forms the Recent Buia graben (Sani et al., 2017). The whole rift segment experiences significant seismicity and dyke emplacement (Gouin, 1979; La Rosa et al., 2023; Moore et al., 2021; Nobile et al., 2012; Ruch et al., 2021). While the margins show significant seismicity, extension in the rift axis accommodates most of the long-term extension (Illsley-Kemp et al., 2018a, 2018b; Moore et al., 2021). In the short term, the InSAR data of Moore et al. (2021) also show that extension is focused in the centre of the Depression. Further north, Viltres et al. (2020) show that the rift axis is situated west of Mt. Ghedem (see Fig. 8).

5.2.2.5. The Red Sea Rift. The Red Sea Rift is probably composed of one single segment in the study area, represented by the central trough of the Red Sea. It likely does not extend further south than the Hanish Islands (see sections 4.3.1 and 5.1.1). It shows significant seismic and magmatic activity, as testified by the formation of new volcanic islands (Ruch et al., 2021; Xu et al., 2015).

5.3. Structural inheritance

Structural inheritance is known to control rift localisation, geometry and evolution (e.g. Brune et al., 2023; Buiter and Torsvik, 2014; Camanni and Ye, 2022; Molnar et al., 2019; Zwaan et al., 2022). In the Afro-Arabian Rift System, there is a general agreement that older structures influence rift development (e.g. Beyth, 1991; Black et al., 1974; Corti et al., 2018a, 2022; Dixon et al., 1987; Ghebreab, 1998; Korme et al., 2004; Varet, 2021). These structures were therefore mapped (Fig. 11) to understand their potential influence on the evolution of the Afar region.

Two types of structures form crustal weaknesses in the study area and were potentially reactivated during the Cenozoic rifting phase: The first type are lineaments and suture zones found in the basement. These structures are often curved and mainly represent ductile deformations developed during the Precambrian East African orogeny cycle (see section 4.1). The prominent sutures relevant to the Afar region are the ones separating the Asir, Tathlith, Abas, Al-Bayda, Al-Mafid and Al-Mukalla terranes (Flowerdew et al., 2013; Fritz et al., 2013; Johnson, 2021; Johnson et al., 2011; Osman and Fowler, 2021; Quick, 1991; Windley et al., 1996). These structures are represented in Fig. 11 and Suppl. Mat. 3 (see Table 3 for references). The second type are straight linear features that developed after this orogeny. Most of them are faults but also dykes that are interpreted to reactivate pre-rift weaknesses. Five major recurrent linear structure orientations have been recognized in the literature and/or mapped in the study area (Fig. 11). For convenience, we name those orientations after localities or names used in the literature.

- **Mekele orientation, NW-SE:** This orientation is ubiquitous throughout the study area (Fig. 11) and was formed during the Upper Jurassic – Lower Cretaceous rifting phase (see section 4.1). Rifting resulted in many grabens and basins, including the Mekele Basin (Beyth, 1972; Black et al., 1974; Sembroni et al., 2017), the Blue Nile Basin, spanning from Sudan to SE Ethiopian (Chernet et al., 2020; Gani et al., 2009; Hunegnaw et al., 1998; McHargue et al., 1992; Salama, 1985, we arbitrarily name them "*Sudanese*", "*Central*" and "*Ogaden*" *Blue Nile* on Fig. 11), numerous rifts in Sudan and South Sudan (e.g. Atbara rift, Melut Basin, Dou et al., 2007; Guiraud et al., 2005; McHargue et al., 1992; Mohamed et al., 2016; Salama, 1985), the Somaliland basins (e.g. Nogal basins, Ali and Lee, 2019; Ali and Watts, 2016))and the southern Yemenites basins (e.g. Marib- Shabwa basin As-Saruri et al., 2010; Redfern and Jones, 1995). Due to their

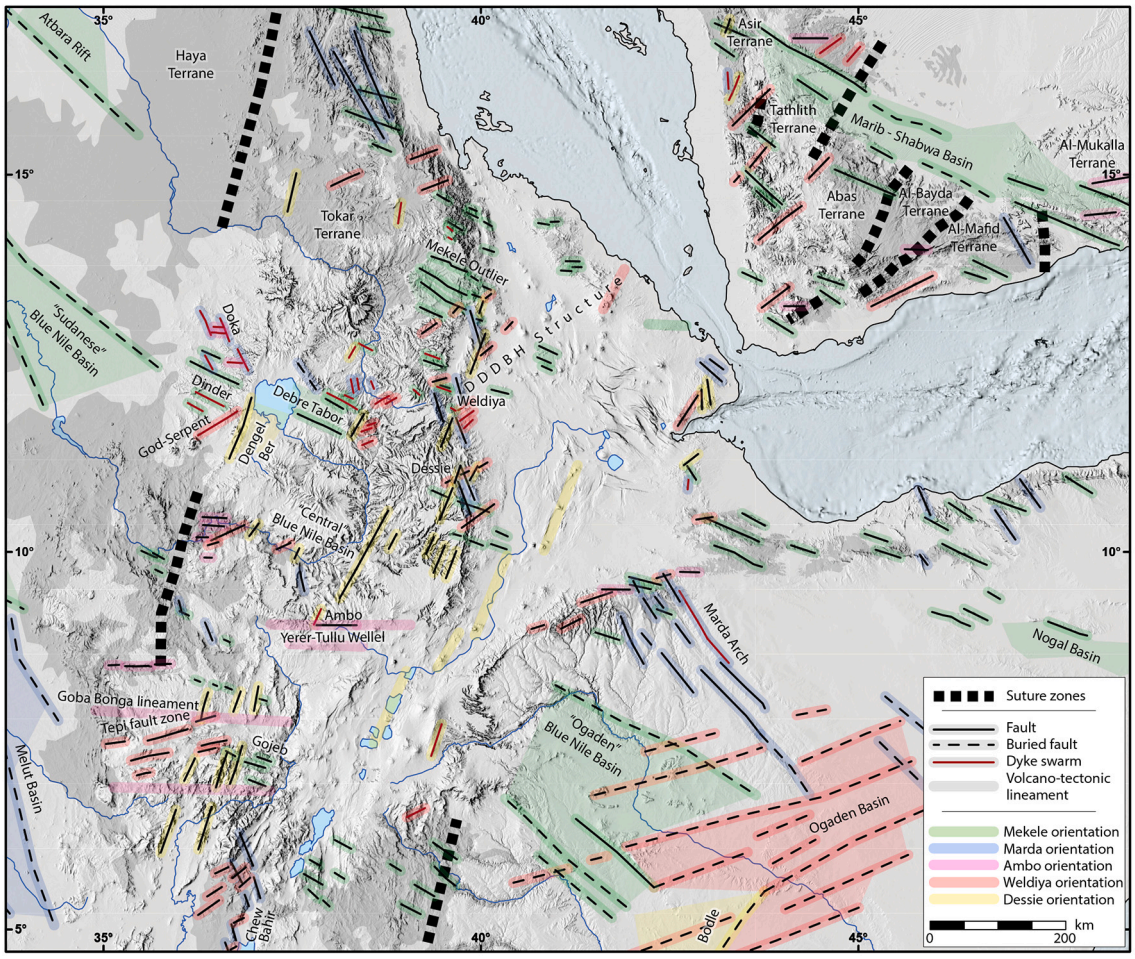

Fig. 11. Main potential inherited structures. Suture zones and linear features are represented. Greyed out areas represent basement outcrop. The restoration of this map to pre-rift configuration is presented in Suppl. Mat. 9. Faults after Ali and Lee (2019), Ali and Watts (2016), Chorowicz et al. (1998), Corti et al. (2018b, 2022), Dou et al. (2007), Gani et al. (2009), Geological Survey of Ethiopia (1996), Hunegnaw et al. (1998), McHargue et al. (1992), Mège and Korme (2004), Mohamed et al. (2016), Mohr and Zanettin (1988), Moore and Davidson (1978), Philippon et al. (2014), Redfern and Jones (1995), Rime et al. (2022a, 2022b), Rooney et al. (2018), Salama (1985), SRTMGL1 and WGM2012 Free Air gravity data (Bonvalot et al., 2012). Suture zones after sources presented in Table 3.

orientation roughly perpendicular to the Arabian - Nubian/Somalian extension, many of these structures were reactivated during the Cenozoic, mainly in the Gulf of Aden (Ali, 2015; Beydoun, 1970; Leroy et al., 2012), but also in the Mekele outlier (Hagos et al., 2020). These structures are also observed in areas covered by syn-rift rocks, e.g. in the Debre Tabor graben (Chorowicz et al., 1998; Hautot et al., 2006), Dinder Dyke Swarm (Mège and Korme, 2004; Rooney et al., 2018) and the Gojeb graben (Corti et al., 2018b, 2022).

- **Marda orientation, NNW-SSE:** This orientation has been recognized for a long time (Black et al., 1974; Ghebreab, 1998; Korme et al., 2004; Mège et al., 2016; Purcell, 1976), forming a prominent fault zone on the Somalian plateau, prolonging in the Ogaden basin (Hunegnaw et al., 1998). It is believed to represent a Precambrian fault zone being reactivated in the late Oligocene resulting in an major dyke swarm (also called Ogaden Dyke Swarm). The orientation is similar to the main Red Sea orientation, structuring most of the Afar western margin (Chorowicz et al., 1999; Zwaan et al., 2020b and Fig. 11). This orientation also forms the Doke Dyke swarm (Rooney et al., 2018), contributes to the structure of the Chew Bahir basin (e.g. Corti et al., 2022; Philippon et al., 2014), the Melut Basin (Dou et al., 2007; Mohamed et al., 2016) and some faults of the Gulf of Aden (Fig. 11).
- **Ambo orientation, E-W**: This orientation is not pervasive over the whole study area but represents a major discontinuity in the western MER margin, forming the *Yerer-Tullu Wellel volcano-tectonic lineament*, of which the Ambo fault is part. This lineament, and the similar *Goba Bonga lineament*, represent major crustal discontinuities, possibly delineating Precambrian crustal weakness (Abebe et al., 1998; Berhe, 1986; Bowden et al., 2022; Corti, 2009; Corti et al., 2018a, 2018b, 2022; Gashawbeza et al., 2004; Keranen and Klemperer, 2008; Korme et al., 2004; Mohr, 1967). They have an significant influence on the structure of the Main Ethiopian Rift. E-W oriented structures are also found on the Afar south-eastern margin, NW of Lake Tana (Rooney et al., 2018) and in south-eastern Yemen, but a clear link is difficult to establish.
- **Weldiya orientation, NE-SW:** This orientation is represented by many faults and dykes throughout the study area (Fig. 11). Faults of this orientation structure the Yemenite eastern margin (Fig. 11, Collet et al., 2000). In central Ethiopia, this orientation represents many dykes, including the God-Serpent dyke swarm (Chorowicz et al., 1998; Mège and Korme, 2004; Rooney et al., 2018), dykes east of Debre Tabor and the ones present near Weldiya, on the central-western Afar margin (Figs. 4 and 11). Multiple faults cutting through the western Afar margin have the same orientation (Fig. 11, Collet et al., 2000; Kronberg et al., 1974b, 1975). It furthermore corresponds to the orientation of the Tepi fault zone (Corti et al., 2018b, 2022; Moore and Davidson, 1978), one of the fault sets structuring the Chew Bahir basin (Corti et al., 2022; Philippon et al., 2014), the south eastern margin of the Afar (Figs. 4 and 11) and the Ogaden basin (Hunegnaw et al., 1998; Worku and Astin, 1992). The

widespread nature of this orientation hints at a pre-rift age (Kronberg et al., 1975) and the similarity with the structures of the Ogaden basin could indicate that this structural trend formed during the Karoo rifting phase in eastern Africa, i.e. being Permian to Triassic in age (see section 4.1).

- **Dessie orientation, NNE-SSW:** This orientation is mainly present in the Nubian part of the study area. It is predominantly present in the Central Blue Nile Basin (Gani et al., 2009; Kronberg et al., 1974b, 1975), reaching the western Afar margin, notably in the vicinity of Dessie (Figs. 4 and 11), but it is also visible in southern Ethiopia and forms the Dengel Ber graben (Chorowicz et al., 1998). It is unclear when these structures formed and whether they represent a structural inheritance. As this orientation is roughly perpendicular to the Nubia – Somalia extension and parallel to the Wonji fault belt, it is plausible that it was formed since the Miocene, when the strain was not yet focused in the MER. The possibility of pre-rift influence is, however, plausible as such structures are also found in northern Ethiopia. Chorowicz et al. (1998) furthermore noted that the Dengel Ber graben predates the termination of flood volcanism indicating at least an Oligocene age. Hunegnaw et al. (1998) and Shawel et al. (2022) show that the *Mandera Bodle Rift* in southern Ogaden has the same orientation and is floored by Carboniferous to Permian sediments. Similarly, Hercynian (Devonian to Carboniferous) structures in eastern Arabia show a similar N-S to NNE-SSW orientation (e.g. Qatar Arch, Faqira et al., 2009; Geert et al., 2001; Stewart, 2016).

Both basement lineaments/suture zones and linear discontinuities certainly play a role in the localisation and segmentation of the rift. When brought back to pre-rift position (section 6.1 and Suppl. Mat. 9), the major sutures between Abas, Al-Bayda and Al-Mafid terranes align with the NMER and could potentially extend under the Yerer-Tullu Wellel volcano-tectonic lineament that represents a crustal-scale discontinuity (see above). These terrane boundaries also align with the pre-rift boundary between the Danakil Block and the Ali Sabieh Block (Suppl. Mat. 9). The presence of these suture zones combined with different linear discontinuities (see Suppl. Mat. 9) formed an significant weakness zone in present-day Afar Depression which probably contributed to the localization of the Afar Rift.

The contribution of the Dessie, Weldiya and Mekele discontinuities to the segmentation of the Afar Depression and NMER is noticeable. The step from the Fantale-Dofen and Issa rift segments corresponds to the presence of Mekele discontinuities potentially extending up to Dire Dawa (Figs. 4 and 13). The difference between the south-western and central-western Afar experiencing slightly different geological histories (Fig. 7) could also be explained by the prominent Weldiya-oriented structures. SE of Dessie, Wolfenden et al. (2005) measured an ENE-striking fault zone (the "Dese-Bati accommodation zone") featuring at least 800 m of sinistral offset. The major eastward step of the western Afar margin between the central-western Afar and the Danakil Depression also coincides with Weldiya and Dessie-oriented faults and dykes (Figs. 4 and 11). This Weldiya-oriented structure can be traced further away from the western margin to the active volcanic range of Dabbayra, the Alayta-Afdera Transfer Zone and the Nabro volcanic range. It is also along this lineament that Tertiary intrusive rocks are outcropping (Limmo, Asa Ale, Affara Dara and Dioita granites). This alignment is believed to represent a transfer zone along a pre-rift crustal weakness (Barberi and Varet, 1977; Black et al., 1972; Tazieff et al., 1972; Varet, 2018). Varet (2018) calls it the *DDDBH Fracture Zone* (Dabbayra-Dababhu-Dubi-Bidu-Hanish) but we instead call it the *DDDBH Structure* to avoid any interpretation. The kinematic reconstruction (section 6.1) postulates that this structure extends to a fault zone of similar orientation identified in Yemen (Suppl. Mat. 9). The DDDBH structure also roughly coincides with the limit between the Arrata Microplate and the southern Danakil Block, i.e., the present-day boundary of the Arabian plate (see section 5.1.1).

It can therefore be postulated that the structural inheritance of both Precambrian lineaments/suture zones and younger faults sets played a role in the localization of the Afar Rift and the segmentation of the rift.

6. Evolution of the Afar region

6.1. Kinematic modelling

A wide range of different models for the evolution of the Afar region has been presented in the literature (Acton et al., 1991, 2000; Barberi and Varet, 1977; Beyene and Abdelsalam, 2005; Bosworth et al., 2005; Collet et al., 2000; Crossley et al., 1992; Eagles et al., 2002; Garfunkel and Beyth, 2006; Gaulier and Huchon, 1991; Hammond et al., 2011; Le Pichon and Francheteau, 1978; Manighetti et al., 2001; McClusky et al., 2010; Mohr, 1970, 1972; Purcell, 2018; Sani et al., 2017; Schettino et al., 2016; Sichler, 1980; Stab et al., 2016; Tazieff et al., 1972; Wolfenden et al., 2004; Zwaan et al., 2020b). However, there is currently no holistic, detailed model for the evolution of the Afar region spanning the complete rift history, considering the complex geological structure of the Depression and including the Red Sea – Gulf of Aden rift system.

The new geological maps of the Afar Depression (Fig. 4), of the southern Red Sea & western Gulf of Aden region (Fig. 6), and the map of basement structures (Suppl. Mat. 3), along with the review of the geological history and tectonic structure of the region (sections 4 and 5) allow proposing a new model for the kinematic evolution of the Afar region. In order to present a kinematically and geometrically coherent and plausible model, modelling was performed using GPlates 2.3.0 (Müller et al., 2018). We did not model complex intraplate deformation but only constructed a model including rigid plates, microplates, blocks or *tectonic elements* (a more generic term than plate or block, see e.g. Vérard, 2021). A movie of the kinematic model is presented in Suppl. Mat 18, and data are available in Suppl. Mat. 19.

The model is constrained by the position of the three main plates (Nubian, Somalian and Arabian) through time. We used the Arabian plate as the reference plate. The Somalian plate was then moved relative to the Arabian plate according to the relatively well-constrained magnetic anomalies of the Gulf of Aden presented by Fournier et al. (2010) with ages updated according to Ogg (2020) (Suppl. Mat. 10). Movement before the last recognized magnetic anomaly is modelled to match structures on both sides of the Gulf of Aden (see Suppl. Mat. 11).

Because of the lack of magnetic anomalies in the Red Sea older than 6.3 Ma (Izzeldin, 1987) or 4.3 Ma (Schettino et al., 2016), the movement of the Nubian plate was tied to the Somalian plate. A study of magnetic anomalies in the southern Indian Ocean defines the relative movement of the two plates, but this movement does not correspond to geological evidence, probably due to structures outside of the MER accommodating a significant amount of strain (DeMets et al., 2021). We thus modelled the movement of the Nubian plate relative to the Somalian one with the following assumptions. The Precambrian basement suture zones and other distinctive features (Fig. 6 and Suppl. Mat. 3) must align between the Nubian and Arabian plates before rifting (see Suppl. Mat. 11, 12 and 13). The movement also needs to be coherent with the opening of the Gulf of Suez and the movement along the Dead Sea fault (section 4.3.1). This defines the position of the Nubian plate relative to the Somalian plate in pre-rift times. They remain fixed relative to each other until rifting begins in the NMER around ~13 Ma (see section 4.9). The present-day position of the plate defines its movement between 13 Ma and the Present. The magnetic anomalies of the Red Sea (Izzeldin, 1987; Schettino et al., 2016, Suppl. Mat. 10) were therefore not used to construct this model but the result led to an excellent match of these anomalies (see Suppl. Mat. 18), highlighting the plausibility of the model.

The movement of the other tectonic elements of the Afar region was then modelled according to the geological evidences described in sections 4 and 5 and considering the correlation of transverse and potentially pre-rift structures (section 5.3, Suppl. Mat. 11 and 12). We used 14 tectonic elements to model the deformation of the Afar region (Suppl.

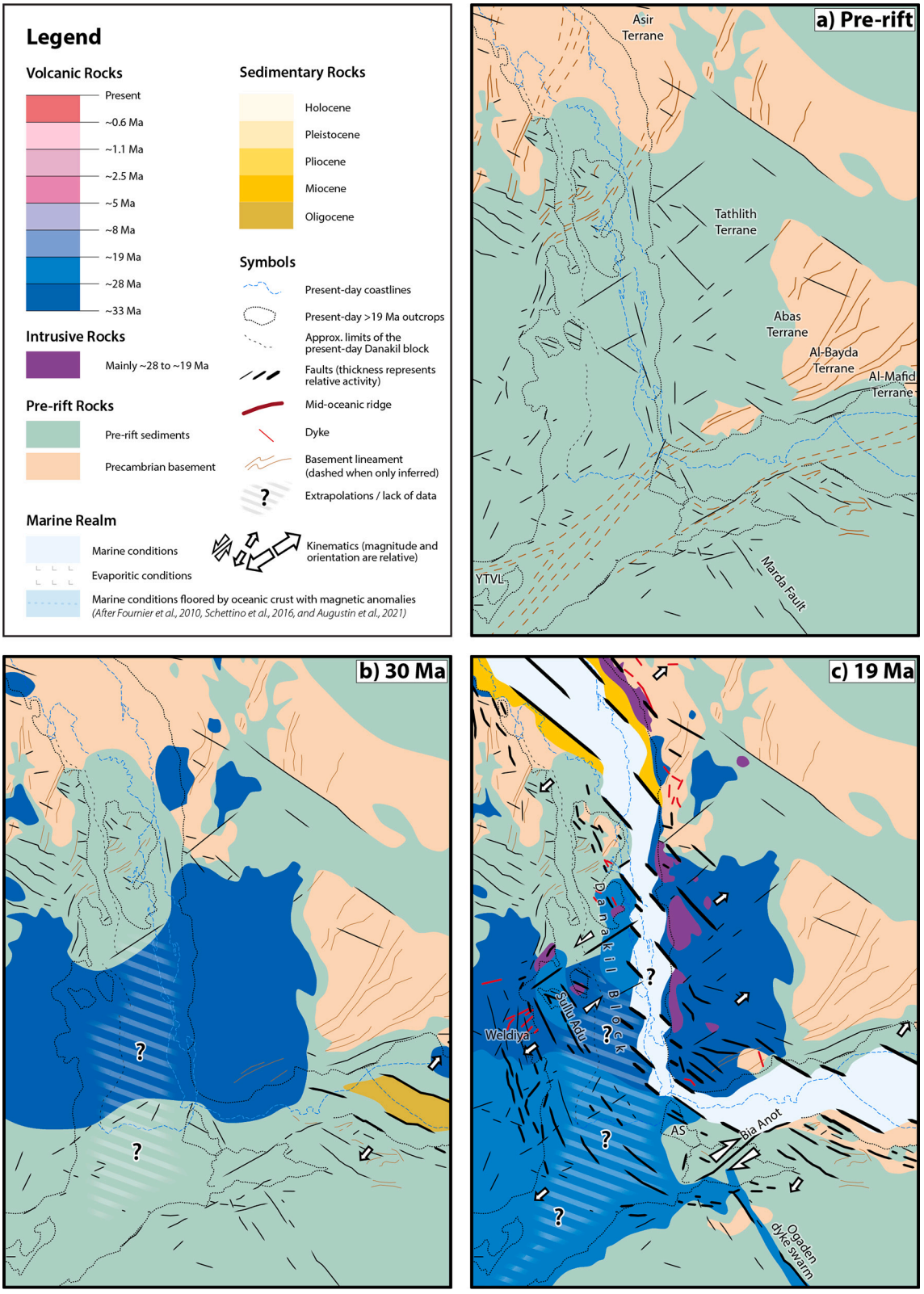

Fig. 12. Tectonostratigraphic evolution of the Afar region. Paleogeological map of the evolution of the Afar Depression and surrounding regions for pre-rift times (a), ~30 Ma (b), ~19 Ma (c), ~13 Ma (d), ~8 Ma (e), ~5 Ma (f), ~2.5 Ma (g), ~1 Ma (h), and present day (i). This model is based on the GPlates kinematic model, our review of the geological history of the region (section 4 and Fig. 7) and on the geological maps presented in Figs. 4 and 6. Note that the model has to be considered as conceptual, schematic and hypothetical. AG = Asal-Ghoubbet, AS = Ali Sabieh Block, F-D = Fentale-Dofen, GoT = Gulf of Tadjoura, YRVL = Yerer-Tullu Wellel volcanotectonic lineament.

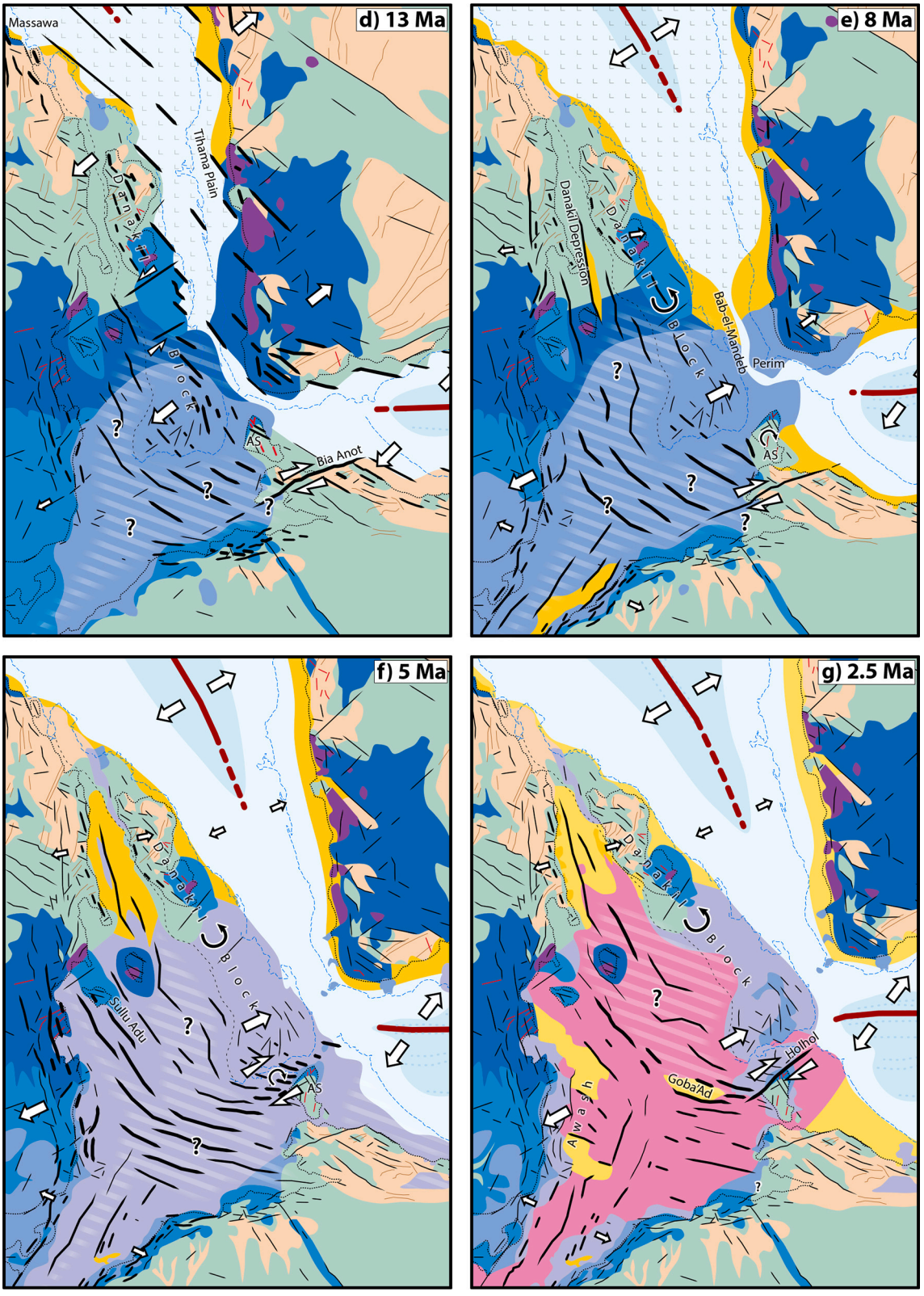

Fig. 12. (*continued*).

Mat. 14). While it is known that the central-eastern Afar does not behave as rigid blocks (Manighetti et al., 2001), these blocks were necessary for the modelling. This is to avoid kinematic incoherence and to serve as a guide to produce a coherent graphical output for the paleogeological maps (Fig. 12).

Unlike all models except the one by Gaulier and Huchon et al. (1991), we did not model the Danakil Block as a single rigid block. Considering the pre-rift configuration of the three main tectonic plates described above and the critical step on the western Afar margin between 12 and 13°N linked to the DDDBH structure, the consideration of

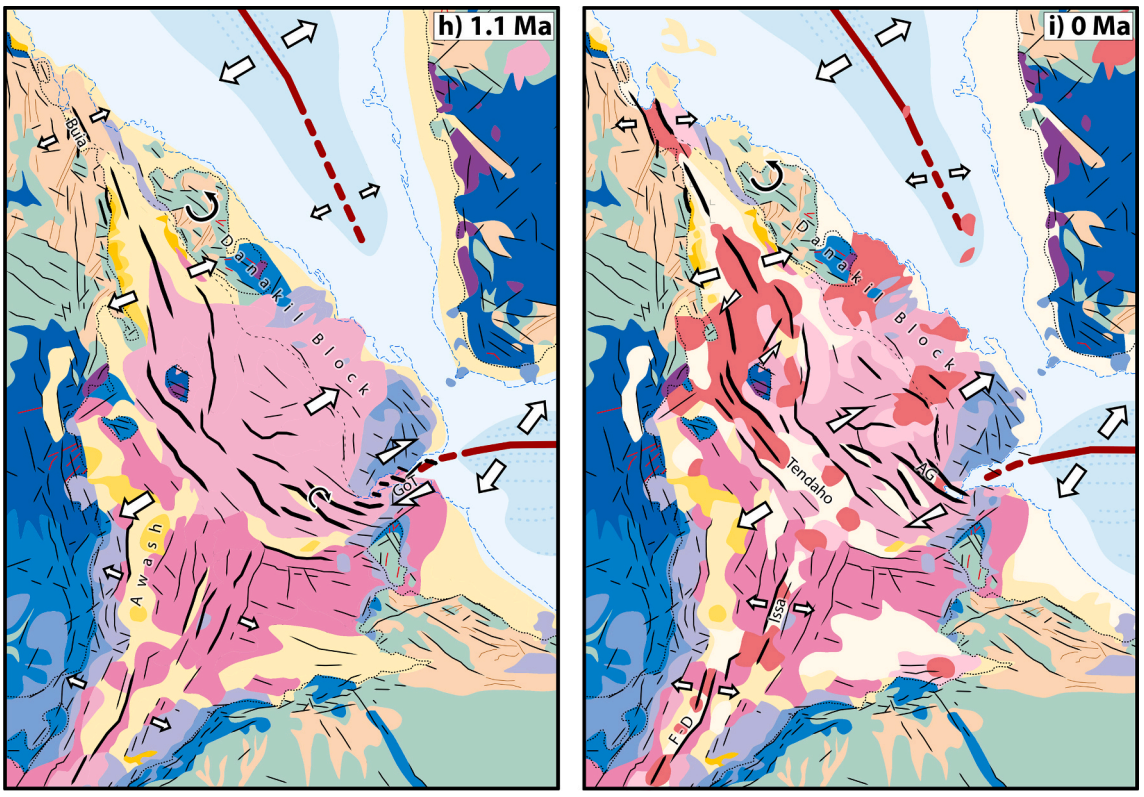

Fig. 12. (*continued*).

a rigid Danakil Block would have implied significant shortening (compression) in the northern part of the Danakil Depression. Conversely, it is known that the Danakil nowadays represent a plate boundary (see section 5.1.1 and Fig. 9) and that the NW-SE- orientated, probably pre-rift DDDBH structure strongly influences the structure of the region (see section 5.3). Near the town of Weldiya, the dykes with the same orientation were dated between 21 and 17 Ma by Ayalew et al. (2019), testifying to the activity of the structure during early rift development. We thus segmented the Danakil Block according to this orientation in the Nabro range and across Beilul Bay. Like other studies (Chu and Gordon, 1998; Eagles et al., 2002; Schettino et al., 2016), we also separated the Buri peninsula from the Danakil Block in the Howlakil Bay that is marked by a positive Bouguer gravity anomaly (Suppl. Mat. 4) and by seismic activity (Fig. 10). This avoids any compression in the north during the rotation of the Danakil Block.

As discussed in section 5.1.2, the kinematics and timing of movement of the Ali Sabieh Block are poorly constrained. The pre-rift configuration suggests that this Block was situated in present-day south-eastern Afar. We modelled movement along the eastern Bia Anot fault since early rifting followed by rotation accommodated in the northern Bia Anot discontinuity. To avoid overlap of the Danakil and Ali Sabieh Block, the latter must rotate ahead of the Danakil Block, consistently with the observation of no rotation since at least 8 Ma (Audin et al., 2004).

6.2. *Tectonostratigraphic evolution of the Afar region*

The tectonostratigraphic evolution of the Afar region is discussed based on the geological history of the different parts of the Afar (section 4, Fig. 7), the tectonic structure of the Afar (section 5), and the new kinematic model (section 6.1). Note that despite the consideration of many sources and references, the kinematic model has to be considered conceptual, schematic and hypothetical.

Prior to rifting and the eruption of the Traps (Fig. 12a), the region was structured by Precambrian and Phanerozoic inherited structures (section 5.3). The suture zones between the Abas, Al-Bayda, Al-Mafid and Al-Mukalla terranes probably extended into the future southern Afar, NMER and possibly continued under the Yerer-Tullu Wellel volcano-tectonic lineament (YTVL). The Marda fault potentially extended under the future Red Sea Rift.

Between 33 and 28 Ma (Fig. 12b), a short pulse of hotspot-related volcanism led to the deposition of a significant thickness of volcanic material (the "Traps") in the northern part of Ethiopia and in Yemen (sections 4.4 and 4.5 and references therein). Before 30 Ma, tectonic movements are only recorded in the eastern and central Gulf of Aden (Fig. 7).

During the late Oligocene and Early Miocene (~28 to ~19 Ma, Fig. 12c), Trap basalts erupted further towards the south (sections 4.4, 4.8 and references therein). The Ogaden dyke swarm, reactivating the Marda fault zone, was also emplaced, along with several plutonic bodies and dykes in the Afar region and along the Yemenite and Saudi coast (sections 4.8, 4.3.1, 4.11 and references therein). Rifting was mainly concentrated in the Gulf of Aden and Red Sea margins, affecting the Eritrean, Somalian and Yemenite coasts, as well as the Danakil Block (sections 4.2, 4.3.1, 4.6 and references therein). In the Afar Depression, the first tectonic movements are reported at the south-western Afar margin and in Sullu Adu (section 4.10 and references therein). As no movement is recorded in the Danakil Depression, a transfer zone probably developed between Sullu Adu and the Red Sea, potentially reactivating Weldiya (SW-NE) oriented inherited structures, as shown by the ~20 Ma dykes of the same orientation observed near the eponym city. It is plausible that the Ali Sabieh Block (AS on Fig. 12) began separating from the Somalian plateaux around the same time, potentially activating the Bia Anot Fault. The different rift segments probably reactivated some of the Mekele (NW-SE) and Marda (NNW-SSE) oriented faults. At that time, an early sea probably made its way from the Gulf of Aden to the Red Sea but the configuration of this sea is unknown (section 4.3.2 and references therein). Oceanic spreading had just begun by ~19.5 Ma east of the Sheba ridge (section 4.2 and references therein).

Between ~19 and ~ 13 Ma (Fig. 12d), the eruption of volcanic material continued on the present-day Ali Sabieh and Southern Danakil Blocks, as well as in the eastern part of the future NMER and the south-western Afar margin (sections 4.7, 4.6, 4.9, 4.10 and references therein). Tectonic movement accelerates with the westward propagation of the Gulf of Aden Rift. At ~16 Ma, oceanic spreading began in the western Gulf of Aden (Fournier et al., 2010). The majority of the tectonic movements in the Afar region are concentrated on the Red Sea and Gulf of Aden margins. The central-western Afar margin experiences a period of volcanic quiescence, but some strain was probably accommodated in present-day southern/central Afar (sections 4.11 and references therein). According to our kinematic model, the Ali Sabieh Block moved away from the Somalian Plateau during this period, possibly dragged by the Arabian plate. As discussed in section 5.1.2, it is unclear how this movement is accommodated, but we model a strike-slip motion on the eastern Bia Anot fault. This is consistent with Gaulier and Huchon et al. (1991) reporting sinistral movements during this period. The marine realm expanded significantly. During the Mid-Miocene, the Sea extended further than today under the Tihama plain (Hakimi et al., 2021) and near Massawa (Sagri et al., 1998), but during the Langhian-Serravallian (~16–12 Ma), conditions became increasingly restricted (section 4.3.2 and references therein).

The period between 13 and 8 Ma (Fig. 12e) corresponds to the most critical changes in the regional geodynamics since rifting initiation. It coincides with a major change in the dynamic of the East African Rift System (Michon et al., 2022). Oceanic spreading in the central Red Sea is believed to begin around 13 Ma (section 4.3.1 and references therein). This period also corresponds to a major reorganisation in the northern part of the Red Sea with the abandonment of the Gulf of Suez and the full strain transfer to the Dead Sea Fault (section 4.3.1). The deposition of sediments of the Chorora Fm in an initial depression marks the initial development of the NMER (section 4.9 and references therein). This changes the Afar region from a two plates system to a triple junction with three distinct major tectonic plates. Another major change is the individualization of the Danakil Block and the beginning of its rotation, caused by the significant reduction in the tectonic activity of the southern Red Sea rift and the related increase in activity of the Afar Rift (sections 4.3.1, 4.13.2 and references therein). This constitutes an major rift jump. The Afar Rift begins its northward propagation, and rifting initiates in the Danakil Depression (section 4.13.2). The Bab-el-Mandeb area is probably devoid of tectonic activity since these times (section 4.3.1). According to our model, the Ali Sabieh Block rotated to reach its present-day position during this period. Eruptions are reported on the southern Ethiopian plateaux, in the NMER, on the southern Danakil Block and near the Bab-el-Mandeb strait (sections 4.4, 4.9, 4.6, 4.3.2 and references therein). The connection between the Gulf of Aden and the Red Sea was strongly reduced, leading to evaporitic conditions throughout the Red Sea (section 4.3.2 and references therein). The temporal coincidence between the end of active rifting of the southernmost Red Sea and the restricted conditions in the Red Sea evidence a potential link. The absence of active rifting coupled with dynamic topography (Moucha and Forte, 2011) caused by the plume probably triggered uplift or at least reduced subsidence, which, coupled with global relative sea level fall during the Mid-Miocene Climatic Transition (MMCT, Miller et al., 2020), led to the isolation of the basin. Sedimentation at the foot of the Yemenite escarpment and the only slightly younger eruption of the Perim volcano might also have played a role in this isolation.

The period between 8 and 5 Ma (Fig. 12f) is marked by the eruption of the Dahla basalts across the Afar Depression and possibly along the Somalian coast (sections 4.6, 4.7, 4.8, 4.9, 4.10, 4.11, 4.13.2, references therein and Ali, 2009, 2015; Ali et al., 2018). Significant tectonic movements are also reported in the western Afar margin, in Sullu Adu and probably in southern Afar (sections 4.8, 4.10, 4.11 and references therein). The development of the Danakil Depression continues, accommodating sediments and a few lava flows (sections 4.13.2 and references therein). The rotation reported at the NW margin of the Ali Sabieh Block probably indicates that strain between the Danakil and Ali Sabieh Blocks was accommodated in that area (Audin et al., 2004). In the NMER, the border faults are gradually less active as strain is concentrated in the central part rift (section 4.9 and references therein). The Red Sea margins were probably nearly devoid of tectonic activity (section 4.3.1 and references therein), the strain being accommodated by the oceanic spreading in the north and by the Afar Rift in the south, forming a relay structure. After the deposition of significant evaporites, the Red Sea again experiences marine conditions (section 4.3.2 and references therein).

Between 5 and 2.5 Ma (Fig. 12 g), the Afar Depression is marked by the eruption of the lower Stratoid Fm nowadays ubiquitously outcropping south of the Tendaho – Goba'Ad discontinuity (section 4.7, 4.8, 4.9, 4.10, 4.11 and references therein). The rotation of the Danakil Block is accommodated along the Holhol fault (Audin et al., 2004) and in southern and central Afar, where sedimentary basins are forming in Goba'Ad (section 4.12), as well as in the Middle and Lower Awash valley. Last being important for the first Hominine ancestors thriving in a lacustrine and fluvial environment (section 4.10 and references therein). The Danakil Depression accumulated sediments and magmatic material (section 4.13.2 and references therein). Extension is primarily accommodated by seafloor spreading in the Red Sea and the Gulf of Aden, (sections 4.2, 4.3 and references therein).

Between 2.5 and 1.1 Ma (Fig. 12 h), the central-eastern Afar experiences voluminous volcanic eruptions forming the upper Stratoid Series (section 4.12 and references therein) and corresponding to a northward shift of tectonic activity from the southern Afar to the central-eastern Afar (Tortelli et al., 2022). It also constitutes a triple junction migration (Hammond et al., 2011; Kalb, 1995; Tesfaye et al., 2003; Wolfenden et al., 2004), probably caused by the significantly higher velocities of the Arabian plate compared to the Somalian one (Maestrelli et al., 2022). The Afar Rift continues its northward propagation with sedimentation in the Danakil basin and the beginning of the opening of the Buia graben (sections 4.13.2, 4.13.3 and references therein). The rotation of the Danakil Block is accommodated by block rotation in central-eastern Afar, and strain is transferred from the Holhol fault to the present-day Gulf of Tadjoura (GoT on Fig. 12, see sections 4.7, 4.12 and references therein). Significant sedimentation is also ongoing in the Awash valley and the Danakil Depression (sections 4.10, 4.13 and references therein).

Between 1.1 Ma and the present day (Fig. 12i), the Afar Depression witnesses the propagation of the Gulf of Aden Rift, forming the Asal-Ghoubbet graben (AG on Fig. 12, see section 4.3 and references therein). The linkage between the Gulf of Aden Rift and the Afar Rift is achieved through a series of en-echelon faults block rotation and rift focussing in central-eastern Afar (sections 4.12 and references therein). Volcanic eruptions focus in active rift segments (Asal, Manda Inakir, Dabbahu-Manda Hararo, Erta Ale, Issa Graben, Fentale, Hanish, Zubair, Jebel at Tair) and volcanoes at the margins (Nabro, Ma'Alalta, Moussa Ali, Dembel, Dabbayra) (sections 4.2, 4.3.1, 4.6, 4.8, 4.9, 4.10, 4.11, 4.12, 4.13 and references therein). Continental sedimentation fills the Tendaho graben and other grabens, as well as the Danakil Depression. The sea starts invading the latter, and the Asal-Ghoubbet graben during sea-level highstands, forming substantial evaporite deposits (sections 4.2, 4.12, 4.13.2 and references therein). In the NMER and southern Afar, the tectonic and volcanic activity is mainly restricted to the Wonji segments (Fantale-Dofen (F—D on Fig. 12) and Issa).

7. Different rifting styles in the Afar Depression

7.1. Central Afar domain versus Danakil domain

Similar to Ahmed et al. (2022), Keir et al. (2013), Le Gall et al. (2018) and Stab et al. (2016), we identify two different domains featuring different rifting styles, magmatic and sedimentary histories: the "Danakil" domain and the "Central Afar" domain (see Table 4, Fig. 13).

Table 4
Comparison between the Central Afar and Danakil domains.

	Central Afar Domain	Danakil Domain
Topography	Wide depression with grabens. Elevation between 350 and 1000 m	Valley shape with elevations below sea level (down to −125 m)
Extension	Significant extension (~200–250 km)	Lower extension (~10–100 km)
Stretching factor	Higher	Smaller
Relative age of rifting	Older	Younger
Crustal thickness	Relatively thick crust with Moho depth of around 24 km	Relatively thin crust with Moho depth of around 22 km, possibly as low as 14 km.
Oligocene to Mid-Miocene magmatism	Voluminous (between 1 and 2 km thickness) flood basalt deposits covering the margin	Only one large magmatic deposit in Adigrat (0.6 km thick). Dykes and plugs on the margins of the Depression.
Basin fill	Vastly dominated by lavas	Dominated by sediments intercalated by lava flows
Syn-rift magmatism	at least 1.5 km of Pleistocene lavas and possibly ~1 km of Mio-Pliocene lavas	Metric- to decametric-scale flows and sills in the Red Bed Series
Recent (<0.6 Ma) magmatic history	Voluminous lava deposits, mainly in the Dabbahu-Manda Hararo range	Voluminous lava deposits in the southern part of the rift axis (Erta Ale range)
Underplating	Evidences for magmatic underplating	No evidence for magmatic underplating
Strain accommodation	Significant magma-accommodated extension	Mechanical extension in the N, magma-accommodated extension in the Erta Ale Range.
Thinning	Magma-compensated thinning	Non-compensated thinning
Rift localization	Distributed extension, incorporation of continental fragments	Clear rift localization in the centre of the rift valley
Hotspot influence	Strong	Less significant

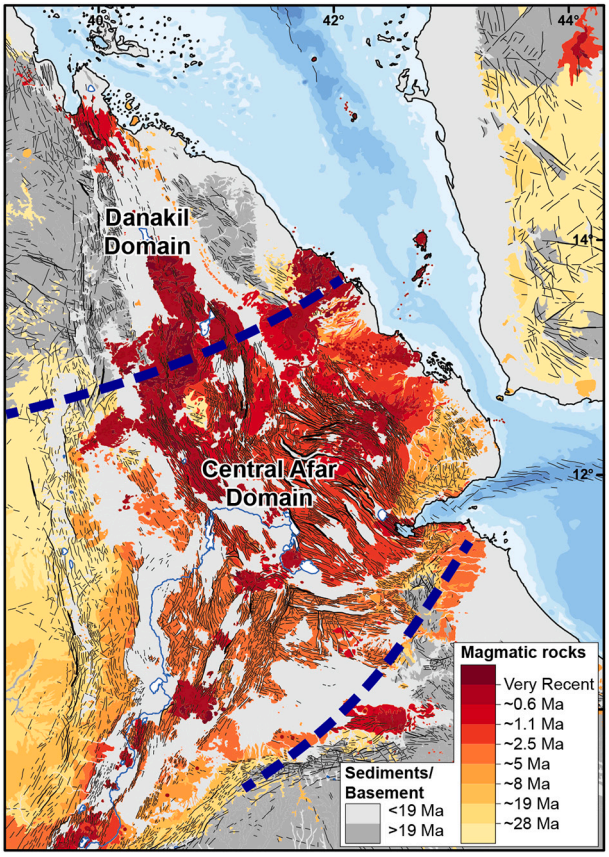

Fig. 13. Illustration of the two main domains of rifting style and magmatic history. Volcanic and intrusive rocks are shown in shades of red indicating their age. Dark grey indicate pre-rift rocks. Dashed blue lines indicate the approximate boundaries between the Danakil and Central Afar Domains. The Central Afar Domain features a much more extensive pre- and *syn*-rift magmatic products. Bathymetry similar to Fig. 4.

Note that the "Central Afar" is meant here in its broad sense, including the central-eastern, central-western, south-western Afar, and possibly the south-eastern Afar. The boundary between these two domains broadly corresponds to the DDDBH Structure (see section 5.3 and Fig. 11).

Central Afar is shaped by a wide depression cut by numerous grabens. Elevations in the Central Afar Depression are usually between 350 and 1000 m, while a single, well-defined valley shapes the Danakil Depression with elevations reaching 125 m below sea level at lake Karum (Fig. 1). According to our kinematic model (section 6.1) and coherently with the northward propagation of the Afar Rift, Central Afar experienced significant extension with high stretching factors (~200–250 km and ~ 2.5–3.3 respectively, see Suppl. Mat. 15) while both the extension and the stretching factors are lower for the Danakil Depression (~10–100 km and ~ 1.2–1.8 respectively). The age of rifting in Central Afar is also older than in the Danakil Depression (see sections 4 and 5.2.1).

While measures of crustal thickness vary considerably between authors (see Suppl. Mat. 16, Appendix A), the average thickness (Ahmed et al., 2022; Dugda et al., 2005; Hammond et al., 2011; Kibret et al., 2019; Lavayssière et al., 2018; Reed et al., 2014; Stuart et al., 2006; Wang et al., 2021) for the central-western and central-eastern Afar or these zones plus the south-western and south-eastern Afar is 24 ± 3 km (N = 90 resp. 103, see Suppl. Mat. 16 for zones considered). In the Danakil Depression, some authors indicate a very shallow Moho depth (14 km by Makris and Ginzburg, 1987; 16 km by Berckhemer et al., 1975 and Hammond et al., 2011) and the average crustal thickness is 22 ± 3 km (N = 19 see Suppl. Mat. 16, Ahmed et al., 2022; Hammond et al., 2011; Lavayssière et al., 2018; Wang et al., 2021), being slightly thinner than for Central Afar. Studies that encompass both the Danakil and Central Afar evidence the presence of a shallower Moho under the Danakil Depression (Berckhemer et al., 1975; Chambers et al., 2019; Hammond et al., 2011; Lavayssière et al., 2018; Makris and Ginzburg, 1987; Mammo, 2004; Tiberi et al., 2005 with the exception of Wang et al., 2021; see also Appendix A). The lower Bouguer gravity anomaly under the Danakil Depression (suppl. Mat. 4) is coherent with the presence of a relatively shallow Moho.

The pre- to early syn-rift (Oligocene to Early Miocene) volcanic activity also differs between both domains (Fig. 13). The margins and plateaus west of Central Afar experienced very significant volcanic activity. Beccaluva et al. (2009) mention 1.8 km of lavas in Lalibela, and Mohr and Zanettin (1988) report thicknesses between >1290 and > 1870 m on the central western Plateau and between >1030 and < 1980 m in the southern western Plateau. Geophysical data shows an altered crust, possibly caused by these magmatic intrusions (Ahmed et al., 2022). Similarly, on the Yemenite plateau, the thickness of magmatic material locally exceeds 1.5 km (Baker et al., 1996; Ukstins Peate et al., 2005). On the margins of the Danakil Depression, however, significant Oligocene to Mid-Miocene lava is only outcropping in the region of Adigrat (approx. 500 m to 650 m thick according to Beccaluva et al., 2009 and Mohr and Zanettin, 1988). Few dykes and plugs are mentioned on the margins of the Depression (Brinckmann and Kürsten, 1971; Geological Survey of Ethiopia, 1978a). Ahmed et al. (2022) evidence unmodified crust in this area. Overall, the Danakil domain experienced less magmatic influence during pre- and early syn-rift times compared to Central Afar.

The syn-rift architecture of both basins is also distinctive. Central Afar is dominated by magmatic products with at least 1.5 km of Pleistocene (Lahitte et al., 2003b) and possibly ~1 km of Mio-Pliocene lavas (Stab et al., 2016). The syn-rift deposits of the Danakil Depression (i.e. the Red Bed Series) are conversely dominated by sedimentary products (Brinckmann and Kürsten, 1971; C.N.R - C.N.R.S. Afar Team, 1973; Le Gall et al., 2018). Le Gall et al. (2018) mention two lava flows (average thickness of 10 m) and seven sills (3–10 m thick) in a ~ 250 m sedimentary succession. Brinckmann and Kürsten (1971) similarly mention one 20–30 m flow and three ≤10 m flows in a ~ 270 m sedimentary log. Our observations match these descriptions.

Both regions experienced significant volcanic activity during Recent times (< 0.6 Ma, Figs. 4 and 13). In Central Afar, eruptions are mainly concentrated in the Dabbahu-Manda Hararo Range and Asal Graben. In the Danakil Depression, voluminous magmatic products are present in the Erta Ale range, interpreted to represent incipient break-up (Barberi et al., 1972a; Bastow and Keir, 2011; Keir et al., 2013; Le Gall et al., 2018).

Central Afar is believed to feature significant magmatic underplating (Stab et al., 2016; Wang et al., 2021), while none have been detected under the Danakil Depression (Wang et al., 2021). This is consistent with the reported extensive magmatic activity of Central Afar throughout its rift history. The volume of underplated material is probably at least as large as the volume of erupted material (Cox, 1980). Underplating may explain the higher elevations by increasing crustal thickness and providing isostatic buoyancy.

A significant part of the strain is believed to be accommodated by magmatic intrusions in Central Afar (Bastow and Keir, 2011; Ebinger et al., 2013; Ferguson et al., 2013a; Hofstetter and Beyth, 2003; Keir et al., 2011, 2013) even though faulting still play an important role outside the magmatic segments (e.g. Polun et al., 2018). In the Danakil Depression, extension is likely accommodated by mechanical extension (faulting and ductile stretching) in the north and magmatic intrusion in the Erta Ale range since Recent times (Ahmed et al., 2022; Bastow et al., 2018; Bastow and Keir, 2011; Hurman et al., 2023; Illsley-Kemp et al., 2018a, 2018b; Keir et al., 2013; La Rosa et al., 2023; Le Gall et al., 2018). The crust in Central Afar is significantly thicker (between 17% and 55%) than expected based on mechanical extension solely (McKenzie, 1978) considering the extension predicted by our tectonic plate reconstruction (see Appendix A) but also the reconstruction of Eagles et al., 2002 (discussion in Ahmed et al., 2022; Bastow and Keir, 2011; Keir et al., 2013; Stab et al., 2016). This indicates that crustal thinning is compensated by underplating, magmatic intrusions and erupted material, a process known as *magma compensated thinning* (Bastow and Keir, 2011; Ferguson et al., 2013b; Stab et al., 2016; Thybo and Nielsen, 2009). It corroborates the hypothesis of magma-accommodated extension. Conversely, the Danakil Depression shows a crustal thickness compatible with mechanical extension (see Appendix A). Thinning in the Danakil Depression is thus probably not compensated, with only localized magmatic intrusions, supporting the hypothesis of extension dominated by mechanical processes.

In Central Afar, the extension is distributed over a large area (>100 km) and vary significantly over times of less than 1 Ma (Doubre et al., 2017; Kogan et al., 2012; Moore et al., 2021; Pagli et al., 2014; Sangha et al., 2022, see also section 5.2.2). In the Danakil Depression, rifting is localized in the centre of the Depression, accommodating most of the long-term extension, even if the margins still experience seismic activity (Illsley-Kemp et al., 2018a, 2018b; Moore et al., 2021).

The contrasting rift styles between Central Afar and the Danakil domain can be explained by distinct volumes of magmatic accretion until Recent times. We tentatively explain this by a stronger influence of the Afar plume in Central Afar compared to the Danakil Depression. This difference in hotspot influence can explain:

1) The abundance of Oligocene to Mid-Miocene volcanic rocks at the margins of Central Afar.
2) The difference in basin fill, including the abundance of Late Miocene to Middle Pleistocene volcanic rocks in Central Afar and the sediment-filled Danakil Depression.
3) The lower crustal thickness of the Danakil Depression and its lower elevation due to the absence or limited magma-compensated thinning.
4) The importance of mechanical extension in the N-Danakil Depression compared to Central Afar, where magmatic intrusion accounts for a significant part of strain accommodation.
5) The apparent contradiction between the near-oceanic state of the Danakil Depression and its younger age, smaller stretching factor and smaller total extension compared to Central Afar. The significant magmatic production of the former compensates for thinning and delays breakup.
6) The absence of penrose-like oceanic crust in the Central Afar – Bab-el-Mandeb region due to magma-compensated thinning. The rest of the Gulf of Aden – central/southern Red Sea rift system experienced comparable extension but feature oceanic crust.

7.2. Stages of rift evolution

One hypothesis presented in the literature is that Central Afar and the Danakil Depression represent two subsequent stages of rift evolution. The Danakil Depression would represent the evolution of what Central Afar is nowadays (Bastow and Keir, 2011; Ebinger and Hayward, 1996; Hayward and Ebinger, 1996; Keir et al., 2013; Moore et al., 2021). Based on this hypothesis, Bastow and Keir et al. (2011) and Keir et al. (2013) postulate that the Danakil Depression experienced, like Central Afar, a long and significant history of magma intrusions. The same authors suggest that the current ductile plate stretching in the Danakil Depression is caused by its history of magmatic intrusions.

The idea of the Danakil Depression representing a more developed stage of the current Central Afar is inconsistent with the northward propagation of the rift (discussed in section 5.2.1), with the younger age of the Danakil Depression (section 4.13.2) and with the lower stretching factor and extension rate it experienced (Suppl. Mat. 15). It is also inconsistent with their contrasting magmatic history and the much more voluminous erupted, intruded and underplated material reported in Central Afar (section 7.1 and references therein). These observations invalidate the idea that the Danakil Depression experienced the same geological history as Central Afar in the past. We therefore consider that the Danakil Depression is not representing the direct evolution of what Central Afar is nowadays. The Danakil Depression is more evolved or more mature in the sense that it is closer to oceanic spreading, but not in the sense that the Danakil Depression was structured like, or was looking like Central Afar a few million years ago. The Danakil Depression and Central Afar represent two different types of rift and not two different stages of evolution of the same rift type. The observations on volumes of magmatic products also preclude that strain was accommodated by significant magma intrusion for a protracted period during the early phase of rift development in the Danakil Depression. This, in turn, calls for a reassessment of the idea that the current ductile plate stretching in Danakil follows - or even is a consequence - of this magmatic intrusion history. We thus argue that the Danakil Depression first experienced mechanical extension since Late Miocene times and that extension in the southern part of the Depression only recently began to be accommodated by magmatic intrusions.

8. Conclusion

This study presents new and revised geological maps of the Afar Depression and the Afro-Arabian Rift System. The maps materialize an up-to-date and integrative representation of the geology of the region. The tectonostratigraphic evolution of the Afar Depression and surrounding regions has been reviewed, allowing for a detailed understanding of the chronology and localization of major tectonic, magmatic and sedimentary events. The review highlights a complex geological history and shows that most geological events are diachronous throughout the different parts of the region.

The Afar region is tectonically structured by four rifts, the Gulf of Aden Rift, the Main Ethiopian Rift, the Afar Rift and the Red Sea Rift separating the Nubian, Arabian and Somalian plates, as well as the Arrata Microplate. Unlike commonly presented, the integrative dataset shows that the Afar Rift propagates northwards and not southwards. It forms a relay structure with the Red Sea Rift and is linked with the counter-clockwise rotation of the Danakil Block. The segmentation and localisation of the different rifts and rift segments is partially inherited by Precambrian and Phanerozoic structures.

The combination of maps, the review of the geological history and the current structure of the Afar region allows us to propose a new kinematic model and paleogeological maps of the evolution of the Afar region. The eruption of the flood basalts began ~33 Ma ago in northern Ethiopia and in Yemen. Rifting began approx. 27 Ma ago in the Afar region. During the first phase, rifting was mainly concentrated in the Gulf of Aden and the Red Sea with more limited extension in Central Afar. This situation changed between 13 and 8 Ma with a major tectonic reorganisation of the region. Tectonic activity significantly decreased in the southernmost Red Sea as the Afar Rift began to accommodate most of the extension while oceanic spreading initiated in the central Red Sea. At the same time, the Northern Main Ethiopian Rift formed and the Afar region developed into a triple junction. Significant magmatism accompanied distributed extension in the Depression since the Pliocene, forming km-thick lava deposits.

The Afar Depression can be segmented into two distinct domains: the Danakil domain and the Central Afar domain. Central Afar experienced significant extension as well as protracted and extensive magmatism during pre- and *syn*-rift times. It is believed to be strongly influenced by the Afar hotspot. Magma-compensated thinning prevented full breakup. Conversely, the Danakil Depression is younger and experienced less magmatic activity until Recent times. Although the extension was lower than in Central Afar, the absence of magma-compensated thinning allowed it to reach an evolved stage of continental breakup. As the Danakil Depression experienced a different geological history compared to Central Afar, it cannot be considered as the simple further evolution of the latter.

Author contributions

VR was responsible for the conceptualization, investigation, literature review, fieldwork, compilation of the database, compilation of the maps, figures, discussion and writing. AF was responsible for the conceptualization, investigation, literature review, fieldwork, discussion, writing, project administration, funding acquisition and supervision. JR was responsible for discussion and writing. TK was responsible for the conceptualization, fieldwork, discussion, writing and supervision.

Declaration of Competing Interest

The authors declare that they have no known competing financial interests or personal relationships that could have appeared to influence the work reported in this paper.

Data availability

Datasets related to this article can be found at doi:https://doi.org/10.5281/zenodo.7351643 and doi:https://doi.org/10.5281/zenodo.7351765, hosted at Zenodo (Rime et al., 2022a, 2022b).

Acknowledgments

This study was funded by the Swiss National Science Foundation (SNF project SERENA – SEdimentary REcord of the Northern Afar 200021_163114). We are grateful to the University of Fribourg (Switzerland), the University of Addis Ababa (Ethiopia), the Ethiopian Ministry of Mines and Energy, the Ethiopian Geological Survey, Circum Minerals, former Allana Potash and Yara Dallol for their support. We particularly acknowledge Samuel Getachew who helped us access some of the geological maps. We thank David Jaramillo-Vogel, Jean-Charles Schaegis, Haileyesus Negga, Addis Endeshaw, Ermias Gebru, Eva De Boever, Juan-Carlos Braga, Pia Wyler, Xenia Haberditz, the Ethioder team as well as the regional and local administration of the Afar for their help and support during fieldwork. We furthermore thank Géraldine Zimmerli, Adeline Marro, Sandra Borderie, Jon Mosar, Lisa McNeill and Audrey Niederer for help, comments and tips. We acknowledge Prof. Paul Cantonneau for the inspiration. We are finally very grateful to Derek Keir and an anonymous reviewer for their constructive comments that helped significantly improve the manuscript.

Appendix A. Crustal balancing

A.1. Introduction

To quantify the mechanisms of accommodation of extension that are important for the Afar Depression, we propose a simple approach of crustal balancing. We distinguish between magma-accommodated rifting and mechanically-accommodated rifting.

In the case of 100% magma-accommodated rifting (Fig. A1a), the theoretical space created by the extension (A_e, defined as the amount of extension (e) multiplied by the initial crustal thickness (T_0)) is entirely compensated by magmatic addition. The crustal thickness remains constant, and the present-day (syn-rift) crustal surface over the cross-section (A_1) is increased by A_e compared to the initial (pre-rift) surface (A_0).

In the case of 100% mechanical accommodation (Fig. A1b), the extension is entirely compensated by crustal thinning. The crustal surface over the cross-section remains constant between pre- and syn-rift ($A_0 = A_1$).

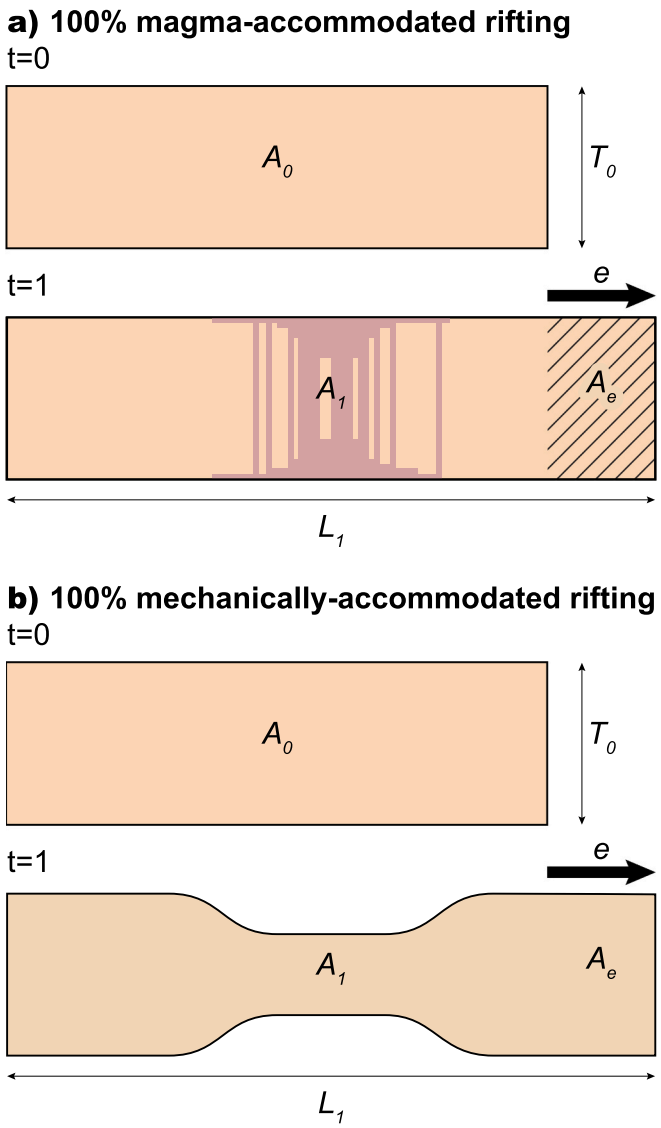

Fig. A1. Schematic representation of a) magma-accommodated rifting and b) mechanically-accommodated rifting.

A.2. Methods

The ratio of magma-accommodated rifting (m) is calculated as:

$$m = \frac{A_1 - A_0}{A_e}$$

$$m = \frac{A_1 - [(L_1 - e)T_0]}{e\,T_0}$$

With L_1 the cross-section length and the other terms defined above.

A_1 is estimated based on the published Moho depths for the Afar Depression (Berckhemer et al., 1975; Makris and Ginzburg, 1987; Tiberi et al., 2005; Dugda and Nyblade, 2006; Hammond et al., 2011; Reed et al., 2014; Lavayssière et al., 2018; Kibret et al., 2019; Wang et al., 2021; Ahmed et al., 2022, see also Suppl. Mat. 14). The data points situated at less than 75 km distance of two cross-sections (one in the Danakil Depression, one in Central Afar) are projected onto them (Fig. A2a, b, c). As the data are very scattered, three estimates of the crustal geometry are suggested: a minimal, best and maximum estimate. The extension (e) is calculated from the GPlates kinematic model (see section 6.1). Initial crustal thicknesses (T_0) are assumed to be 38 km and 42 km for the Danakil and Central Afar, respectively (Ahmed et al., 2022).

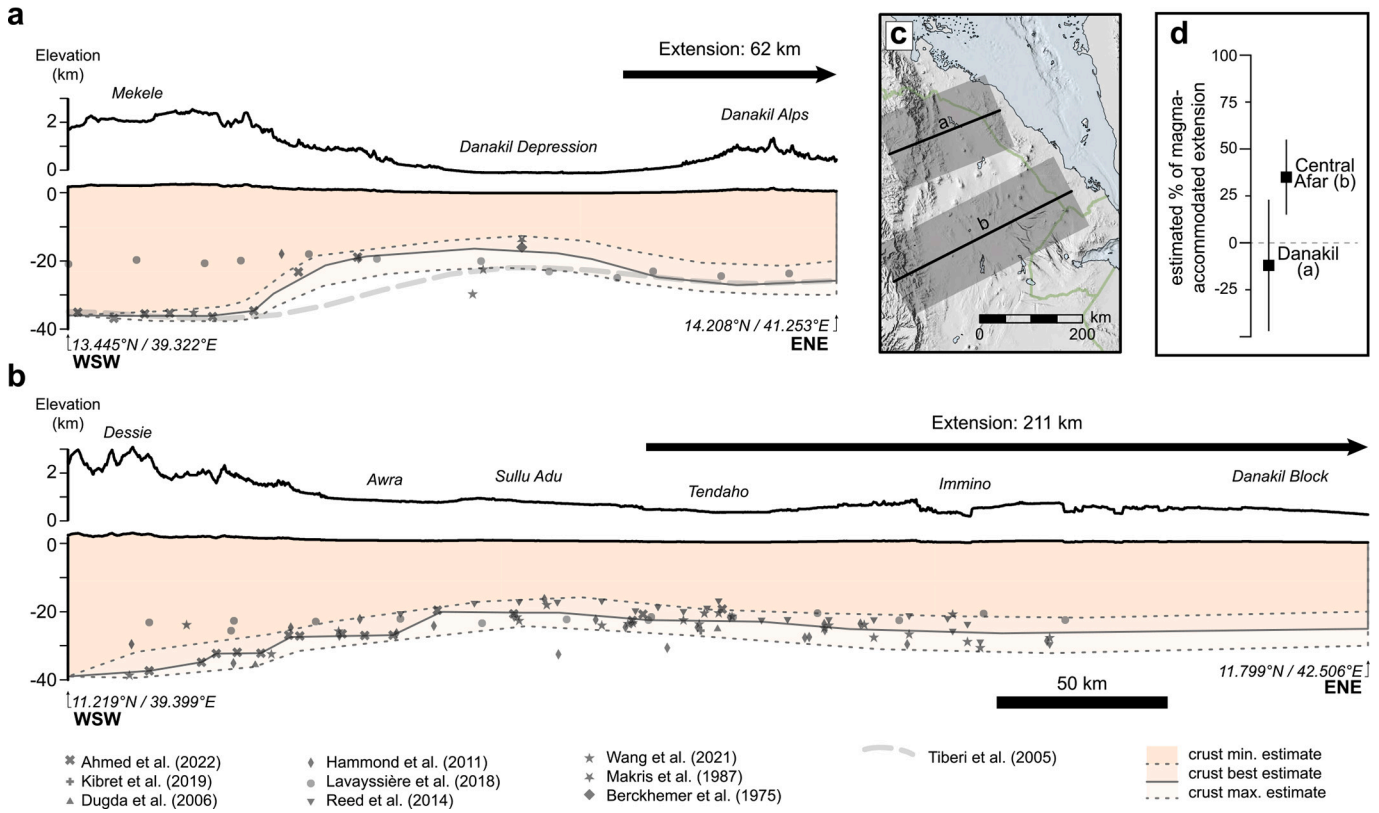

Fig. A2. Crustal balancing in the Danakil Depression (a) and Central Afar (b). Symbols represent projected Moho depth by different authors. Coloured polygons indicate minimum, best and maximum estimates of crustal geometry. Surface topography is also indicated. c) Position of the cross-sections. Only the data situated in the shaded areas were projected on the cross-sections. d) Results of the proportion of magma-accommodated extension. Black square represents the best estimates and bars indicate min. and max. estimates. [2-columns fitting image]

A.3. Results

For the Danakil cross-section (Fig. A2a), the results (Fig. A2d) show that the percentage of magma-accommodated extension ranges from −47% (minimum estimate of crust surface), −12% (best estimate) and + 23% (maximum estimate). For Central Afar (Fig. A2b), the percentages are 17% (minimum estimate), 36% (best estimate) and 55% (maximum estimate).

A.4. Discussion

In accordance with the scattered Moho depth data, the results show an large spread and should thus be interpreted with caution. The best estimate for the Danakil Depression tend to indicate slightly negative values. This would mean that material was removed from the crust, which we consider not realistic. These low values could indicate that 1) the Moho depth data are underestimated, 2) the extension value is underestimated, 3) the initial crustal thickness is overestimated. However, considering that positive values are within the range of calculated uncertainty, we interpret these results as valid. They show low magma addition to the crust, consistently with outcrop evidences (see section 7.1). Conversely, calculations for Central Afar shows that a significant proportion of extension is accommodated by magmatic addition to the crust, consistently with other evidences discussed in section 7.1.

Even considering the large uncertainties, these results show a remarkable difference between the Danakil and Central Afar domains.

Appendix B. Supplementary data

Supplementary data to this article can be found online at https://doi.org/10.1016/j.earscirev.2023.104519.

References

Abbate, E., Sagri, M., 2012. Early to Middle Pleistocene Homo dispersals from Africa to Eurasia: Geological, climatic and environmental constraints. Quat. Int. 267, 3–19. https://doi.org/10.1016/J.QUAINT.2011.02.043.

Abbate, E., Albianelli, A., Azzaroli, A., Benvenuti, M., Tesfamariam, B., Bruni, P., Cipriani, N., Clarke, R.J., Ficcarelli, G., Macchiarelli, R., Napoleons, G., Papini, M., Rook, L., Sagri, M., Teclei, T.M., Torret, D., Villa, I., 1998. A one-million-year-old Homo cranium from the Danakil (Afar) depression of Eritrea. Nature 393, 458–460. https://doi.org/10.1038/30954.

Abbate, E., Balestrieri, M.L., Bigazzi, G., 2002. Morphostructural development of the Eritrean rift flank (southern Red Sea) inferred from apatite fission track analysis. J. Geophys. Res. Solid Earth 107. https://doi.org/10.1029/2001JB001009. ETG 12-1-ETG 12-12.

Abbate, E., Woldehaimanot, B., Bruni, P., Falorni, P., Papini, M., Sagri, M., Girmay, S., Tecle, T.M., 2004. Geology of the Homo-bearing Pleistocene Dandiero Basin (Buia region, Eritrean Danakil depression). Riv. Ital. Paleontol. Stratigr. 110, 5–34. https://doi.org/10.13130/2039-4942/5761.

Abbate, E., Bruni, P., Sagri, M., 2015. Geology of Ethiopia: A review and geomorphological perspectives. In: Billi, P. (Ed.), Landscapes and Landforms of

Ethiopia. Springer, Dordrecht, pp. 33–65. https://doi.org/10.1007/978-94-017-8026-1.
Abdallah, A., Courtillot, V., Kasser, M., Le Dain, A.Y., Lépine, J.C., Robineau, B., Ruegg, J.C., Tapponnier, P., Tarantola, A., 1979. Relevance of Afar seismicity and volcanism to the mechanics of accreting plate boundaries. Nature 282, 17–23. https://doi.org/10.1038/282017a0.
Abebe, T., Mazzarini, F., Innocenti, F., Manetti, P., 1998. The Yerer-Tullu Wellel volcanotectonic lineament: a transtensional structure in Central Ethiopia and the associated magmatic activity. J. Afr. Earth Sci. 26, 135–150. https://doi.org/10.1016/S0899-5362(97)00141-3.
Abebe, T., Manetti, P., Bonini, M., Corti, G., Innocenti, F., Mazzarini, F., 2005. Geological Map of the Northern Main Ethiopian Rift. Geol. Soc. Am.
Abebe, T., Balestrieri, M.L., Bigazzi, G., 2010. The Central Main Ethiopian Rift is younger than 8 Ma: confirmation through apatite fission-track thermochronology. Terra Nova 22, 470–476. https://doi.org/10.1111/j.1365-3121.2010.00968.x.
Acocella, V., 2010. Coupling volcanism and tectonics along divergent plate boundaries: Collapsed rifts from Central Afar, Ethiopia. GSA Bull. 122, 1717–1728. https://doi.org/10.1130/B30105.1.
Acocella, V., Abebe, B., Korme, T., Barberi, F., 2008. Structure of Tendaho Graben and Manda Hararo Rift: Implications for the evolution of the southern Red Sea propagator in Central Afar. Tectonics 27, TC4016. https://doi.org/10.1029/2007TC002236.
Acton, G.D., Stein, S., Engeln, J.F., 1991. Block rotation and continental extension in Afar: a comparison to oceanic microplate systems. Tectonics 10, 501–526. https://doi.org/10.1029/90TC01792.
Acton, G.D., Tessema, A., Jackson, M., Bilham, R., 2000. The tectonic and geomagnetic significance of paleomagnetic observations from volcanic rocks from Central Afar, Africa. Earth Planet. Sci. Lett. 180, 225–241. https://doi.org/10.1016/S0012-821X(00)00173-4.
Adamson, D.A., Williams, M.A.J., 1987. Geological setting of Pliocene rifting and deposition in the Afar Depression of Ethiopia. J. Hum. Evol. 16, 597–610. https://doi.org/10.1016/0047-2484(87)90015-7.
Aghanabati, A., 1993. Geological Map of the Middle East. Geol. Surv, Iran.
Ahmed, A., Tiberi, C., Leroy, S., Stuart, G.W., Keir, D., Sholan, J., Khanbari, K., Al-Ganad, I., Basuyau, C., 2013. Crustal structure of the rifted volcanic margins and uplifted plateau of Western Yemen from receiver function analysis. Geophys. J. Int. 193, 1673–1690. https://doi.org/10.1093/gji/ggt072.
Ahmed, A., Doubre, C., Leroy, S., Keir, D., Pagli, C., Hammond, J.O.S., Ayele, A., Be de Berc, M., Grunberg, M., Vergne, J., Pestourie, R., Mamo, D., Kibret, B., Cubas, N., Lavayssière, A., Janowski, M., Lengliné, O., La Rosa, A., Chambers, E.L., Illsley-Kemp, F., 2022. Across and along-strike crustal structure variations of the western Afar margin and adjacent plateau: Insights from receiver functions analysis. J. Afr. Earth Sci. 192, 104570 https://doi.org/10.1016/J.JAFREARSCI.2022.104570.
Ahn, H.S., Kidane, T., Yamamoto, Y., Otofuji, Y.I., 2016. Low geomagnetic field intensity in the Matuyama Chron: palaeomagnetic study of a lava sequence from Afar depression, East Africa. Geophys. J. Int. 204, 127–146. https://doi.org/10.1093/GJI/GGV303.
Aksu, A.E., Hall, J., Yaltırak, C., 2021. Miocene–Quaternary tectonic, kinematic and sedimentary evolution of the eastern Mediterranean Sea: A regional synthesis. Earth-Sci. Rev. 220, 103719 https://doi.org/10.1016/j.earscirev.2021.103719.
Aldaajani, T.Z., Almalki, K.A., Betts, P.G., 2021. Plume Versus Slab-pull: example from the Arabian Plate. Front. Earth Sci. 9, 494. https://doi.org/10.3389/FEART.2021.700550.
Alemseged, Z., Spoor, F., Kimbel, W.H., Bobe, R., Geraads, D., Reed, D., Wynn, J.G., 2006. A juvenile early hominin skeleton from Dikika, Ethiopia. Nature 443, 296–301. https://doi.org/10.1038/nature05047.
Alemseged, Z., Wynn, J.G., Geraads, D., Reed, D., Andrew Barr, W., Bobe, R., McPherron, S.P., Deino, A., Alene, M., Sier, J., Roman, D., Mohan, J., 2020. Fossils from Mille-Logya, Afar, Ethiopia, elucidate the link between Pliocene environmental changes and Homo origins. Nat. Commun. 11, 2480. https://doi.org/10.1038/s41467-020-16060-8.
Alene, M., Hart, W.K., Saylor, B.Z., Deino, A., Mertzman, S., Haile-Selassie, Y., Gibert, L. B., 2017. Geochemistry of Woranso–Mille Pliocene basalts from west-central Afar, Ethiopia: Implications for mantle source characteristics and rift evolution. Lithos 282–283, 187–200. https://doi.org/10.1016/J.LITHOS.2017.03.005.
Ali, M.Y., 2009. Geology and coal potential of Somaliland. Int. J. Oil, Gas Coal Technol. 2, 168–185. https://doi.org/10.1504/IJOGCT.2009.024885.
Ali, M.Y., 2015. Petroleum geology and hydrocarbon potential of the Guban Basin, Northern Somaliland. J. Pet. Geol. 38, 433–457. https://doi.org/10.1111/jpg.12620.
Ali, M.Y., Lee, J., 2019. Petroleum geology of the Nogal Basin and surrounding area, northern Somalia: part 1, stratigraphy and tectonic evolution. J. Pet. Geol. 42, 91–120. https://doi.org/10.1111/JPG.12726.
Ali, M.Y., Watts, A.B., 2013. Subsidence history, crustal structure, and evolution of the Somaliland-Yemen conjugate margin. J. Geophys. Res. Solid Earth 118, 1638–1649. https://doi.org/10.1002/jgrb.50113.
Ali, M.Y., Watts, A.B., 2016. Tectonic evolution of sedimentary basins of northern Somalia. Basin Res. 28, 340–364. https://doi.org/10.1111/bre.12113.
Ali, M.Y., Hibberd, P., Stoikovich, B., 2018. Origin and prospectivity of heavy mineral enriched sand deposits along the Somaliland coastal areas. J. Afr. Earth Sci. 140, 60–75. https://doi.org/10.1016/J.JAFREARSCI.2017.12.024.
Ali, M., Decarlis, A., Ligi, M., Ball, P., Bosworth, W., Ceriani, A., 2022. The Red Sea rifting in Central Egypt: constraints from the offshore Quseir. J. Geol. Soc. Lond. https://doi.org/10.1144/JGS2022-105.
Almalki, K.A., Betts, P.G., Ailleres, L., 2014. Episodic Sea-floor spreading in the Southern Red Sea. Tectonophysics 617, 140–149. https://doi.org/10.1016/J.TECTO.2014.01.030.
Almalki, K.A., Betts, P.G., Ailleres, L., 2015. The Red Sea – 50 years of geological and geophysical research. Earth-Sci. Rev. 147, 109–140. https://doi.org/10.1016/J.EARSCIREV.2015.05.002.
Almalki, K.A., Betts, P.G., Ailleres, L., 2016. Incipient seafloor spreading segments: Insights from the Red Sea. Geophys. Res. Lett. 43, 2709–2715. https://doi.org/10.1002/2016GL068069.
Al-Mikhlafi, A.S., Edwards, L.R., Cheng, H., 2018. Sea-level history and tectonic uplift during the last-interglacial period (LIG): Inferred from the Bab al-Mandab coral reef terraces, southern Red Sea. J. Afr. Earth Sci. 138, 133–148. https://doi.org/10.1016/j.jafrearsci.2017.10.023.
Altherr, R., Mertz-Kraus, R., Volker, F., Kreuzer, H., Henjes-Kunst, F., Lange, U., 2019. Geodynamic setting of Upper Miocene to Quaternary alkaline basalts from Harrat al 'Uwayrid (NW Saudi Arabia): Constraints from K–Ar dating, chemical and Sr-Nd-Pb isotope compositions, and petrological modeling. Lithos 330–331, 120–138. https://doi.org/10.1016/j.lithos.2019.02.007.
Angelucci, A., Civitelli, G., Funiciello, R., Mariotti, G., Matteucci, R., Passeri, L., Pialli, G., Praturlon, A., Sirna, G., 1975. Preliminary report on the carbonate sedimentation oat the Dahlak Islands (Red Sea, Ethiopia). Geol. Romana 14, 41–61.
Antonielli, B., Fidolini, F., Righini, G., 2009. Landsat TM and Quickbird images for geological mapping in the syn-rift lower Dogali formation (Red Sea coast, NE Eritrea). Photo Interpret. 45, 107.
Armitage, J.J., Ferguson, D.J., Goes, S., Hammond, J.O.S., Calais, E., Rychert, C.A., Harmon, N., 2015. Upper mantle temperature and the onset of extension and break-up in Afar, Africa. Earth Planet. Sci. Lett. 418, 78–90. https://doi.org/10.1016/J.EPSL.2015.02.039.
Aronson, J.L., Schmitt, T.J., Walter, R.C., Taieb, M., Tiercelin, J.J., Johanson, D.C., Naeser, C.W., Nairn, A.E.M., 1977. New geochronologic and palaeomagnetic data for the hominid-bearing Hadar Formation of Ethiopia. Nature 267, 323–327. https://doi.org/10.1038/267323a0.
ArRajehi, A., McClusky, S., Reilinger, R., Daoud, M., Alchalbi, A., Ergintav, S., Gomez, F., Sholan, J., Bou-Rabee, F., Ogubazghi, G., Haileab, B., Fisseha, S., Asfaw, L., Mahmoud, S., Rayan, A., Bendik, R., Kogan, L., 2010. Geodetic constraints on present-day motion of the Arabian Plate: Implications for Red Sea and Gulf of Aden rifting. Tectonics 29, TC3011. https://doi.org/10.1029/2009TC002482.
Arthaud, F., Choukroune, P., Robineau, B., 1980. Evolution structurale de la zone transformante d'Arta (Rep. de Djibouti). Bull. Soc. Géol. Fr. S7-XXII, 909–915. https://doi.org/10.2113/gssgfbull.s7-xxii.6.909.
Asfaw, B., Gilbert, W.H., Beyene, Y., Hart, W.K., Renne, P.R., WoldeGabriel, G., Vrba, E. S., White, T.D., 2002. Remains of Homo erectus from Bouri, Middle Awash, Ethiopia. Nature 416, 317–320. https://doi.org/10.1038/416317a.
As-Saruri, M.A., Sorkhabi, R., Baraba, R., 2010. Sedimentary basins of Yemen: their tectonic development and lithostratigraphic cover. Arab. J. Geosci. 3, 515–527. https://doi.org/10.1007/s12517-010-0189-z.
Atnafu, B., Kidane, T., Foubert, A., Jaramillo-Vogel, D., Schaegis, J.C., Henriet, J.P., 2015. Reading history from Afar. Eos 98, 12–15.
Audin, J., Vellutini, P.J., Coulon, C., Piguet, P., Vincent, J., 1990. The 1928-1929 eruption of Kammourta volcano-evidence of tectono-magmatic activity in the Manda-Inakir rift and comparison with the Asal Rift, Afar depression, Republic of Djibuti. Bull. Volcanol. 52, 551–561. https://doi.org/10.1007/BF00301536.
Audin, L., Manighetti, I., Tapponnier, P., Métivier, F., Jacques, E., Huchon, P., 2001. Fault propagation and climatic control of sedimentation on the Ghoubbet Rift Floor: insights from the Tadjouraden cruise in the western Gulf of Aden. Geophys. J. Int. 144, 391–413. https://doi.org/10.1046/j.0956-540x.2000.01322.x.
Audin, L., Quidelleur, X., Coulié, E., Courtillot, V., Gilder, S., Manighetti, I., Gillot, P.-Y., Tapponnier, P., Kidane, T., 2004. Palaeomagnetism and K-Ar and ^{40}Ar/^{39}Ar ages in the Ali Sabieh area (Republic of Djibouti and Ethiopia): constraints on the mechanism of Aden ridge propagation into southeastern Afar during the last 10 Myr. Geophys. J. Int. 158, 327–345. https://doi.org/10.1111/j.1365-246X.2004.02286.x.
Augustin, N., Devey, C.W., van der Zwan, F.M., Feldens, P., Tominaga, M., Bantan, R.A., Kwasnitschka, T., 2014. The rifting to spreading transition in the Red Sea. Earth Planet. Sci. Lett. 395, 217–230. https://doi.org/10.1016/J.EPSL.2014.03.047.
Augustin, N., van der Zwan, F.M., Devey, C.W., Ligi, M., Kwasnitschka, T., Feldens, P., Bantan, R.A., Basaham, A.S., 2016. Geomorphology of the Central Red Sea Rift: determining spreading processes. Geomorphology 274, 162–179. https://doi.org/10.1016/J.GEOMORPH.2016.08.028.
Augustin, N., van der Zwan, F.M., Devey, C.W., Brandsdóttir, B., 2021. 13 million years of seafloor spreading throughout the Red Sea Basin. Nat. Commun. 12, 2427. https://doi.org/10.1038/s41467-021-22586-2.
Ayalew, D., Pik, R., Bellahsen, N., France, L., Yirgu, G., 2019. Differential Fractionation of Rhyolites during the Course of Crustal Extension, Western Afar (Ethiopian Rift). Geochemistry. Geophys. Geosyst. 20, 571–593. https://doi.org/10.1029/2018GC007446.
Ayalew, D., Getaneh, W., Pik, R., Atnafu, B., Zemelak, A., Belay, E., 2021. Stratigraphic framework of the northeastern part of the Ethiopian flood basalt province. Bull. Volcanol. 83, 1–13. https://doi.org/10.1007/S00445-021-01482-Z.
Ayele, A., Jacques, E., Kassim, M., Kidane, T., Omar, A., Tait, S., Nercessian, A., de Chabalier, J.B., King, G., 2007. The volcano–seismic crisis in Afar, Ethiopia, starting September 2005. Earth Planet. Sci. Lett. 255, 177–187. https://doi.org/10.1016/J.EPSL.2006.12.014.
Ayele, A., Keir, D., Ebinger, C., Wright, T.J., Stuart, G.W., Buck, W.R., Jacques, E., Ogubazghi, G., Sholan, J., 2009. September 2005 mega-dike emplacement in the Manda-Harraro nascent oceanic rift (Afar depression). Geophys. Res. Lett. 36, L20306. https://doi.org/10.1029/2009GL039605.

Baker, J., Snee, L., Menzies, M., 1996. A brief Oligocene period of flood volcanism in Yemen: Implications for the duration and rate of continental flood volcanism at the Afro-Arabian triple junction. Earth Planet. Sci. Lett. 138, 39–55. https://doi.org/10.1016/0012-821x(95)00229-6.

Balestrieri, M.L., Stuart, F.M., Persano, C., Abbate, E., Bigazzi, G., 2005. Geomorphic development of the escarpment of the Eritrean margin, southern Red Sea from combined apatite fission-track and (U–Th)/he thermochronometry. Earth Planet. Sci. Lett. 231, 97–110. https://doi.org/10.1016/J.EPSL.2004.12.011.

Bannert, D., Brinckmann, J., Käding, K.C., Knetsch, G., Kürsten, M., Mayrhofer, H., 1970. Zur Geologie der Danakil-Senke - Nördliches Afar-Gebiet, NE-Äthiopien. Geol. Rundsch. 59, 409–443. https://doi.org/10.1007/BF01823804.

Barberi, F., Varet, J., 1970. The Erta Ale volcanic range (Danakil depression, northern afar, Ethiopia). Bull. Volcanol. 34, 848–917. https://doi.org/10.1007/BF02596805.

Barberi, F., Varet, J., 1972. Geological map of the Erta Ale volcanic range (Danakil depression, Ethiopia), approximate scale 1: 100.000. CNR-CNRS. Geotech.

Barberi, F., Varet, J., 1975. Recent volcanic units of Afar and their structural significance. In: Pilger, A., Rösler, A. (Eds.), Afar Depression of Ethiopia: Proceedings of an International Symposium on the Afar Region and Related Rift Problems. E. Schweizerbart'sche Verlagsbuchhandlung, Stuttgart, pp. 174–178.

Barberi, F., Varet, J., 1977. Volcanism of Afar: Small-scale plate tectonics implications. Geol. Soc. Am. Bull. 88, 1251–1266. https://doi.org/10.1130/0016-7606(1977)88<1251:VOASPT>2.0.CO;2.

Barberi, F., Borsi, S., Ferrara, G., Marinelli, G., Varet, J., 1970. Relations between tectonics and magmatology in the northern Danakil Depression (Ethiopia). Philos. Trans. R. Soc. Lond. A 267, 293–311. https://doi.org/10.1098/rsta.1970.0037.

Barberi, F., Giglia, G., Marinelli, G., Santacroce, R., Tazieff, H., Varet, J., Bonatti, S., Borsi, S., Cheminée, J.L., Faure, H., Ferrara, G., Martini, M., Chèdeville, E., 1971. Carte Géologique de la dépression des Danakil (1:500′000). CNRS/CNR.

Barberi, F., Borsi, S., Ferrara, G., Marinelli, G., Santacroce, R., Tazieff, H., Varet, J., 1972a. Evolution of the Danakil Depression (Afar, Ethiopia) in Light of Radiometric Age Determinations. J. Geol. 80, 720–729.

Barberi, F., Tazieff, H., Varet, J., 1972b. Volcanism in the Afar Depression: its tectonic and magmatic significance. Tectonophysics 15, 19–29. https://doi.org/10.1016/B978-0-444-41087-0.50007-5.

Barberi, F., Bonatti, E., Marinelli, G., Varet, J., 1974. Transverse tectonics during the split of a continent: Data from the afar rift. Tectonophysics 23, 17–29. https://doi.org/10.1016/0040-1951(74)90108-5.

Barberi, F., Ferrara, G., Santacroce, R., Varet, J., 1975. Structural evolution of the Afar triple junction. In: Pilger, A., Rösler, A. (Eds.), Afar Depression of Ethiopia: Proceedings of an International Symposium on the Afar Region and Related Rift Problems. E. Schweizerbart'sche Verlagsbuchhandlung, Stuttgart, pp. 38–54.

Barnie, T.D., Keir, D., Hamling, I., Hofmann, B., Belachew, M., Carn, S., Eastwell, D., Hammond, J.O.S., Ayele, A., Oppenheimer, C., Wright, T., 2016. A Multidisciplinary Study of the Final Episode of the Manda Hararo Dyke Sequence, Ethiopia, and Implications for Trends in Volcanism during the Rifting Cycle. Geological Society Special Publication. Geological Society of London, pp. 149–163. https://doi.org/10.1144/SP420.6.

Barrat, J.A., Fourcade, S., Jahn, B.M., Cheminée, J.L., Capdevila, R., 1998. Isotope (Sr, Nd, Pb, O) and trace-element geochemistry of volcanics from the Erta'Ale range (Ethiopia). J. Volcanol. Geotherm. Res. 80, 85–100. https://doi.org/10.1016/S0377-0273(97)00016-4.

Barrier, E., Chamot-Rooke, N., Giordano, G., 2004. Geodynamic Map of the Mediterranean. CCGM-CGMW.

Bastow, I.D., Keir, D., 2011. The protracted development of the continent-ocean transition in Afar. Nat. Geosci. 4, 248–250. https://doi.org/10.1038/ngeo1095.

Bastow, I.D., Stuart, G.W., Kendall, J.M., Ebinger, C.J., 2005. Upper-mantle seismic structure in a region of incipient continental breakup: Northern Ethiopian rift. Geophys. J. Int. 162, 479–493. https://doi.org/10.1111/J.1365-246X.2005.02666.X/3/162-2-479-FIG 009.JPEG.

Bastow, I.D., Booth, A.D., Corti, G., Keir, D., Magee, C., Jackson, C.A.-L., Warren, J., Wilkinson, J., Lascialfari, M., 2018. The Development of Late-Stage Continental Breakup: Seismic Reflection and Borehole evidence from the Danakil Depression, Ethiopia. Tectonics 37, 2848–2862. https://doi.org/10.1029/2017TC004798.

Battistelli, A., Yiheyis, A., Calore, C., Ferragina, C., Abatneh, W., 2002. Reservoir engineering assessment of Dubti geothermal field, Northern Tendaho Rift, Ethiopia. Geothermics 31, 381–406. https://doi.org/10.1016/S0375-6505(01)00039-6.

Beccaluva, L., Bianchini, G., Natali, C., Siena, F., 2009. Continental Flood Basalts and Mantle Plumes: a Case Study of the Northern Ethiopian Plateau. J. Petrol. 50, 1377–1403. https://doi.org/10.1093/PETROLOGY/EGP024.

Behle, A., Makris, J., Baier, B., Delibasis, N., 1975. Salt thickness near Dallol (Ethiopia) from seismic reflection measurements and gravity data. In: Pilger, A., Rösler, A. (Eds.), Afar Depression of Ethiopia: Proceedings of an International Symposium on the Afar Region and Related Rift Problems. E. Schweizerbart'sche Verlagsbuchhandlung, Stuttgart, pp. 156–167.

Belilla, J., Iniesto, M., Moreira, D., Benzerara, K., López-García, J., López-Archilla, A., Reboul, G., Deschamps, P., Gérard, E., López-García, P., 2021. Archaeal overdominance close to life-limiting conditions in geothermally influenced hypersaline lakes at the Danakil Depression. Ethiopia. Environ. Microbiol. 23, 7168–7182. https://doi.org/10.1111/1462-2920.15771.

Bellahsen, N., Faccenna, C., Funiciello, F., Daniel, J.M., Jolivet, L., 2003. Why did Arabia separate from Africa? Insights from 3-D laboratory experiments. Earth Planet. Sci. Lett. 216, 365–381. https://doi.org/10.1016/S0012-821X(03)00516-8.

Benes, V., Scott, S.D., 1996. Oblique rifting in the Havre trough and its propagation into the continental margin of New Zealand: Comparison with analogue experiments. Mar. Geophys. Res. 18, 189–201. https://doi.org/10.1007/BF00286077.

Benito-Calvo, A., Barfod, D.N., McHenry, L.J., de la Torre, I., 2014. The geology and chronology of the Acheulean deposits in the Mieso area (East-Central Ethiopia). J. Hum. Evol. 76, 26–38. https://doi.org/10.1016/j.jhevol.2014.08.013.

Berckhemer, H., Baier, B., Bartelsen, H., Behle, A., Burkhardt, H., Gebrande, H., Makris, J., Menzel, H., Miller, H., Vees, R., 1975. Deep seismic soundings in the Afar region and on the highland of Ethiopia. In: Pilger, A., Rösler, A. (Eds.), Afar Depression of Ethiopia: Proceedings of an International Symposium on the Afar Region and Related Rift Problems. E. Schweizerbart'sche Verlagsbuchhandlung, Stuttgart, pp. 89–107.

Berhe, S.M., 1986. Geologic and geochronologic constraints on the evolution of the Red Sea-Gulf of Aden and Afar depression. J. Afr. Earth Sci. 5, 101–117. https://doi.org/10.1016/0899-5362(86)90001-1.

Berhe, S.M., Desta, B., Nicoletti, M., Teferra, M., 1987. Geology, geochronology and geodynamic implications of the Cenozoic magmatic province in W and SE Ethiopia. J. Geol. Soc. Lond. 144, 213–226. https://doi.org/10.1144/gsjgs.144.2.0213.

Beydoun, Z.R., 1970. Southern Arabia and northern Somalia: comparative geology. Philos. Trans. R. Soc. London. Ser. A. Math. Phys. Sci. 267, 267–292.

Beyene, A., Abdelsalam, M.G., 2005. Tectonics of the Afar Depression: a review and synthesis. J. Afr. Earth Sci. 41, 41–59. https://doi.org/10.1016/j.jafrearsci.2005.03.003.

Beyin, A., 2006. The Bab al Mandab vs the Nile-Levant: an appraisal of the two dispersal routes for early modern humans out of Africa. Afr. Archaeol. Rev. 23, 5–30. https://doi.org/10.1007/S10437-006-9005-2/TABLES/2.

Beyin, A., 2021. The Western Periphery of the Red Sea as a Hominin Habitat and Dispersal Corridor: marginal or Central? J. World Prehist. 2021 (34), 1–38. https://doi.org/10.1007/S10963-021-09157-5.

Beyth, M., 1972. Paleozoic-Mesozoic Sedimentary Basin of Mekele Outlier, Northern Ethiopia. Am. Assoc. Pet. Geol. Bull. 56, 2426–2439. https://doi.org/10.1306/819A422A-16C5-11D7-8645000102C1865D.

Beyth, M., 1973. Interpretation of the stratigraphy of northern Ethiopia according to the model of plate tectonics. Geology 1, 81–82. https://doi.org/10.1130/0091-7613(1973)1<81:IOTSON>2.0.CO;2.

Beyth, M., 1978. A comparative study of the sedimentary fills of the Danakil depression (Ethiopia) and Dead Sea rift (Israel). Tectonophysics 46, 357–367. https://doi.org/10.1016/0040-1951(78)90213-5.

Beyth, M., 1991. "Smooth" and "rough" propagation of spreading Southern Red Sea - Afar depression. J. Afr. Earth Sci. 13, 157–171. https://doi.org/10.1016/0899-5362(91)90001-F.

Billi, P., 2022. Fluvial Landscape of the Dabaan Basin, Northern Somalia. In: Billi, P. (Ed.), Landscapes and Landforms of the Horn of Africa. Springer, Cham, pp. 265–280. https://doi.org/10.1007/978-3-031-05487-7_12.

Black, R., Morton, W.H., Rex, D.C., Shackleton, R.M., 1972. Sur la découverte en Afar (Ethiopie) d'un granite hyperalcalin miocène: le massif de Limmo. Comptes rendus Hebd. des séances l'Académie des Sci. Série D 274, 1453–1456.

Black, R., Morton, W.H., Hailu, T., 1974. Early structures around the Afar triple junction. Nature 248, 496–497. https://doi.org/10.1038/248496a0.

Black, R., Morton, W.H., Rex, D.C., 1975. Block tilting and volcanism within the Afar in the light of recent K/Ar age data. In: Pilger, A., Rösler, A. (Eds.), Afar Depression of Ethiopia: Proceedings of an International Symposium on the Afar Region and Related Rift Problems. E. Schweizerbart'sche Verlagsbuchhandlung, Stuttgart, pp. 296–300.

Blanford, W.T., 1869. On the Geology of a portion of Abyssinia. Q. J. Geol. Soc. 25, 401–406. https://doi.org/10.1144/GSL.JGS.1869.025.01-02.68.

Bohannon, R.G., 1986. Tectonic configuration of the Western Arabian Continental margin, southern Red Sea. Tectonics 5, 477–499. https://doi.org/10.1029/TC005I004P00477.

Bohannon, R.G., Eittreim, S.L., 1991. Tectonic development of passive continental margins of the southern and Central Red Sea with a comparison to Wilkes Land, Antarctica. Tectonophysics 198, 129–154. https://doi.org/10.1016/0040-1951(91)90148-L.

Bohannon, R.G., Naeser, C.W., Schmidt, D.L., Zimmermann, R.A., 1989. The timing of uplift, volcanism, and rifting peripheral to the Red Sea: a case for passive rifting? J. Geophys. Res. 94, 1683. https://doi.org/10.1029/JB094iB02p01683.

Bonatti, E., 1985. Punctiform initiation of seafloor spreading in the Red Sea during transition from a continental to an oceanic rift. Nature 316, 33–37. https://doi.org/10.1038/316033a0.

Bonatti, E., Seyler, M., 1987. Crustal underplating and evolution in the Red Sea Rift: Uplifted gabbro/gneiss crustal complexes on Zabargad and Brothers Islands. J. Geophys. Res. 92, 12803. https://doi.org/10.1029/JB092iB12p12803.

Bonatti, E., Hamlyn, P., Ottonello, G., 1981. Upper mantle beneath a young oceanic rift: Peridotites from the island of Zabargad (Red Sea). Geology 9, 474–479. https://doi.org/10.1130/0091-7613(1981)9<474:UMBAYO>2.0.CO;2.

Bonatti, E., Cipriani, A., Lupi, L., 2015. The Red Sea: Birth of an Ocean. In: Rasul, N.M.A., Stewart, I.C.F. (Eds.), The Red Sea - the Formation, Morphology, Oceanography and Environment of a Young Ocean Basin. Springer, Berlin, Heidelberg.

Bondár, I., Storchak, D., 2011. Improved location procedures at the International Seismological Centre. Geophys. J. Int. 186, 1220–1244. https://doi.org/10.1111/J.1365-246X.2011.05107.X.

Bonini, M., Corti, G., Innocenti, F., Manetti, P., Mazzarini, F., Abebe, T., Pecskay, Z., 2005. Evolution of the Main Ethiopian Rift in the frame of Afar and Kenya rifts propagation. Tectonics 24, TC1007. https://doi.org/10.1029/2004TC001680.

Bonvalot, S., Balmino, G., Briais, A., Kuhn, M., Peyrefitte, A., Biancale, R., Gabalda, G., Reinquin, F., Sarrailh, M., 2012. World Gravity Map. Comm. Geol. Map World. BGI-CGMW-CNES-IRD, Paris.

Bosellini, A., Russo, A., Assefa, G., 2001. The Mesozoic succession of Dire Dawa, Harar Province, Ethiopia. J. Afr. Earth Sci. 32, 403–417. https://doi.org/10.1016/S0899-5362(01)90105-8.

Bosworth, W., Stockli, D.F., 2016. Early magmatism in the greater Red Sea rift: timing and significance. Can. J. Earth Sci. 53, 1158–1176. https://doi.org/10.1139/cjes-2016-0019.
Bosworth, W., Sultan, M., Stern, R.J., Arvidson, R.E., Shore, P., Becker, R., 1993. Nature of the Red Sea crust: a controversy revisited: comment and Reply. Geology 21, 574. https://doi.org/10.1130/0091-7613(1993)021<0574:NOTRSC>2.3.CO;2.
Bosworth, W., Crevello, P., Winn Jr., R.D., Steinmetz, J., 1998. Structure, sedimentation, and basin dynamics during rifting of the Gulf of Suez and North-Western Red Sea. In: Purser, B.H., Bosence, D.W. (Eds.), Sedimentation and Tectonics in Rift Basins Red: Sea - Gulf of Aden. Chapman & Hall, pp. 77–96. https://doi.org/10.1007/978-94-011-4930-3_6.
Bosworth, W., Huchon, P., McClay, K., 2005. The Red Sea and Gulf of Aden Basins. J. Afr. Earth Sci. 43, 334–378. https://doi.org/10.1016/J.JAFREARSCI.2005.07.020.
Boucarut, M., Clin, M., Pouchan, P., Thibault, C., 1985. Impact des événements tectono-volcaniques plio-pléistocènes sur la sédimentation en République de Djibouti (Afar Central). Geol. Rundsch. 74, 123–137. https://doi.org/10.1007/BF01764575.
Bourgeois, O., Dauteuil, O., Hallot, E., 2005. Rifting above a mantle plume: Structure and development of the Iceland Plateau. Geodin. Acta 18, 59–80. https://doi.org/10.3166/GA.18.59-80.
Bowden, S., Gani, N.D., Furman, T., Gani, M.R., Vansoest, M., Abebe, T., Alemu, T., O'Sullivan, P., Tadesse, K., Abebe, B., 2022. Feedback between topography and lithosphere–asthenosphere dynamics beneath the Yerer-Tulu Wellel volcano-tectonic lineament: Insights from apatite thermochronology and basalt geochemistry. Geol. J. 57, 3569–3586. https://doi.org/10.1002/GJ.4488.
Braun, D.R., Aldeias, V., Archer, W., Arrowsmith, J.R., Baraki, N., Campisano, C.J., Deino, A.L., DiMaggio, E.N., Dupont-Nivet, G., Engda, B., Feary, D.A., Garello, D.I., Kerfelew, Z., McPherron, S.P., Patterson, D.B., Reeves, J.S., Thompson, J.C., Reed, K. E., 2019. Earliest known Oldowan artifacts at >2.58 Ma from Ledi-Geraru, Ethiopia, highlight early technological diversity. Proc. Natl. Acad. Sci. U. S. A. 116, 11712–11717. https://doi.org/10.1073/pnas.1820177116.
Bridges, D.L., Mickus, K., Gao, S.S., Abdelsalam, M.G., Alemu, A., 2012. Magnetic stripes of a transitional continental rift in Afar. Geology 40, 203–206. https://doi.org/10.1130/G32697.1.
Brinckmann, J., Kürsten, M., 1970. Geological Sketchmap of the Danakil Depression (1: 250′000). Bundesanstalt für Bodenforschung, Hannover.
Brinckmann, J., Kürsten, M., 1971. Stratigraphie und Tektonik der Danakil-Senke (NE-Äthiopien). Beihefte Geol. Jahrb. 116, 5–87.
Brown, G.F., Schmidt, D.L., Huffman, A.C.J., 1989. Geology of the Arabian Peninsula; shield area of western Saudi Arabia. U.S. Geol. Surv. Prof. https://doi.org/10.3133/pp560A. Pap. 560-A.
Bruggemann, J.H., Buffler, R.T., Guillaume, M.M.M., Walter, R.C., Von Cosel, R., Ghebretensae, B.N., Berhe, S.M., 2004. Stratigraphy, palaeoenvironments and model for the deposition of the Abdur Reef Limestone: Context for an important archaeological site from the last interglacial on the Red Sea coast of Eritrea. Palaeogeogr. Palaeoclimatol. Palaeoecol. 203, 179–206. https://doi.org/10.1016/S0031-0182(03)00659-X.
Brune, S., Kolawole, F., Olive, J.-A., Stamps, D.S., Buck, W.R., Buiter, S.J.H., Furman, T., Shillington, D.J., 2023. Geodynamics of continental rift initiation and evolution. Nat. Rev. Earth Environ. https://doi.org/10.1038/s43017-023-00391-3.
Buffler, R.T., Bruggemann, J.H., Ghebretensae, B.N., Walter, R.C., Guillaume, M.M.M., Berhe, S.M., McIntosh, W., Park, L.E., 2010. Geologic setting of the Abdur Archaeological Site on the Red Sea coast of Eritrea, Africa. Glob. Planet. Chang. 72, 429–450. https://doi.org/10.1016/J.GLOPLACHA.2010.01.017.
Buiter, S.J.H., Torsvik, T.H., 2014. A review of Wilson Cycle plate margins: a role for mantle plumes in continental break-up along sutures? Gondwana Res. 26, 627–653. https://doi.org/10.1016/J.GR.2014.02.007.
Bunter, M.A.G., Debretsion, T., Woldegiorgis, L., 1998. New developments in the pre-rift prospectivity of the Eritrean Red Sea. J. Pet. Geol. 21, 373–400. https://doi.org/10.1111/j.1747-5457.1998.tb00792.x.
Burgi, P.-Y., Caillet, M., Haefeli, S., 2002. Field temperature measurements at Erta'Ale Lava Lake, Ethiopia. Bull. Volcanol. 64, 472–485. https://doi.org/10.1007/S00445-002-0224-3.
C.N.R - C.N.R.S. Afar Team, 1973. Geology of Northern Afar (Ethiopia). Rev. Géogr. Phys. Géol. Dyn. 14, 443–490.
Camanni, G., Ye, Q., 2022. The significance of fault reactivation on the Wilson cycle undergone by the northern South China Sea area in the last 60 Myr. Earth-Sci. Rev. 225, 103893 https://doi.org/10.1016/J.EARSCIREV.2021.103893.
Camp, V.E., Roobol, M.J., 1989. The Arabian continental alkali basalt province: part I. Evolution of Harrat Rahat, Kingdom of Saudi Arabia. Geol. Soc. Am. Bull. 101, 71–95. https://doi.org/10.1130/0016-7606(1989)101<0071:TACABP>2.3.CO;2.
Camp, V.E., Roobol, M.J., Hooper, P.R., 1991. The Arabian continental alkali basalt province: Part II. Evolution of Harrats Khaybar, Ithnayn, and Kura, Kingdom of Saudi Arabia. Geol. Soc. Am. Bull. 103, 363–391. https://doi.org/10.1130/0016-7606(1991)103<0363:TACABP>2.3.CO;2.
Camp, V.E., Roobol, M.J., Hooper, P.R., 1992. The Arabian continental alkali basalt province: Part III. Evolution of Harrat Kishb, Kingdom of Saudi Arabia. Geol. Soc. Am. Bull. 104, 379–396. https://doi.org/10.1130/0016-7606(1992)104<0379:TACABP>2.3.CO;2.
Campisano, C.J., 2012. Geological summary of the Busidima Formation (Plio-Pleistocene) at the Hadar paleoanthropological site, Afar Depression, Ethiopia. J. Hum. Evol. 62, 338–352. https://doi.org/10.1016/j.jhevol.2011.05.002.
Capaldi, G., Chiesa, S., Conticelli, S., Manetti, P., 1987a. Jabal an Nar: an upper miocene volcanic Centre near Al Mukha (Yemen Arab Republic). J. Volcanol. Geotherm. Res. 31, 345–351. https://doi.org/10.1016/0377-0273(87)90077-1.
Capaldi, G., Chiesa, S., Manetti, P., Orsi, G., Poli, G., 1987b. Tertiary anorogenic granites of the western border of the Yemen Plateau. Lithos 20, 433–444. https://doi.org/10.1016/0024-4937(87)90028-4.
Carbone, F., Matteucci, R., Angelucci, A., 1998. Present-day sedimentation on the carbonate platform of the Dahlak Islands, Eritrea. In: Purser, B.H., Bosence, D.W. (Eds.), Sedimentation and Tectonics in Rift Basins: Red Sea - Gulf of Aden. Springer, Dordrecht, pp. 523–536. https://doi.org/10.1007/978-94-011-4930-3_28.
Cattin, R., Doubre, C., de Chabalier, J.B., King, G., Vigny, C., Avouac, J.P., Ruegg, J.C., 2005. Numerical modelling of quaternary deformation and post-rifting displacement in the Asal–Ghoubbet rift (Djibouti, Africa). Earth Planet. Sci. Lett. 239, 352–367. https://doi.org/10.1016/J.EPSL.2005.07.028.
Cavalazzi, B., Barbieri, R., Gómez, F., Capaccioni, B., Olsson-Francis, K., Pondrelli, M., Rossi, A.P., Hickman-Lewis, K., Agangi, A., Gasparotto, G., Glamoclija, M., Ori, G.G., Rodriguez, N., Hagos, M., 2019. The Dallol Geothermal Area, Northern Afar (Ethiopia)—an Exceptional Planetary Field Analog on Earth. Astrobiology 19, 553–578. https://doi.org/10.1089/ast.2018.1926.
Chambers, E.L., Harmon, N., Keir, D., Rychert, C.A., 2019. Using Ambient Noise to image the Northern East African Rift. Geochem. Geophys. Geosyst. 20, 2091–2109. https://doi.org/10.1029/2018GC008129.
Chang, S.-J., Van der Lee, S., 2011. Mantle plumes and associated flow beneath Arabia and East Africa. Earth Planet. Sci. Lett. 302, 448–454. https://doi.org/10.1016/J.EPSL.2010.12.050.
Chang, S., Kendall, E., Davaille, A., Ferreira, A.M.G., 2020. The evolution of mantle plumes in East Africa. J. Geophys. Res. Solid Earth 125, e2020JB019929. https://doi.org/10.1029/2020JB019929.
Chauvet, F., Geoffroy, L., Le Gall, B., Jaud, M., 2023. Volcanic passive margins and break-up processes in the Southern Red Sea. Gondwana Res. 117, 169–193. https://doi.org/10.1016/J.GR.2023.01.004.
Chernet, T., Hart, W.K., Aronson, J.L., Walter, R.C., 1998. New age constraints on the timing of volcanism and tectonism in the northern Main Ethiopian Rift–southern Afar transition zone (Ethiopia). J. Volcanol. Geotherm. Res. 80, 267–280. https://doi.org/10.1016/S0377-0273(97)00035-8.
Chernet, S.G., Atnafu, B., Asrat, A., 2020. Stratigraphic and lithofacies analysis of the Gohatsion Formation in the Blue Nile basin, Central Ethiopia: Implications for depositional setting. J. Afr. Earth Sci. 162, 103693 https://doi.org/10.1016/j.jafrearsci.2019.103693.
Chessex, R., Delaloye, M., Muller, J., Weidmann, M., 1975. Evolution of the volcanic region of Ali Sabieh (T.F.A.I.), in the light of K-Ar age determinations. In: Pilger, A., Rösler, A. (Eds.), Afar Depression of Ethiopia: Proceedings of an International Symposium on the Afar Region and Related Rift Problems. E. Schweizerbart'sche Verlagsbuchhandlung, Stuttgart, pp. 221–227.
Chorowicz, J., 2005. The East African rift system. J. Afr. Earth Sci. 43, 379–410. https://doi.org/10.1016/J.JAFREARSCI.2005.07.019.
Chorowicz, J., Collet, B., Bonavia, F.F., Mohr, P., Parrot, J.F., Korme, T., 1998. The Tana basin, Ethiopia: Intra-plateau uplift, rifting and subsidence. Tectonophysics 295, 351–367. https://doi.org/10.1016/S0040-1951(98)00128-0.
Chorowicz, J., Collet, B., Bonavia, F., Korme, T., 1999. Left-lateral strike-slip tectonics and gravity induced individualisation of wide continental blocks in the western Afar margin. Eclogae Geol. Helv. 92, 149–158. doi:10.5169/seals-168656.
Christiansen, T.B., Schaefer, H.-U., Schönfeld, M., 1975. Southern Afar and adjacent areas: Geology, Petrology, Geochemistry. In: Pilger, A., Rösler, A. (Eds.), Afar Depression of Ethiopia: Proceedings of an International Symposium on the Afar Region and Related Rift Problems. E. Schweizerbart'sche Verlagsbuchhandlung, Stuttgart, pp. 259–277.
Chu, D., Gordon, R.G., 1998. Current plate motions across the Red Sea. Geophys. J. Int. 135, 313–328. https://doi.org/10.1046/j.1365-246X.1998.00658.x.
Civetta, L., De Fino, M., La Volpe, L., Lirer, L., 1974. Geochemical trends in the alkali basaltic suite of the Assab range (Ethiopia). Chem. Geol. 13, 149–162. https://doi.org/10.1016/0009-2541(74)90017-5.
Civetta, L., De Fino, M., Gasparini, P., Ghiara, M.R., La Volpe, L., Lirer, L., 1975a. Geology of the Central-Eastern Afar (Ethiopia). In: Pilger, A., Rösler, A. (Eds.), Afar Depression of Ethiopia: Proceedings of an International Symposium on the Afar Region and Related Rift Problems. E. Schweizerbart'sche Verlagsbuchhandlung, Stuttgart, pp. 201–206.
Civetta, L., De Fino, M., Gasparini, P., Ghiara, M.R., La Volpe, L., Lirer, L., 1975b. Structural meaning of east-Central Afar Volcanism (Ethiopia, T.F.A.I.). J. Geol. 83, 363–373. https://doi.org/10.1017/CBO9781107415324.004.
Civiero, C., Hammond, J.O.S., Goes, S., Fishwick, S., Ahmed, A., Ayele, A., Doubre, C., Goitom, B., Keir, D., Kendall, J.M., Leroy, S., Ogubazghi, G., Rümpker, G., Stuart, G. W., 2015. Multiple mantle upwellings in the transition zone beneath the northern East-African Rift system from relative P-wave travel-time tomography. Geochem. Geophys. Geosyst. 16, 2949–2968. https://doi.org/10.1002/2015GC005948.
Civiero, C., Lebedev, S., Celli, N.L., 2022. A complex Mantle Plume Head Below East Africa-Arabia shaped by the Lithosphere-Asthenosphere Boundary Topography. Geochem. Geophys. Geosyst. 23, e2022GC010610 https://doi.org/10.1029/2022GC010610.
Clark, J.D., Asfaw, B., Assefa, G., Harris, J.W.K., Kurashina, H., Walter, R.C., White, T.D., Williams, M.A.J., 1984. Palaeoanthropological discoveries in the Middle Awash Valley, Ethiopia. Nature 307, 423–428. https://doi.org/10.1038/307423a0.
Clark, J.D., De Heinzelin, J., Schick, K.D., Hart, W.K., White, T.D., WoldeGabriel, G., Walter, R.C., Suwa, G., Asfaw, B., Vrba, E., Selassie, Y.H., 1994. African Homo erectus: Old radiometric ages and young oldowan assemblages in the Middle Awash Valley, Ethiopia. Science 264, 1907–1910. https://doi.org/10.1126/science.8009220.
Clark, J.D., Beyene, Y., WoldeGabriel, G., Hart, W.K., Renne, P.R., Gilbert, H., Defieur, A., Suwa, G., Katoh, S., Ludwig, K.R., Boisserie, J.R., Asfaw, B., White, T.D.,

2003. Stratigraphic, chronological and behavioural contexts of Pleistocene Homo sapiens from Middle Awash, Ethiopia. Nature 423, 747–752. https://doi.org/10.1038/nature01670.
Cochran, J.R., 1983. A model for development of Red Sea. Am. Assoc. Pet. Geol. Bull. 67, 41–69. https://doi.org/10.1306/03B5ACBE-16D1-11D7-8645000102C1865D.
Cochran, J.R., 2005. Northern Red Sea: Nucleation of an oceanic spreading center within a continental rift. Geochem. Geophys. Geosyst. 6, Q03006. https://doi.org/10.1029/2004GC000826.
Collet, B., Taud, H., Parrot, J.F., Bonavia, F., Chorowicz, J., 2000. A new kinematic approach for the Danakil block using a Digital Elevation Model representation. Tectonophysics 316, 343–357. https://doi.org/10.1016/S0040-1951(99)00263-2.
Conforto, L., Delitala, M.C., Taddeucci, A., 1976. Datazioni col 230Th di alcune formazioni coralligene delle Isole Dahlak (Mar Rosso). Riv. Ital. Mineral. Petrol. 32, 153–158.
Corti, G., 2009. Continental rift evolution: from rift initiation to incipient break-up in the Main Ethiopian Rift, East Africa. Earth-Sci. Rev. 96, 1–53. https://doi.org/10.1016/J.EARSCIREV.2009.06.005.
Corti, G., Molin, P., Sembroni, A., Bastow, I.D., Keir, D., 2018a. Control of Pre-rift Lithospheric Structure on the Architecture and Evolution of Continental Rifts: Insights from the Main Ethiopian Rift, East Africa. Tectonics 37, 477–496. https://doi.org/10.1002/2017TC004799.
Corti, G., Sani, F., Agostini, S., Philippon, M., Sokoutis, D., Willingshofer, E., 2018b. Off-axis volcano-tectonic activity during continental rifting: Insights from the transversal Goba-Bonga lineament, Main Ethiopian Rift (East Africa). Tectonophysics 728–729, 75–91. https://doi.org/10.1016/J.TECTO.2018.02.011.
Corti, G., Maestrelli, D., Sani, F., 2022. Large-to Local-Scale Control of Pre-existing Structures on Continental Rifting: examples from the Main Ethiopian Rift, East Africa. Front. Earth Sci. 10 https://doi.org/10.3389/FEART.2022.808503.
Cottaar, S., Lekic, V., 2016. Morphology of seismically slow lower-mantle structures. Geophys. J. Int. 207, 1122–1136. https://doi.org/10.1093/gji/ggw324.
Coulié, E., 2001. Chronologie 40Ar/39Ar et K/Ar de la dislocation du plateau éthiopien et de la déchirure continentale à la corne de l'Afrique depuis 30 Ma. University Paris 11, France.
Coulié, E., Quidelleur, X., Gillot, P.-Y., Courtillot, V., Lefèvre, J.-C., Chiesa, S., 2003. Comparative K–Ar and Ar/Ar dating of Ethiopian and Yemenite Oligocene volcanism: implications for timing and duration of the Ethiopian traps. Earth Planet. Sci. Lett. 206, 477–492. https://doi.org/10.1016/S0012-821X(02)01089-0.
Courtillot, V.E., 1980. Opening of the Gulf of Aden and Afar by progressive tearing. Phys. Earth Planet. Inter. 21, 343–350. https://doi.org/10.1016/0031-9201(80)90137-5.
Courtillot, V., 1982. Propagating rifts and continental breakup. Tectonics 1, 239–250. https://doi.org/10.1029/TC001I003P00239.
Courtillot, V., Achache, J., Landre, F., Bonhommet, N., Montigny, R., Féraud, G., 1984. Episodic spreading and rift propagation: New paleomagnetic and geochronologic data from the Afar Nascent passive margin. J. Geophys. Res. Solid Earth 89, 3315–3333. https://doi.org/10.1029/JB089iB05p03315.
Courtillot, V., Armijo, R., Tapponnier, P., 1987. Kinematics of the Sinai triple junction and a two-phase model of Arabia-Africa rifting. Geol. Soc. Spec. Publ. 28, 559–573. https://doi.org/10.1144/GSL.SP.1987.028.01.37.
Courtillot, V., Davaille, A., Besse, J., Stock, J., 2003. Three distinct types of hotspots in the Earth's mantle. Earth Planet. Sci. Lett. 205, 295–308. https://doi.org/10.1016/S0012-821X(02)01048-8.
Cox, K.G., 1980. A Model for Flood Basalt Vulcanism. J. Petrol. 21, 629–650. https://doi.org/10.1093/petrology/21.4.629.
Craddock, J.P., Nuriel, P., Kylander-Clark, A.R.C., Hacker, B.R., Luczaj, J., Weinberger, R., 2021. Long-term (7 Ma) strain fluctuations within the Dead Sea transform system from high-resolution U-Pb dating of a calcite vein. GSA Bull. 134, 1231–1246. https://doi.org/10.1130/B36000.1.
Crossley, R., Watkins, C., Raven, M., Cripps, D., Carnell, A., Williams, D., 1992. The Sedimentary Evolution of the Red Sea and Gulf of Aden. J. Pet. Geol. 15, 157–172. https://doi.org/10.1111/j.1747-5457.1992.tb00960.x.
Daoud, M.A., Le Gall, B., Maury, R.C., Rolet, J., Huchon, P., Guillou, H., 2011. Young rift kinematics in the Tadjoura rift, western Gulf of Aden, Republic of Djibouti. Tectonics 30, TC1002. https://doi.org/10.1029/2009TC002614.
Darin, M.H., Umhoefer, P.J., 2022. Diachronous initiation of Arabia–Eurasia collision from eastern Anatolia to the southeastern Zagros Mountains since middle Eocene time. Int. Geol. Rev. 64, 2653–2681. https://doi.org/10.1080/00206814.2022.2048272.
Dauteuil, O., Huchon, P., Quemeneur, F., Souriot, T., 2001. Propagation of an oblique spreading Centre: the western Gulf of Aden. Tectonophysics 332, 423–442. https://doi.org/10.1016/S0040-1951(00)00295-X.
Davison, I., Al-Kadasi, M., Al-Khirbash, S., Al-Subbary, A.K., Baker, J., Blakey, S., Bosence, D., Dart, C., Heaton, R., McClay, K., Menzies, M., Nichols, G., Owen, L., Yelland, A., 1994. Geological evolution of the southeastern Red Sea Rift margin, Republic of Yemen. Geol. Soc. Am. Bull. 106, 1474–1493. https://doi.org/10.1130/0016-7606(1994)106<1474:GEOTSR>2.3.CO;2.
Davison, I., Tatnell, M.R., Owen, L.A., Jenkins, G., Baker, J., 1998. Tectonic geomorphology and rates of crustal processes along the Red Sea margin, north-West Yemen. In: Purser, B.H., Bosence, D.W. (Eds.), Sedimentation and Tectonics in Rift Basins: Red Sea - Gulf of Aden. Chapman & Hall, London, pp. 595–612. https://doi.org/10.1007/978-94-011-4930-3_32.
Dawit, E.L., 2016. Paleoclimatic records of late Triassic paleosols from Central Ethiopia. Palaeogeogr. Palaeoclimatol. Palaeoecol. 449, 127–140. https://doi.org/10.1016/J.PALAEO.2016.02.011.
De Fino, M., La Volpe, L., Lirer, L., 1973. Volcanology and petrology of the Assab Range (Ethiopia). Bull. Volcanol. 37, 95–110. https://doi.org/10.1007/BF02596882.
De Fino, M., La Volpe, L., Lirer, L., 1978. Geology and volcanology of the Edd-Bahar Assoli area (Ethiopia). Bull. Volcanol. 41, 32–42. https://doi.org/10.1007/BF02597681.
De Heinzelin, J., Clark, J.D., White, T., Hart, W., Renne, P., WoldeGabriel, G., Beyene, Y., Vrba, E., 1999. Environment and behavior of 2.5-million-year-old Bouri hominids. Science 284, 625–629. https://doi.org/10.1126/science.284.5414.625.
Deino, A.L., Scott, G.R., Saylor, B., Alene, M., Angelini, J.D., Haile-Selassie, Y., 2010. 40Ar/39Ar dating, paleomagnetism, and tephrochemistry of Pliocene strata of the hominid-bearing Woranso-Mille area, west-Central Afar Rift, Ethiopia. J. Hum. Evol. 58, 111–126. https://doi.org/10.1016/j.jhevol.2009.11.001.
DeMets, C., Merkouriev, S., 2016. High-resolution estimates of Nubia-Somalia plate motion since 20 Ma from reconstructions of the Southwest Indian Ridge, Red Sea and Gulf of Aden. Geophys. J. Int. 207, 317–332. https://doi.org/10.1093/gji/ggw276.
DeMets, C., Merkouriev, S., Sauter, D., 2021. High resolution reconstructions of the Southwest Indian Ridge, 52 Ma to present: Implications for the breakup and absolute motion of the Africa plate. Geophys. J. Int. 142, 1461–1497. https://doi.org/10.1093/gji/ggab107.
Desissa, M., Johnson, N.E., Whaler, K.A., Hautot, S., Fisseha, S., Dawes, G.J.K., 2013. A mantle magma reservoir beneath an incipient mid-ocean ridge in Afar, Ethiopia. Nat. Geosci. 6, 861–865. https://doi.org/10.1038/ngeo1925.
Didana, Y.L., Thiel, S., Heinson, G., 2014. Magnetotelluric imaging of upper crustal partial melt at Tendaho graben in Afar, Ethiopia. Geophys. Res. Lett. 41, 3089–3095. https://doi.org/10.1002/2014GL060000.
DiMaggio, E., Arrowsmith, J., Reed, K., Campisano, C., Oswald, L., 2009. Filling the Temporal Gap in Plio-Pleistocene Sedimentological Records from the Southern Afar Depression. EOS Trans, Ethiopia, in (AGU Fall Meeting Suppl., EP53A-0622).
DiMaggio, E.N., Arrowsmith, J.R., Campisano, C.J., Johnson, R., Deino, A.L., Warren, M., Fisseha, S., Cohen, A.S., 2015a. Tephrostratigraphy and depositional environment of young (< 2.94 Ma) Hadar Formation deposits at Ledi-Geraru, Afar, Ethiopia. J. Afr. Earth Sci. 112, 234–250. https://doi.org/10.1016/j.jafrearsci.2015.09.018.
DiMaggio, E.N., Campisano, C.J., Rowan, J., Dupont-Nivet, G., Deino, A.L., Bibi, F., Lewis, M.E., Souron, A., Garello, D., Werdelin, L., Reed, K.E., Arrowsmith, J.R., 2015b. Late Pliocene fossiliferous sedimentary record and the environmental context of early Homo from Afar, Ethiopia. Science 347, 1355–1359. https://doi.org/10.1126/science.aaa1415.
Dixon, T.H., Stern, R.J., Hussein, I.M., 1987. Control of Red Sea rift geometry by Precambrian structures. Tectonics 6, 551–571. https://doi.org/10.1029/TC006I005P00551.
Dou, L., Xiao, K., Cheng, D., Shi, B., Li, Z., 2007. Petroleum geology of the Melut Basin and the Great Palogue Field, Sudan. Mar. Pet. Geol. 24, 129–144. https://doi.org/10.1016/J.MARPETGEO.2006.11.001.
Doubre, C., Déprez, A., Masson, F., Socquet, A., Lewi, E., Grandin, R., Nercessian, A., Ulrich, P., De Chabalier, J.-B., Saad, I., Abayazid, A., Peltzer, G., Delorme, A., Calais, E., Wright, T., 2017. Current deformation in Central Afar and triple junction kinematics deduced from GPS and InSAR measurements. Geophys. J. Int. 208, 936–953. https://doi.org/10.1093/gji/ggw434.
Drury, S.A., Kelley, S.P., Berhe, S.M., Collier, R.E.L., Abraha, M., 1994. Structures related to Red Sea evolution in northern Eritrea. Tectonics 13, 1371–1380. https://doi.org/10.1029/94TC01990.
Duffield, W.A., Bullen, T.D., Clynne, M.A., Fournier, R.O., Janik, C.J., Lanphere, M.A., Lowenstern, J., Smith, J.G., Giorgis, L.W., Kahsai, G., Mariam, K.W., Tesfai, T., 1997. Geothermal potential of the Alid Volcanic center, Danakil depression, Eritrea. US Geol. Surv. Open-File Rep. 97-291 68 pp. https://doi.org/10.3133/ofr97291.
Dugda, M.T., Nyblade, A.A., 2006. New constraints on crustal structure in eastern Afar from the analysis of receiver functions and surface wave dispersion in Djibouti. Geol. Soc. London. Spec. Publ. 259, 239–251. https://doi.org/10.1144/GSL.SP.2006.259.01.19.
Dugda, M.T., Nyblade, A.A., Julia, J., Langston, C.A., Ammon, C.J., Simiyu, S., 2005. Crustal structure in Ethiopia and Kenya from receiver function analysis: Implications for rift development in eastern Africa. J. Geophys. Res. Solid Earth 110, 1–15. https://doi.org/10.1029/2004JB003065.
Dumont, S., Klinger, Y., Socquet, A., Doubre, C., Jacques, E., 2017. Magma influence on propagation of normal faults: evidence from cumulative slip profiles along Dabbahu-Manda-Hararo rift segment (Afar, Ethiopia). J. Struct. Geol. 95, 48–59. https://doi.org/10.1016/j.jsg.2016.12.008.
Dumont, S., Klinger, Y., Socquet, A., Escartín, J., Grandin, R., Jacques, E., Medynski, S., Doubre, C., 2019. Rifting Processes at a Continent-Ocean transition Rift Revealed by Fault Analysis: example of Dabbahu-Manda-Hararo Rift (Ethiopia). Tectonics 38, 190–214. https://doi.org/10.1029/2018TC005141.
Duncan, R.A., Al-Amri, A.M., 2013. Timing and composition of volcanic activity at Harrat Lunayyir, western Saudi Arabia. J. Volcanol. Geotherm. Res. 260, 103–116. https://doi.org/10.1016/j.jvolgeores.2013.05.006.
Dziewonski, A.M., Chou, T.A., Woodhouse, J.H., 1981. Determination of earthquake source parameters from waveform data for studies of global and regional seismicity. J. Geophys. Res. Solid Earth 86, 2825–2852. https://doi.org/10.1029/JB086IB04P02825.
Eagles, G., Gloaguen, R., Ebinger, C., 2002. Kinematics of the Danakil microplate. Earth Planet. Sci. Lett. 203, 607–620. https://doi.org/10.1016/S0012-821X(02)00916-0.
Earth Resources Observation and Science (EROS) Center, 2018a. Landsat 8 OLI (Operational Land Imager) and TIRS (Thermal Infrared Sensor) Level-1 Data Products. https://doi.org/10.5066/F71835S6.
Earth Resources Observation and Science (EROS) Center, 2018b. Shuttle Radar Topography Mission (SRTM) 1 Arc-Second Global. https://doi.org/10.5066/f7pr7tft.

Ebinger, C.J., Hayward, N.J., 1996. Soft plates and hot spots: views from Afar. J. Geophys. Res. Solid Earth 101, 21859–21876. https://doi.org/10.1029/96JB02118.
Ebinger, C.J., Sleep, N.H., 1998. Cenozoic magmatism throughout East Africa resulting from impact of a single plume. Nature 395, 788–791. https://doi.org/10.1038/27417.
Ebinger, C., Ayele, A., Keir, D., Rowland, J., Yirgu, G., Wright, T., Belachew, M., Hamling, I., 2010. Length and Timescales of Rift Faulting and Magma Intrusion: the Afar Rifting Cycle from 2005 to present. Annu. Rev. Earth Planet. Sci. 38, 439–466. https://doi.org/10.1146/annurev-earth-040809-152333.
Ebinger, C., Van Wijk, J., Keir, D., 2013. The time scales of continental rifting: Implications for global processes. Geol. Soc. Am. Spec. Pap. 500, 371–396. https://doi.org/10.1130/2013.2500(11).
Egloff, F., Rihm, R., Makris, J., Izzeldin, Y.A., Bobsien, M., Meier, K., Junge, P., Noman, T., Warsi, W., 1991. Contrasting structural styles of the eastern and western margins of the southern Red Sea: the 1988 SONNE experiment. Tectonophysics 198, 329–353. https://doi.org/10.1016/0040-1951(91)90159-P.
Egyptian Geological Survey, 1981. Geological Map of Egypt, 1:2′000’000. Egypt. Geol. Surv. Min, Auth.
Eid, B., Lhuillier, F., Gilder, S.A., Pfänder, J.A., Gebru, E.F., Aßbichler, D., 2021. Exceptionally High Emplacement Rate of the Afar Mantle Plume Head. Geophys. Res. Lett. 48, e2021GL094755 https://doi.org/10.1029/2021GL094755.
Ekström, G., Nettles, M., Dziewoński, A.M., 2012. The global CMT project 2004–2010: Centroid-moment tensors for 13,017 earthquakes. Phys. Earth Planet. Inter. 200–201, 1–9. https://doi.org/10.1016/J.PEPI.2012.04.002.
El Khrepy, S., Koulakov, I., Gerya, T., Al-Arifi, N., Alajmi, M.S., Qadrouh, A.N., 2021. Transition from continental rifting to oceanic spreading in the northern Red Sea area. Sci. Rep. 11, 5594. https://doi.org/10.1038/s41598-021-84952-w.
El-Sharkawy, A., Meier, T., Hübscher, C., Lebedev, S., Dannowski, A., Kopp, H., Behrmann, J.H., McGrandle, A., Hamada, M., 2021. Lithospheric structure of the eastern Mediterranean Sea: Inferences from surface wave tomography and stochastic inversions constrained by wide-angle refraction measurements. Tectonophysics 821, 229159. https://doi.org/10.1016/J.TECTO.2021.229159.
Evans, A.L., 1988. Neogene tectonic and stratigraphic events in the Gulf of Suez rift area, Egypt. Tectonophysics 153, 235–247. https://doi.org/10.1016/0040-1951(88)90018-2.
Faccenna, C., Becker, T.W., Jolivet, L., Keskin, M., 2013. Mantle convection in the Middle East: Reconciling Afar upwelling, Arabia indentation and Aegean trench rollback. Earth Planet. Sci. Lett. 375, 254–269. https://doi.org/10.1016/J.EPSL.2013.05.043.
Fairer, G.M., 1985. Geologic Map of the Wadi Baysh quadrangle, Sheet 17F, Kingdom of Saudi Arabia. Min. Pet. Miner. Resour. Deputy Minist. Miner. Resour. (Geosci. map GM-77 A).
Fantozzi, P., Ali Kassim, M., 2002. Geological mapping in northeastern Somalia (Midjiurtinia region): Field evidence of the structural and paleogeographic evolution of the northern margin of the Somalian plate. J. Afr. Earth Sci. 34, 21–55. https://doi.org/10.1016/S0899-5362(01)00100-2.
Faqira, M., Rademakers, M., Afifi, A.K.M., 2009. New insights into the Hercynian Orogeny, and their implications for the Paleozoic Hydrocarbon System in the Arabian Plate. GeoArabia 14, 199–228. https://doi.org/10.2113/GEOARABIA1403199.
Faure, H., Hoang, C.T., Lalou, C., 1980. Datations 230 Th/ 234 U des calcaires coralliens et mouvements verticaux a Djibouti. Bull. Soc. Géol. Fr. 7, 959–962.
Ferguson, D.J., Calvert, A.T., Pyle, D.M., Blundy, J.D., Yirgu, G., Wright, T.J., 2013a. Constraining timescales of focused magmatic accretion and extension in the Afar crust using lava geochronology. Nat. Commun. 4, 1416. https://doi.org/10.1038/ncomms2410.
Ferguson, D.J., Maclennan, J., Bastow, I.D., Pyle, D.M., Jones, S.M., Keir, D., Blundy, J. D., Plank, T., Yirgu, G., 2013b. Melting during late-stage rifting in Afar is hot and deep. Nature 499, 70–73. https://doi.org/10.1038/nature12292.
Feyissa, D.H., Shinjo, R., Kitagawa, H., Meshesha, D., Nakamura, E., 2017. Petrologic and geochemical characterization of rift-related magmatism at the northernmost Main Ethiopian Rift: Implications for plume-lithosphere interaction and the evolution of rift mantle sources. Lithos 282–283, 240–261. https://doi.org/10.1016/J.LITHOS.2017.03.011.
Field, L., Blundy, J., Calvert, A., Yirgu, G., 2013. Magmatic history of Dabbahu, a composite volcano in the Afar Rift, Ethiopia. Bull. Geol. Soc. Am. 125, 128–147. https://doi.org/10.1130/B30560.1.
Flowerdew, M.J., Whitehouse, M.J., Stoeser, D.B., 2013. The Nabitah fault zone, Saudi Arabia: a Pan-African suture separating juvenile oceanic arcs. Precambrian Res. 239, 95–105. https://doi.org/10.1016/J.PRECAMRES.2013.08.004.
Forte, A.M., Whipple, K.X., 2019. Short communication: the Topographic Analysis Kit (TAK) for TopoToolbox. Earth Surf. Dyn. 7, 87–95. https://doi.org/10.5194/esurf-7-87-2019.
Foulger, G.R., Jahn, C.H., Seeber, G., Einarsson, P., Julian, B.R., Heki, K., 1992. Post-rifting stress relaxation at the divergent plate boundary in Northeast Iceland. Nature 358, 488–490. https://doi.org/10.1038/358488a0.
Foulger, G.R., Doré, T., Emeleus, C.H., Franke, D., Geoffroy, L., Gernigon, L., Hey, R., Holdsworth, R.E., Hole, M., Höskuldsson, Á., Julian, B., Kusznir, N., Martinez, F., McCaffrey, K.J.W., Natland, J.H., Peace, A.L., Petersen, K., Schiffer, C., Stephenson, R., Stoker, M., 2020. The Iceland Microcontinent and a continental Greenland-Iceland-Faroe Ridge. Earth-Sci. Rev. 206, 102926 https://doi.org/10.1016/j.earscirev.2019.102926.
Fournier, M., Chamot-Rooke, N., Petit, C., Huchon, P., Al-Kathiri, A., Audin, L., Beslier, M.-O., D’Acremont, E., Fabbri, O., Fleury, J.-M., Khanbari, K., Lepvrier, C., Leroy, S., Maillot, B., Merkouriev, S., 2010. Arabia-Somalia plate kinematics, evolution of the Aden-Owen-Carlsberg triple junction, and opening of the Gulf of Aden. J. Geophys. Res. 115, B04102. https://doi.org/10.1029/2008JB006257.
Franke, D., 2013. Rifting, lithosphere breakup and volcanism: Comparison of magma-poor and volcanic rifted margins. Mar. Pet. Geol. 43, 63–87. https://doi.org/10.1016/J.MARPETGEO.2012.11.003.
Frazier, S.B., 1970. Adjacent structures of Ethiopia: that portion of the Red Sea Coast including Dahlak Kebir Island and the Gulf of Zula. Philos. Trans. R. Soc. Lond. Ser. A Math. Phys. Sci. 267, 131–141. https://doi.org/10.2307/73613.
Fritz, H., Abdelsalam, M., Ali, K.A., Bingen, B., Collins, A.S., Fowler, A.R., Ghebreab, W., Hauzenberger, C.A., Johnson, P.R., Kusky, T.M., Macey, P., Muhongo, S., Stern, R.J., Viola, G., 2013. Orogen styles in the East African Orogen: a review of the Neoproterozoic to Cambrian tectonic evolution. J. Afr. Earth Sci. 86, 65–106. https://doi.org/10.1016/J.JAFREARSCI.2013.06.004.
Frizon de Lamotte, D., Fourdan, B., Leleu, S., Leparmentier, F., de Clarens, P., 2015. Style of rifting and the stages of Pangea breakup. Tectonics 34, 1009–1029. https://doi.org/10.1002/2014TC003760.
Furman, T., Kaleta, K.M., Bryce, J.G., Hanan, B.B., 2006. Tertiary Mafic Lavas of Turkana, Kenya: Constraints on East African Plume Structure and the Occurrence of High-μ Volcanism in Africa. J. Petrol. 47, 1221–1244. https://doi.org/10.1093/PETROLOGY/EGL009.
Ganci, G., Cappello, A., Bilotta, G., Del Negro, C., 2020. How the variety of satellite remote sensing data over volcanoes can assist hazard monitoring efforts: the 2011 eruption of Nabro volcano. Remote Sens. Environ. 236, 111426 https://doi.org/10.1016/j.rse.2019.111426.
Gani, N.D., Abdelsalam, M.G., Gera, S., Gani, M.R., 2009. Stratigraphic and structural evolution of the Blue Nile Basin, Northwestern Ethiopian Plateau. Geol. J. 44, 30–56. https://doi.org/10.1002/gj.1127.
Gardo, I.A., Varet, J., 2018. Ta’Ali Geothermal Site, Afdera Woreda, Northern Afar, Ethiopia, in: Proceedings, 7th African Rift Geothermal Conference Kigali, Rwanda.
Garello, D.I., 2019. Tephrostratigraphy of Pliocene Drill Cores from Kenya and Ethiopia, and Pleistocene Exposures in the Ledi-Geraru Research Project Area. Geological Context for the Evolution of Australopithecus and Homo. Arizona State University, Ethiopia.
Garfunkel, Z., 2014. Lateral motion and deformation along the Dead Sea transform. In: Garfunkel, Z., Ben-Avraham, Z., Kagan, E. (Eds.), Dead Sea Transform Fault System: Reviews. Modern Approaches in Solid Earth Sciences. Springer, Dordrecht, pp. 109–150. https://doi.org/10.1007/978-94-017-8872-4_5.
Garfunkel, Z., Beyth, M., 2006. Constraints on the structural development of Afar imposed by the kinematics of the major surrounding plates. Geol. Soc. London. Spec. Publ. 259, 23–42. https://doi.org/10.1144/GSL.SP.2006.259.01.04.
Garzanti, E., Vezzoli, G., Andò, S., Castiglioni, G., 2001. Petrology of Rifted-margin sand (Red Sea and Gulf of Aden, Yemen). J. Geol. 109, 277–297. https://doi.org/10.1086/319973.
Gashawbeza, E.M., Klemperer, S.L., Nyblade, A.A., Walker, K.T., Keranen, K.M., 2004. Shear-wave splitting in Ethiopia: Precambrian mantle anisotropy locally modified by Neogene rifting. Geophys. Res. Lett. 31, 18602. https://doi.org/10.1029/2004GL020471.
Gass, I.G., Mallick, D.I.J., Cox, K.G.I., 1973. Volcanic islands of the Red Sea. J. Geol. Soc. Lond. 129, 275–309. https://doi.org/10.1144/gsjgs.129.3.0275.
Gasse, F., 1974. Les Diatomées des Sédiments Holocènes du Bassin du Lac Afrera (Giulietti) (Afar Septentrional, Ethiopie). Essai de Reconstitution de l’Évolution du Milieu. Int. Rev. Gesamten Hydrobiol. Hydrogr. 59, 95–122. https://doi.org/10.1002/iroh.19740590112.
Gasse, F., Fontes, J.C., 1989. Palaeoenvironments and palaeohydrology of a tropical closed lake (lake Asal, Djibouti) since 10,000 yr B.P. Palaeogeogr. Palaeoclimatol. Palaeoecol. 69, 67–102. https://doi.org/10.1016/0031-0182(89)90156-9.
Gasse, E., Street, F.A., 1978. Late Quaternary Lake-level fluctuations and environments of the northern Rift valley and Afar region (Ethiopia and Djibouti). Palaeogeogr. Palaeoclimatol. Palaeoecol. 24, 279–325. https://doi.org/10.1016/0031-0182(78)90011-1.
Gasse, F., Fontes, J.C., Rognon, P., 1974. Variations hydrologiques et extension des lacs holocenes du Desert Danakil. Palaeogeogr. Palaeoclimatol. Palaeoecol. 15, 109–148. https://doi.org/10.1016/0031-0182(74)90028-5.
Gasse, F., Richard, O., Robbe, D., Rognon, P., Williams, M.A.J., 1980. Evolution tectonique et climatique de l’Afar central d’apres les sediments plio-pleistocenes. Bull. Soc. Géol. Fr. S7-XXII, 987–1001. https://doi.org/10.2113/gssgfbull.s7-xxii.6.987.
Gasse, F., Varet, J., Mazet, G., Recroix, F., Ruegg, J.C., 1986. Carte géologique de la République de Djibouti à 1:100 000. Eali Sabih. Map and explanatory note.
Gasse, F., Dagain, J., Mazet, G., Richard, O., Fournier, M., 1987. Carte géologique de la République de Djibouti à 1:100 000. Dikhil. Map and explanatory note.
Gaulier, J.M., Huchon, P., 1991. Tectonic Evolution of Afar Triple Junction. Bull. La Soc. Geol. Fr. 162, 451–464. https://doi.org/10.2113/gssgfbull.162.3.451.
GEBCO Compilation Group, 2020. GEBCO 2020 Grid. https://doi.org/10.5285/a29c5465-b138-234d-e053-6c86abc040b9.
Geert, K., Afifi, A.M., Al-Hajri, S.A., Droste, H.J., 2001. Paleozoic Stratigraphy and Hydrocarbon Habitat of the Arabian Plate. GeoArabia 6, 407–442. https://doi.org/10.2113/geoarabia0603407.
Geoffroy, L., Le Gall, B., Daoud, M.A., Jalludin, M., 2014. Flip-flop detachment tectonics at nascent passive margins in SE Afar. J. Geol. Soc. Lond. 171, 689–694. https://doi.org/10.1144/jgs2013-135.
Geological Survey of Ethiopia, 1971. Mekele, 1:250,000 geological map and accompanying report.
Geological Survey of Ethiopia, 1973. Geological Map of Ethiopia (1:2′000’000).
Geological Survey of Ethiopia, 1978a. Adigrat, 1:250,000 geological map and accompanying report.

Geological Survey of Ethiopia, 1978b. Nazret, 1:250,000 geological map.
Geological Survey of Ethiopia, 1985. Dire Dawa, 1:250,000 geological map and accompanying report.
Geological Survey of Ethiopia, 1996. Geological map of Ethiopia (1:2'000'000).
Geological Survey of Ethiopia, 2007. Bedesa, 1:250,000 geological map and accompanying report.
Geological Survey of Ethiopia, 2009a. Were-Ilu, 1:250,000 geological map and accompanying report.
Geological Survey of Ethiopia, 2009b. Debre Birhan, 1:250,000 geological map.
Geological Survey of Ethiopia, 2010a. Harar, 1:250,000 geological map and accompanying report.
Geological Survey of Ethiopia, 2010b. Dessie, 1:250,000 geological map and accompanying report.
Geological Survey of Ethiopia, 2011. Maychew, 1:250,000 geological map and accompanying report.
Geological Survey of Ethiopia, 2013a. Serdo, 1:250,000 geological map and accompanying report.
Geological Survey of Ethiopia, 2013b. Urikemam Terar and Alulu Meda, 1:250,000 geological map and accompanying report.
Geological Survey of Ethiopia, 2014. Ayelu Terara, 1:250,000 geological map and accompanying report.
Geological Survey of Ethiopia, 2015. Ayisha, 1:250,000 geological map and accompanying report.
Geological Survey Somali Democratic Republic, 1957. Qabri Bahar (Sheet 21), 1:125,000 Geological Map.
Geological Survey Somali Democratic Republic, 1970a. Gocti (Sheet 19), 1:125,000 Geological Map.
Geological Survey Somali Democratic Republic, 1970b. Las Dureh (Sheet 25), 1:125,000 Geological Map.
Geological Survey Somali Democratic Republic, 1970c. El Dur Elan (Sheet 26), 1: 125,000 Geological Map.
Geological Survey Somali Democratic Republic, 1970d. Burao (Sheet 37), 1:125,000 Geological Map.
Geological Survey Somali Democratic Republic, 1970e. Habaji (Sheet 38), 1:125,000 Geological Map.
Geological Survey Somali Democratic Republic, 1971a. Abdal Quadr (Sheet 7), 1: 125,000 Geological Map.
Geological Survey Somali Democratic Republic, 1971b. Bawn (Sheet 20), 1:125,000 Geological Map.
Geological Survey Somali Democratic Republic, 1971c. Laferug (Sheet 23), 1:125,000 Geological Map.
Geological Survey Somaliland Protectorate, 1954. Sheikh (Sheet 36), 1:125,000 Geological Map.
Geological Survey Somaliland Protectorate, 1956. Adadleh (Sheet 35), 1:125,000 Geological Map.
Geological Survey Somaliland Protectorate, 1959a. Heis Area (Sheet 14), 1:125,000 Geological Map.
Geological Survey Somaliland Protectorate, 1959b. Erigavo (Sheet 15), 1:125,000 Geological Map.
Geological Survey Somaliland Protectorate, 1959c. Medishe (Sheet 16), 1:125,000 Geological Map.
George, R., Rogers, N., Kelley, S., 1998. Earliest magmatism in Ethiopia: evidence for two mantle plumes in one flood basalt province. Geology 26, 923–926. https://doi.org/10.1130/0091-7613(1998)026<0923:EMIEEF>2.3.CO;2.
Geraads, D., Alemseged, Z., Bellon, H., 2002. The late Miocene mammalian fauna of Chorora, Awash basin, Ethiopia: systematics, biochronology and 40K-40Ar ages of the associated volcanics. Tertiary Res. 21, 113–122.
Geraads, D., Reed, D., Barr, W.A., Bobe, R., Stamos, P., Alemseged, Z., 2021. Plio-Pleistocene mammals from Mille-Logya, Ethiopia, and the post-Hadar faunal change. J. Quat. Sci. 36, 1073–1089. https://doi.org/10.1002/jqs.3345.
Ghebreab, W., 1998. Tectonics of the Red Sea region reassessed. Earth-Sci. Rev. 45, 1–44. https://doi.org/10.1016/S0012-8252(98)00036-1.
Ghebreab, W., 1999. Tectono-metamorphic history of Neoproterozoic rocks in eastern Eritrea. Precambrian Res. 98, 83–105. https://doi.org/10.1016/S0301-9268(99)00040-6.
Ghebreab, W., Talbot, C.J., 2000. Red Sea extension influenced by Pan-African tectonic grain in eastern Eritrea. J. Struct. Geol. 22, 931–946. https://doi.org/10.1016/S0191-8141(00)00022-5.
Ghebreab, W., Carter, A., Hurford, A.J., Talbot, C.J., 2002. Constraints for timing of extensional tectonics in the western margin of the Red Sea in Eritrea. Earth Planet. Sci. Lett. 200, 107–119. https://doi.org/10.1016/S0012-821X(02)00621-0.
Ghinassi, M., Libsekal, Y., Papini, M., Rook, L., 2009. Palaeoenvironments of the Buia Homo site: High-resolution facies analysis and non-marine sequence stratigraphy in the Alat formation (Pleistocene Dandiero Basin, Danakil depression, Eritrea). Palaeogeogr. Palaeoclimatol. Palaeoecol. 280, 415–431. https://doi.org/10.1016/j.palaeo.2009.06.029.
Ghinassi, M., Billi, P., Libsekal, Y., Papini, M., Rook, L., 2014. Inferring Fluvial Morphodynamics and Overbank Flow Control from 3D Outcrop Sections of a Pleistocene Point Bar, Dandiero Basin, Eritrea. J. Sediment. Res. 83, 1065–1083. https://doi.org/10.2110/jsr.2013.80.
Girdler, R.W., 1985. Problems concerning the evolution of oceanic lithosphere in the northern Red Sea. Tectonophysics 116, 109–122. https://doi.org/10.1016/0040-1951(85)90224-0.
Girdler, R.W., 1991. The Afro-Arabian rift system—an overview. Tectonophysics 197, 139–153. https://doi.org/10.1016/0040-1951(91)90038-T.
Girdler, R.W., Southren, T.C., 1987. Structure and evolution of the northern Red Sea. Nature 330, 716–721. https://doi.org/10.1038/330716a0.
Girdler, R.W., Styles, P., 1974. Two Stage Red Sea Floor Spreading. Nature 247, 7–11. https://doi.org/10.1038/247007a0.
Girdler, R.W., Underwood, M., 1985. The evolution of early oceanic lithosphere in the southern Red Sea. Tectonophysics 116, 95–108. https://doi.org/10.1016/0040-1951(85)90223-9.
Global Volcanism Program, 2013. In: Venzke, E. (Ed.), Volcanoes of the World, v. 4.10.4 (09 Dec 2021). Smithson. Inst. https://doi.org/10.5479/si.GVP.VOTW4-2013.
Global Volcanism Program, 2018. Report on Erta Ale (Ethiopia). In: Crafford, A.E., Venzke, E. (Eds.), Bull. Glob. Volcanism Network, 43. Smithonian Inst. https://doi.org/10.5479/si.GVP.BGVN201804-221080.
Global Volcanism Program, 2019. Report on Erta Ale (Ethiopia). In: Venzke, E. (Ed.), Bull. Glob. Volcanism Network, 44. Smithonian Inst. https://doi.org/10.5479/si.GVP.BGVN201911-221080.
Global Volcanism Program, 2021. Report on Erta Ale (Ethiopia). In: Bennis, K.L., Venzke, E. (Eds.), Bull. Glob. Volcanism Network, 46. Smithonian Inst. https://doi.org/10.5479/si.GVP.BGVN202102-221080.
Goitom, B., Oppenheimer, C., Hammond, J.O.S., Grandin, R., Barnie, T., Donovan, A., Ogubazghi, G., Yohannes, E., Kibrom, G., Kendall, J.-M., Carn, S.A., Fee, D., Sealing, C., Keir, D., Ayele, A., Blundy, J., Hamlyn, J., Wright, T., Berhe, S., 2015. First recorded eruption of Nabro volcano, Eritrea, 2011. Bull. Volcanol. 77, 85. https://doi.org/10.1007/s00445-015-0966-3.
Gouin, P., 1979. Earthquake History of Ethiopia and the Horn of Africa. IDRC, Ottawa, ON, CA.
Grandin, R., Socquet, A., Binet, R., Klinger, Y., Jacques, E., De Chabalier, J.B., King, G.C.P., Lasserre, C., Tait, S., Tapponnier, P., Delorme, A., Pinzuti, P., 2009. September 2005 Manda Hararo-Dabbahu rifting event, Afar (Ethiopia): Constraints provided by geodetic data. J. Geophys. Res. Solid Earth 114, 8404. https://doi.org/10.1029/2008JB005843.
Grandin, R., Socquet, A., Jacques, E., Mazzoni, N., de Chabalier, J.-B., King, G.C.P., 2010. Sequence of rifting in Afar, Manda-Hararo rift, Ethiopia, 2005–2009: Time-space evolution and interactions between dikes from interferometric synthetic aperture radar and static stress change modeling. J. Geophys. Res. 115, B10413. https://doi.org/10.1029/2009JB000815.
Grolier, M.J., Overstreet, W.C., 1978. Geologic map of the Yemen Arab Republic (Sana). U.S. Geol. Surv. Misc. Investig. (Ser. Map I-1143-b).
Guan, H., Geoffroy, L., Xu, M., 2021. Magma-assisted fragmentation of Pangea: Continental breakup initiation and propagation. Gondwana Res. 96, 56–75. https://doi.org/10.1016/J.GR.2021.04.003.
Guiraud, R., Bosworth, W., Thierry, J., Delplanque, A., 2005. Phanerozoic geological evolution of Northern and Central Africa: an overview. J. Afr. Earth Sci. 43, 83–143. https://doi.org/10.1016/J.JAFREARSCI.2005.07.017.
van der Gun, J., 1995. Geological map of Yemen (Fig 2.3 in "The Water Resources of Yemen"). https://doi.org/10.13140/RG.2.1.3566.4085.
van der Gun, J.A.M., Ahmed, A.A., 1995. The water resources of Yemen: a summary and digest of available information. Water Resour. Assess. Yemen. https://doi.org/10.13140/RG.2.1.2616.1362.
Hagos, M., Koeberl, C., van Wyk de Vries, B., 2016a. The Quaternary volcanic rocks of the northern Afar Depression (northern Ethiopia): Perspectives on petrology, geochemistry, and tectonics. J. Afr. Earth Sci. 117, 29–47. https://doi.org/10.1016/j.jafrearsci.2015.11.022.
Hagos, M., Konka, B., Ahmed, J., 2016b. A preliminary Geological and Generalized Stratigraphy of Western margin of Northern Afar Depression, Dallol Area, Northern Ethiopia. Mom. Ethiop. J. Sci. 8, 1–22. https://doi.org/10.4314/mejs.v8i1.1.
Hagos, M., Koeberl, C., Jourdan, F., 2017. Geochemistry and Geochronology of Phonolitic and Trachytic Source Rocks of the Axum Obelisks and Other Stone Artifacts, Axum, Ethiopia. Geoheritage 9, 479–494. https://doi.org/10.1007/s12371-016-0199-7.
Hagos, M., Gebreyohannes, T., Amare, K., Hussien, A., Berhane, G., Walraevens, K., Koeberl, C., De Vries, Van Wyk, Cavalazzi, B., 2020. Tectonic link between the Neoproterozoic dextral shear fabrics and Cenozoic extension structures of the Mekelle basin, Northern Ethiopia. Int. J. Earth Sci. 109, 1957–1974. https://doi.org/10.1007/s00531-020-01882-0.
Haile-Selassie, Y., Gibert, L., Melillo, S.M., Ryan, T.M., Alene, M., Deino, A., Levin, N.E., Scott, G., Saylor, B.Z., 2015. New species from Ethiopia further expands Middle Pliocene hominin diversity. Nature 521, 483–488. https://doi.org/10.1038/nature14448.
Hakimi, M.H., Ahmed, A.F., Abdullah, W.H., 2016. Organic geochemical and petrographic characteristics of the Miocene Salif organic-rich shales in the Tihama Basin, Red Sea of Yemen: Implications for paleoenvironmental conditions and oil-generation potential. Int. J. Coal Geol. 154–155, 193–204. https://doi.org/10.1016/j.coal.2016.01.004.
Hakimi, M.H., Gharib, A.F., Abidin, N.S.Z., Yahya, M.M.A., 2021. Preliminary investigation of the hydrocarbon generation potential from the post-rift Abbas shale Formation (Pliocene) in the Tihamah Basin, south-eastern Yemeni Red Sea. J. Pet. Explor. Prod. Technol. 11, 63–73. https://doi.org/10.1007/s13202-020-01045-6.
Hakimi, M.H., Lashin, A., Gharib, A.F., Rahim, A., Yelwa, N.A., Nasher, M.A., Lotfy, N. M., Afify, W.E., 2022. The effect of Pliocene volcanic intrusive rocks and thermogenic gas generation from the Miocene Salif Formation in the offshore Tihamah Basin, Yemeni Red Sea. Mar. Pet. Geol. 146, 105923 https://doi.org/10.1016/j.marpetgeo.2022.105923.
Hall, S.A., 1989. Magnetic evidence for the Nature of the Crust beneath the Southen Red Sea. J. Geophys. Res. Earth Planets 94, 12267–12279. https://doi.org/10.1029/Jb094ib09p12267.

Hall, C.M., Walter, R.C., Westgate, J.A., York, D., 1984. Geochronology, stratigraphy and geochemistry of Cindery Tuff in Pliocene hominid-bearing sediments of the Middle Awash, Ethiopia. Nature 308, 26–31. https://doi.org/10.1038/308026a0.
Halldórsson, S.A., Hilton, D.R., Scarsi, P., Abebe, T., Hopp, J., 2014. A common mantle plume source beneath the entire East African Rift System revealed by coupled helium-neon systematics. Geophys. Res. Lett. 41, 2304–2311. https://doi.org/10.1002/2014GL059424.
Hammond, J.O.S., Kendall, J.-M., Stuart, G.W., Keir, D., Ebinger, C., Ayele, A., Belachew, M., 2011. The nature of the crust beneath the Afar triple junction: Evidence from receiver functions. Geochem. Geophys. Geosyst. 12 https://doi.org/10.1029/2011GC003738. Q12004.
Hammond, J.O.S., Kendall, J.-M., Stuart, G.W., Ebinger, C.J., Bastow, I.D., Keir, D., Ayele, A., Belachew, M., Goitom, B., Ogubazghi, G., Wright, T.J., 2013. Mantle upwelling and initiation of rift segmentation beneath the Afar Depression. Geology 41, 635–638. https://doi.org/10.1130/G33925.1.
Hansen, S.E., Nyblade, A.A., Benoit, M.H., 2012. Mantle structure beneath Africa and Arabia from adaptively parameterized P-wave tomography: Implications for the origin of Cenozoic Afro-Arabian tectonism. Earth Planet. Sci. Lett. 319–320, 23–34. https://doi.org/10.1016/J.EPSL.2011.12.023.
Hassan, R., Williams, S.E., Gurnis, M., Müller, D., 2020. East African topography and volcanism explained by a single, migrating plume. Geosci. Front. 11, 1669–1680. https://doi.org/10.1016/j.gsf.2020.01.003.
Hautot, S., Whaler, K., Gebru, W., Desissa, M., 2006. The structure of a Mesozoic basin beneath the Lake Tana area, Ethiopia, revealed by magnetotelluric imaging. J. Afr. Earth Sci. 44, 331–338. https://doi.org/10.1016/j.jafrearsci.2005.11.027.
Hayward, N.J., Ebinger, C.J., 1996. Variations in the along-axis segmentation of the Afar Rift system. Tectonics 15, 244–257. https://doi.org/10.1029/95TC02292.
Hearn, G.J., 2022. Some of the geological challenges and opportunities associated with the dynamics of the Cenozoic East African Rift System. Q. J. Eng. Geol. Hydrogeol. 55 https://doi.org/10.1144/qjegh2021-060 qjegh2021-060.
Hébert, H., Deplus, C., Huchon, P., Khanbari, K., Audin, L., 2001. Lithospheric structure of a nascent spreading ridge inferred from gravity data: the western Gulf of Aden. J. Geophys. Res. Solid Earth 106, 26345–26363. https://doi.org/10.1029/2000JB900391.
Hofmann, C., Courtillot, V., Féraud, G., Rochette, P., Yirgu, G., Ketefo, E., Pik, R., 1997. Timing of the ethiopian flood basalt event and implications for plume birth and global change. Nature 389, 838–841. https://doi.org/10.1038/39853.
Hofstetter, R., Beyth, M., 2003. The Afar Depression: interpretation of the 1960-2000 earthquakes. Geophys. J. Int. 155, 715–732. https://doi.org/10.1046/j.1365-246X.2003.02080.x.
Holwerda, U.G., Hutchinson, R.W., 1968. Potash-bearing Evaporites in the Danakhil Region, Etiopia. Econ. Geol. 2, 124–150. https://doi.org/10.2113/gsecongeo.63.2.124.
Huchon, P., Jestin, F., Cantagrel, J.M., Gaulier, J.M., Al Khirbash, S., Gafaneh, A., 1991. Extensional deformations in Yemen since Oligocene and the Africa- Arabia-Somalia triple junction. Ann. Tecton. 5, 141–163.
Hughes, G.W., Beydoun, Z.R., 1992. The Red Sea — Gulf of Aden: Biostratigraphy, Lithostratigraphy and Palaeoenvironments. J. Pet. Geol. 15, 135–156. https://doi.org/10.1111/j.1747-5457.1992.tb00959.x.
Hughes, G.W., Varol, O., Beydoun, Z.R., 1991. Evidence for Middle Oligocene rifting of the Gulf of Aden and for late Oligocene rifting of the southern Red Sea. Mar. Pet. Geol. 8, 354–358. https://doi.org/10.1016/0264-8172(91)90088-I.
Hughes, G.W., Aramco, S., Perincek, D., Grainger, D.J., Abu-Bshait, A.-J., Jarad, A.-R.M., 1999. Lithostratigraphy and Depositional history of part of the Midyan Region, Northwestern Saudi Arabia. GeoArabia 4, 503–542. https://doi.org/10.2113/geoarabia0404503.
Hujer, W., Kuiper, K., Viola, T.B., Wagreich, M., Faupl, P., 2015. Lithostratigraphy of the late Miocene to early Pleistocene, hominidbearing Galili Formation, Southern Afar Depression, Ethiopia. Aust. J. Earth Sci. 108, 105–127. https://doi.org/10.17738/ajes.2015.0016.
Hunegnaw, A., Sage, L., Gonnard, R., 1998. Hydrocarbon potential of the intracratonic Ogaden Basin, SE Ethiopia. J. Pet. Geol. 21, 401–425. https://doi.org/10.1111/J.1747-5457.1998.TB00793.X.
Illsley-Kemp, F., Keir, D., Bull, J.M., Gernon, T.M., Ebinger, C., Ayele, A., Hammond, J.O. S., Kendall, J.M., Goitom, B., Belachew, M., 2018a. Seismicity during continental breakup in the Red Sea rift of Northern Afar. J. Geophys. Res. Earth 123, 2345–2362. https://doi.org/10.17605/OSF.IO/A7QTD.
Hurman, G.L., Keir, D., Bull, J.M., McNeill, L.C., Booth, A.D., Bastow, I.D., 2023. Quantitative Analysis of Faulting in the Danakil Depression Rift of Afar: The Importance of Faulting in the Final Stages of Magma-Rich Rifting. Tectonics 42. https://doi.org/10.1029/2022TC007607.
Illsley-Kemp, F., Bull, J.M., Keir, D., Gerya, T.V., Pagli, C., Gernon, T., Ayele, A., Goitom, B., Hammond, J., Kendall, J.M., 2018b. Initiation of a Proto-Transform Fault prior to Seafloor Spreading. Geochem. Geophys. Geosyst. 2018GC007947 https://doi.org/10.1029/2018GC007947.
International Seismological Centre, 2021. On-line Bulletin. https://doi.org/10.31905/D808B830.
Issachar, R., Ebbing, J., Dilixiati, Y., 2022. New magnetic anomaly map for the Red Sea reveals transtensional structures associated with rotational rifting. Sci. Rep. 12, 1–13. https://doi.org/10.1038/s41598-022-09770-0.
Izzeldin, A.Y., 1987. Seismic, gravity and magnetic surveys in the central part of the Red Sea: their interpretation and implications for the structure and evolution of the Red Sea. Tectonophysics 143, 269–306. https://doi.org/10.1016/0040-1951(87)90214-9.
Jaramillo-Vogel, D., Foubert, A., Braga, J.C., Schaegis, J.-C., Atnafu, B., Grobety, B., Kidane, T., 2019. Pleistocene Sea-floor fibrous crusts and spherulites in the Danakil Depression (Afar, Ethiopia). Sedimentology 66, 480–512. https://doi.org/10.1111/sed.12484.
Jaramillo-Vogel, D., Braga, J.C., Negga, H.A., Vennemann, T., De Boever, E., Schaegis, J. C., Rime, V., Atnafu, B., Kidane, T., Foubert, A., 2023. Pleistocene aragonite crust diagenesis mimics microbialite fabrics (Danakil Depression, Ethiopia). Sediment. Geol. 106341 https://doi.org/10.1016/J.SEDGEO.2023.106341.
Johanson, D.C., Lovejoy, C.O., Kimbel, W.H., White, T.D., Ward, S.C., Bush, M.E., Latimer, B.M., Coppens, Y., 1982. Morphology of the Pliocene partial hominid skeleton (a.L. 288-1) from the Hadar formation, Ethiopia. Am. J. Phys. Anthropol. 57, 403–451. https://doi.org/10.1002/AJPA.1330570403.
Johnson, P.R., 2021. The Arabian–Nubian Shield, an Introduction: Historic Overview, Concepts, Interpretations, and Future Issues. In: Hamimi, Z., Fowler, A.R., Liégeois, J.P., Collins, A., Abdelsalam, M.G., Abd EI-Wahed M. (Eds.), The Geology of the Arabian-Nubian Shield. Springer, Cham, pp. 1–38. https://doi.org/10.1007/978-3-030-72995-0_1.
Johnson, P.R., Andresen, A., Collins, A.S., Fowler, A.R., Fritz, H., Ghebreab, W., Kusky, T., Stern, R.J., 2011. Late Cryogenian–Ediacaran history of the Arabian–Nubian Shield: A review of depositional, plutonic, structural, and tectonic events in the closing stages of the northern East African Orogen. J. Afr. Earth Sci. 61, 167–232. https://doi.org/10.1016/J.JAFREARSCI.2011.07.003.
Johnson, N.E., Whaler, K.A., Hautot, S., Fisseha, S., Desissa, M., Dawes, G.J.K., 2016. Magma imaged magnetotellurically beneath an active and an inactive magmatic segment in Afar, Ethiopia. Geol. Soc. Spec. Publ. 420, 105–125. https://doi.org/10.1144/SP420.11.
Jolivet, L., Faccenna, C., 2000. Mediterranean extension and the Africa-Eurasia collision. Tectonics 19, 1095–1106. https://doi.org/10.1029/2000TC900018.
Juch, D., 1975. Geology of the South-Eastern Escarpment of Ethiopia between 39° and 42° long. east. In: Pilger, A., Rösler, A. (Eds.), Afar Depression of Ethiopia. E. Schweizerbart'sche Verlagsbuchhandlung, Stuttgart, pp. 310–316.
Justin-Visentin, E., 1974. Petrografia, chimismo e petrogenesi dei corpi subvulcanici di Macallè (Tigrai Etiopia). Mem. dell'Istituto di Geol. e Mineral. Univ. Padova 31, 1–33.
Justin-Visentin, E., Zanettin, B., 1974. Dike swarms, volcanism and tectonics of the western Afar margin along the Kombolcha-Eloa traverse (Ethiopia). Bull. Volcanol. 38, 187–205. https://doi.org/10.1007/BF02597810.
Kalb, J.E., 1995. Fossil elephantoids, Awash paleolake basins, and the Afar triple junction, Ethiopia. Palaeogeogr. Palaeoclimatol. Palaeoecol. 114, 357–368. https://doi.org/10.1016/0031-0182(94)00088-P.
Kalb, J.E., Oswald, E.B., Tebedge, S., Mebrate, A., Tola, E., Peak, D., 1982. Geology and stratigraphy of Neogene deposits, Middle Awash Valley, Ethiopia. Nature 298, 17–25. https://doi.org/10.1038/298017a0.
Kasser, M., Lepine, J.C., Ruegg, J.C., Tarantula, A., 1981. Geodetic results in Afar: the rifting episode of November 1978 in the Asal-Ghoubbet rift. Tectonophysics 71, 73–74. https://doi.org/10.1016/0040-1951(81)90048-2.
Kazmin, V., Seife, M.B., Nicoletti, M., Petrucciani, C., 1980. Evolution of the Northern part of the Ethiopian Rift, in: Geodynamic Evolution of the Afro-Arabian Rift System, Accademia Nazionale Dei Lincei, International meeting April 1979. Atti Dei Convegni Lincei 47, 275–292.
Keir, D., Belachew, M., Ebinger, C.J., Kendall, J.M., Hammond, J.O.S., Stuart, G.W., Ayele, A., Rowland, J.V., 2011. Mapping the evolving strain field during continental breakup from crustal anisotropy in the Afar Depression. Nat. Commun. 2, 285–287. https://doi.org/10.1038/ncomms1287.
Keir, D., Bastow, I.D., Pagli, C., Chambers, E.L., 2013. The development of extension and magmatism in the Red Sea rift of Afar. Tectonophysics 607, 98–114. https://doi.org/10.1016/j.tecto.2012.10.015.
Kendall, J.-M., Lithgow-Bertelloni, C., 2016. Why is Africa rifting? Geol. Soc. London Spec. Publ. 420, 11–30. https://doi.org/10.1144/SP420.17.
Kenea, N.H., Ebinger, C.J., Rex, D.C., 2001. Late Oligocene volcanism and extension in the southern Red Sea Hills, Sudan. J. Geol. Soc. Lond. 158, 285–294. https://doi.org/10.1144/JGS.158.2.285.
Keranen, K., Klemperer, S.L., 2008. Discontinuous and diachronous evolution of the Main Ethiopian Rift: Implications for development of continental rifts. Earth Planet. Sci. Lett. 265, 96–111. https://doi.org/10.1016/J.EPSL.2007.09.038.
Khalil, H.M., Capitanio, F.A., Betts, P.G., Cruden, A.R., 2020. 3-D Analog Modeling Constraints on Rifting in the Afar Region. Tectonics 39, e2020TC006339. https://doi.org/10.1029/2020TC006339.
Kibret, B.A., Ayele, A., Keir, D., 2019. Crustal thickness estimates beneath four seismic stations in Ethiopia inferred from p-wave receiver function studies. J. Afr. Earth Sci. 150, 264–271. https://doi.org/10.1016/J.JAFREARSCI.2018.11.005.
Kidane, T., 2016. Strong clockwise block rotation of the Ali-Sabieh/Aïsha Block: evidence for opening of the Afar Depression by a 'saloon-door' mechanism. Geol. Soc. London Spec. Publ. 420, 209–219. https://doi.org/10.1144/SP420.10.
Kidane, T., Carlut, J., Courtillot, V., Gallet, Y., Quidelleur, X., Gillot, P.Y., Haile, T., 1999. Paleomagnetic and geochronological identification of the Réunion subchron in Ethiopian Afar. J. Geophys. Res. Solid Earth 104, 10405–10419. https://doi.org/10.1029/1999JB900014.
Kidane, T., Courtillot, V., Manighetti, I., Audin, L., Lahitte, P., Quidelleur, X., Gillot, P.-Y., Gallet, Y., Carlut, J., Haile, T., 2003. New paleomagnetic and geochronologic results from Ethiopian Afar: Block rotations linked to rift overlap and propagation and determination of a 2 Ma reference pole for stable Africa. J. Geophys. Res. Solid Earth 108, 2102. https://doi.org/10.1029/2001JB000645.
Kidane, T., Platzman, E., Ebinger, C.J., Abebe, B., Rochette, P., 2006. Palaeomagnetic constraints on continental break-up processes: Observations from the Main Ethiopian Rift. Geol. Soc. Spec. Publ. 259, 165–183. https://doi.org/10.1144/GSL.SP.2006.259.01.14.

Kidane, T., Otofuji, Y.I., Komatsu, Y., Shibasaki, H., Yokoyama, M., 2010. Structural and geochronological implications of the Fentale Volcanics at a nascent passive margin of the Main Ethiopian Rift: Constraints from magnetostratigraphy study at the Kereyou Lodge, Ethiopia. Tectonophysics 495, 159–170. https://doi.org/10.1016/j.tecto.2010.09.004.

Kidane, T., Bachtadse, V., Alene, M., Kirscher, U., 2013. Palaeomagnetism of Palaeozoic glacial sediments of Northern Ethiopia: a contribution towards African Permian palaeogeography. Geophys. J. Int. 195, 1551–1565. https://doi.org/10.1093/GJI/GGT336.

Kieffer, B., Arndt, N., Lapierre, H., Bastien, F., Bosch, D., Pecher, A., Yirgu, G., Ayalew, D., Weis, D., Jerram, D.A., Keller, F., Meugniot, C., 2004. Flood and Shield Basalts from Ethiopia: Magmas from the African Superswell. J. Petrol. 45, 793–834. https://doi.org/10.1093/petrology/egg112.

Kleinsasser, L., Quade, J., McIntosh, W.C., Levin, N.E., Simpson, S.W., Semaw, S., 2008. Stratigraphy and geochronology of the late Miocene Adu-Asa Fromation at Gona, Ethiopia. In: Quade, J., Wynn, J.G. (Eds.), The Geology of Early Humans in the Horn of Africa. The Geological Society of America, pp. 33–65. https://doi.org/10.1130/2008.2446(02).

Kogan, L., Fisseha, S., Bendick, R., Reilinger, R., McClusky, S., King, R., Solomon, T., 2012. Lithospheric strength and strain localization in continental extension from observations of the East African Rift. J. Geophys. Res. Solid Earth 117, B03402. https://doi.org/10.1029/2011JB008516.

Koptev, A., Cloetingh, S., Gerya, T., Calais, E., Leroy, S., 2018a. Non-uniform splitting of a single mantle plume by double cratonic roots: Insight into the origin of the central and southern East African Rift System. Terra Nova 30, 125–134. https://doi.org/10.1111/ter.12317.

Koptev, A., Gerya, T., Calais, E., Leroy, S., Burov, E., 2018b. Afar triple junction triggered by plume-assisted bi-directional continental break-up. Sci. Rep. 8, 14742. https://doi.org/10.1038/s41598-018-33117-3.

Korme, T., Acocella, V., Abebe, B., 2004. The Role of Pre-existing Structures in the Origin, Propagation and Architecture of Faults in the Main Ethiopian Rift. Gondwana Res. 7, 467–479. https://doi.org/10.1016/S1342-937X(05)70798-X.

Kronberg, P., Bannert, D., Schönfeld, M., Günther, R., Tsombos, P., Gundlach, A., 1974a. Lithological Map of the Afar/Ethiopia and Adjacent Regions as Mapped from ERTS 1-Imagery. In: Pilger, A., Rösler, A. (Eds.), Afar Depression of Ethiopia: Proceedings of an International Symposium on the Afar Region and Related Rift Problems. E. Schweizerbart'sche Verlagsbuchhandlung, Stuttgart.

Kronberg, P., Bannert, D., Schönfeld, M., Günther, R., Tsombos, P., Polyzos, A., 1974b. Surface Structures of the Afar/Ethiopia and Adjacent Regions as Mapped from ERTS 1-Imagery. In: Pilger, A., Rösler, A. (Eds.), Afar Depression of Ethiopia: Proceedings of an International Symposium on the Afar Region and Related Rift Problems. E. Schweizerbart'sche Verlagsbuchhandlung, Stuttgart.

Kronberg, P., Schönfeld, M., Günther, R., Tsombos, P., 1975. Tectonic relations of the Afar region and adjacent areas - ERTS 1-data on the geology and tectonics of the Afar/Ethiopia and adjacent regions. In: Pilger, A., Rösler, A. (Eds.), Afar Depression of Ethiopia: Proceedings of an International Symposium on the Afar Region and Related Rift Problems. E. Schweizerbart'sche Verlagsbuchhandlung, Stuttgart, pp. 19–27.

Kruck, W., 1980. Geological Map of the Yemen Arab Republic, Sheet Al Hazm 1:250 000. Fed. Inst. Geosci. Nat. Resour, Hann.

Kruck, W., 1984. Geological Map of the Yemen Arab Republic, Sheet San'a' 1:250 000. Fed. Inst. Geosci. Nat. Resour, Hann.

Kruck, W., Al Anissi, A., Saif, M., 1984. Geological Map of the Yemen Arab Republic, Sheet Al Hudaydah 1:250 000 (Fed. Inst. Geosci. Nat. Resour. Hann. / Yemen Oil Miner. Resour. Corp. San'a').

Kunz, K., Kreuzer, H., Müller, P., 1975. Potassium-Argon age determinations of the Trap basalt of the south-eastern part of the Afar Rift. In: Pilger, A., Rösler, A. (Eds.), Afar Depression of Ethiopia: Proceedings of an International Symposium on the Afar Region and Related Rift Problems. E. Schweizerbart'sche Verlagsbuchhandlung, Stuttgart, pp. 370–374.

Kürsten, M., 1975. Tectonic inventory of the Danakil Depression. In: Pilger, A., Rösler, A. (Eds.), Afar Depression of Ethiopia: Proceedings of an International Symposium on the Afar Region and Related Rift Problems. E. Schweizerbart'sche Verlagsbuchhandlung, Stuttgart, pp. 170–174.

Kurz, T., Gloaguen, R., Ebinger, C., Casey, M., Abebe, B., 2007. Deformation distribution and type in the Main Ethiopian Rift (MER): a remote sensing study. J. Afr. Earth Sci. 48, 100–114. https://doi.org/10.1016/J.JAFREARSCI.2006.10.008.

La Rosa, A., 2020. Strain Partitioning between Border Faults and Axial Magmatic Segments in the Afar Rift (PhD Thesis).. Università degli Studi di Firenze.

La Rosa, A., Pagli, C., Keir, D., Sani, F., Corti, G., Wang, H., Possee, D., 2019. Observing Oblique Slip during Rift Linkage in Northern Afar. Geophys. Res. Lett. 46, 10782–10790. https://doi.org/10.1029/2019GL084801.

La Rosa, A., Pagli, C., Wang, H., Doubre, C., Leroy, S., Sani, F., Corti, G., Ayele, A., Keir, D., 2021. Plate-Boundary Kinematics of the Afrera Linkage Zone (Afar) from InSAR and Seismicity. J. Geophys. Res. Solid Earth 126, e2020JB021387. https://doi.org/10.1029/2020JB021387.

La Rosa, A., Pagli, C., Hurman, G.L., Keir, D., 2022. Strain Accommodation by Intrusion and Faulting in a Rift Linkage Zone: Evidences from High-Resolution Topography Data of the Afrera Plain (Afar, East Africa). Tectonics 41, e2021TC007115. https://doi.org/10.1029/2021TC007115.

La Rosa, A., Raggiunti, M., Pagli, C., Keir, D., Wang, H., Ayele, A., 2023. Extensional Earthquakes in the Absence of Magma in Northern Afar: Insights from InSAR. Geophys. Res. Lett. 50, e2023GL102826 https://doi.org/10.1029/2023GL102826.

LaFemina, P.C., Dixon, T.H., Malservisi, R., Árnadóttir, T., Sturkell, E., Sigmundsson, F., Einarsson, P., 2005. Geodetic GPS measurements in South Iceland: Strain accumulation and partitioning in a propagating ridge system. J. Geophys. Res. Solid Earth 110, 1–21. https://doi.org/10.1029/2005JB003675.

Lahitte, P., Gillot, P.-Y., Courtillot, V., 2003a. Silicic central volcanoes as precursors to rift propagation: the Afar case. Earth Planet. Sci. Lett. 207, 103–116. https://doi.org/10.1016/S0012-821X(02)01130-5.

Lahitte, P., Gillot, P.-Y., Kidane, T., Courtillot, V., Bekele, A., 2003b. New age constraints on the timing of volcanism in Central Afar, in the presence of propagating rifts. J. Geophys. Res. Solid Earth 108, 2123. https://doi.org/10.1029/2001JB001689.

Lambeck, K., Purcell, A., Flemming, N.C., Vita-Finzi, C., Alsharekh, A.M., Bailey, G.N., 2011. Sea level and shoreline reconstructions for the Red Sea: isostatic and tectonic considerations and implications for hominin migration out of Africa. Quat. Sci. Rev. 30, 3542–3574. https://doi.org/10.1016/J.QUASCIREV.2011.08.008.

Lavayssière, A., Rychert, C., Harmon, N., Keir, D., Hammond, J.O.S., Kendall, J.M., Doubre, C., Leroy, S., 2018. Imaging Lithospheric Discontinuities beneath the Northern East African Rift using S-to-P Receiver Functions. Geochemistry. Geophys. Geosyst. 19, 4048–4062. https://doi.org/10.1029/2018GC007463.

Le Gall, B., Daoud, M.A., Maury, R.C., Rolet, J., Guillou, H., Sue, C., 2010. Magma-driven antiform structures in the Afar rift: the Ali Sabieh range, Djibouti. J. Struct. Geol. 32, 843–854. https://doi.org/10.1016/J.JSG.2010.06.007.

Le Gall, B., Daoud, M.A., Rolet, J., Egueh, N.M., 2011. Large-scale flexuring and antithetic extensional faulting along a nascent plate boundary in the SE Afar rift. Terra Nova 23, 416–420. https://doi.org/10.1111/j.1365-3121.2011.01029.x.

Le Gall, B., Daoud, M.A., Maury, R., Gasse, F., Rolet, J., Jalludin, M., Caminiti, A.-M., Moussa, N., 2015. Carte géologique de la République de Djibouti. Cent. d'Etude Rech. Djibouti CCGM.

Le Gall, B., Leleu, S., Pik, R., Jourdan, F., Chazot, G., Ayalew, D., Yirgu, G., Cloquet, C., Chauvet, F., 2018. The Red Beds series in the Erta Ale segment, North Afar. Evidence for a 6 Ma-old post-rift basin prior to continental rupturing. Tectonophysics 747–748, 373–389. https://doi.org/10.1016/j.tecto.2018.10.002.

Le Magoarou, C., Hirsch, K., Fleury, C., Martin, R., Johana, R.-B., Ball, P., 2021. Integration of gravity, magnetic and seismic data for sub-salt modelling in the Northern Red Sea. Interpretation 1–37. https://doi.org/10.1190/int-2019-0232.1.

Le Pichon, X., Francheteau, J., 1978. A plate-tectonic analysis of the Red Sea-Gulf of Aden Area. Tectonophysics 46, 369–406. https://doi.org/10.1016/0040-1951(78)90214-7.

Le Pichon, X., Gaulier, J.M., 1988. The rotation of Arabia and the Levant fault system. Tectonophysics 153, 271–294. https://doi.org/10.1016/0040-1951(88)90020-0.

Le Pourhiet, L., Chamot-rooke, N., Delescluse, M., May, D.A., Watremez, L., Pubellier, M., 2018. Continental break-up of the South China Sea stalled by far-field compression. Nat. Geosci. 11, 605–610. https://doi.org/10.1038/s41561-018-0178-5.

Leroy, S., Razin, P., Autin, J., Bache, F., d'Acremont, E., Watremez, L., Robinet, J., Baurion, C., Denèle, Y., Bellahsen, N., Lucazeau, F., Rolandone, F., Rouzo, S., Kiel, J. S., Robin, C., Guillocheau, F., Tiberi, C., Basuyau, C., Beslier, M.-O., Ebinger, C., Stuart, G., Ahmed, A., Khanbari, K., Al Ganad, I., de Clarens, P., Unternehr, P., Al Toubi, K., Al Lazki, A., 2012. From rifting to oceanic spreading in the Gulf of Aden: a synthesis. Arab. J. Geosci. 52012, 859–901. https://doi.org/10.1007/s12517-011-0475-4.

Levin, N.E., Quade, J., Simpson, S.W., Semaw, S., Rogers, M., 2004. Isotopic evidence for Plio-Pleistocene environmental change at Gona, Ethiopia. Earth Planet. Sci. Lett. 219, 93–110. https://doi.org/10.1016/S0012-821X(03)00707-6.

Lewi, E., Keir, D., Birhanu, Y., Blundy, J., Stuart, G., Wright, T., Calais, E., 2016. Use of a high-precision gravity survey to understand the formation of oceanic crust and the role of melt at the southern Red Sea rift in Afar, Ethiopia. Geol. Soc. London Spec. Publ. 420, 165–180. https://doi.org/10.1144/SP420.13.

Ligi, M., Bonatti, E., Bosworth, W., Cai, Y., Cipriani, A., Palmiotto, C., Ronca, S., Seyler, M., 2018. Birth of an ocean in the Red Sea: Oceanic-type basaltic melt intrusions precede continental rupture. Gondwana Res. 54, 150–160. https://doi.org/10.1016/J.GR.2017.11.002.

Lin, S.C., Kuo, B.Y., Chiao, L.Y., van Keken, P.E., 2005. Thermal plume models and melt generation in East Africa: a dynamic modeling approach. Earth Planet. Sci. Lett. 237, 175–192. https://doi.org/10.1016/J.EPSL.2005.04.049.

Lithgow-Bertelloni, C., Silver, P.G., 1998. Dynamic topography, plate driving forces and the African superswell. Nature 395, 269–272. https://doi.org/10.1038/26212.

López, S., van Dorp, L., Hellenthal, G., 2015. Human dispersal out of Africa: a lasting debate. Evol. Bioinforma. 11, 57–68. https://doi.org/10.4137/EBO.S33489/ASSET/IMAGES/LARGE/10.4137_EBO.S33489-FIG 1.JPEG.

López-García, J.M., Moreira, D., Benzerara, K., Grunewald, O., López-García, P., 2020. Origin and Evolution of the Halo-Volcanic complex of Dallol: Proto-Volcanism in Northern Afar (Ethiopia). Front. Earth Sci. 7, 351. https://doi.org/10.3389/feart.2019.00351.

Lowenstern, J.B., Charlier, B.L.A., Clynne, M.A., Wooden, J.L., 2006. Extreme U-Th Disequilibrium in Rift-Related Basalts, Rhyolites and Granophyric Granite and the Timescale of Rhyolite Generation, Intrusion and Crystallization at Alid Volcanic Center, Eritrea. J. Petrol. 47, 2105–2122. https://doi.org/10.1093/petrology/egl038.

Lucassen, F., Franz, G., Romer, R.L., Pudlo, D., Dulski, P., 2008. Nd, Pb, and Sr isotope composition of late Mesozoic to Quaternary intra-plate magmatism in NE-Africa (Sudan, Egypt): High-μ signatures from the mantle lithosphere. Contrib. Mineral. Petrol. 156, 765–784. https://doi.org/10.1007/S00410-008-0314-0/FIGURES/7.

Macgregor, D., 2015. History of the development of the East African Rift System: a series of interpreted maps through time. J. Afr. Earth Sci. 101, 232–252. https://doi.org/10.1016/J.JAFREARSCI.2014.09.016.

Macgregor, D., 2018. History of the development of Permian–Cretaceous rifts in East Africa: a series of interpreted maps through time. Pet. Geosci. 24, 8–20. https://doi.org/10.1144/petgeo2016-155.

Maestrelli, D., Montanari, D., Corti, G., Del Ventisette, C., Moratti, G., Bonini, M., 2020. Exploring the Interactions between Rift Propagation and Inherited Crustal Fabrics through Experimental Modeling. Tectonics 39, e2020TC006211. https://doi.org/10.1029/2020TC006211.

Maestrelli, D., Brune, S., Corti, G., Keir, D., Muluneh, A.A., Sani, F., 2022. Analog and Numerical Modeling of Rift-Rift-Rift Triple Junctions. Tectonics 41, e2022TC007491. https://doi.org/10.1029/2022TC007491.

Magee, C., Bastow, I.D., van Wyk de Vries, B., Jackson, C.A.-L., Hetherington, R., Hagos, M., Hoggett, M., 2017. Structure and dynamics of surface uplift induced by incremental sill emplacement. Geology 45, 431–434. https://doi.org/10.1130/G38839.1.

Makris, J., Ginzburg, A., 1987. The Afar Depression: transition between continental rifting and sea-floor spreading. Tectonophysics 141, 199–214. https://doi.org/10.1016/0040-1951(87)90186-7.

Makris, J., Rihm, R., 1991. Shear-controlled evolution of the Red Sea: pull apart model. Tectonophysics 198, 441–466. https://doi.org/10.1016/0040-1951(91)90166-P.

Makris, J., Menzel, H., Zimmermann, J., Gouin, P., 1975. Gravity field and crustal structure of North Ethiopia. In: Pilger, A., Rösler, A. (Eds.), Afar Depression of Ethiopia: Proceedings of an International Symposium on the Afar Region and Related Rift Problems. E. Schweizerbart'sche Verlagsbuchhandlung, Stuttgart, pp. 135–144.

Makris, J., Henke, C.H., Egloff, F., Akamaluk, T., 1991. The gravity field of the Red Sea and East Africa. Tectonophysics 198, 369–381.

Mallick, D.I.J., Gass, I.G., Cox, K.G., De Vries, B.V.W., Tindle, A.G., 1990. Perim Island, a volcanic remnant in the southern entrance to the Red Sea. Geol. Mag. 127, 309–318. https://doi.org/10.1017/S0016756800014874.

Mammo, T., 2004. Mapping the Crust-Mantle Boundary beneath Afar Depression. Gondwana Res. 7, 855–861. https://doi.org/10.1016/S1342-937X(05)71069-8.

Mandur, M.M., 2009. Calcareous Nannoplankton Biostratigraphy of the lower and Middle Miocene of the Gulf of Suez, Egypt. Aust. J. Basic Appl. Sci. 3, 2290–2303.

Manighetti, I., Tapponnier, P., Gillot, P.-Y., 1997. Propagation of rifling along the Arabia-Somalia plate boundary: the Gulfs of Aden and Tadjoura. J. Geophys. Res. Solid Earth 102, 2681–2710. https://doi.org/10.1029/96JB01185.

Manighetti, I., Tapponnier, P., Gillot, P.Y., Jacques, E., Courtillot, V., Armijo, R., Ruegg, J.C., King, G., 1998. Propagation of rifting along the Arabia-Somalia Plate Boundary: into Afar. J. Geophys. Res. Solid Earth 103, 4947–4974. https://doi.org/10.1029/97JB02758.

Manighetti, I., Tapponnier, P., Courtillot, V., Gallet, Y., Jacques, E., Gillot, P.-Y., 2001. Strain transfer between disconnected, propagating rifts in Afar. J. Geophys. Res. 106, 13,613–13,665. https://doi.org/10.1029/2001JB900017.

McClusky, S., Reilinger, R., Mahmoud, S., Ben Sari, D., Tealeb, A., 2003. GPS constraints on Africa (Nubia) and Arabia plate motions. Geophys. J. Int. 155, 126–138. https://doi.org/10.1046/J.1365-246X.2003.02023.X/3/155-1-126-FIG 006.JPEG.

McClusky, S., Reilinger, R., Ogubazghi, G., Amleson, A., Healeb, B., Vernant, P., Sholan, J., Fisseha, S., Asfaw, L., Bendick, R., Kogan, L., 2010. Kinematics of the southern Red Sea-Afar Triple Junction and implications for plate dynamics. Geophys. Res. Lett. 37, 1–5. https://doi.org/10.1029/2009GL041127.

McHargue, T.R., Heidrick, T.L., Livingston, J.E., 1992. Tectonostratigraphic development of the Interior Sudan rifts, Central Africa. Tectonophysics 213, 187–202. https://doi.org/10.1016/0040-1951(92)90258-8.

McKenzie, D., 1978. Some remarks on the development of sedimentary basins. Earth Planet. Sci. Lett. 40, 25–32. https://doi.org/10.1016/0012-821X(78)90071-7.

McKenzie, D.P., Davies, D., Molnar, P., 1970. Plate Tectonics of the Red Sea and East Africa. Nature 226, 243–248. https://doi.org/10.1038/226243a0.

McQuarrie, N., Stock, J.M., Verdel, C., Wernicke, B.P., 2003. Cenozoic evolution of Neotethys and implications for the causes of plate motions. Geophys. Res. Lett. 30, 2036. https://doi.org/10.1029/2003GL017992.

Medynski, S., Pik, R., Burnard, P., Vye-Brown, C., France, L., Schimmelpfennig, I., Whaler, K., Johnson, N., Benedetti, L., Ayelew, D., Yirgu, G., 2015. Stability of rift axis magma reservoirs: Spatial and temporal evolution of magma supply in the Dabbahu rift segment (Afar, Ethiopia) over the past 30 kyr. Earth Planet. Sci. Lett. 409, 278–289. https://doi.org/10.1016/J.EPSL.2014.11.002.

Medynski, S., Pik, R., Burnard, P., Dumont, S., Grandin, R., Williams, A., Blard, P.H., Schimmelpfennig, I., Vye-Brown, C., France, L., Ayalew, D., Benedetti, L., Yirgu, G., Arnold, M., Aumaître, G., Bourlès, D., Ked-Dadouche, K., 2016. Magmatic cycles pace tectonic and morphological expression of rifting (Afar depression, Ethiopia). Earth Planet. Sci. Lett. 446, 77–88. doi:https://doi.org/10.1016/j.epsl.2016.04.014.

Mège, D., Korme, T., 2004. Dyke swarm emplacement in the Ethiopian large Igneous Province: not only a matter of stress. J. Volcanol. Geotherm. Res. 132, 283–310. https://doi.org/10.1016/S0377-0273(03)00318-4.

Mège, D., Purcell, P., Bézos, A., Jourdan, F., La, C., 2016. A major dyke swarm in the Ogaden region south of Afar and the early evolution of the Afar triple junction. Geol. Soc. London. Spec. Publ. 420, 221–248. https://doi.org/10.1144/SP420.7.

Mège, D., Hauber, E., Allemand, P., Moors, H., de Craen, M., Choe, H., Dyment, J., 2021. The 2004 tectonic and hydrothermal crisis in the Danakil depression: documenting the last continental step prior to oceanic spreading (Preprint v1, accessed on 13.01.2022). ESSOAr. https://doi.org/10.1002/ESSOAR.10505758.1.

Menzies, M.A., Baker, J., Bosence, D., Dart, C., Davison, I., Hurford, A., Al'Kadasi, M., McClay, K., Nichols, G., Al'Subbary, A., Yelland, A., 1992. The timing of magmatism, uplift and crustal extension: preliminary observations from Yemen. Geol. Soc. London Spec. Publ. 68, 293–304. https://doi.org/10.1144/GSL.SP.1992.068.01.18.

Michon, L., Famin, V., Quidelleur, X., 2022. Evolution of the East African Rift System from trap-scale to plate-scale rifting. Earth-Sci. Rev. 231, 104089 https://doi.org/10.1016/J.EARSCIREV.2022.104089.

Miller, K.G., Browning, J.V., Schmelz, W.J., Kopp, R.E., Mountain, G.S., Wright, J.D., 2020. Cenozoic Sea-level and cryospheric evolution from deep-sea geochemical and continental margin records. Sci. Adv. 6 https://doi.org/10.1126/sciadv.aaz1346.

Ministry of mines and energy, A.A., 1985. Geological map of the Ogaden and surrounding area.

Ministry of Petroleum and Mining, 2004. Geological map of the Republic of South Sudan.

Mitchell, N.C., Park, Y., 2014. Nature of crust in the Central Red Sea. Tectonophysics 628, 123–139. https://doi.org/10.1016/J.TECTO.2014.04.029.

Mitchell, D.J.W., Allen, R.B., Salama, W., Abouzakm, A., 1992. Tectonostratigraphic framework and hydrocarbon potential of the Red Sea. J. Pet. Geol. 15, 187–210. https://doi.org/10.1111/j.1747-5457.1992.tb00962.x.

Mitchell, N.C., Shi, W., Izzeldin, A., Stewart, I.C.F., 2021. Reconstructing the level of the Central Red Sea evaporites at the end of the Miocene. Basin Res. 33, 1266–1292. https://doi.org/10.1111/bre.12513.

Mohamed, A.Y., Whiteman, A.J., Archer, S.G., Bowden, S.A., 2016. Thermal modelling of the Melut basin Sudan and South Sudan: Implications for hydrocarbon generation and migration. Mar. Pet. Geol. 77, 746–762. https://doi.org/10.1016/J.MARPETGEO.2016.07.007.

Mohr, P.A., 1965. Re-classification of the Ethiopian Cainozoic Volcanic Succession. Nature 208, 177–178. https://doi.org/10.1038/208177b0.

Mohr, P.A., 1967. Major Volcano-Tectonic Lineament in the Ethiopian Rift System. Nature 216, 664–665. https://doi.org/10.1038/213664a0.

Mohr, P.A., 1970. The Afar Triple Junction and sea-floor spreading. J. Geophys. Res. 75, 7340–7352. https://doi.org/10.1029/JB075i035p07340.

Mohr, P.A., 1972. Surface structure and plate tectonics of Afar. Tectonophysics 15, 3–18. https://doi.org/10.1016/0040-1951(72)90045-5.

Mohr, P., 1983. The Morton-black hypothesis for the thinning of continental crust—revisited in western afar. Tectonophysics 94, 509–528. https://doi.org/10.1016/B978-0-444-42198-2.50034-1.

Mohr, P., Zanettin, B., 1988. The Ethiopian flood basalt province. Cont. Flood Basalts 63–110. https://doi.org/10.1007/978-94-015-7805-9_3.

Molnar, N.E., Cruden, A.R., Betts, P.G., 2017. Interactions between propagating rotational rifts and linear rheological heterogeneities: Insights from three-dimensional laboratory experiments. Tectonics 36, 420–443. https://doi.org/10.1002/2016TC004447.

Molnar, N.E., Cruden, A.R., Betts, P.G., 2018. Unzipping continents and the birth of microcontinents. Geology 46, 451–454. https://doi.org/10.1130/G40021.1.

Molnar, N.E., Cruden, A.R., Betts, P.G., 2019. Interactions between propagating rifts and linear weaknesses in the lower crust. Geosphere 15, 1617–1640. https://doi.org/10.1130/GES02119.1.

Molnar, N., Cruden, A., Betts, P., 2020. The role of inherited crustal and lithospheric architecture during the evolution of the Red Sea: Insights from three dimensional analogue experiments. Earth Planet. Sci. Lett. 544, 116377 https://doi.org/10.1016/j.epsl.2020.116377.

Mologni, C., Bruxelles, L., Schuster, M., Davtian, G., Ménard, C., Orange, F., Doubre, C., Cauliez, J., Taezaz, H.B., Revel, M., Khalidi, L., 2021. Holocene East African monsoonal variations recorded in wave-dominated clastic paleo-shorelines of Lake Abhe, Central Afar region (Ethiopia & Djibouti). Geomorphology 391, 107896. https://doi.org/10.1016/j.geomorph.2021.107896.

Mondy, L.S., Rey, P.F., Duclaux, G., Moresi, L., 2018. The role of asthenospheric flow during rift propagation and breakup. Geology 46, 103–106. https://doi.org/10.1130/G39674.1.

Montelli, R., Nolet, G., Dahlen, F.A., Masters, G., 2006. A catalogue of deep mantle plumes: New results from finite-frequency tomography. Geochem. Geophys. Geosyst. 7, Q11007. https://doi.org/10.1029/2006GC001248.

Montenat, C., Orszag-Sperber, F., Plaziat, J.-C., Purser, B.H., 1998. The sedimentary record of the initial stages of Oligo-Miocene rifting in the Gulf of Suez and the northern Red Sea. In: Purser, B.H., Bosence, D.W. (Eds.), Sedimentation and Tectonics in Rift Basins: Red Sea - Gulf of Aden. Chapman & Hall, London, pp. 146–161. https://doi.org/10.1007/978-94-011-4930-3_10.

Mooney, W.D., Gettings, M.E., Blank, H.R., Healy, J.H., 1985. Saudi Arabian seismic-refraction profile: a traveltime interpretation of crustal and upper mantle structure. Tectonophysics 111, 173–246. https://doi.org/10.1016/0040-1951(85)90287-2.

Moore, J.M., Davidson, A., 1978. Rift structure in southern Ethiopia. Tectonophysics 46, 159–173. https://doi.org/10.1016/0040-1951(78)90111-7.

Moore, C., Wright, T.J., Hooper, A., 2021. Rift focusing and Magmatism during Late-Stage Rifting in Afar. J. Geophys. Res. Solid Earth 126, e2020JB021542. https://doi.org/10.1029/2020JB021542.

Morag, N., Haviv, I., Eyal, M., Kohn, B.P., Feinstein, S., 2019. Early flank uplift along the Suez Rift: Implications for the role of mantle plumes and the onset of the Dead Sea Transform. Earth Planet. Sci. Lett. 516, 56–65. https://doi.org/10.1016/J.EPSL.2019.03.002.

Morbidelli, L., Nicoletti, M., Petrucciani, C., Piccirillo, E.M., 1975. Ethiopian South-Eastern Plateau and related escarpment: K/Ar ages of the main volcanic events (Main Ethiopian Rift from 8 10 to 9 00 lat. North). In: Pilger, A., Rösler, A. (Eds.), Afar Depression of Ethiopia: Proceedings of an International Symposium on the Afar Region and Related Rift Problems. E. Schweizerbart'sche Verlagsbuchhandlung, Stuttgart, pp. 362–369.

Morton, W.H., Rex, D.C., Mitchell, J.G., Mohr, P., 1979. Riftward younging of volcanic units in the Addis Ababa region, Ethiopian rift valley. Nature 280, 284–288. https://doi.org/10.1038/280284a0.

Moucha, R., Forte, A.M., 2011. Changes in African topography driven by mantle convection. Nat. Geosci. 4, 707–712. https://doi.org/10.1038/ngeo1235.

Moufti, M.R., Moghazi, A.M., Ali, K.A., 2012. Geochemistry and Sr–Nd–Pb isotopic composition of the Harrat Al-Madinah Volcanic Field, Saudi Arabia. Gondwana Res. 21, 670–689. https://doi.org/10.1016/J.GR.2011.06.003.

Mouthereau, F., Lacombe, O., Vergés, J., 2012. Building the Zagros collisional orogen: timing, strain distribution and the dynamics of Arabia/Eurasia plate convergence. Tectonophysics 532–535, 27–60. https://doi.org/10.1016/J.TECTO.2012.01.022.

Muller, J., Boucarut, M., 1975. Evolution structurale de la région d'Arta-Ali Sabieh (T.F. A.I.), Afrique Orientale. In: Pilger, A., Rösler, A. (Eds.), Afar Depression of Ethiopia: Proceedings of an International Symposium on the Afar Region and Related Rift Problems. E. Schweizerbart'sche Verlagsbuchhandlung, Stuttgart, pp. 228–231.
Müller, R.D., Cannon, J., Qin, X., Watson, R.J., Gurnis, M., Williams, S., Pfaffelmoser, T., Seton, M., Russell, S.H.J., Zahirovic, S., 2018. GPlates: building a virtual earth through deep time. Geochem. Geophys. Geosyst. 19, 2243–2261. https://doi.org/10.1029/2018GC007584.
Muluneh, A.A., Kidane, T., Rowland, J., Bachtadse, V., 2013. Counterclockwise block rotation linked to southward propagation and overlap of sub-aerial Red Sea Rift segments, Afar Depression: Insight from paleomagnetism. Tectonophysics 593, 111–120. https://doi.org/10.1016/j.tecto.2013.02.030.
Muluneh, A.A., Cuffaro, M., Kidane, T., 2017. Along-strike variation in deformation style inferred from kinematic reconstruction and strain rate analysis: a case study of the Ethiopian Rift. Phys. Earth Planet. Inter. 270, 176–182. https://doi.org/10.1016/j.pepi.2017.07.009.
Munzinger, W., 1869. Narrative of a Journey through the Afar Country. J. R. Geogr. Soc. Lond. 39, 188–232. https://doi.org/10.2307/1798551.
Mutebi, S., Ozumba, B.M., Adeigbe, O.C., 2019. An Aspect of Palyno Stratigraphy of "XM" Field located in Semliki Basin South Western Uganda. J. Pet. Environ. Biotechnol. 10, 1–9. https://doi.org/10.35248/2157-7463.19.10.388.
Nanis, H., Aly, M.H., 2020. Desegregation of remote sensing and GIS to characterize fluctuations in the surface water area of Afar Lakes, Ethiopia. Geocarto Int. 35, 976–990. https://doi.org/10.1080/10106049.2018.1559884.
Natali, C., Beccaluva, L., Bianchini, G., Siena, F., 2013. The Axum-Adwa basalt-trachyte complex: a late magmatic activity at the periphery of the Afar plume. Contrib. Mineral. Petrol. 166, 351–370. https://doi.org/10.1007/s00410-013-0879-0.
Nelson, R.A., Patton, T.L., Morley, C.K., 1992. Rift-segment interaction and its relation to hydrocarbon exploration in continental rift systems. Am. Assoc. Pet. Geol. Bull. 76, 1153–1169. https://doi.org/10.1306/bdff898e-1718-11d7-8645000102c1865d.
Niespolo, E.M., WoldeGabriel, G., Hart, W.K., Renne, P.R., Sharp, W.D., Shackley, M.S., Ambrose, S.H., Asfaw, B., Beyene, Y., Brasil, M.F., Carlson, J.P., Sahle, Y., White, T. D., 2021. Integrative geochronology calibrates the Middle and late Stone Ages of Ethiopia's Afar Rift. Proc. Natl. Acad. Sci. 118, e2116329118 https://doi.org/10.1073/PNAS.2116329118.
Nobile, A., Pagli, C., Keir, D., Wright, T.J., Ayele, A., Ruch, J., Acocella, V., 2012. Dike-fault interaction during the 2004 Dallol intrusion at the northern edge of the Erta Ale Ridge (Afar, Ethiopia). Geophys. Res. Lett. 39, L19305. https://doi.org/10.1029/2012GL053152.
Nonn, C., Leroy, S., Lescanne, M., Castilla, R., 2019. Central Gulf of Aden conjugate margins (Yemen-Somalia): Tectono-sedimentary and magmatism evolution in hybrid-type margins. Mar. Pet. Geol. 105, 100–123. https://doi.org/10.1016/j.marpetgeo.2018.11.053.
Nuriel, P., Weinberger, R., Kylander-Clark, A.R.C., Hacker, B.R., Craddock, J.P., 2017. The onset of the Dead Sea transform based on calcite age-strain analyses. Geology 45, 587–590. https://doi.org/10.1130/G38903.1.
Ogg, J.G., 2020. Geomagnetic polarity time scale. In: Gradstein, F.M., Ogg, James G., Schmitz, M.D., Ogg, G.M. (Eds.), Geologic Time Scale. Elsevier, pp. 159–192. https://doi.org/10.1016/B978-0-12-824360-2.00005-X.
Okwokwo, O.I., Mitchell, N.C., Shi, W., Stewart, I.C.F., Izzeldin, A.Y., 2022. How have thick evaporites affected early seafloor spreading magnetic anomalies in the Central Red Sea? Geophys. J. Int. 229, 1550–1566. https://doi.org/10.1093/gji/ggac012.
Omar, G.I., Steckler, M.S., 1995. Fission Track evidence on the initial rifting of the Red Sea: two pulses, no propagation. Science 270, 1341–1344. https://doi.org/10.1126/science.270.5240.1341.
Orszag-Sperber, F., Harwood, G., Kendall, A., Purser, B.H., 1998. A review of the evaporites of the Red Sea - Gulf of Suez rift. In: Purser, B.H., Bosence, D.W. (Eds.), Sedimentation and Tectonics in Rift Basins: Red Sea - Gulf of Aden. Chapman & Hall, London, pp. 409–426. https://doi.org/10.1007/978-94-011-4930-3_22.
Osman, A.F., Fowler, A.-R., 2021. Terrane Accretion within the Arabian-Nubian Shield. In: Hamimi, Z., Fowler, A.R., Liégeois, J.P., Collins, A., Abdelsalam, M.G., Abd El-Wahed M. (Eds.), The Geology of the Arabian-Nubian Shield. Springer, Cham, pp. 221–266. https://doi.org/10.1007/978-3-030-72995-0_10.
Otálora, F., Palero, F., Papaslioti, E.-M., García-Ruiz, J.M., 2022. Mineralochemical Mechanism for the Formation of Salt Volcanoes: the Case of Mount Dallol (Afar Triangle, Ethiopia). ACS Earth Sp. Chem. 6, 2767–2778. https://doi.org/10.1021/acsearthspacechem.2c00075.
Pagli, C., Wright, T.J., Ebinger, C.J., Yun, S.-H., Cann, J.R., Barnie, T., Ayele, A., 2012. Shallow axial magma chamber at the slow-spreading Erta Ale Ridge. Nat. Geosci. 5, 284–288. https://doi.org/10.1038/ngeo1414.
Pagli, C., Wang, H., Wright, T.J., Calais, E., Lewi, E., 2014. Current plate boundary deformation of the Afar rift from a 3-D velocity field inversion of InSAR and GPS. J. Geophys. Res. Solid Earth 119, 8562–8575. https://doi.org/10.1002/2014JB011391.
Pagli, C., Yun, S.-H., Ebinger, C., Keir, D., Wang, H., 2019. Strike-slip tectonics during rift linkage. Geology 47, 31–34. https://doi.org/10.1130/G45345.1.
Pan, M., Sjöberg, L.E., Asfaw, L.M., Asenjo, E., Alemu, A., Hunegnaw, A., 2002. An analysis of the Ethiopian Rift Valley GPS campaigns in 1994 and 1999. J. Geodyn. 33, 333–343. https://doi.org/10.1016/S0264-3707(01)00076-X.
Papini, M., Ghinassi, M., Libsekal, Y., Rook, L., 2014. Facies associations of the northern Dandiero Basin (Danakil depression, Eritrea, including the Pleistocene Buya homo site). J. Maps 10, 126–135. https://doi.org/10.1080/17445647.2013.862748.
Park, L.E., 2010. New Neogene Fluvio-Lacustrine Faunal Archives from the Danakil Depression, East Africa: Implications for Human Origins, Paleoclimate and Continental Rifting. In: Oral Presentation, 2010 GSA Denver Annual Meeting.
Pasquet, G., Hassan, R.H., Sissmann, O., Varet, J., Moretti, I., 2022. An Attempt to Study Natural H2 Resources across an Oceanic Ridge Penetrating a continent: the Asal-Ghoubbet Rift (Republic of Djibouti). Geosciences 12, 16. https://doi.org/10.3390/GEOSCIENCES12010016.
Peace, A.L., Phethean, J.J.J., Franke, D., Foulger, G.R., Schiffer, C., Welford, J.K., McHone, G., Rocchi, S., Schnabel, M., Doré, A.G., 2020. A review of Pangaea dispersal and large Igneous Provinces – in search of a causative mechanism. Earth-Sci. Rev. 206, 102902 https://doi.org/10.1016/j.earscirev.2019.102902.
Petrunin, A.G., Kaban, M.K., El Khrepy, S., Al-Arifi, N., 2020. Mantle Convection patterns Reveal the Mechanism of the Red Sea Rifting. Tectonics 39, e2019TC005829. https://doi.org/10.1029/2019TC005829.
Philippon, M., Corti, G., Sani, F., Bonini, M., Balestrieri, M.L., Molin, P., Willingshofer, E., Sokoutis, D., Cloetingh, S., 2014. Evolution, distribution, and characteristics of rifting in southern Ethiopia. Tectonics 33, 485–508. https://doi.org/10.1002/2013TC003430.
Piguet, P., Vellutini, P., 1991. Données nouvelles sur le volcan Moussa Ali (République de Djibouti). Compt. Rend. l'Acad. Sci. Sér. 2 (313), 1611–1618.
Plaziat, J.-C., Montenat, C., Barrier, P., Janin, M.-C., Orszag-Sperber, F., Philobbos, E., 1998. Stratigraphy of the Egyptian syn-rift deposits: Correlations between axial and peripheral sequences of the North-Western Red Sea and Gulf of Suez and their relations with tectonics and eustacy. In: Purcell, P.G., Bosence, D.W.J. (Eds.), Sedimentation and Tectonics in Rift Basins: Red Sea - Gulf of Aden. Chapman & Hall, pp. 211–222. https://doi.org/10.1007/978-94-011-4930-3_13.
Pollastro, R.M., Karshbaum, A.S., Viger, R.J., 1999. Maps showing geology, oil and gas fields and geologic provinces of the Arabian Peninsula. U.S. Geol. Surv. Open-File Rep. https://doi.org/10.3133/ofr97470B, 97-470-B.
Polun, S.G., Gomez, F., Tesfaye, S., 2018. Scaling properties of normal faults in the Central Afar, Ethiopia and Djibouti: Implications for strain partitioning during the final stages of continental breakup. J. Struct. Geol. 115, 178–189. https://doi.org/10.1016/j.jsg.2018.07.018.
Popp, F., Scholger, R., 2017. Paleomagnetic constraints on stratigraphy and rift-related tectonics of Pliocene and early Pleistocene volcano-sedimentary strata: the Mt. Galili hominid research area, Southern Afar Depression, Ethiopia. Aust. J. Earth Sci. 110 https://doi.org/10.17738/ajes.2017.0018.
Prinz, W.C., 1984. Geologic map of the Wadi Haliy quadrangle, Sheet 18E, Kingdom of Saudi Arabia. Min. Pet. Miner. Resour. Deputy Minist. Miner. Resour. (Geosci. map GM-74 A).
Pubelier, M., 2008. Structural Map of Eastern Eurasia. CCGM-CGMW.
Purcell, P.G., 1976. The Marda Fault Zone, Ethiopia. Nature 261, 569–571. https://doi.org/10.1038/261569a0.
Purcell, P.G., 2018. Re-imagining and re-imaging the development of the East African Rift. Pet. Geosci. 24, 21–40. https://doi.org/10.1144/petgeo2017-036.
Purkis, S.J., Harris, P.M., Ellis, J., 2012. Patterns of sedimentation in the contemporary Red Sea as an analog for ancient carbonates in rift settings. J. Sediment. Res. 82, 859–870. https://doi.org/10.2110/jsr.2012.77.
Quade, J., Levin, N., Semaw, S., Stout, D., Renne, P., Rogers, M., Simpson, S., 2004. Paleoenvironments of the earliest stone toolmakers, Gona, Ethiopia. Bull. Geol. Soc. Am. 116, 1529–1544. https://doi.org/10.1130/B25358.1.
Quade, J., Levin, N.E., Simpson, S.W., Butler, R., McIntosh, W.C., Semaw, S., Kleinsasser, L., Dupont-Nivet, G., Renne, P., Dunbar, N., 2008. The geology of Gona, Afar, Ethiopia. In: Quade, J., Wynn, J.G. (Eds.), The Geology of Early Humans in the Horn of Africa. Geological Society of America, pp. 1–31. https://doi.org/10.1130/2008.2446(01).
Quennell, A.M., 1958. The structural and geomorphic evolution of the Dead Sea Rift. Q. J. Geol. Soc. 114, 1–24. https://doi.org/10.1144/GSJGS.114.1.0001.
Quick, J.E., 1991. Late Proterozoic transpression on the Nabitah fault system—implications for the assembly of the Arabian Shield. Precambrian Res. 53, 119–147. https://doi.org/10.1016/0301-9268(91)90008-X.
Redfern, P., Jones, J.A., 1995. The interior rifts of the Yemen - analysis of basin structure and stratigraphy in a regional plate tectonic context. Basin Res. 7, 337–356. https://doi.org/10.1111/j.1365-2117.1995.tb00121.x.
Redfield, T.F., Wheeler, W.H., Often, M., 2003. A kinematic model for the development of the Afar Depression and its paleogeographic implications. Earth Planet. Sci. Lett. 216, 383–398. https://doi.org/10.1016/S0012-821X(03)00488-6.
Reed, C.A., Almadani, S., Gao, S.S., Elsheikh, A.A., Cherie, S., Abdelsalam, M.G., Thurmond, A.K., Liu, K.H., 2014. Receiver function constraints on crustal seismic velocities and partial melting beneath the Red Sea rift and adjacent regions, Afar Depression. J. Geophys. Res. Solid Earth 119, 2138–2152. https://doi.org/10.1002/2013JB010719.
Rees, R., Gernon, T.M., Keir, D., Taylor, R.N., Pagli, C., 2023. The spatial and volcanic evolution of Ayelu, Abida and Yangudi volcanoes in the Northern Main Ethiopian Rift – Southern Afar, Ethiopia. J. Volcanol. Geotherm. Res. 107846 https://doi.org/10.1016/j.jvolgeores.2023.107846.
Reilinger, R., McClusky, S., 2011. Nubia-Arabia-Eurasia plate motions and the dynamics of Mediterranean and Middle East tectonics. Geophys. J. Int. 186, 971–979. https://doi.org/10.1111/j.1365-246X.2011.05133.x.
Reilinger, R., McClusky, S., Vernant, P., Lawrence, S., Ergintav, S., Cakmak, R., Ozener, H., Kadirov, F., Guliev, I., Stepanyan, R., Nadariya, M., Hahubia, G., Mahmoud, S., Sakr, K., ArRajehi, A., Paradissis, D., Al-Aydrus, A., Prilepin, M., Guseva, T., Evren, E., Dmitrotsa, A., Filikov, S.V., Gomez, F., Al-Ghazzi, R., Karam, G., 2006. GPS constraints on continental deformation in the Africa-Arabia-Eurasia continental collision zone and implications for the dynamics of plate interactions. J. Geophys. Res. Solid Earth 111, B05411. https://doi.org/10.1029/2005JB004051.
Reilinger, R., McClusky, S., ArRajehi, A., 2015. Geodetic Constraints on the Geodynamic Evolution of the Red Sea. In: Rasul, N., Stewart, I.C.F. (Eds.), The Red Sea - the

Formation, Morphology, Oceanography and Environment of a Young Ocean Basin. Springer, Berlin, Heidelberg, pp. 135–149. https://doi.org/10.1007/978-3-662-45201-1_7.
Renne, P.R., WoldeGabriel, G., Hart, W.K., Heiken, G., White, T.D., 1999. Chronostratigraphy of the Miocene-Pliocene Sagantole formation, Middle Awash Valley, Afar rift, Ethiopia. Bull. Geol. Soc. Am. 111, 869–885. https://doi.org/10.1130/0016-7606(1999)111<0869:COTMPS>2.3.CO;2.
Rihm, R., Henke, C.H., 1998. Geophysical studies on early tectonic controls on Red Sea rifting, opening and segmentation. In: Purser, B.H., Bosence, D.W. (Eds.), Sedimentation and Tectonics in Rift Basins: Red Sea - Gulf of Aden. Chapman & Hall, London, pp. 29–49. https://doi.org/10.1007/978-94-011-4930-3_3.
Riisager, P., Knight, K.B., Baker, J.A., Ukstins Peate, I., Al-Kadasi, M., Al-Subbary, A., Renne, P.R., 2005. Paleomagnetism and 40Ar / 39Ar Geochronology of Yemeni Oligocene volcanics: Implications for timing and duration of Afro-Arabian traps and geometry of the Oligocene paleomagnetic field. Earth Planet. Sci. Lett. 237, 647–672. https://doi.org/10.1016/J.EPSL.2005.06.016.
Rime, V., Foubert, A., Atnafu, B., Kidane, T., 2022a. Geological map of the Afar Depression. Zenodo. https://doi.org/10.5281/zenodo.7351643.
Rime, V., Foubert, A., Atnafu, B., Kidane, T., 2022b. Geological map of the southern Red Sea & western Gulf of Aden region. Zenodo. https://doi.org/10.5281/zenodo.7351765.
Ritsema, J., Deuss, A., van Heijst, H.J., Woodhouse, J.H., 2011. S40RTS: a degree-40 shear-velocity model for the mantle from new Rayleigh wave dispersion, teleseismic traveltime and normal-mode splitting function measurements. Geophys. J. Int. 184, 1223–1236. https://doi.org/10.1111/j.1365-246X.2010.04884.x.
Rizzello, D., Armadillo, E., Pasqua, C., Pisani, P., Balsotti, R., Kebede, S., Mengiste, A., Kebede, Y., Hailegiorgis, G., Mengesha, K., 2021. The geophysical recognition of a vapor-cored geothermal system in divergent plate tectonics: the Alalobeda (Alalobad) field, Ethiopia. Tectonophysics 813, 228933. https://doi.org/10.1016/j.tecto.2021.228933.
Rogers, N., Macdonald, R., Fitton, J.G., George, R., Smith, M., Barreiro, B., 2000. Two mantle plumes beneath the East African rift system: Sr, Nd and Pb isotope evidence from Kenya Rift basalts. Earth Planet. Sci. Lett. 176, 387–400. https://doi.org/10.1016/S0012-821X(00)00012-1.
Rooney, T.O., 2017. The Cenozoic magmatism of East-Africa: part I — Flood basalts and pulsed magmatism. Lithos 286–287, 264–301. https://doi.org/10.1016/j.lithos.2017.05.014.
Rooney, T.O., 2020a. The Cenozoic magmatism of East Africa: Part IV – the terminal stages of rifting preserved in the Northern East African Rift System. Lithos 360–361, 105381. https://doi.org/10.1016/j.lithos.2020.105381.
Rooney, T.O., 2020b. The Cenozoic magmatism of East Africa: Part II – Rifting of the mobile belt. Lithos 360–361, 105291. https://doi.org/10.1016/j.lithos.2019.105291.
Rooney, T.O., 2020c. The Cenozoic magmatism of East Africa: Part V – Magma sources and processes in the East African Rift. Lithos 360–361, 105296. https://doi.org/10.1016/j.lithos.2019.105296.
Rooney, T., Furman, T., Bastow, I., Ayalew, D., Yirgu, G., 2007. Lithospheric modification during crustal extension in the Main Ethiopian Rift. J. Geophys. Res. Solid Earth 112, 10201. https://doi.org/10.1029/2006JB004916.
Rooney, T.O., Herzberg, C., Bastow, I.D., 2012. Elevated mantle temperature beneath East Africa. Geology 40, 27–30. https://doi.org/10.1130/G32382.1.
Rooney, T.O., Mohr, P., Dosso, L., Hall, C., 2013. Geochemical evidence of mantle reservoir evolution during progressive rifting along the western Afar margin. Geochim. Cosmochim. Acta 102, 65–88. https://doi.org/10.1016/j.gca.2012.08.019.
Rooney, T.O., Krans, S.R., Mège, D., Arnaud, N., Korme, T., Kappelman, J., Yirgu, G., 2018. Constraining the Magmatic Plumbing System in a Zoned Continental Flood Basalt Province. Geochem. Geophys. Geosyst. 19, 3917–3944. https://doi.org/10.1029/2018GC007724.
Rowan, J., Lazagabaster, I.A., Campisano, C.J., Bibi, F., Bobe, R., Boisserie, J.-R., Frost, S. R., Getachew, T., Gilbert, C.C., Lewis, M.E., Melaku, S., Scott, E., Souron, A., Werdelin, L., Kimbel, W.H., Reed, K.E., 2022. Early Pleistocene large mammals from Maka'amitalu, Hadar, lower Awash Valley, Ethiopia. PeerJ 10, e13210. https://doi.org/10.7717/PEERJ.13210.
Rowland, J.V., Baker, E., Ebinger, C.J., Keir, D., Kidane, T., Biggs, J., Hayward, N., Wright, T.J., 2007. Fault growth at a nascent slow-spreading ridge: 2005 Dabbahu rifting episode. Afar. Geophys. J. Int. 171, 1226–1246. https://doi.org/10.1111/j.1365-246X.2007.03584.x.
Ruch, J., Wang, T., Xu, W., Hensch, M., Jónsson, S., 2016. Oblique rift opening revealed by reoccurring magma injection in Central Iceland. Nat. Commun. 7, 1–7. https://doi.org/10.1038/ncomms12352.
Ruch, J., Keir, D., Passarelli, L., Di Giacomo, D., Ogubazghi, G., Jónsson, S., 2021. Revealing 60 years of Earthquake Swarms in the Southern Red Sea, Afar and the Gulf of Aden. Front. Earth Sci. 9, 690. https://doi.org/10.3389/feart.2021.664673.
Rüppel, W., 1834. Skizze der geologischen Formation Abyssiniens. Abhandlungen Museum Senkenbergianum 1, 286–288.
Rychert, C.A., Hammond, J.O.S., Harmon, N., Michael Kendall, J., Keir, D., Ebinger, C., Bastow, I.D., Ayele, A., Belachew, M., Stuart, G., 2012. Volcanism in the Afar Rift sustained by decompression melting with minimal plume influence. Nat. Geosci. 5, 406–409. https://doi.org/10.1038/ngeo1455.
Saada, S.A., Mickus, K., Eldosouky, A.M., Ibrahim, A., 2021. Insights on the tectonic styles of the Red Sea rift using gravity and magnetic data. Mar. Pet. Geol. 133, 105253 https://doi.org/10.1016/j.marpetgeo.2021.105253.
Sagri, M., Abbate, E., Azzaroli, A., Balestrieri, M.L., Benvenuti, M., Bruni, P., Fazzuoli, M., Ficcarelli, G., Marcucci, M., Papini, M., Pavia, G., Reale, V., Rook, L., Tecle, T.M., 1998. New data on the Jurassic and Neogene sedimentation in the Danakil Horst and northern Afar Depression, Eritrea. In: Crasquin-Soleau, S., Barrier, E. (Eds.), Peri-Tethys Memoir 3; Stratigraphy and Evolution of Peri-Tethyan Platforms. Mémoires du Muséum national d'Histoire naturelle, Paris, pp. 193–214.
Salama, R.B., 1985. Buried troughs, grabens and rifts in Sudan. J. Afr. Earth Sci. 3, 381–390. https://doi.org/10.1016/0899-5362(85)90012-0.
Sandwell, D.T., Müller, R.D., Smith, W.H.F., Garcia, E., Francis, R., 2014. New global marine gravity model from CryoSat-2 and Jason-1 reveals buried tectonic structure. Science 346, 65–67. https://doi.org/10.1126/SCIENCE.1258213/SUPPL_FILE/SANDWELL.SM.PDF.
Sangha, S.S., 2021. Characterizing the Deformation Field in Afar from Radar Interferometry and Topography Data (PhD Thesis). University of California, Los Angeles.
Sangha, S.S., Peltzer, G., Doubre, C., 2022. The evolving deformation field in Central Afar from two decades of InSAR observations: implications for the decoupling between the upper and lower crusts (Preprint). ESSOAr 1–32. https://doi.org/10.1002/essoar.10508772.1.
Sani, F., Ghinassi, M., Papini, M., Oms, O., Finotello, A., 2017. Evolution of the northern tip of Afar triangle: Inferences from the Quaternary succession of the Dandiero — Massawa area (Eritrea). Tectonophysics 717, 339–357. https://doi.org/10.1016/j.tecto.2017.08.026.
Sanz, J.L., Rodríguez, N., Escudero, C., Carrizo, D., Amils, R., Gómez, F., 2021. Methanogenesis at High Temperature, High Ionic Strength and Low pH in the Volcanic Area of Dallol, Ethiopia. Microorganisms 9, 1231. https://doi.org/10.3390/microorganisms9061231.
Savoyat, E., Shiferaw, A., Balcha, T., 1989. Petroleum exploration in the Ethiopian Red Sea. J. Pet. Geol. 12, 187–204. https://doi.org/10.1111/j.1747-5457.1989.tb00232.x.
Saylor, B.Z., Gibert, L., Deino, A., Alene, M., Levin, N.E., Melillo, S.M., Peaple, M.D., Feakins, S.J., Bourel, B., Barboni, D., Novello, A., Sylvestre, F., Mertzman, S.A., Haile-Selassie, Y., 2019. Age and context of mid-Pliocene hominin cranium from Woranso-Mille, Ethiopia. Nature 573, 220–224. https://doi.org/10.1038/s41586-019-1514-7.
Schaegis, J.-C., Rime, V., Kidane, T., Mosar, J., Filfilu Gebru, E., Atnafu, B., Foubert, A., Augustin, N., Illsley-Kemp, F., Pagli, C., 2021. Novel Bathymetry of Lake Afdera reveals Fault Structures and Volcano-Tectonic Features of an Incipient Transform Zone (Afar, Ethiopia). Front. Earth Sci. 9, 1. https://doi.org/10.3389/feart.2021.706643.
Schettino, A., Macchiavelli, C., Pierantoni, P.P., Zanoni, D., Rasul, N., 2016. Recent kinematics of the tectonic plates surrounding the Red Sea and Gulf of Aden. Geophys. J. Int. 207, 457–480. https://doi.org/10.1093/gji/ggw280.
Schmid, T.C., Schreurs, G., Adam, J., 2022. Characteristics of continental rifting in rotational systems: New findings from spatiotemporal high resolution quantified crustal scale analogue models. Tectonophysics 822, 229174. https://doi.org/10.1016/j.tecto.2021.229174.
Schult, A., 1974. Palaeomagnetism of Tertiary Volcanic Rocks from the Ethiopian Southern Plateau and the Danakil Block. J. Gephys. 40, 203–212.
Scoon, R.N., 2020. Geotourism, Iconic Landforms and Island-style Speciation patterns in National Parks of East Africa. Geoheritage 12, 1–19. https://doi.org/10.1007/S12371-020-00486-Z/FIGURES/16.
Sebai, A., Zumbo, V., Féraud, G., Bertrand, H., Hussain, A.G., Giannérini, G., Campredon, R., 1991. 40Ar39Ar dating of alkaline and tholeiitic magmatism of Saudi Arabia related to the early Red Sea Rifting. Earth Planet. Sci. Lett. 104, 473–487. https://doi.org/10.1016/0012-821X(91)90223-5.
Semaw, S., Simpson, S.W., Quade, J., Renne, P.R., Butter, R.F., McIntosh, W.C., Levin, H., Domingues-Rodrigo, M., Rodgers, M.J., 2005. Early Pliocene hominids from Gona, Ethiopa. Nature 433, 301–305. https://doi.org/10.1038/nature03177.
Sembroni, A., Molin, P., Dramis, F., Faccenna, C., Abebe, B., 2017. Erosion-tectonics feedbacks in shaping the landscape: an example from the Mekele Outlier (Tigray, Ethiopia). J. Afr. Earth Sci. 129, 870–886. https://doi.org/10.1016/J.JAFREARSCI.2017.02.028.
Shawel, M., Unnithan, V., Mammo, T., 2022. Seismic sequence stratigraphy of the Permo- Triassic Karoo Group and its implication for hydrocarbon exploration, southwestern Ogaden Basin, Ethiopia. Mar. Pet. Geol. 139, 105480 https://doi.org/10.1016/J.MARPETGEO.2021.105480.
Shi, W., Mitchell, N.C., Kalnins, L.M., Izzeldin, A.Y., 2018. Oceanic-like axial crustal high in the Central Red Sea. Tectonophysics 747–748, 327–342. https://doi.org/10.1016/J.TECTO.2018.10.011.
Shoshani, J., Walter, R.C., Abraha, M., Berhe, S., Tassy, P., Sanders, W.J., Marchant, G. H., Libsekal, Y., Ghirmai, T., Zinner, D., 2006. A proboscidean from the late oligocene of Eritrea, a "missing link" between early elephantiformes and elephantimorpha, and biogeographic implications. Proc. Natl. Acad. Sci. U. S. A. 103, 17296–17301. https://doi.org/10.1073/pnas.0603689103.
Sichler, B., 1980. La biellette danakile : un modèle pour l'évolution géodynamique de l'Afar. Bull. Soc. Géol. Fr. 22, 925–932.
Sickenberg, O., Schönfeld, M., 1975. The Chorora Formation - lower Pliocene limnical sediments in the southern Afar (Ethiopia). In: Pilger, A., Rösler, A. (Eds.), Afar Depression of Ethiopia: Proceedings of an International Symposium on the Afar Region and Related Rift Problems. E. Schweizerbart'sche Verlagsbuchhandlung, Stuttgart, pp. 277–284.
Siegburg, M., Gernon, T.M., Bull, J.M., Keir, D., Barfod, D.N., Taylor, R.N., Abebe, B., Ayele, A., 2018. Geological evolution of the Boset-Bericha Volcanic complex, Main Ethiopian Rift: 40Ar/39Ar evidence for episodic Pleistocene to Holocene volcanism. J. Volcanol. Geotherm. Res. 351, 115–133. https://doi.org/10.1016/j.jvolgeores.2017.12.014.
Sigmundsson, F., 2006. Iceland Geodynamics, Springer Praxis Books. Springer, Berlin Heidelberg. https://doi.org/10.1007/3-540-37666-6.

Smith, J.E., Santamarina, J.C., 2022. Red Sea evaporites: Formation, creep and dissolution. Earth-Sci. Rev. 232, 104115 https://doi.org/10.1016/j.earscirev.2022.104115.
Smittarello, D., Grandin, R., De Chabalier, J.B., Doubre, C., Deprez, A., Masson, F., Socquet, A., Saad, I.A., 2016. Transient deformation in the Asal-Ghoubbet Rift (Djibouti) since the 1978 diking event: is deformation controlled by magma supply rates? J. Geophys. Res. Solid Earth 121, 6030–6052. https://doi.org/10.1002/2016JB013069.
Sneh, A., Bartov, Y., Rosensaft, M., 1997a. Geological Map of Israel - Sheet 1. Geol. Surv. Isr.
Sneh, A., Bartov, Y., Rosensaft, M., 1997b. Geological Map of Israel - Sheet 2. Geol. Surv. Isr.
Sneh, A., Bartov, Y., Weissbrod, T., Rosensaft, M., 1997c. Geological Map of Israel - Sheet 3. Geol. Surv. Isr.
Sneh, A., Bartov, Y., Weissbrod, T., Rosensaft, M., 1997d. Geological Map of Israel - Sheet 4. Geol. Surv. Isr.
Souriot, T., Brun, J.P., 1992. Faulting and block rotation in the Afar triangle, East Africa: the Danakil "crank-arm" model. Geology 20, 911–914. https://doi.org/10.1130/0091-7613(1992)020<0911:FABRIT>2.3.CO;2.
Speijer, R.P., Pälike, H., Hollis, C.J., Hooker, J.J., Ogg, J.G., 2020. The Paleogene Period. In: Gradstein, F.M., Ogg, J.G., Schmitz, M.D., Ogg, G.M. (Eds.), Geologic Time Scale 2020. Elsevier, pp. 1087–1140. https://doi.org/10.1016/B978-0-12-824360-2.00028-0.
Stab, M., Bellahsen, N., Pik, R., Quidelleur, X., Ayalew, D., Leroy, S., 2016. Modes of rifting in magma-rich settings: Tectono-magmatic evolution of Central Afar. Tectonics 35, 2–38. https://doi.org/10.1002/2015TC003893.
Stamps, D.S., Flesch, L.M., Calais, E., Ghosh, A., 2014. Current kinematics and dynamics of Africa and the East African Rift System. J. Geophys. Res. Solid Earth 119, 5161–5186. https://doi.org/10.1002/2013JB010717.
Stamps, D.S., Iaffaldano, G., Calais, E., 2015. Role of mantle flow in Nubia-Somalia plate divergence. Geophys. Res. Lett. 42, 290–296. https://doi.org/10.1002/2014GL062515.
Stamps, D.S., Kreemer, C., Fernandes, R., Rajaonarison, T.A., Rambolamanana, G., 2021. Redefining East African Rift System kinematics. Geology 49, 150–155. https://doi.org/10.1130/g47985.1.
Steckler, M.S., ten Brink, U.S., 1986. Lithospheric strength variations as a control on new plate boundaries: examples from the northern Red Sea region. Earth Planet. Sci. Lett. 79, 120–132. https://doi.org/10.1016/0012-821X(86)90045-2.
Stern, R.J., Johnson, P.R., 2019. Constraining the opening of the Red Sea: Evidence from the Neoproterozoic margins and Cenozoic Magmatism for a Volcanic Rifted margin. In: Rasul, N.M.A., Stewart, I.C.F. (Eds.), Geological Setting, Palaeoenvironment and Archaeology of the Red Sea. Springer, pp. 53–79. https://doi.org/10.1007/978-3-319-99408-6.
Stewart, S.A., 2016. Structural geology of the Rub' Al-Khali Basin, Saudi Arabia. Tectonics 35, 2417–2438. https://doi.org/10.1002/2016TC004212.
Stockli, D.F., Bosworth, W.B., 2019. Timing of extensional faulting along the magma-poor central and northern red sea rift margin-transition from regional extension to necking along a hyperextended rifted margin. In: Geological Setting, Palaeoenvironment and Archaeology of the Red Sea. Springer International Publishing, pp. 81–111. https://doi.org/10.1007/978-3-319-99408-6_5.
Stoffers, P., Ross, D., 1974. Sedimentary history of the Red Sea. Initial Rep. Deep Sea Drill. Proj. 23, 849–865. https://doi.org/10.2973/dsdp.proc.23.123.1974.
Storchak, D.A., Harris, J., Brown, L., Lieser, K., Shumba, B., Verney, R., Di Giacomo, D., Korger, E.I.M., 2017. Rebuild of the Bulletin of the International Seismological Centre (ISC), part 1: 1964–1979. Geosci. Lett. 4, 1–14. https://doi.org/10.1186/S40562-017-0098-Z/TABLES/1.
Storchak, D.A., Harris, J., Brown, L., Lieser, K., Shumba, B., Di Giacomo, D., 2020. Rebuild of the Bulletin of the International Seismological Centre (ISC)—part 2: 1980–2010. Geosci. Lett. 7, 1–21. https://doi.org/10.1186/S40562-020-00164-6/FIGURES/16.
Stuart, G.W., Bastow, I.D., Ebinger, C.J., 2006. Crustal structure of the northern Main Ethiopian Rift from receiver function studies. Geol. Soc. London. Spec. Publ. 259, 253–267. https://doi.org/10.1144/GSL.SP.2006.259.01.20.
Sultan, M., 1992. Nature of the Red Sea crust: a controversy revisited. Geology 20, 593–596. https://doi.org/10.1130/0091-7613(1992)020<0593:NOTRSC>2.3.CO;2.
Sultan, M., Becker, R., Arvidson, R.E., Shore, P., Stern, R.J., El Alfy, Z., Attia, R.I., 1993. New constraints on Red Sea rifting from correlations of Arabian and Nubian Neoproterozoic outcrops. Tectonics 12, 1303–1319. https://doi.org/10.1029/93TC00819.
Survey of Kenya, 1962. Kenya Geological Map - 1:3′000′000.
Szymanski, E., Stockli, D.F., Johnson, P.R., Hager, C., 2016. Thermochronometric evidence for diffuse extension and two-phase rifting within the Central Arabian margin of the Red Sea Rift. Tectonics 35, 2863–2895. https://doi.org/10.1002/2016TC004336.
Taieb, M., Johanson, D.C., Coppens, Y., Aronson, J.L., 1976. Geological and palaeontological background of Hadar hominid site, Afar, Ethiopia. Nature 260, 289–293. https://doi.org/10.1038/260289a0.
Tapponnier, P., Varet, J., 1974. La zone de Mak'arrasou en Afar: un équivlent émergé des "failles transformantes" océaniques. Compt. Rend. Hebd. Séances l'Acad. Sci. Sér. B 278, 209–212.
Tapponnier, P., Armijo, R., Manighetti, I., Courtillot, V., 1990. Bookshelf faulting and horizontal block rotations between overlapping rifts in southern Afar. Geophys. Res. Lett. 17, 1–4. https://doi.org/10.1029/GL017i001p00001.
Tard, F., Masse, P., Walgenwitz, F., Gruneisen, P., 1991. The volcanic passive margin in the vicinity of Aden, Yemen. Bull. Centres Rech Explor. Prod. Elf-Aquitaine 15, 1–9.
Tazieff, H., Varet, J., Barberi, F., Giglia, G., 1972. Tectonic significance of the Afar (or Danakil) depression. Nature 235, 144–147. https://doi.org/10.1038/235144a0.
Teilhard de Chardin, P., 1930. Observations géologiques en Samalie française et au Harrar. Mém. Soc. Géol. Fr. 6, 5–12.
Teklay, M., Asmerom, Y., Toulkeridis, T., 2005. Geochemical and Sr-Nd isotope ratios in Cenozoic basalts from Eritrea: evidence for temporal evolution from low-Ti tholeiitic to high-Ti alkaline basalts in Afro-Arabian Continental Flood Basalt Province. Period. Mineral. 74, 167–182.
Tesfamichael, G., De Smedt, F., Miruts, H., Solomon, G., Kassa, A., Kurkura, K., Abdulwassie, H., Bauer, H., Nyssen, J., Moeyersons, J., Deckers, J., Mitiku, H., Nurhussen, T., 2010. Large-Scale Geological mapping of the Geba basin, northern Ethiopia. Tigray Livelihood Pap. No 9, VLIR – Mekelle Univ. IUC Progr. 1–46.
Tesfaye, S., Harding, D.J., Kusky, T.M., 2003. Early continental breakup boundary and migration of the Afar triple junction, Ethiopia. Bull. Geol. Soc. Am. 115, 1053–1067. https://doi.org/10.1130/B25149.1.
Thiélemont, D., 2016. Carte géologique de l'Afrique à l'échelle du 1/10M. CCGM-BRGM.
Thines, J.E., Ukstins, I.A., Wall, C., Schmitz, M., 2021. Volumetric extrusive rates of silicic supereruptions from the Afro-Arabian large igneous province. Nat. Commun. 12, 1–9. https://doi.org/10.1038/s41467-021-26468-5.
Thybo, H., Nielsen, C.A., 2009. Magma-compensated crustal thinning in continental rift zones. Nature 457, 873–876. https://doi.org/10.1038/nature07688.
Tiberi, C., Ebinger, C., Ballu, V., Stuart, G., Oluma, B., 2005. Inverse models of gravity data from the Red Sea-Aden-East African rifts triple junction zone. Geophys. J. Int. 163, 775–787. https://doi.org/10.1111/j.1365-246X.2005.02736.x.
Tiercelin, J.J., 1986. The Pliocene Hadar Formation, Afar depression of Ethiopia. Geol. Soc. Spec. Publ. 25, 221–240. https://doi.org/10.1144/GSL.SP.1986.025.01.19.
Tiercelin, J.J., Michaux, J., Bandet, Y., 1979. Le Miocene superieur du sud de la depression de l'Afar, Ethiopie; sediments, faunes, ages isotopiques. Bull. Soc. Géol. Fr. S7-XXI, 255–258. https://doi.org/10.2113/gssgfbull.S7-XXI.3.255.
Tierney, J.E., deMenocal, P.B., Zander, P.D., 2017. A climatic context for the out-of-Africa migration. Geology 45, 1023–1026. https://doi.org/10.1130/G39457.1.
Tortelli, G., Gioncada, A., Pagli, C., Rosi, M., De Dosso, L., Keir, D., 2021. Evidence of active magmatic rifting at the Ma'Alalta volcanic field (Afar, Ethiopia). Bull. Volcanol. 83, 38. https://doi.org/10.1007/s00445-021-01461-4.
Tortelli, G., Gioncada, A., Pagli, C., Braschi, E., Gebru, E.F., Keir, D., 2022. Constraints on the Magma Source and Rift Evolution from Geochemistry of the Stratoid Flood Basalts (Afar, Ethiopia). Geochem. Geophys. Geosyst. 23, e2022GC010434 https://doi.org/10.1029/2022GC010434.
Trifonov, V.G., Dodonov, A.E., Sharkov, E.V., Golovin, D.I., Chernyshev, I.V., Lebedev, V. A., Ivanova, T.P., Bachmanov, D.M., Rukieh, M., Ammar, O., Minini, H., Al Kafri, A. M., Ali, O., 2011. New data on the late Cenozoic basaltic volcanism in Syria, applied to its origin. J. Volcanol. Geotherm. Res. 199, 177–192. https://doi.org/10.1016/J.JVOLGEORES.2010.01.013.
Ukstins Peate, I., Baker, J.A., Al-Kadasi, M., Al-Subbary, A., Knight, K.B., Riisager, P., Thirlwall, M.F., Peate, D.W., Renne, P.R., Menzies, M.A., 2005. Volcanic stratigraphy of large-volume silicic pyroclastic eruptions during Oligocene Afro-Arabian flood volcanism in Yemen. Bull. Volcanol. 68, 135–156. https://doi.org/10.1007/S00445-005-0428-4/TABLES/4.
Ukstins, I.A., Renne, P.R., Wolfenden, E., Baker, J., Ayalew, D., Menzies, M., 2002. Matching conjugate volcanic rifted margins: 40Ar/39Ar chrono-stratigraphy of pre- and syn-rift bimodal flood volcanism in Ethiopia and Yemen. Earth Planet. Sci. Lett. 198, 289–306. https://doi.org/10.1016/S0012-821X(02)00525-3.
USGS, 1963. Geologic map of the Arabian Peninsula. U.S. Geol. Surv. IMAP 270-A. https://doi.org/10.3133/i270A.
USGS, Arabian American Oil Company, 1963. Geologic Map of the Arabian Peninsula.
Varet, J., 2018. Geology of Afar (East Africa). Springer, Cham. https://doi.org/10.1007/978-3-319-60865-5.
Varet, J., 2021. Relationship of the Pan-African Tectonic Structures with the opening of the Afar Triple Junction. In: Hamimi, Z., Fowler, A., Liégeois, J., Collins, A., Abdelsalam, M.G., Abd EI-Wahed, M. (Eds.), The Geology of the Arabian-Nubian Shield. Springer, Cham, pp. 737–771. https://doi.org/10.1007/978-3-030-72995-0_27.
Varet, J., Gardo, I.A., 2020. Another geothermal site in North-Eastern Afar: Harak (Bidu woreda, Afar regional state, Ethiopia), that marks the southernmost extension of the Danakil Sea 110m bsl. In: Proceeding of the 8th African Rift Geothermal Conference. Nairobi, pp. 1–13.
Varet, J., Barberi, F., Borsi, S., Cheminée, J.L., Giglia, G., Marinelli, G., Santacroce, R., Stieltjes, H., Tazieff, H., La Volpe, L., Lirer, L., Di Paola, M., Demange, J., Black, R., Morton, W., Gasse, F., Taieb, M., Chèdeville, E., 1975. Geological Map of Central and Southern Afar (1:500′000). CNRS/CNR.
Vérard, C., 2021. 888–444 Ma Global Plate Tectonic Reconstruction with Emphasis on the Formation of Gondwana. Front. Earth Sci. 9, 404. https://doi.org/10.3389/feart.2021.666153.
Vigny, C., de Chabalier, J.-B., Ruegg, J.-C., Huchon, P., Feigl, K.L., Cattin, R., Asfaw, L., Kanbari, K., 2007. Twenty-five years of geodetic measurements along the Tadjoura-Asal rift system, Djibouti, East Africa. J. Geophys. Res. 112, B06410. https://doi.org/10.1029/2004JB003230.
Villmoare, B., Kimbel, W.H., Seyoum, C., Campisano, C.J., DiMaggio, E.N., Rowan, J., Braun, D.R., Arrowsmith, J.R., Reed, K.E., 2015. Early Homo at 2.8 Ma from Ledi-Geraru, Afar, Ethiopia. Science 347, 1352–1355. https://doi.org/10.1126/SCIENCE.AAA1343/SUPPL_FILE/AAA1343-VILLMOARE-SM.PDF.
Viltres, R., Jónsson, S., Ruch, J., Doubre, C., Reilinger, R., Floyd, M., Ogubazghi, G., 2020. Kinematics and deformation of the southern Red Sea region from GPS observations. Geophys. J. Int. 221, 2143–2154. https://doi.org/10.1093/gji/ggaa109.

Viltres, R., Jónsson, S., Alothman, A.O., Liu, S., Leroy, S., Masson, F., Doubre, C., Reilinger, R., 2022. Present-Day Motion of the Arabian Plate. Tectonics 41, e2021TC007013. https://doi.org/10.1029/2021TC007013.
Vogel, N., Nomade, S., Negash, A., Renne, P.R., 2006. Forensic 40Ar/39Ar dating: a provenance study of Middle Stone Age obsidian artifacts from Ethiopia. J. Archaeol. Sci. 33, 1749–1765. https://doi.org/10.1016/j.jas.2006.03.008.
Vrbka, P., Bussert, R., Abdalla, O.A.E., 2008. Groundwater in North and Central Sudan. Appl. Groundw. Stud. Afr. IAH Sel. Pap. Hydrogeol. 13, 337–349.
Walter, R.C., Buffler, R.T., Bruggemann, J.H., Guillaume, M.M.M., Berhe, S.M., Negassi, B., Libsekal, Y., Cheng, H., Edwards, R.L., von Cosel, R., Néraudeau, D., Gagnon, M., 2000. Early human occupation of the Red Sea coast of Eritrea during the last interglacial. Nature 405, 65–69. https://doi.org/10.1038/35011048.
Wang, T., Gao, S.S., Yang, Q., Liu, K.H., 2021. Crustal structure beneath the Ethiopian Plateau and adjacent areas from receiver functions: Implications for partial melting and magmatic underplating. Tectonophysics 809, 228857. https://doi.org/10.1016/j.tecto.2021.228857.
Watchorn, F., Nichols, G.J., Bosence, D.W., 1998. Rift-related sedimentation and stratigraphy, southern Yemen (Gulf of Aden). In: Purser, B.H., Bosence, D.W. (Eds.), Sedimentation and Tectonics in Rift Basins: Red Sea - Gulf of Aden. Chapman & Hall, London, pp. 165–189. https://doi.org/10.1007/978-94-011-4930-3_11.
Watts, E.J., Gernon, T.M., Taylor, R.N., Keir, D., Siegburg, M., Jarman, J., Pagli, C., Gioncada, A., 2020. Evolution of the Alu-Dalafilla and Borale volcanoes, Afar, Ethiopia. J. Volcanol. Geotherm. Res. 408, 107094 https://doi.org/10.1016/j.jvolgeores.2020.107094.
Wegener, A., 1929. Die Entstehung der Kontinente und Ozeane. Druck und. ed. Braunschweig.
White, T.D., Suwa, G., Hart, W.K., Walter, R.C., Woldegabriel, G., De Heinzelin, J., Clark, J.D., Asfaw, B., Vrba, E., 1993. New discoveries of australopithecus at maka in Ethiopia. Nature 366, 261–265. https://doi.org/10.1038/366261a0.
Wiart, P., Oppenheimer, C., 2000. Largest known historical eruption in Africa: Dubbi volcano, Eritrea, 1861. Geology 28, 291. https://doi.org/10.1130/0091-7613(2000)28<291:LKHEIA>2.0.CO;2.
Wiart, P., Oppenheimer, C., 2005. Large magnitude silicic volcanism in North Afar: the Nabro Volcanic Range and Ma'alalta volcano. Bull. Volcanol. 67, 99–115. https://doi.org/10.1007/s00445-004-0362-x.
Wiart, P.A.M., Oppenheimer, C., Francis, P., 2000. Eruptive history of Dubbi volcano, Northeast Afar (Eritrea), revealed by optical and SAR image interpretation. Int. J. Remote Sens. 21, 911–936. https://doi.org/10.1080/014311600210353.
Willemann, R.J., Storchak, D.A., 2001. Data Collection at the International Seismological Centre. Seismol. Res. Lett. 72, 440–453. https://doi.org/10.1785/GSSRL.72.4.440.
Williams, F.M., 2016. The Rift margins and the Great Western Escarpment. In: Understanding Ethiopia. GeoGuide. Springer, Cham, pp. 225–242. https://doi.org/10.1007/978-3-319-02180-5.
Williams, F.M., Williams, M.A.J., Aumento, F., 2004. Tensional fissures and crustal extension rates in the northern part of the Main Ethiopian Rift. J. Afr. Earth Sci. 38, 183–197. https://doi.org/10.1016/j.jafrearsci.2003.10.007.
Windley, B.F., Whitehouse, M.J., Ba-Bttat, M.A.O., 1996. Early Precambrian gneiss terranes and Pan-African island arcs in Yemen: Crustal accretion of the eastern Arabian Shield. Geology 24, 131. https://doi.org/10.1130/0091-7613(1996)024<0131:EPGTAP>2.3.CO;2.
WoldeGabriel, G., 1987. Unpublished. PhD thesis. Case West. Reserv. Univ.
WoldeGabriel, G., Walter, R.C., Aronson, J.L., Hart, W.K., 1992a. Geochronology and distribution of silicic volcanic rocks of Plio-Pleistocene age from the central sector of the Main Ethiopian Rift. Quat. Int. 13–14, 69–76. https://doi.org/10.1016/1040-6182(92)90011-P.
WoldeGabriel, G., White, T., Suwa, G., Semaw, S., Beyene, Y., Asfaw, B., Walter, R., 1992b. Kesem-Kebena: a newly Discovered Paleoanthropological Research Area in Ethiopia. J. F. Archaeol. 19, 471. https://doi.org/10.2307/530428.
WoldeGabriel, G., Haile-Selassie, Y., Renne, P.R., Hart, W.K., Ambrose, S.H., Asfaw, B., Heiken, G., White, T., 2001. Geology and palaeontology of the late Miocene Middle Awash valley, Afar rift, Ethiopia. Nature 412, 175–178. https://doi.org/10.1038/35084058.
WoldeGabriel, G., Endale, T., White, T.D., Thouveny, N., Hart, W.K., Renne, P.R., Asfaw, B., 2013. The role of tephra studies in African paleoanthropology as exemplified by the Sidi Hakoma Tuff. J. Afr. Earth Sci. 77, 41–58. https://doi.org/10.1016/j.jafrearsci.2012.09.004.
Wolfenden, E., Ebinger, C., Yirgu, G., Deino, A., Ayalew, D., 2004. Evolution of the northern Main Ethiopian rift: Birth of a triple junction. Earth Planet. Sci. Lett. 224, 213–228. https://doi.org/10.1016/j.epsl.2004.04.022.
Wolfenden, E., Ebinger, C., Yirgu, G., Renne, P.R., Kelley, S.P., 2005. Evolution of a volcanic rifted margin: Southern Red Sea, Ethiopia. Geol. Soc. Am. Bull. 117, 846. https://doi.org/10.1130/B25516.1.
Worku, T., Astin, T.R., 1992. The Karoo sediments (late Palaeozoic to early Jurassic) of the Ogaden Basin, Ethiopia. Sediment. Geol. 76, 7–21. https://doi.org/10.1016/0037-0738(92)90136-F.
Wright, T.J., Ebinger, C., Biggs, J., Ayele, A., Yirgu, G., Keir, D., Stork, A., 2006. Magma-maintained rift segmentation at continental rupture in the 2005 Afar dyking episode. Nature 442, 291–294. https://doi.org/10.1038/nature04978.
Wright, T.J., Sigmundsson, F., Pagli, C., Belachew, M., Hamling, I.J., Brandsdóttir, B., Keir, D., Pedersen, R., Ayele, A., Ebinger, C., Einarsson, P., Lewi, E., Calais, E., 2012. Geophysical constraints on the dynamics of spreading centres from rifting episodes on land. Nat. Geosci. 5, 242–250. https://doi.org/10.1038/ngeo1428.
Wynn, J.G., Roman, D.C., Alemseged, Z., Reed, D., Geraads, D., Munro, S., 2008. Stratigraphy, depositional environments, and basin structure of the hadar and busidima formations at dikika, Ethiopia. Spec. Pap. Geol. Soc. Am. 446, 87–118. https://doi.org/10.1130/2008.2446(04).
Xu, W., Ruch, J., Jónsson, S., 2015. Birth of two volcanic islands in the southern Red Sea. Nat. Commun. 6, 7104. https://doi.org/10.1038/ncomms8104.
Xu, W., Rivalta, E., Li, X., 2017. Magmatic architecture within a rift segment: Articulate axial magma storage at Erta Ale volcano, Ethiopia. Earth Planet. Sci. Lett. 476, 79–86. https://doi.org/10.1016/J.EPSL.2017.07.051.
Xu, W., Xie, L., Aoki, Y., Rivalta, E., Jónsson, S., 2020. Volcano-Wide Deformation after the 2017 Erta Ale Dike Intrusion, Ethiopia, Observed with Radar Interferometry. J. Geophys. Res. Solid Earth 125, e2020JB019562. https://doi.org/10.1029/2020JB019562.
Zanettin, B., Justin-Visentin, E., 1975. Tectonical and volcanological evolution of the western Afar margin (Ethiopia). In: Pilger, A., Rösler, A. (Eds.), Afar Depression of Ethiopia: Proceedings of an International Symposium on the Afar Region and Related Rift Problems. E. Schweizerbart'sche Verlagsbuchhandlung, Stuttgart, pp. 300–309.
Zanettin, B., Bellieni, G., Justin-Visentin, E., 2006. New radiometric age of volcanic rocks in the central Eritrean plateau (from Asmara to Adi Quala): Considerations on stratigraphy and correlations. J. Afr. Earth Sci. 45, 156–161. https://doi.org/10.1016/j.jafrearsci.2006.01.010.
Zawacki, E.E., van Soest, M.C., Hodges, K.V., Scott, J.J., Barboni, M., Strecker, M.R., Feibel, C.S., Campisano, C.J., Arrowsmith, J.R., 2022. Sediment provenance and silicic volcano-tectonic evolution of the northern East African Rift System from U/Pb and (U-Th)/he laser ablation double dating of detrital zircons. Earth Planet. Sci. Lett. 580, 117375 https://doi.org/10.1016/J.EPSL.2022.117375.
Zumbo, V., Féraud, G., Bertrand, H., Chazot, G., 1995a. 40Ar39Ar chronology of tertiary magmatic activity in Southern Yemen during the early Red Sea-Aden rifting. J. Volcanol. Geotherm. Res. 65, 265–279. https://doi.org/10.1016/0377-0273(94)00106-Q.
Zumbo, V., Féraud, G., Vellutini, P., Piguet, P., Vincent, J., 1995b. First 40Ar39Ar dating on early pliocene to plio-pleistocene magmatic events of the Afar — Republic of Djibouti. J. Volcanol. Geotherm. Res. 65, 281–295. https://doi.org/10.1016/0377-0273(94)00107-R.
Zwaan, F., Schreurs, G., 2020. Rift segment interaction in orthogonal and rotational extension experiments: Implications for the large-scale development of rift systems. J. Struct. Geol. 140, 104119 https://doi.org/10.1016/j.jsg.2020.104119.
Zwaan, F., Schreurs, G., Rosenau, M., 2019. Rift propagation in rotational versus orthogonal extension: Insights from 4D analogue models. J. Struct. Geol. 135, 103946 https://doi.org/10.1016/j.jsg.2019.103946.
Zwaan, F., Corti, G., Keir, D., Sani, F., Muluneh, A., Illsley-Kemp, F., Papini, M., 2020a. Geological Data from the Western Afar Margin, East Africa. GFZ Data Serv.
Zwaan, F., Corti, G., Sani, F., Keir, D., Muluneh, A.A., Illsley-Kemp, F., Papini, M., 2020b. Structural Analysis of the Western Afar margin, East Africa: evidence for Multiphase Rotational Rifting. Tectonics 39, e2019TC006043. https://doi.org/10.1029/2019TC006043.
Zwaan, F., Chenin, P., Erratt, D., Manatschal, G., Schreurs, G., 2022. Competition between 3D structural inheritance and kinematics during rifting: Insights from analogue models. Basin Res. 34, 824–854. https://doi.org/10.1111/BRE.12642.